UNIVERSITY OF Southampton

University of Southampton Research Repository

Copyright © and Moral Rights for this thesis and, where applicable, any accompanying data are retained by the author and/or other copyright owners. A copy can be downloaded for personal non-commercial research or study, without prior permission or charge. This thesis and the accompanying data cannot be reproduced or quoted extensively from without first obtaining permission in writing from the copyright holder/s. The content of the thesis and accompanying research data (where applicable) must not be changed in any way or sold commercially in any format or medium without the formal permission of the copyright holder/s.

When referring to this thesis and any accompanying data, full bibliographic details must be given, e.g.

Thesis: Author (Year of Submission) "Full thesis title", University of Southampton, name of the University Faculty or School or Department, PhD Thesis, pagination.

Data: Author (Year) Title. URI [dataset]

University of Southampton

Faculty of Medicine

Clinical and Experimental Sciences

Recognition of viral peptides by inhibitory and activating Killer Immunoglobulin-like Receptors

by

Leidy Yamile Bastidas Legarda

https://orcid.org/0000-0001-8743-1863

Thesis for the degree of Doctor of Philosophy

January 2020

University of Southampton

Abstract

Faculty of Medicine

Clinical and Experimental Sciences

Thesis for the degree of Doctor of Philosophy

Recognition of viral peptides by inhibitory and activating Killer Immunoglobulin-like Receptors

by

Leidy Yamile Bastidas Legarda

Background and Aim: Natural killer (NK) cells are lymphocytes from the innate immunity critical in the control of viral infections. NK cell functions against viruses are largely regulated by the interaction between Killer Immunoglobulin-like receptors (KIR) and Major Histocompatibility Complex class I (MHC-I):peptide ligands. Recently, our group reported that highly conserved peptides derived from viruses of the family *Flaviviridae* bind the HLA-C*0102 allele and together induce strong KIR2DS2-mediated NK cell functions. Given the enormous allelic diversity of the MHC-I locus, this thesis aimed to investigate the ability of *Flaviviridae*-derived peptides to bind different Human Leukocyte Antigen C (HLA-C) alleles and to activate NK cells through engagement with KIR2DS2.

Methods: An *in vitro* co-culture system using different combinations of target and effector cell lines was optimized. As target cells, we used Transporter-associated with Antigen Processing (TAP)-deficient or TAP-competent cells expressing different HLA-C alleles and presenting exogenous or endogenous viral peptides containing the AT motif and derived from the non-structural 3 (NS3) proteins of Hepatitis C virus (HCV; LNPSVAATL), Dengue/Zika virus (DENV/ZIKV; IVDLMCHATF), Yellow Fever virus (YFV; VIDAMCHATL) and West Nile/Japanese Encephalitis virus (WNV/JEV; IVDVMCHATL). As effector cells, NKL cell lines or primary NK cells expressing inhibitory KIR2DL2 or activating KIR2DS2 receptors, were used. Activation of NK cells to different targets was determined by assessing NK cell cytotoxicity, degranulation and inhibition of viral replication.

Results: Huh-7 cells expressing the HCV replicon and presenting endogenous viral peptides in the context of HLA-C*0304 or HLA-C*0802 were strongly recognized by the

Natural Killer Cell Leukaemia (NKL) cell line expressing KIR2DS2; this effect was independent of LNPSVAATL peptide. TAP-deficient 721.221 cells expressing HLA-C*0802 or HLA-C*0501 and loaded with IVDLMCHATF peptide strongly bound KIR2DS2-PE tetramers; however only TAP-competent 721.221 cells expressing HLA-C*0802 and endogenously presenting DENV/NS3-derived peptides induced strong NK cell effector functions through canonical interaction with KIR2DS2. Finally, 721.221 cells co-expressing HLA-C*0802 and IVDLMCHATF peptide generated robust NK cell degranulation and cytotoxic activity. Unlike LNPSVAATL, IVDLMCHATF peptide is predicted to have a broad HLA-C specificity.

Conclusion: This research identified a Flaviviral peptide carrying the highly conserved “MCHAT” motif (IVDLMCHATF) that in complex with HLA-C*0802 specifically interacted with KIR2DS2 leading to robust NK cell effector functions. This is the first viral peptide defined that binds an activating KIR and more than one HLA-C type. These data imply that Flaviviruses are credible drivers of the evolution of KIR2DS2.

Table of Contents

Table of Contents

Table of Tables

Table of Figures

Table of Figures

Research Thesis: Declaration of Authorship

Print name:	Leidy Yamile Bastidas Legarda

Title of thesis:	Recognition of viral peptides by inhibitory and activating Killer Immunoglobulin-like Receptors

I declare that this thesis and the work presented in it are my own and has been generated by me as the result of my own original research.

I confirm that:

1. This work was done wholly or mainly while in candidature for a research degree at this University;
2. Where any part of this thesis has previously been submitted for a degree or any other qualification at this University or any other institution, this has been clearly stated;
3. Where I have consulted the published work of others, this is always clearly attributed;
4. Where I have quoted from the work of others, the source is always given. With the exception of such quotations, this thesis is entirely my own work;
5. I have acknowledged all main sources of help;
6. Where the thesis is based on work done by myself jointly with others, I have made clear exactly what was done by others and what I have contributed myself;
7. None of this work has been published before submission

Signature:		Date:	30th of January, 2020

Acknowledgements

I would like to express my gratitude to my supervisor, Professor Salim Khakoo, for his continuous support and motivation throughout this process and for always encouraging me to achieve excellence. I can say with complete certainty that I was mentored by one of the worldwide experts in the NK field. I also want to thank Chris McCormick for his contributions.

Besides my supervisors, I also would like to thank all the past and present members of the NK group. The help I received from the post-docs, technician and students was essential during the planning and execution of my experiments as well as the analysis of my results. Thanks to all the people from Level E, the Flow Cytometry facility in Level F and CCI building and all the blood donors.

A special thanks to Professor David Wilson for always being there for me. I will always cherish the memory of the moment I met him in Colombia and appreciate all the valuable help that I received from him since that day. Likewise, this thesis would not have been possible without the scholarships from Colciencias, the University of Southampton and the British Council through the Newton Fund.

My most sincere thanks go to my Mom Estella for all her love, care, dedication and support in all my decisions throughout my life. My education and all the success I achieved so far is because of her. To my sister Julie and my nephew Juan Pablo for being always there for me with their good vibes and for reminding me the value of family. To my Dad Carlos for always having me in his prayers and for his constant care.

A big thank you to all my friends, the ones that have always been there, the ones I met here in Southampton, the ones that were, and the ones that are not with us anymore.

Finally, I want to acknowledge all the people that somehow guided me to make the decision of studying this PhD, as this experience has not only increased my scientific knowledge, but also has enormously contributed to my personal growth and development.

Definitions and Abbreviations

ADCC	Antibody-Dependent Cellular Cytotoxicity
AKT	Protein kinase B
ATCC	American Type Culture Collection
BLIMP1	B lymphocyte-induced maturation protein-1
C	Core
CCL	Chemokine (C-C motif) Ligand
CTL	Cytotoxic T-Lymphocyte
CD	Cluster of Differentiation
CDC	Centres for Disease Control and Prevention
CLP	Common Lymphoid Progenitor
CMV	Cytomegalovirus
CXCL	C-X-C motif Chemokine Ligand
DAA	Direct-Acting Anti-viral
DAP	DNAX-activation protein
DENV	Dengue Virus
DMEM	Dulbecco's Modified Eagle Medium
DNAM	DNAX Accessory Molecule
D0	Domain 0
D1	Domain 1
D2	Domain 2
E	Envelope
EBOV	Ebolavirus
EBV	Epstein-Barr Virus
ECDC	European Centres for Disease Control and Prevention
Eomes	Eomesodermin
ER	Endoplasmic Reticulum
ERAAP	Endoplasmic Reticulum Aminopeptidase Associated with Antigen Processing
ETS-1	E26 transformation-specific
E4BP4	E4 promoter–binding protein 4
E:T	Effector:Target
Fab	Antigen-binding Fragment
FACS	Fluorescence-Activated Cell Sorting
FBS	Fetal Bovine Serum
Fc	Fragment Crystallizable

FcγR	Fc-gamma Receptor
FL	Fluorescence
Flt3L	Fms-like Tyrosine Kinase 3 Ligand
FMDV	Foot-and-Mouth Disease Virus
GATA-3	GATA-binding factor 3
GFP	Green Fluorescent Protein
GM-CSF	Granulocyte-Macrophage Colony-Stimulating Factor
HBV	Hepatitis B Virus
HCC	Hepatocellular Carcinoma
HCV	Hepatitis C Virus
HIV-1	Human Immunodeficiency Virus type 1
HLA	Human Leukocyte Antigen
HSC	Hematopoietic Stem Cells
HSV	Herpes Simplex Virus
IAV	Influenza A Virus
ICP47	Infected cell protein 47
Id2	DNA-binding protein inhibitor
IFNγ	Interferon gamma
IL	Interleukin
IL1R1	IL-1 Receptor type 1
IL2Rβ	IL-2 Receptor beta
IMDM	Iscove's Modified Dulbecco's Medium
ITAM	Immune-receptor Tyrosine-based Activation Motif
ITIM	Immune-receptor Tyrosine-based Inhibition Motif
iNK	Immature Natural Killer cell
JAK	Janus Kinase
JEV	Japanese Encephalitis Virus
KanR	Kanamycin Resistance
KIR	Killer Immunoglobulin-like Receptor
KIR2D	Killer Immunoglobulin-like Receptor 2 domains
KIR3D	Killer Immunoglobulin-like Receptor 3 domains
KLRF1	Killer cell Lectin-like Receptor subfamily F member 1
KLRG1	Killer cell Lectin-like Receptor subfamily G member 1
KL	c-kit Ligand
LAMP	Lysosome-Associated Membrane Protein
LB	Lysogeny Broth
LILR	Leukocyte Immunoglobulin-like Receptors
LIV	Louping-ill Virus

LMPP	Lymphoid-primed Multipotential Progenitor
LRC	Leukocyte Receptor Complex
Luc	Luciferase
M	Membrane
MAPK	Mitogen-Activated Protein Kinase
MDC	Macrophage-derived Chemokine
MFI	Mean Fluorescence Intensity
MHC-I	Major Histocompatibility Complex Class I
MHC-II	Major Histocompatibility Complex Class II
MICA	MHC class I Chain-related sequence A
MICB	MHC class I Chain-related sequence B
MIP-1α	Macrophage Inflammatory Protein 1 alpha
MIP-1β	Macrophage Inflammatory Protein 1 beta
mNK	Mature Natural Killer cell
NCAM	Neural Cell Adhesion Molecule
NCR	Natural Cytotoxicity Receptors
NK	Natural Killer
NKG2A	Natural Killer Group 2 member A
NKG2D	Natural Killer Group 2 member D
NKL	Natural Killer Cell Leukemia
NKP	Natural Killer Precursor
NS	Non-structural
OHFV	Omsk Hemorrrhagic Fever Virus
PAC	Puromycin-N-Acetyltransferase
PBMC	Peripheral Blood Mononuclear Cells
PBS	Phosphate Buffered Saline
PCR	Polymerase Chain Reaction
PFA	Paraformaldehyde
PI3K	Phosphatidylinositol-3-kinase
PLC	Peptide Loading Complex
POWV	Powassan Encephalitis Virus
P7	Viroporin
Raf	Rapidly Accelerated Fibrosarcoma
RANTES	Regulated on Activation, Normal T Cell Expressed and Secreted
Ras	Proto-Oncogene Proteins p21
RH	Recombinant human
RLU	Relative Luciferase Units
RPMI	Roswell Park Memorial Institute

SD	Standard Deviation
SH2	Src Homology 2
SHP	Src homology 2 (SH2) domain-containing protein tyrosine phosphatase
STAT	Signal Transducer and Activator of Transcription
TAP	Transporter-associated with Antigen Processing
TaV	Thosea asigna Virus
TBEV	Tick-borne Encephalitis Virus
TCA3	T-cell activation gene-3
TF	Transcription Factor
TNFα	Tumour Necrosis Factor Alpha
Tox2	Thymocyte selection-associated high mobility group box protein 2
TRAIL	TNF-related apoptosis-inducing ligand
T-bet	T-box protein expressed in T cells
VACV	Vaccinia Virus
WHO	World Health Organization
WNV	West Nile Virus
WT	Wild type
XCL	X-C motif Chemokine Ligand
YFP	Yellow Fluorescent Protein
YFV	Yellow Fever Virus
ZAP	Zeta Chain of T cell Receptor Associated Protein Kinase
ZIKV	Zika Virus
ZYk	Spleen Tyrosine Kinase

Chapter 1 - Introduction

1.1 Natural killer cells

Natural Killer (NK) cells were identified in the early 1970's from their ability to spontaneously kill murine tumour cells without prior sensitization via undefined receptor-ligand interactions. (Kiessling, Klein and Wigzell, 1975; Phillips, Ortaldo and Herberman, 1980). Later on, new evidence emerged showing that these cells expressed unique cell surface markers that mediated their effector functions (Ortaldo *et al.*, 1981; Lanier *et al.*, 1983). Currently, human NK cells are defined as a population of lymphocytes expressing a broad repertoire of germline-encoded inhibitory and activating receptors and represent an essential first line of defence against invading pathogens and in tumour surveillance (Abel *et al.*, 2018).

1.1.1 NK cell development and maturation

Development of NK cells primarily occur in the perivascular regions of the bone marrow; however, secondary lymphoid tissues are also an important site for NK cell differentiation and maturation (Freud *et al.*, 2005; Freud, Yu and Caligiuri, 2014). Initially, cluster of differentiation (CD) 34+ multipotent hematopoietic stem cells (HSC) differentiate into lymphoid-primed multi-potential progenitors (LMPP) that, in turn, transform into common lymphoid progenitors (CLP). At this point, CLP can differentiate into B cells, T cells or other innate lymphoid cells (Abel *et al.*, 2018). CLP also give rise to NK precursors (NKP), which are cells exclusively committed to the NK cell lineage (Abel *et al.*, 2018; Vivier *et al.*, 2018).

The interplay of intrinsic and extrinsic signals contributes to the transition of NKP to immature NK cells (iNK) and subsequently, to mature NK cells (mNK). Intrinsic cellular signalling comes from transcription factors (TF) that determine the expression of particular genes. Studies in mice and human NK cells have shown that E26 transformation-specific (ETS-1) is essential for the early stages of NK cell development whereas E4 promoter–binding protein 4 (E4bp4) is crucial in the transition from NKP to iNK and from iNK to mNK (Gascoyne *et al.*, 2009; Ramirez *et al.*, 2012). Other TF such as B lymphocyte-induced maturation protein-1 (Blimp1), Eomesodermin (Eomes), GATA-binding factor 3 (GATA-3),

T-box protein expressed in T cells (T-bet), Thymocyte selection-associated high mobility group box protein 2 (Tox2) and DNA-binding protein inhibitor (Id2) are involved in later stages of NK cell development (Townsend *et al.*, 2004; Carotta *et al.*, 2011; Vong *et al.*, 2014; Ali *et al.*, 2016). It has been demonstrated that GATA-3 plays a role in NK progression from the bone marrow to the periphery (Ali *et al.*, 2016) whereas Eomes and T-bet are up-regulated in peripheral NK cells, with the expression of T-bet being higher in mNK cells compared to iNK cells (Townsend *et al.*, 2004; Knox *et al.*, 2016).

Extrinsic signals that promote development, survival and proliferation of NK cells are given by a rich cytokine environment that includes fms-like tyrosine kinase 3 ligand (Flt3L), c-kit ligand (KL), and a variety of interleukins (IL) such as IL-2, IL-3, IL-7, IL-10, IL-12, IL-15, IL-18, IL-21 and IL-27. IL-3 and IL-7, along with Flt3L and KL (ligands for Flt-3 and c-kit receptors, respectively), promote proliferation of HSC into CLP and NKP (Lyman and Jacobsen, 1998; Yu *et al.*, 1998; Wu, Tian and Wei, 2017). The c-kit:KL interaction also takes place in later stages of NK cell maturation and it has been described to play essential roles in the formation of mNK cells in mice (Colucci and Di Santo, 2000).

The cytokines IL-2 and IL-15 play major roles in NK cell development as they lead NK cell commitment and maturation (Mrozek, Anderson and Caligiuri, 1996). IL-2 and IL-15 signal through receptor complexes located on the NK cell surface. Thus, soluble IL-2 binds IL-2Rα (CD25) in complex with IL-2R/IL-15Rβ chain (CD122) and the common gamma chain (γc; CD132) whereas IL-15 signals through the heterotrimeric IL-15R composed by the IL-15Rα chain (CD215), the IL-2R/IL-15Rβ chain and the common γc. Membrane-bound IL-15 in complex with IL-15Rα is presented in *trans* to NK cells expressing IL-2R/IL-15Rβ and γc chain (Budagian *et al.*, 2006; Waldmann, 2015). Both cytokines, along with others that use γc cytokine receptors (IL-4, IL-7, IL9 and IL-21), trigger intracellular signalling cascades that involve phosphorylation of Janus Kinase/Signal Transducer and Activator of Transcription (Jak/STAT), Proto-Oncogene Proteins p21/ Rapidly Accelerated Fibrosarcoma/ Mitogen-Activated Protein Kinase (Ras/Raf/MAPK) and Phosphatidylinositol-3-kinase/ Protein kinase B (PI3K/Akt) to regulate transcription (Becknell and Caligiuri, 2005).

1.1.1.1 Stages of NK cell maturation

Six distinct stages of NK cell development and maturation have been recognized and are characterized by the lack of expression of lineage markers (CD3, CD14 and CD19) and the systematic acquisition or loss of distinct cell surface markers **(Figure 1.1)** (Abel *et al.*, 2018).

Stage 1 corresponds to the initial stage of development in which LMPP are derived and express CD34, CD133, CD45RA and 2B4 (CD244). Stage 2 divides into 2a and 2b: stage 2a comprises CLP, which acquire CD7, CD10, CD38, CD117 and CD127 markers. After stage 2a, CLP express IL-1 receptor type 1 (IL1R1) and IL-2 receptor beta (IL2Rβ; CD122) and transform into NKP. From this stage, cells are exclusively committed to the NK cell lineage, which means that they are no longer able to differentiate into other cell types. Stage 3 includes iNK that are characterized by the loss of CD34 and gain of natural killer group 2 member D (NKG2D; CD314) and natural cytotoxicity receptors (NCR) such as NKp46 (CD335) and NKp30 (CD337), which are maintained until the last stage of maturation. Developing NK cells at stage 4 (4a and 4b) acquire a pre-maturity status and express neural cell adhesion molecule (NCAM; CD56) and natural killer group 2 member A (NKG2A; CD159a). What differentiates stages 4a and 4b is the expression of NKp80 (KLRF1). Stage 5 comprises mNK, whose expression of CD56 is reduced. These mature subsets also acquire expression of killer immunoglobulin-like receptors (KIR; CD158) and Fc-gamma receptor III (FcγRIII; CD16). The 6th stage includes mNK cells that express CD57, a marker of terminal differentiation (Freud *et al.*, 2006; Abel *et al.*, 2018).

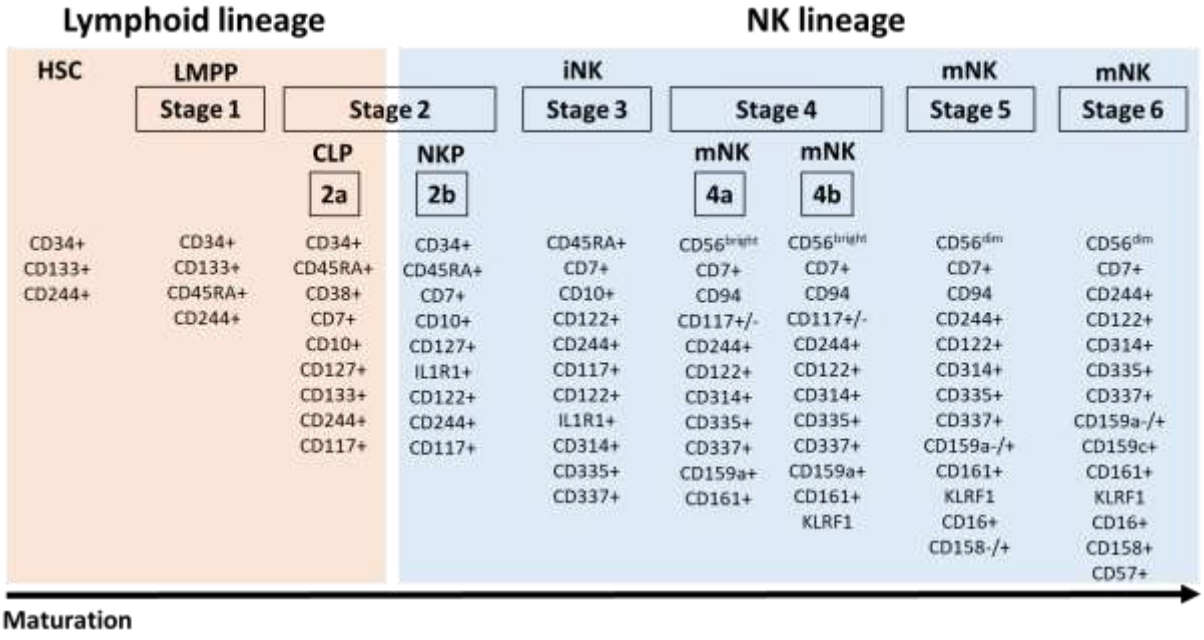

Figure 1.1 Stages of NK cell differentiation and maturation. HSC from the bone marrow undergo a series of divisions that give rise to LMPP and CLP. These cells have the potential to develop into all immune cells from the lymphoid lineage (orange). Conversion of CLP to NKP occurs at stage 2 under the influence of intrinsic and extrinsic signals. From this stage, NKP are committed exclusively to the NK cell lineage (blue) and develop into immature and subsequently into mature NK cells. Figure adapted from Abel *et al* and originally published by Frontiers in Immunology (Abel *et al.*, 2018).

The 140 kDa isoform of CD56 is mainly expressed by NK cells and a small subpopulation of T lymphocytes (Lanier *et al.*, 1991). This molecule is the phenotypic marker that defines NK cells and its expression through the different stages of NK cell development is progressive, reaching a peak at stages 4a and 4b ($CD56^{bright}$) and then decreasing at stages 5 and 6 ($CD56^{dim}$) (Freud *et al.*, 2006; Abel *et al.*, 2018). Expression of CD56 allows to discriminate between two mature NK cell phenotypes, which exhibit major differences in the expression of surface markers, maturation status, localization and functions **(Figure 1.2)**.

The $CD56^{bright}$ NK cells mainly reside in secondary lymphoid organs and uterus (~90%), whereas a small proportion is present in peripheral blood (~10%). The $CD56^{bright}$ subset in lymph nodes include two subgroups of cells, namely $CD56^{bright}$ CD16- NK cells (50-70%) and $CD56^{bright}$ $CD16^{dim}$ NK cells (30-50%) (Poli *et al.*, 2009). These cells are characterized by their ability to proliferate in response to IL-2 and IL-21 and to produce high amounts of cytokines such as interferon gamma (IFNγ), tumour necrosis factor alpha (TNFα), granulocyte-macrophage colony-stimulating factor (GM-CSF), IL-10 and IL-14. Overall, the cytotoxic capacity of $CD56^{bright}$ NK cells is low (Angelo *et al.*, 2015; Michel *et al.*, 2016).

Conversely, $CD56^{dim}$ NK cells are more abundant in peripheral blood (~90%) and express CD16 and KIR. Contrary to $CD56^{bright}$ NK cells, $CD56^{dim}$ NK cells are characterized by their low cytokine production and potent cytotoxic activity as they highly express perforin, granzymes and cytolytic granules. The expression of CD57 and CD160 on $CD56^{dim}$ NK cells is indicative of maturation and terminal differentiation (Poli *et al.*, 2009; Moretta, 2010). Controversy exists as whether $CD56^{dim}$ are derived from $CD56^{bright}$ NK cells or they develop as two distinct subpopulations (Michel *et al.*, 2016). Evidence has shown that $CD56^{bright}$ NK cells have longer telomeres compared to $CD56^{dim}$ NK cells, which indicates that NK cells undergo a maturation process (Romagnani *et al.*, 2007). Nevertheless, other studies have shown the differential expression of genes and metabolic activity of both subsets, which might suggest that $CD56^{bright}$ and $CD56^{dim}$ are individual NK cell subpopulations (Wendt *et al.*, 2006; Keating *et al.*, 2016).

Overall, mature NK cells are recognized as large, granular cells, which comprise 5 to 20% of peripheral blood mononuclear cells (PBMC) and represent the third largest subset of lymphocytes. Mature NK cells mainly circulate in the peripheral blood but also exist as tissue-resident cells in lymph nodes, spleen, tonsils, thymus, skin, intestine, kidneys, lungs, uterus and liver (Yokoyama *et al.*, 2013; Vivier *et al.*, 2018). The tissue-resident NK cell sub-populations are developmentally and phenotypically different from circulating NK cells.

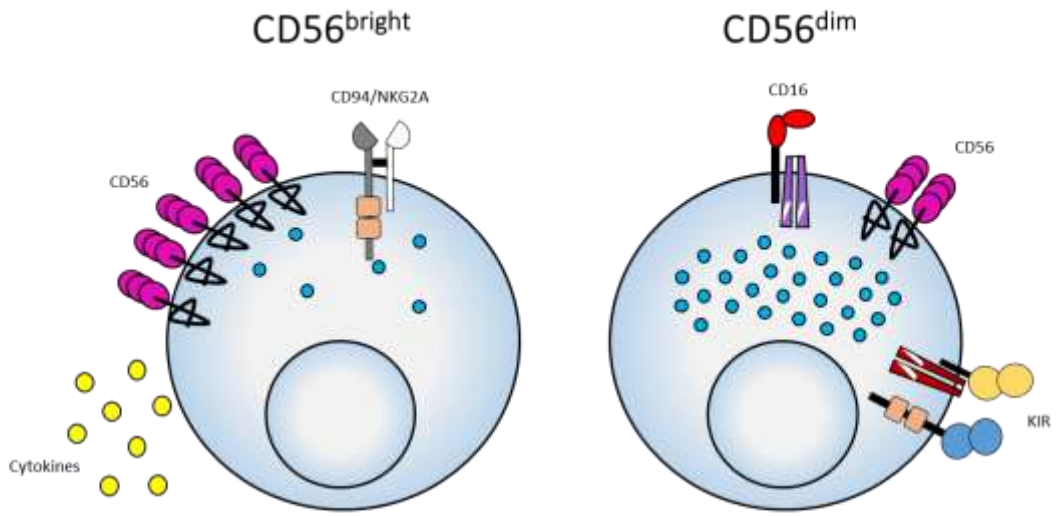

	CD56bright	CD56dim
Surface markers	CD94/NKG2A, NKp46, CD117, IL-2R, IL-1R1, IL-18R, CCR7, CXCR3, CD2, CD11c, CD44, CD49e, CD54, CD62L	KIR, CD16, CD11a, CXCR1, CX3CR1, CD57, CD160, granzimes, perforin, cytolytic granules
Localization	75-95% in secondary lymphoid organs. ~10% in peripheral blood Uterus	~90% in peripheral blood. 7-50% in spleen
Functions	Production of cytokines	Cytotoxicity, Antibody dependent cellular cytotoxicity (ADCC)
Proliferation	High proliferation in response to IL-2 and IL-21	Low responsiveness to IL-2 or IL-15

Figure 1.2 Subsets of mature NK cells. Expression of the phenotypic marker CD56 defines two subpopulations of mature NK cells that differ phenotypically and functionally: $CD56^{bright}$ and $CD56^{dim}$ NK cells. The $CD56^{bright}$ subset (left) highly express CD56 and CD94/NKG2A receptor and mainly produce cytokines. Conversely, $CD56^{dim}$ NK cells (right) have a reduced expression of CD56 and express KIR receptors and CD16. These cells have high cytotoxic activity and mediate antibody-dependent cellular cytotoxicity (ADCC).

1.1.2 NK cell education

In order to become functionally competent, NK cells undergo a maturation process termed licensing or education. NK cell education refers to the mechanism by which NK cells become tolerant to self while specifically react against non-self or altered-self. This process requires the interaction between NK cells and normal cells through a receptor/ligand system, resulting in the formation of functionally mature NK cells (Gasser and Raulet, 2006). NK cell education is a complex and controversial topic and different models explaining this mechanism have been proposed. However, they are not mutually exclusive and provide clear insights into how NK cells achieve immunological tolerance.

The **"at least one" model** proposes that NK cells must express "at least one" inhibitory NK receptor that interacts with its ligand in order to become functional. Despite this, it has been demonstrated that some NK cells may not express inhibitory receptors and yet retain tolerance; however, their functionality has shown to be reduced (Fernandez *et al.*, 2005; Raulet, 2006; Yawata *et al.*, 2008). In the **arming model** of NK cell education, it has been proposed that unlicensed NK cells are hypo-responsive whereas an "armed" or "educated" NK cell results from the engagement between an inhibitory KIR receptor and its Major Histocompatibility Complex class I (MHC-I) ligand **(Figure 1.3)**. This interaction generates an inhibitory signal that leads to the recruitment of phosphatases, which prevent NK cells from becoming activated (Raulet, 2006; Elliott and Yokoyama, 2011). Unlike the arming model, the **disarming model** suggests that uneducated NK cells are originally hyper-responsive. Lack of interaction between inhibitory KIR and MHC-I generates a chronic activating signal that leaves NK cells "disarmed" or anergic **(Figure 1.3)** (Raulet, 2006; Elliott and Yokoyama, 2011). This has been demonstrated for different activating receptors such as Ly49 in mice and KIR2DS1 and NKG2D in humans (He and Tian, 2017). Down-regulation of activating receptors as well as low responsiveness to activating ligands promote disarming of NK cells.

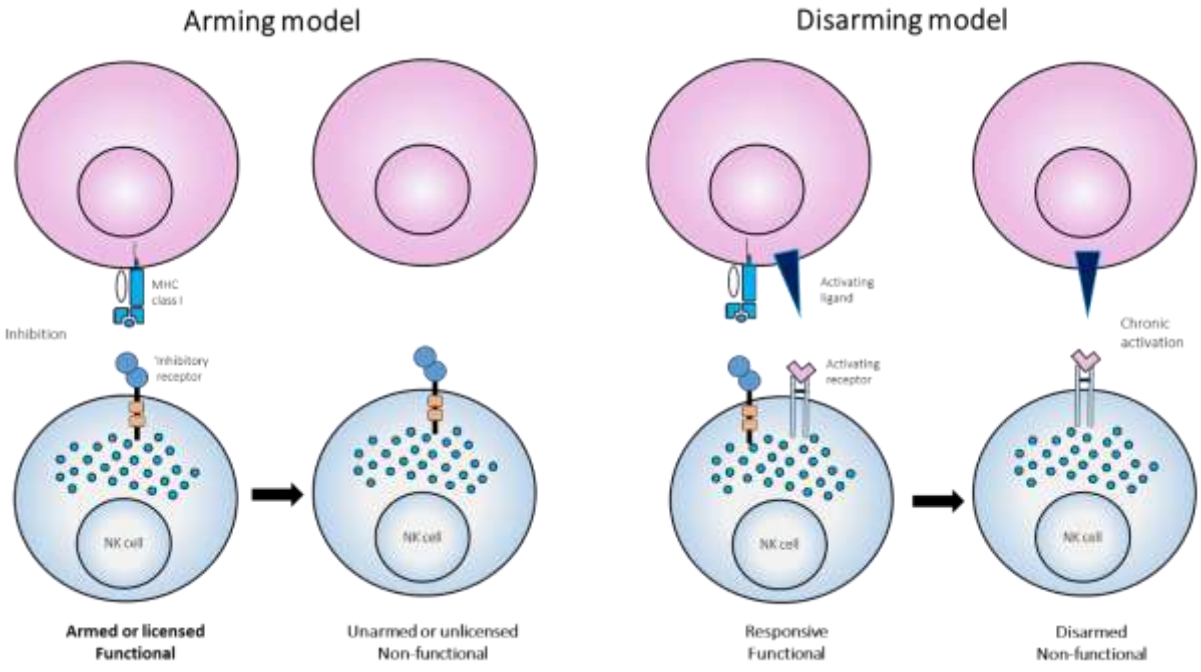

Figure 1.3 **Arming and disarming models of NK cell education**. Two of the most accepted and controversial models of NK cell education are the arming and disarming model. While the arming model base its assumptions on the generation of inhibitory signals, the disarming model proposes that activating signals are also relevant in NK cell education.

Other models of NK cell education include the **rheostat model**, which postulates that NK cell responses depend on the number of inhibitory receptors that they express as well as the strength of the inhibitory signal, which is given by the type of inhibitory receptor. In this way, a strong signal is consistent with inhibition whereas a weak signal impairs the inhibitory response (Brodin, Karre and Hoglund, 2009; Joncker *et al.*, 2009). Finally, the **confining model** refers to the physical association of inhibitory, activating and adhesion molecules at the NK cell surface, being educated NK cells the ones that display more stable contacts. It has been shown that activating receptors cluster in nano-domains on the cell membrane of educated NK cells, which does not occur on uneducated cells (Guia *et al.*, 2011; He and Tian, 2017).

There is increasing evidence showing that NK cell education also occurs through the interaction between non-classical MHC class I (e.g. HLA-E) with non-KIR inhibitory receptors (e.g. CD94/NKG2A); however it has been suggested that these interactions are only relevant in the education of foetal and peripheral NK cells (Ivarsson *et al.*, 2013; He and Tian, 2017). Interactions between other non-KIR inhibitory NK receptors and their ligands are also involved in NK cell education. For instance, interactions between 2B4:CD48, SLAMF6:SLAMF6 or TIGIT:CD155 have been shown to be sufficient for NK cells to achieve self-tolerance (Lee *et al.*, 2006; He and Tian, 2017).

Once educated, mature NK cells become functionally competent effector cells from the innate immunity with the ability to discriminate healthy from non-healthy cells. Some insights regarding NK cell functional potential have been recently provided and suggest that educated NK cells regulate the lysosomal compartment and accumulate granzyme B in order to generate strong responses against abnormal cells (Goodridge *et al.*, 2019). Although additional molecular mechanisms of NK cell education remain to be elucidated, the aforementioned models are widely accepted and continue to be a major area of NK cell research.

1.2 Functions of peripheral NK cells

The human immune system comprises a complex and organised network of molecules, cells and tissues that together provide defence mechanisms to protect the body from foreign invaders. The innate immunity is defined as the earliest line of defence against microorganisms with a genetically determined specificity whereas the adaptive system is

highly specialized and characteristically involve receptors that rearrange gene segments in order to generate molecules with an exquisite specificity for the invading pathogens, with the subsequent development of immunological memory and enhanced reactivity on repeat challenge (Janeway, Travers and M, 2001). NK cells are a fundamental component of the innate arm of the immunity against intracellular pathogens such as viruses and parasites, and are responsible for the early recognition and elimination of infected cells and for the control of the spread of the infection. NK cells have also critical roles in tumour surveillance and elimination of cancer cells. It has recently shown that NK cells are key drivers of the adaptive immune response and exhibit adaptive-like characteristics (Vivier *et al.*, 2011). The functions exerted by NK cells as part of the innate and adaptive immunity are described below.

1.2.1 Functions in innate immunity

1.2.1.1 NK cell-mediated cytotoxicity

Natural killing of infected or tumour cells occurs through two distinct mechanisms via direct cell-cell contact: release of cytotoxic granules containing granzymes and perforin, or the binding of death receptors to their ligands.

Degranulation is the main function attributed to the $CD56^{dim}$ NK cell subset. NK cells store cytolytic granules in secretory lysosomes, which mainly contain perforin, granulysin, cathepsins, lysosome-associated membrane proteins (LAMP-1, -2, -3) and granzymes A, B, H, K and M (Smyth *et al.*, 2005; de Saint Basile, Menasche and Fischer, 2010). Contact of NK cells with target cells results in the formation of an immunological synapse. Recognition of target cells triggers an increase in the cytosolic Ca^{2+} and reorganization of the cytoskeleton within NK cells, which allows lysosomes to migrate towards the synapse where they fuse with the cell membrane. Thus, perforin and granzymes are secreted into the target cell. Perforin is a pore-forming protein that, after oligomerization, binds and inserts into the target cell membrane (Topham and Hewitt, 2009; Voskoboinik, Whisstock and Trapani, 2015). Once the pore has been formed (16-22 nm approximately), granzymes, a family of small serine proteases, penetrate into the target cell. Granzymes A and B induce caspase-dependent and independent apoptosis, with granzyme B activity being much more rapid than that of granzyme A (Topham and Hewitt, 2009; Voskoboinik, Whisstock and

Trapani, 2015). In the absence of granzymes A and B, granzyme M has shown to promote target cell apoptosis (Kelly *et al.*, 2004).

Exocytosis of cytotoxic granules is a highly coordinated process that must prevent self-attack by toxic proteins. To avoid this, NK cells recycle these harmful proteins from the surface back to the cytoplasm or synthesize inhibitors that block their functions (Li *et al.*, 2010; Lopez *et al.*, 2012). It has recently been shown that reduction of LAMP-1 (CD107a) expression is associated with NK cell apoptosis, suggesting a protective role for this protein against NK self-destruction (Cohnen *et al.*, 2013). Other studies have shown that down-regulation of this protein impairs NK cell-mediated cytotoxicity, which indicates a central role for LAMP-1 in the effector functions of NK cells (Krzewski *et al.*, 2013).

The second mechanism of target cell death involves the interaction of death receptors with their ligands on NK cells. NK cells use Fas/FasL and TNF-related apoptosis-inducing ligand (TRAIL) systems in order to mediate target cell cytotoxicity. After activation, NK cells up-regulate expression of FasL and TRAIL, which engage Fas and TRAIL receptors on target cells, respectively. Such interactions trigger intracellular signalling cascades that result in the activation of the caspases cascade, DNA fragmentation and death of the target cell (Chua, Serov and Brahmi, 2004; Mirandola *et al.*, 2004).

1.2.1.2 Production of cytokines

The $CD56^{bright}$ NK cell subpopulation is characterized by their high efficiency in the production of pro-inflammatory cytokines and chemokines upon target cell recognition. Among the cytokines produced by $CD56^{bright}$ NK cells are IFNγ, TNFα, GM-CSF, IL-5, IL-10, IL-12, IL-13, IL-15 and IL-18. NK cells are the most important source of IFNγ, a cytokine that possess potent anti-viral and anti-tumour activity (Schroder *et al.*, 2004). Production of IFNγ induces expression of death receptors in target cells and activation of different immune cells such as neutrophils, macrophages, dendritic cells and T cells (Martín-Fontecha *et al.*, 2004). Activated monocytes and dendritic cells synthesise IFNα/β, IL-12, IL-15, L-18 and TNFα, which in turn, activate NK cells and promote the transcription of genes encoding pro-inflammatory cytokines, including IFNγ. This positive feedback ensures that elevated amounts of pro-inflammatory cytokines are maintained before the establishment of the adaptive immune response.

Likewise, activated NK cells produce different chemokines such as Chemokine (C-C motif) ligand 1 (CCL1;TCA3), CCL3 (Macrophage Inflammatory protein; MIP-1α), CCL4 (MIP-1β), CCL5 (Regulated on Activation, Normal T Cell Expressed and Secreted RANTES), CCL22 (Macrophage-derived Chemokine; MDC), XCL1 (X-C motif Chemokine Ligand 1; lymphotoxin) and CXCL8 (IL-8). These molecules promote the migration of neutrophils, dendritic cells, T and B cells as well as other NK cells to the sites of the infection (Robertson, 2002). It has been described that the absence of certain chemokines is associated with impaired NK effector functions, suggesting that these molecules play important roles in the induction of NK cell activation and subsequent elimination of target cells (Bernardini, Gismondi and Santoni, 2012).

1.2.2 Functions in adaptive immunity

Besides their functions as pro-inflammatory mediators, cytokines produced by NK cells act as a bridge between innate and adaptive immunity. Both, IFNγ and IL-12 promote differentiation of T CD4+ lymphocytes into Th1 helper cells. As mentioned above, a positive feedback loop maintains high levels of both cytokines in the pro-inflammatory milieu and thus, the adaptive response is directed towards a Th1 phenotype (Schroder *et al.*, 2004). Similarly, during the adaptive immune response, antibodies produced by B cells opsonize target cells through its antigen-binding fragment (Fab), leading the fragment crystallizable (Fc) region available for interaction with effector cells that express Fc receptors (Zahavi *et al.*, 2018). The $CD56^{dim}$ NK cell subpopulation express FcγRIII (CD16) and thus, recognize antibody-coated target cells leading to NK cell activation and target cell death. This phenomenon is known as Antibody-Dependent Cellular Cytotoxicity (ADCC) and is of great importance in the treatment of cancer with monoclonal antibodies (Ochoa *et al.*, 2017).

Finally, the generation of immunological memory by NK cells during the adaptive response is being increasingly recognized. After an encounter with a pathogen, some antigen-specific T and B lymphocytes become long-lived memory cells and develop the ability to mount rapid and robust responses in subsequent encounters against the same pathogen. It has been recently described that some subsets of NK cells exhibit memory responses and the molecular mechanisms behind this phenomenon have been investigated in several murine models of viral infection including murine cytomegalovirus (CMV), herpes simplex virus (HSV), influenza A virus (IAV) and human immunodeficiency virus type 1 (HIV-1) (O'Sullivan, Sun and Lanier, 2015).

In order to develop memory against viruses, NK cells follow a sequence of events that lead them to efficiently respond in a second encounter with the same antigen. First, in the *expansion stage*, activated NK cells proliferate in response to the signals received by their surface receptors and the cytokines produced by other immune cells. Second, during the *contraction stage*, most of activated NK cells undergo apoptosis and only a small subset survives. These cells enter to the *memory phase* and show antigen-specific cytotoxic responses against infected cells. They are characterized by exhibiting a more mature phenotype. Finally, during the *recall phase*, long-lived memory NK cells generate robust effector functions during a secondary infection (Sun, Beilke and Lanier, 2009; Sun *et al.*, 2011; O'Sullivan, Sun and Lanier, 2015). In humans, it has been reported that a subset of NK cells from human CMV-seropositive donors exhibit memory responses when re-exposed to CMV-infected cells (Newhook, Fudge and Grant, 2017).

1.3 Receptors of NK cells

Unlike T or B cells that undergo somatic recombination of gene segments encoding surface receptors, NK cells express a broad array of germline-encoded, non-rearranging receptors that mediate their responses against target cells. These receptors transduce negative or positive signals and the balance between them determines NK cell activation or inhibition of their effector functions **(Figure 1.4)** (Borhis and Khakoo, 2011).

1.3.1 Inhibitory NK cell receptors

Inhibitory receptors of NK cells include KIR, the CD94/NKG2A heterodimer, leukocyte immunoglobulin-like receptors (LILR), 2B4 (CD244) and killer cell lectin-like receptor subfamily G member 1 (KLRG1). These receptors signal through immune-receptor tyrosine-based inhibition motifs (ITIM) located in their cytoplasmic tails. After phosphorylation of a tyrosine residue, the ITIM recruit Src homology 2 (SH2) domain-containing protein tyrosine phosphatase (SHP) 1 and 2. These phosphatases dephosphorylate intracellular proteins leading to inhibition of the NK cell response (Billadeau and Leibson, 2002).

Ligands for inhibitory receptors are well known and mainly include molecules from the MHC-I and related proteins **(Figure 1.4)**. Inhibitory KIR interact with classical MHC-I (Human

Leukocyte Antigen; HLA-A, -B, -C) whereas inhibitory CD94/NKG2A interact with the non-classical HLA-E. CD94:NKG2A indirectly monitors expression of classical MHC-I as HLA-E presents peptides from the leader sequence of those molecules (Pegram *et al.*, 2011). LILR, specifically LILRB1 has also been shown to bind classical and non-classical MHC-I. Indeed, interaction of LILRB1 with HLA-G has shown to be relevant in preventing NK cell activation at the maternal-foetal interface (Apps *et al.*, 2007). Other inhibitory receptors such as 2B4 and KLRG1 bind non-MHC-I ligands and play roles in the maintenance of self-tolerance (McNerney, Guzior and Kumar, 2005; Ito *et al.*, 2006).

1.3.2 Activating NK cell receptors

Activating receptors of NK cells include KIR, CD94/NKG2C, CD94/NKG2E, NKG2D, 2B4, DNAX accessory molecule 1 (DNAM-1; CD226) and NCR such as NKp30, NKp44, NKp46 and NKp80. These receptors interact through a positively charged residue (lysine) with immune-receptor tyrosine-based activation motifs (ITAM)-containing accessory proteins, such as DNAX-activation protein of 12 kDa (DAP12).

Following phosphorylation of a tyrosine residue, DAP12 recruits SH2 domain-containing kinases (Spleen Tyrosine Kinase; Zyk or Zeta Chain of T cell Receptor Associated Protein Kinase; ZAP70) (Pegram *et al.*, 2011). These kinases initiate an activation cascade that includes phosphorylation of the guanine nucleotide exchange factor Vav1, which promotes reorganization of the cytoskeleton (Riteau, Barber and Long, 2003). As a result of the phosphorylation cascade, NK cells become activated and exert their cytotoxic or cytokine production functions against target cells.

Unlike inhibitory receptors, ligands for some activating receptors are poorly defined. It has been suggested that activating KIR bind classical MHC-I with the same specificity as their inhibitory counterparts (see below). The same is true for CD94/NKG2C, which binds HLA-E and whose expression has shown to be relevant in the control of human CMV infection (Gumá *et al.*, 2004). NKG2D recognizes stress ligands on target cells such as MHC class I chain-related proteins MICA, MICB and ULBP (1 to 4) **(Figure 1.4)**. This receptor recruits the accessory protein DAP10 instead DAP12 and binds PI3K to initiate the phosphorylation cascade. NKG2D along with NCR and DNAM-1 have important roles in the recognition of malignant cells (Pegram *et al.*, 2011).

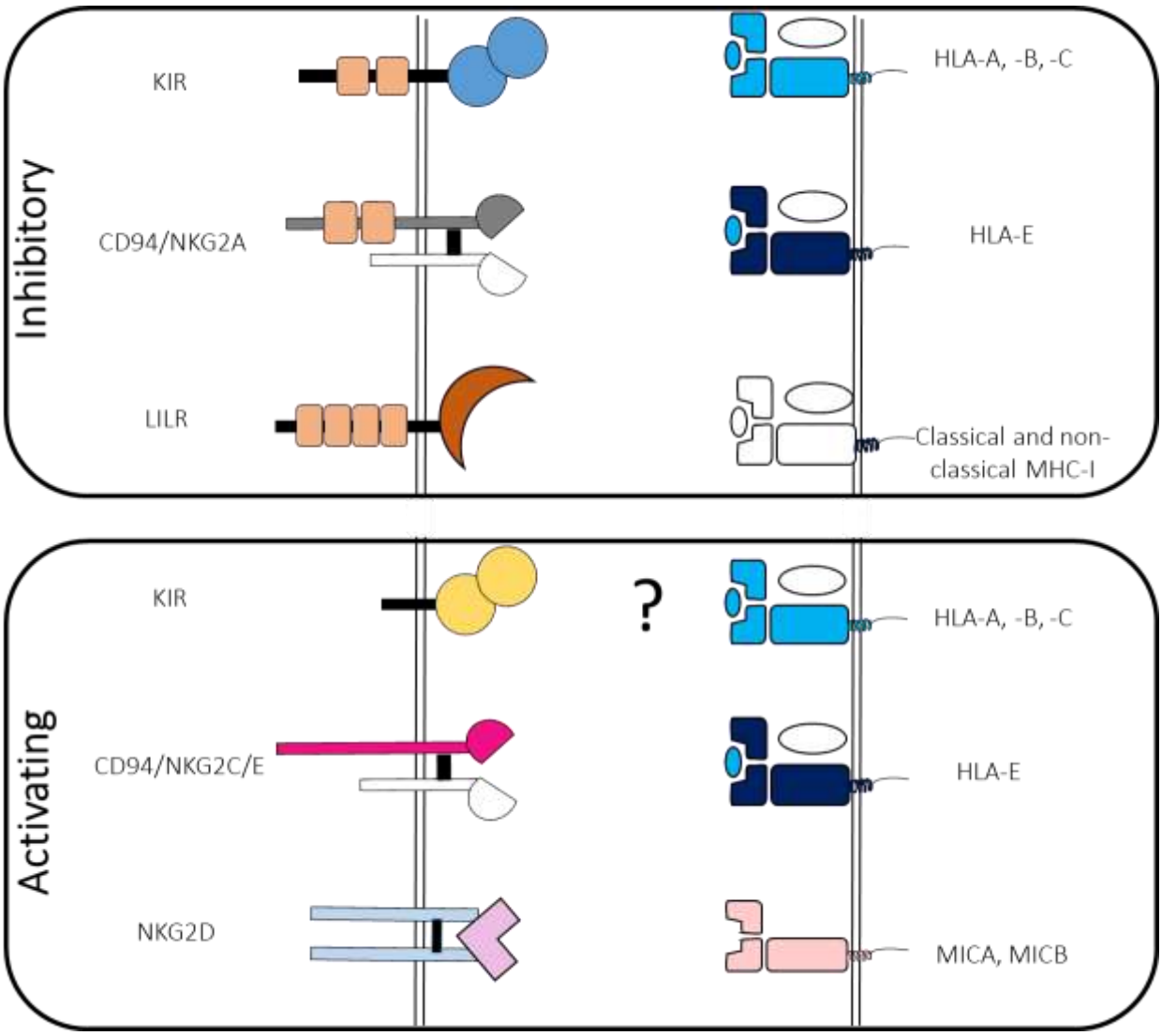

Figure 1.4 NK cell receptors for MHC class I. NK cells express a wide array of inhibitory (top) and activating receptors (bottom) whose ligands are MHC-I or MHC-I-related proteins. Ligands for activating KIR are poorly defined, however they have shown to interact with the same ligands as their inhibitory counterparts.

1.3.3 Combinatorial diversity of NK cells

One of the most striking features of NK cells is their ability to express different combinations of inhibitory and activating receptors at the cell surface. This diversity is enhanced by the expression of KIR receptors, which are one of the most polymorphic within the human genome. Horowitz et al estimated that between 6.000 and 30.000 different NK cell phenotypes are present within an individual and more than 100000 exist in a cohort of 22 individuals (Horowitz *et al.*, 2013). This enormous diversity in NK cell receptor repertoires facilitates the generation of rapid and efficient responses to a broad spectrum of pathogens.

Particularly, the combinatorial expression of MHC-I receptors (KIR and CD94/NKG2 heterodimers) is advantageous in the recognition of virus-infected cells. Both types of receptors have different evolutionary trajectories, being CD94/NKG2A highly conserved whereas KIR receptors have rapidly adapted to the environment. By working in combination, the breadth of signals received by NK cells through these receptors increases. This translates into a system exquisitely tuned to detect minimal changes in MHC-I expression that ultimately strengthen the anti-viral response (Bastidas-Legarda and Khakoo, 2018).

1.4 The family of KIR receptors

The family of KIR receptors constitute one of the most intriguing set of NK cell receptors due to their extensive polymorphism, stochastic expression and association with infectious and non-infectious diseases. These receptors transduce either inhibitory or activating signals upon engagement with their MHC-I ligands and play a fundamental role in regulating NK cell functions.

1.4.1 Structure and nomenclature of KIR receptors

Killer immunoglobulin-like receptors (KIR) are a group of 15 structurally related type 1 glycoproteins, eight of which are inhibitory (KIR2DL1, KIR2DL2, KIR2DL3, KIR2DL5A, KIR2DL5B, KIR3DL1, KIR3DL2 and KIR3DL3) and seven are activating (KIR2DS1, KIR2DS2, KIR2DS3, KIR2DL4, KIR2DS4, KIR2DS5 and KIR3DS1) (Campbell and Purdy, 2011). This family of receptors consist of extracellular, transmembrane and intracellular domains that dictate their functions and define their nomenclature **(Figure 1.5)**.

The extracellular region of KIR receptors is characterized by the presence of two or three C2 type immunoglobulin-like domains (KIR**2D** or KIR**3D**, respectively). The N-terminal domain 1 (D1) and the C-terminus domain 2 (D2) of KIR2D receptors form a hinge (66º to 81º), whose rotation alters the configuration of the ligand-binding site and therefore impacts their specificity to MHC-I ligands (Boyington, Brooks and Sun, 2001; Moesta and Parham, 2012). KIR3D receptors possess D0, D1 and D2 domains, being D1 and D2 the ones that directly contact the ligand in a similar fashion than KIR2D receptors (Vivian *et al.*, 2011). Controversy exists as to whether D0 is involved in the interaction of KIR3D receptors with

MHC-I ligands; however recent evidence suggests that D0 is an “innate HLA sensor domain” as it contacts a conserved region of the HLA molecule (Khakoo *et al.*, 2002; Sharma *et al.*, 2009; Vivian *et al.*, 2011). KIR2DL4, KIR2DL5A and KIR2DL5B lack D1 and only possess D0 and D2 domains; however, D0 seems not to be involved in the contact with MHC-I (Moradi *et al.*, 2015; Saunders *et al.*, 2015).

The transmembrane region of inhibitory and activating KIR differ inasmuch as amino acids from this domain interact with residues from intracellular proteins, thereby influencing KIR activity. Thus, inhibitory KIR possess hydrophobic residues whereas activating KIR contain a positively charged residue (lysine) available to interact with acidic amino acids from ITAM-containing adaptor proteins **(Figure 1.5)** (Campbell and Purdy, 2011). It has been described that hydrophobic amino acids in the transmembrane of a KIR2DS2 allelic variant may prevent association with DAP12 leading to a reduced activation (Bottino *et al.*, 2000; Campbell and Purdy, 2011).

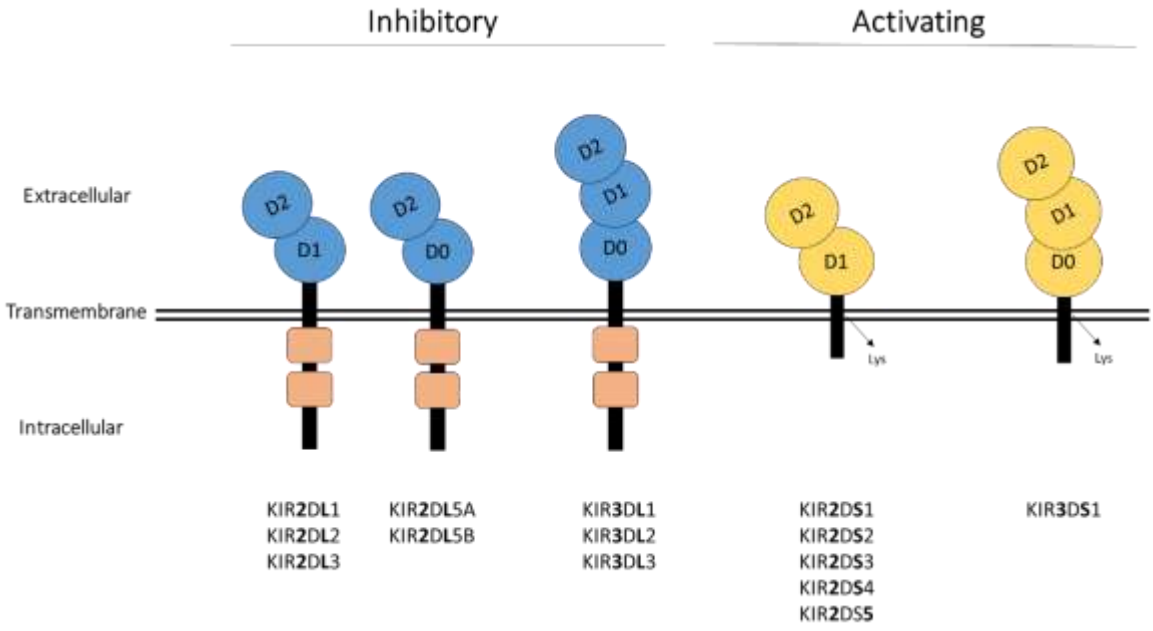

Figure 1.5 Structure of KIR receptors. The family of KIR receptors is composed by 15 receptors that transduce either inhibitory or activating signals. KIR receptors are composed of extracellular domains that interact with the MHC-I molecule, a transmembrane region and an intracellular tail, which recruits proteins to either inhibit or trigger NK cell responses. Inhibitory KIR possess a long cytoplasmic tail containing 2 ITIM whereas activating KIR have short cytoplasmic tails that interact with adaptor proteins. KIR2DL4 does not follow this classification and is not included in the figure.

Finally, the cytoplasmic tails of KIR receptors dictate the transduction of downstream inhibitory or activating signals. Inhibitory KIRs have long (L) cytoplasmic tails (KIR2D**L** or KIR3D**L**) and two ITIMs. Phosphorylation of tyrosine residues on both ITIMs results in the recruitment of SHP-1 and SHP-2 phosphatases which transduce negative signals and direct NK cells to remain quiescent. Conversely, activating receptors consist of short (S) cytoplasmic tails (KIR2D**S** or KIR3D**S**) and associate with ITAM-containing DAP-12 adaptor molecule resulting in NK cell activation (Billadeau and Leibson, 2002; Pegram *et al.*, 2011). This classification applies for all KIR with the exception of KIR2DL4, which has a long cytoplasmic tail and one ITIM, however, its functions are activating (Kikuchi-Maki, Catina and Campbell, 2005; MacFarlane and Campbell, 2006). The transmembrane region of KIR2DL4 contains one positively charged residue (arginine) that interacts with FcεRIγ chain and transduces activating signals through an endosomal compartment (Rajagopalan and Long, 2012; Moradi *et al.*, 2015).

1.4.2 Genetic diversity of KIR receptors

Genes encoding KIR receptors are located in the Leukocyte Receptor Complex (LRC), which is contained on the long arm of the chromosome 19 (19q13) and comprise a large set of genes encoding proteins with immunological functions (Carrington and Norman, 2003). The KIR locus contains 13 genes: *KIR2DL1, KIR2DL2/KIR2DL3, KIR2DL4, KIR2DL5A, KIR2DL5B, KIR2DS1, KIR2DS2, KIR2DS3, KIR2DS4, KIR2DS5, KIR3DL1/KIR3DS1, KIR3DL2, KIR3DL3* and 2 pseudogenes named *KIR2DP1* and *KIR3DP1*. Of note, *KIR3DL1* and *KIR3DS1* are alleles of the same gene (Uhrberg, Parham and Wernet, 2002; Kelley, Walter and Trowsdale, 2005; Parham, 2005; Middleton and Gonzelez, 2010). The structure of KIR genes defines an additional classification of KIR2D genes. Thus, type 1 two-domain KIR genes (*KIR2DL1, KIR2DL2/L3* and all *2DS*) contain 8 exons (1-2 and 4-9) and 1 pseudoexon encoding D0 (3), which is not incorporated into the mRNA. Conversely, type 2 two-domain KIR genes (*KIR2DL4, KIR2DL5A* and *KIR2DL5B*) contain 1 pseudoexon (3) and 7 exons (1-2 and 5-9) due to the absence of exon 4 that encodes D1. *KIR3D* genes contain the complete set of 9 exons encoding the signal sequence and the extracellular, transmembrane and cytoplasmic domains (Carrington and Norman, 2003).

As mentioned above, KIR genes do not undergo somatic recombination; however, their remarkable diversity is influenced by epigenetic regulation, gene content, copy number and variability at the allelic and haplotype level (Santourlidis *et al.*, 2002; Middleton and

Gonzelez, 2010; Rajalingam, 2011). All these factors contribute to generating different KIR repertoires on NK clones from a single individual, as well as among individuals from the same population. To date, there are reported 660 different KIR genotypes in 24950 individuals from 191 populations (Gonzalez-Galarza *et al.*, 2015). Different KIR genotypes stochastically expressed give rise to NK clones with unique phenotypes that generate diversity in the specificity of the innate response.

1.4.2.1 Haplotypic variability

The KIR genotypes are grouped into two major haplotypes: A and B. Both haplotypes contain 4 framework genes: *KIR3DL3* at the centromeric end, *KIR2DL4* and *KIR3DP1 i*n the middle and *KIR3DL2* at the telomeric end. Haplotype A contains a maximum of 9 genes including the 4 framework genes plus *KIR2DL1, KIR2DL3, KIR3DL1, KIR2DS4* and the pseudogene *KIR2DP1* **(Figure1.6)**. A total of 15 AA genotypes have been reported, with the genotype 1 (which contains the maximum number of genes) being the most frequent in Chinese (67.9%), Japanese (63.8%) and Brazilian (61%) populations (Gonzalez-Galarza *et al.*, 2015). Lack of KIR2DL4 and KIR2DS4 expression at the cell surface has also been reported, which means that some individuals homozygous for haplotype A may not express any activating receptor. Haplotype A is characterized by their high allelic variability (Middleton and Gonzelez, 2010).

Haplotype B includes a broad number of inhibitory and activating KIR **(Figure 1.6)**. To date, there are reported 645 B genotypes (AB and BB), with the genotype 2 (*KIR3DL1, KIR2DL1, KIR2DL3, KIR2DS4, KIR2DL5, KIR3DS1, KIR2DS1, KIR2DS5, KIR2DL4, KIR3DL2, KIR3DL3, KIR2DP1, KIR3DP1*) being highly frequent in populations from North and South America such as Mexico (41.5%), Brazil (36.5%) and Venezuela (26.25%). Haplotype B displays large variation in gene content rather than allelic variability. Different gene arrangements in haplotype B generate distinct KIR repertoires that enormously contribute to the combinatorial diversity of receptor expression on NK cells (Hsu *et al.*, 2002; Borhis and Khakoo, 2011; Pegram *et al.*, 2011). Evolutionary studies suggest that haplotype B is associated with reproductive success whereas haplotype A is more relevant in the control of infections. Such phenomenon has been explained by the struggle of different selective forces (infectious diseases vs reproductive) that promote either the emergence of haplotype A or B (Penman *et al.*, 2016).

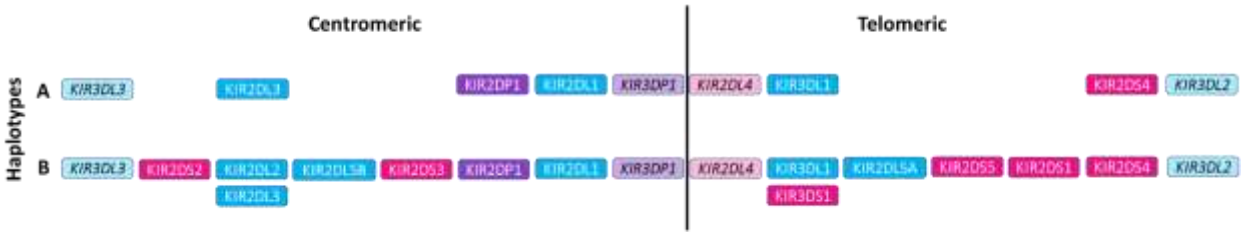

Figure 1.6 KIR haplotypes. Genes encoding KIR receptors are grouped into haplotype A or B. Different arrangements of KIR genes in both haplotypes exist, which results in the expression of unique KIR repertoires among individuals. Haplotype A is influenced by allelic diversity whereas haplotype B also has variability in gene content. *KIR3DL1/KIR3DS1* are alleles from the same gene. Inhibitory genes (blue), activating genes (pink), pseudogenes (purple), framework genes (light blue, light purple and light pink).

1.4.2.2 Allelic variability

Allelic variants of KIR genes contribute to generate KIR polymorphism. It has been reported that inhibitory KIR are the ones that have a major number of alleles compared to activating KIR. *KIR3DL3, KIR3DL2* and *KIR3DL1* genes have 164, 161 and 147 alleles, respectively (Robinson *et al.*, 2015). Conversely, *KIR2DS2* and *KIR2DS5* genes have 24 alleles each, followed by *KIR2DS1* and *KIR2DS3* with 16 alleles (Robinson *et al.*, 2015). Currently, high throughput technologies are being developed in order to detect new allele sequences that would contribute to characterize and understand the complexity of KIR allelic diversity (Norman *et al.*, 2016).

1.4.3 Frequencies of KIR receptors

Frequencies of KIR genes vary among different populations, being the ones encoding inhibitory receptors the most prevalent worldwide. Most inhibitory KIR have frequencies of 100% in several populations, except *KIR2DL2* and *KIR2DL5*. Thus, the highest frequency for *KIR2DL2* is 95.5% in Papua New Guinea followed by 80.6% in the Israel Jew population. *KIR2DL5A* and *KIR2DL5B* frequencies are relatively low compared to other inhibitory KIR, with the highest frequency being around 45% in Uruguay and Thailand for *KIR2DL5A* and the same percentage in Equatorial and Vietnamese populations for *KIR2DL5B* (Gonzalez-Galarza *et al.*, 2015).

The scenario for activating KIR genes is slightly different, as only a few populations exhibit very high gene frequencies. Thus, *KIR2DS1* and *KIR2DS2* are found in 90% of individuals in Papua New Guinea, *KIR3DS1* and *KIR2DS5* in 80 and 90% in Brazil, respectively, whereas *KIR2DS3* is present in 80% of Australians. However, this is not the case for *KIR2DL4* and *KIR2DS4* as the frequency of *KIR2DS4* is more than 90% and the one of *KIR2DL4* reaches 100% in a vast number of populations around the globe (Gonzalez-Galarza *et al.*, 2015). The differences in KIR gene frequencies are thought to be the result of evolutionary processes in which environmental factors, such as pathogens, act as a strong selective pressure driving KIR genes diversification (Brodin *et al.*, 2015; Mangino *et al.*, 2017). These selective forces favour host fitness and the preservation of heterozygosity in the populations.

1.5 KIR ligands: the major histocompatibility complex

Discovery of the MHC occurred after the observation of transplant rejection from one individual to another. In the search for cellular determinants of graft rejection, a group of genes were found to be responsible for this outcome and were named histocompatibility genes. Then, serological studies led to the identification of antibodies that reacted against antigens expressed by leukocytes. These determinants were named Human Leukocyte Antigens (HLA) and their encoding genes are clustered within a genetic locus known as the major histocompatibility complex (Abbas Abul, 2014). This group of genes are the most polymorphic within the human genome and their products are responsible for the processing and presentation of intracellular or extracellular peptide fragments at the cell surface for recognition by immune cells (Janeway, Travers and M, 2001).

1.5.1 The MHC locus

The MHC is a large genetic complex located within the short arm of the chromosome 6 (6p21.3) (Mungall *et al.*, 2003). This region harbours a broad set of immune genes including those encoding proteins with functions in antigen processing and presentation. Two groups of MHC genes are present in this locus, whose products differ in structure, expression patterns and recognition by immune cells. The *MHC class I* comprises the classical HLA-A, -B and -C genes and the non-classical HLA-E, -F -G, MHC class I polypeptide-related sequence A (MICA) and B (MICB). MHC-I are expressed on all nucleated cells and present

intracellular-derived peptides to NK cells and T CD8+ lymphocytes. The *MHC class II* (MHC-II) includes HLA-DR, -DQ and –DP, which are expressed by specialized cells (antigen-presenting cells) and present extracellular peptides to T CD4+ lymphocytes (Janeway, Travers and M, 2001).

The extensive polymorphism of MHC class I genes is mainly driven by allelic diversity. The number of reported alleles has enormously increased the last decade and was 17191 alleles by September 2019. Within classical MHC-I, HLA-B-encoding genes display the highest number of allelic variants (6537), followed by HLA-A (5266) and HLA-C (5140) (Robinson *et al.*, 2015). Thus, a heterozygous individual is equipped with 6 different classical MHC-I molecules with an exquisite specificity for self or non-self (pathogen-derived) peptides. Conversely, non-classical MHC-I present low allelic diversity, being 69 alleles for HLA-G, 44 for HLA-F and 43 for HLA-E (Robinson *et al.*, 2015). These proteins are less polymorphic and have diverse immunological and regulatory functions (Janeway, Travers and M, 2001).

1.5.2 Structure of MHC class I

Major histocompatibility complex class I molecules are transmembrane proteins composed of two polypeptide chains: α or heavy chain and β or light chain. The α chain is subdivided into α1, α2 and α3 and the β chain is known as β2-microglobulin, which is encoded in a different region of the genome (chromosome 15). β2-microglobulin interacts non-covalently with α3 whereas α1 along with α2 form a cleft or groove that serves to present small peptides derived from intracellularly processed proteins **(Figure 1.7)** (Janeway, Travers and M, 2001). Although MHC-I mainly accommodate peptides of 8 to 11 amino acids length, longer peptides can also be presented as their N- or C-terminus are able to extend from the peptide-binding groove (Pymm *et al.*, 2017). The presented peptides confer stability to the MHC-I molecule at the cell surface and therefore are considered essential elements of the MHC-I:peptide complex.

Binding of peptides to MHC-I requires the interactions between the N- and C- terminal regions of the peptide with the ends of the peptide-binding cleft. Furthermore, the side chains of specific residues of the peptide act as anchors and insert into pockets formed by amino acids in the MHC-I molecule. The peptide-binding region is therefore the most polymorphic segment within the MHC-I molecule as different combinations of amino acids

need to be accommodated into the cleft (Li and Raghavan, 2010). This diversity facilitates the presentation of a vast number of self or foreign peptides to immune cells.

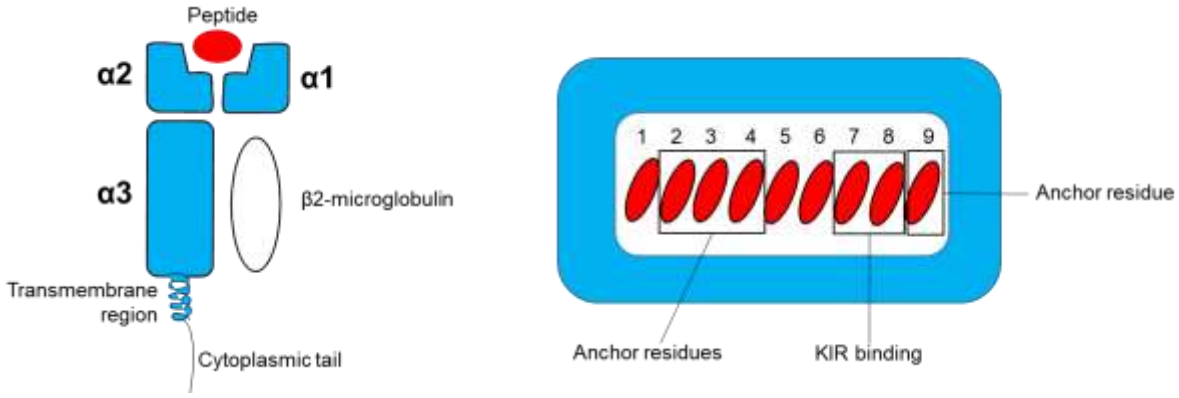

Figure 1.7 Structure of the MHC-I:peptide complex. The MHC-I molecule is composed by three α chains (α1, α2 and α3) and the β2 microglobulin subunit, which interacts with α1 and α3 (left). The peptide-binding site (right) accommodates intracellularly processed peptides from 8 to 11 amino acids length. Some amino acids act as anchor residues that interact with the MHC-I molecule whereas others dictate the affinity to KIR. A 9-mer peptide is shown.

1.5.3 Protein processing and peptide presentation

Presentation of endogenous peptides through MHC-I molecules is a mechanism of immune surveillance that allows cells to alert immune NK cells and CD8+ T lymphocytes to infections or malignant change. This process requires the processing of intracellular proteins into small peptides which are then loaded onto the MHC-I proteins. After intracellular proteins are processed by the immunoproteasome, peptides between 3 and 22 amino acids length are generated and transferred to the Endoplasmic Reticulum (ER). The Transporter-associated with Antigen Processing (TAP) is the protein responsible of such process and is also involved in the loading of the peptide onto empty class I molecules (Vukmanović *et al.*, 2001).

Peptide loading is a coordinated process performed by the peptide loading complex (PLC) that results in the generation of MHC-I:peptide complexes **(Figure 1.8)**. During this process, long peptides (more than 11 amino acids) are trimmed by ER aminopeptidase associated with antigen processing (ERAP1/2). An empty MHC-I molecule interacts with tapasin, a chaperone protein that acts as a bridge between MHC-I and TAP. Then, the peptide is released from TAP and binds to the MHC-I groove, being the high-affinity peptides the ones

that bind with the maximal strength. Finally, MHC-I:peptide complexes travel through the Golgi apparatus and reach the plasma membrane **(Figure 1.8)** (Vukmanović *et al.*, 2001; Dong *et al.*, 2009).

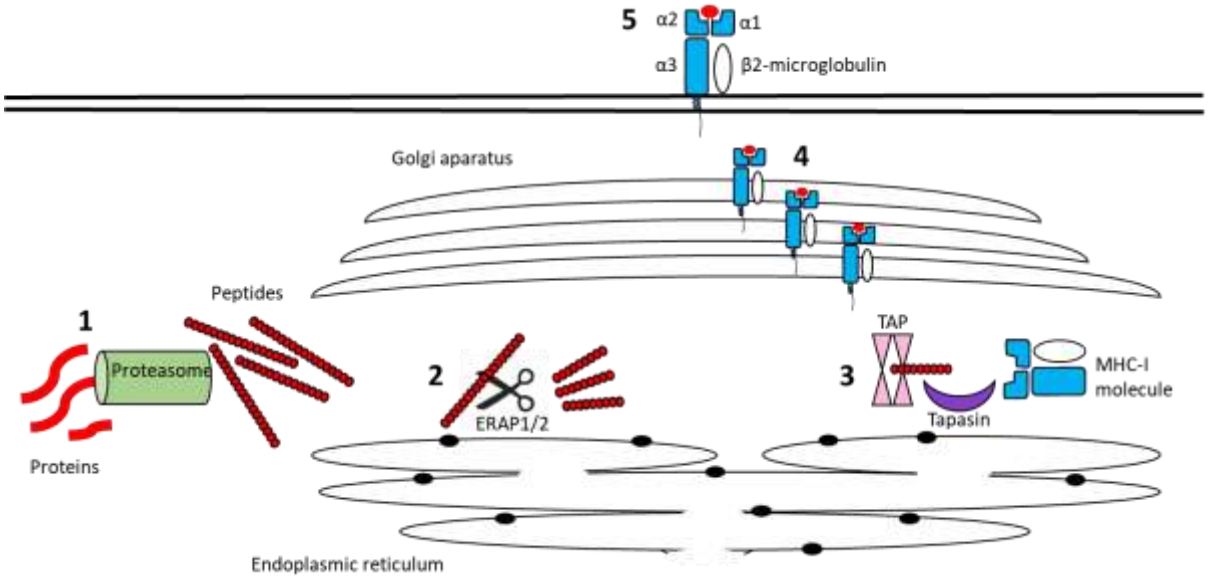

Figure 1.8 **Antigen processing and presentation.** Peptide presentation is a mechanism that allows body cells to present peptides to immune cells. **1.** Intracellular proteins are processed by the immunoproteasome in peptides of different lengths. **2.** ERAAP trim peptides in order to generate shorter peptides that can be accommodated onto MHC-I. **3.** The MHC-I molecule is loaded with peptides by a peptide loading complex comprised of TAP, tapasin and chaperones. **4.** MHC-I:peptide complexes travel through Golgi Apparatus. **5.** Finally, MHC:I:peptide complexes reach the cell surface and are available to interact with immune cells (NK and T cells).

1.6 An overview of KIR/MHC-I interactions

During the course of evolution, KIR and MHC-I loci have been under the influence of pathogen-mediated selection and evolve together despite their distant chromosomal locations. Co-evolution of KIR and MHC-I occurs through balancing selection, a mechanism that favours variability in regions involved in the interaction with the ligand and at the peptide binding site (Norman *et al.*, 2013). The result from this and other evolutionary pressures is the emergence of a vast number of different KIR/MHC-I combinations with diverse affinities and selective advantages against specific pathogens. These interactions have a major role in determining diseases outcomes.

1.6.1 KIR/MHC-I binding affinities

Interaction of inhibitory and activating KIR receptors with MHC-I ligands differ in their binding specificities and strength. Ligands for most of the inhibitory KIR are well known and include HLA-A*03 and A*11 that interact with KIR3DL2, HLA-Bw4 that is recognized by KIR3DL1 and HLA-C that binds KIR2DL1, KIR2DL2 and KIR2DL3 (Parham and Moffett, 2013). In contrast to inhibitory KIR, ligands for activating KIR are less well defined; however, it has been suggested that they have the same specificities as their inhibitory counterparts but display a reduced affinity (Stewart *et al.*, 2005b). Thus, KIR2DS1 and KIR2DS2 mainly associate with HLA-C2 and C1 alleles, respectively. KIR2DS4 has been described to interact with HLA-A11 and some HLA-C alleles whereas KIR2DL4 binds HLA-G. KIR2DS5 is thought to bind HLA-C2 alleles and KIR3DS1 recognizes HLA-Bw4^{80I} and HLA-F. (Graef *et al.*, 2009; Rajagopalan and Long, 2012; Garcia-Beltran *et al.*, 2016; Blokhuis *et al.*, 2017; Chapel *et al.*, 2017; Naiyer *et al.*, 2017; Lunemann *et al.*, 2018). Ligands for KIR2DL5, KIR3DL3 and KIR2DS3 are unknown

Binding of inhibitory KIR to HLA-C molecules differ as there are two groups of HLA-C ligands that determine binding specificity. HLA-C from group 1 (HLA-C1) contain serine at position 77 (Ser77) and asparagine at position 80 (Asn80) whereas HLA-C from group 2 (HLA-C2) contain asparagine at position 77 (Asn77) and lysine at position 80 (Lys80). In this way, KIR2DL2/KIR2DL3 recognize HLA-C1 whereas KIR2DL1 binds HLA-C2 molecules (Jamil and Khakoo, 2011). Both interactions differ in their binding strengths as it has been demonstrated that the KIR2DL3:HLA-C1 interaction is weaker than KIR2DL2:HLA-C1, and both are weaker compared to KIR2DL1:HLA-C2 (Kulkarni, Martin and Carrington, 2008; Sim *et al.*, 2017). The same is true for activating receptors as KIR2DS2 recognizes HLA-C1 and KIR2DS1 binds HLA-C2 (Stewart *et al.*, 2005a).

1.6.2 KIR/MHC-I interactions at a super-resolution level

Crystal structures of KIR have revealed the molecular determinants of KIR binding to MHC-I. To date, the crystal structures of 9 KIR have been resolved, four of which are in complex with the MHC-I molecule (Boyington *et al.*, 2000; Fan, Long and Wiley, 2001; Vivian *et al.*, 2011; Liu *et al.*, 2014). Overall, KIR contact the MHC-I molecule through amino acids from the D1 and D2 regions whereas MHC-I contacts KIR through α1 and α2 helices, respectively **(Figure 1.9)**. The electrostatic forces between these molecules involve

hydrogen bonds and salt bridges, which determine the affinity of the interaction (Moesta and Parham, 2012).

Specific KIR residues at positions 44, 45 and 71 have shown to influence binding to their ligand. Thus, KIR2DL2 has a lysine at position 44 (D1) whereas KIR2DL1 has methionine at the same position. Binding of Lys44 from KIR2DL2 to Asn80 from HLA-C1 is a key interaction that determines KIR specificity as mutation of Lys44 for Phe44 (K44F) impairs KIR binding. Likewise, Met44 from KIR2DL1 binds Lys80 from HLA-C2 and it has been shown that the point mutation Met44 for Lys44 (M44K) reverts the specificity from C2 to C1 and vice versa (Winter and Long, 1997). In addition to this, KIR2DL2 and KIR2DL3 present a phenylalanine at position 45 that, when mutated to tyrosine (F45Y), reduces the KIR/MHC-I affinity as this polar amino acid disrupts the hydrophobic interactions between both molecules. Interestingly, KIR2DS2 has a tyrosine at position 45 and the crystal structure of KIR2DS2 showed that the side chains of Tyr45 and Gln71 are displaced and this may prevent hydrogen bonds from forming **(Figure 1.9)**. These features may explain the low affinity of KIR2DS2 to HLA-C1 molecules (Boyington, Brooks and Sun, 2001; Saulquin, Gastinel and Vivier, 2003).

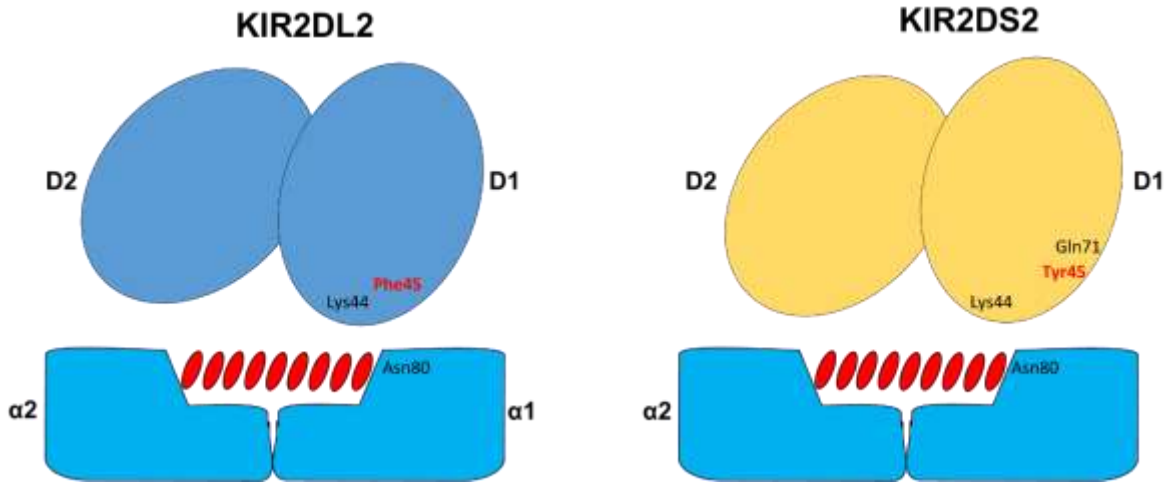

Figure 1.9 **The KIR/MHC-I:peptide interaction.** Crystal structures of KIR with their ligands have been determined and showed that the interaction of the amino acid 44 in the D1 domain of KIR with the residue 80 of the HLA-C molecule is determinant for KIR binding. Electric charge and position of residue 45 of KIR may play a role in their affinity to the HLA-C allele. Positions of key amino acids of KIR2DL2 and KIR2DS2 are shown.

1.6.3 Peptides as determinants of KIR binding to MHC-I

There is increasing evidence showing that KIR receptors bind the MHC-I molecule and additionally contact the presented peptide (Boyington, Brooks and Sun, 2001; Cassidy, Cheent and Khakoo, 2014; Das and Khakoo, 2015). The crystal structure of KIR2DL2 in complex with the HLA-C*0304 allele (C1) has shown that KIR2DL2 contacts the α1 and α2 chains of the HLA-C molecule along with the C-terminus end of the peptide. Specifically, KIR2DL2 contact amino acids at positions 7 (P7) and 8 (P8) of the bound peptide (Boyington *et al.*, 2000). Point mutations of P7 and P8 have shown to disrupt recognition by KIR, being the influence of P8 critical for such interaction (Boyington, Brooks and Sun, 2001). Overall, it has been shown that small residues at P8 promote KIR binding whereas large or negatively charged amino acids at that position abrogate KIR recognition (Boyington *et al.*, 2000; Liu *et al.*, 2014). Nevertheless, it has been described that other residues besides P7 and P8 also contribute to KIR binding (Sim *et al.*, 2017).

The MHC-I peptide repertoire has shown to be determinant in KIR binding and NK cell functions. The study conducted by Sim *et al* showed that multiple peptides favour the canonical interaction between HLA-C*0501 (C2) and KIR2DL1 whereas a smaller repertoire of peptides promote canonical binding of HLA-C*0802 (C1) to KIR2DL2/KIR2DL3, indicating that the latter interaction is more peptide selective. Cross-reactivity between HLA-C*0501 with KIR2DL2/KIR2DL3 showed high dependence on the peptide sequence and suggest that non-canonical interactions may occur in the context of specific residues. Only two residues with arginine at position 8 promoted cross-reactive binding of HLA-C*0802 to KIR2DL1 (Sim *et al.*, 2017). Thus, the contribution of the peptide sequence presented by MHC-I molecules enormously impacts recognition by KIR and the NK cell response.

Changes in the content of presented peptides have a profound effect in the strength of the association between MHC-I:peptide complexes with inhibitory KIR receptors and have repercussions in NK cell functions. Fadda *et al* studied the effect of the natural peptide VAPWNSLSL and several variants with amino acid substitutions at P7 and P8 on KIR binding and NK cell inhibition. These authors found peptides with different binding strengths to KIR2DL2 and KIR2DL3. Thus, peptides promoting a strong binding led to NK cell inhibition whereas the ones inducing a weak interaction antagonized the inhibition and triggered NK cell activation (Fadda *et al.*, 2010). Interestingly, using this same set of peptides, Cassidy *et al* found that KIR2DL3 is more sensitive to small changes in peptide content compared to KIR2DL2 (Cassidy *et al.*, 2015). This indicates that peptide repertoires

can be major determinants of KIR-mediated responses and this may have implications in disease outcomes.

1.7 Role of the KIR/MHC-I system in viral infections

Polymorphisms of genes encoding KIR receptors and MHC-I result in a wide range of possible receptor/ligand combinations. Genetic association studies have reported that some KIR/MHC-I interactions are associated with protection or susceptibility against a broad range of diseases, including pregnancy disorders, haematological malignancies, different types of cancer, autoimmune syndromes and infections (Rajagopalan and Long, 2005). Amongst infectious diseases, associations of KIR/MHC with tuberculosis, malaria, HIV-1, CMV, Herpes simplex virus (HSV), Epstein-bar virus (EBV), Ebola virus (EBOV), Hepatitis B virus (HBV), Hepatitis C virus (HCV) and Dengue virus (DENV) infections have been reported (Gonzalez-Galarza *et al.*, 2015).

1.7.1 Genetic association studies

In the context of viral infections, a large number of association studies in different worldwide populations have shown that KIR/MHC-I combinations impact the outcome of the disease (Gonzalez-Galarza *et al.*, 2015). Overall, the presence of either inhibitory or activating KIR with or without their ligands have shown to act as risk or protective factors against several infectious diseases **(Table 1.1)**. Thus, KIR/MHC-I combinations that promote NK cell inhibition render individuals more susceptible whereas those triggering NK cell reactivity have been associated with disease resistance. The mechanisms behind these associations are not completely understood; however some factors including binding strength, allelic diversity and peptide repertoire have shown to play an important role in the outcome of the infection (Kulkarni, Martin and Carrington, 2008). Some examples of KIR/MHC-I combinations that are associated with disease susceptibility in specific populations include KIR2DL3/HLA-C1 and KIR3DL1/HLA-Bw4 pairings, which are associated with HIV-1 seropositivity in African female sex workers (Jennes *et al.*, 2006). Likewise, presence of KIR3DS1/HLA-Bw4, KIR3DL1/HLA-Bw4, KIR2DL1/C2 and KIR2DS1/C2 have been positively associated with DENV infection in a Brazilian population (Beltrame *et al.*, 2013).

Table 1.1 Disease associations of the KIR/MHC-I system

Contribution	Viral infection	KIR/MHC-I	Population	Reference
Risk factor	Cytomegalovirus	Homozygosity for haplotype A and HLA-Bw4	Italian	(Di Bona *et al.*, 2014)
	Dengue virus	KIR3DL1	Indian	(Alagarasu *et al.*, 2015)
		KIR3DS1:HLA-Bw4, KIR3DL1: HLA-Bw4, KIR2DL1-HLA-C2 and KIR2DS1:HLA-C2	Brazilian	(Beltrame *et al.*, 2013)
	Epstein-Barr virus	KIR2DS5	Chinese	(Qiang *et al.*, 2012)
	Hepatitis C virus	KIR2DL2 and KIR2DS2	Polish	(Kusnierczyk *et al.*, 2015)
	Human immunodeficiency virus	KIR2DL3:HLA-C1 and KIR3DL1:HLA-Bw4	Ivorian	(Jennes *et al.*, 2006)
	Human papillomavirus	KIR2DL2:HLA-C1 and KIR2DL3:HLA-C1	Italian	(Rizzo *et al.*, 2014)
		KIR3DS1	Multicentric	(Carrington *et al.*, 2005)
	Ebolavirus	KIR2DS1 and KIR2DS3	Gabonese	(Wauquier *et al.*, 2010)
Protective factor	Dengue virus	KIR2DL3:HLA-C1:C1 and haplotype AA	Brazilian	(Beltrame *et al.*, 2013)
	Hepatitis B virus	KIR2DL1:HLA-C2	Dutch	(Stelma *et al.*, 2016)
	Hepatitis C virus	KIR2DL3:HLA-C1	British	(Khakoo *et al.*, 2004; Knapp *et al.*, 2010)
		KIR2DS2 without KIR2DS5	Polish	(Kusnierczyk *et al.*, 2015)
	Herpes simplex virus type 1	KIR2DL2 and KIR2DS2	Spanish	(Estefania *et al.*, 2007)
	Human immunodeficiency virus	KIR3DS1:HLA-Bw4:HLA-Bw4 and KIR2DL3	Chinese	(Wang *et al.*, 2018)
		KIR3D:HLA:Bw4	Mexican	(Hernandez-Ramirez *et al.*, 2015)
		KIR2DL2 and KIR2DL3 without HLA-C1 and KIR3DL1 without HLA-Bw4	Ivorian	(Jennes *et al.*, 2006)
	Human papillomavirus	KIR3DS1 and KIR2DS1	American	(Bonagura *et al.*, 2010)
	Ebolavirus	Haplotype AA	Gabonese	(Wauquier *et al.*, 2010)

Conversely, other KIR/MHC-I interactions have shown to be protective factors as they are associated with resolution of infections. In this regard, interaction of KIR3DS1 with HLA-Bw4 showed to confer protection against HIV-1 infection in a Chinese population (Martin *et al.*, 2018; Wang *et al.*, 2018). Likewise, homozygosity for KIR2DL3 and HLA-C1 is a protective factor for HCV and is associated with clearance of the virus in Caucasian and African Americans individuals. Such protection was not evident in individuals carrying one or two copies of the KIR2DL2 gene (Khakoo *et al.*, 2004). Despite KIR2DL2 and KIR2DL3 segregate as alleles of the same gene and share high sequence homology, the KIR2DL2 interaction with its ligand displays higher affinity compared to that of KIR2DL3. Therefore, a weaker inhibitory KIR/MHC-I interaction promotes NK cell activity and is consistent with a protective effect in HCV infection (Khakoo *et al.*, 2004).

The presence of specific haplotypes has also been shown to impact the course of viral infections. Thus, haplotype A in an Italian population has been associated with susceptibility to symptomatic CMV infection. In contrast, homozygosity for haplotype A has shown to be protective against DENV infection in a population from southern Brazil and against EBOV infection in a Gabonese cohort (Wauquier *et al.*, 2010; Beltrame *et al.*, 2013; Di Bona *et al.*, 2014). Overall, these disease association studies demonstrate that selective pressures imposed by pathogens on different populations around the world have driven evolution of these polymorphic genes. More studies are needed in order to elucidate the molecular mechanisms behind the protection associated with KIR/MHC-I that could be exploited in the selection of anti-viral strategies for individuals from specific populations.

1.8 Recognition of virus-infected cells and NK cell activation mechanisms

Several studies have highlighted the role of viruses as a major selective force on the human innate system (Prugnolle *et al.*, 2005; Enard *et al.*, 2016). The mechanisms that NK cells have evolved to scan and discriminate normal from virus-infected cells involve the interaction of inhibitory or activating receptors with their ligands. In health, engagement of inhibitory KIR with MHC-I results in the inhibition of NK cell functions **(Figure 1.10)** (Raulet, 2006). However, during viral infections, these interactions may be disrupted as a result of down-regulation or absence of MHC-I on the cell surface. Additionally, virally-infected cells may present peptides associated with cell stress or derived from viral proteins. These scenarios induce activation of NK cells through different mechanisms explained below.

1.8.1 The missing-self hypothesis

The immune defence mechanisms employed by NK cells to fight viruses operate as a selective antagonistic force against these pathogens. Viruses respond to such pressure by generating opposing responses to escape from the host attack (Miletić, Krmpotić and Jonjić, 2013). One of the main cellular processes targeted by viruses to avoid immune recognition is the processing and presentation of viral peptides, which results in down-modulation of surface MHC-I. Some of these strategies include the restriction of viral protein access into proteasome (Gilbert *et al.*, 1996; Dantuma, Sharipo and Masucci, 2002), blocking the active site of TAP (Früh *et al.*, 1995; Hewitt, 2003), retention of MHC- I heavy chains (Jones *et al.*, 1996; Ahn *et al.*, 1997; Abendroth *et al.*, 2001) and protein degradation (Wiertz *et al.*, 1996; Hudson, Howley and Ploegh, 2001).

The missing-self hypothesis states that loss of expression of NK cell ligands induces activation of NK cells. Down-regulation of MHC-I induced by viruses prevents them from being recognized by CD8+ T lymphocytes; however, this escape mechanism leads infected cells susceptible to NK cell attack through missing-self. Hence, inhibitory KIR fail to engage MHC-I and this prevents cells to generate an inhibitory signal. Lack of an inhibitory signal within NK cells results in a dominant activating response leading to NK cell cytotoxicity or cytokine production **(Figure 1.10)** (Raulet, 2006).

1.8.2 Induced-self mechanism

The induced-self mechanism refers to the activation of NK cells after activating receptors recognize induced ligands on target cells. These ligands are self-molecules that may be up-regulated during pathological processes and are associated with cell damage or stress **(Figure 1.10)** (Orr and Lanier, 2010). This mechanism is well described for the activating receptor NKG2D and its ligands Rae1 and MIC (Diefenbach *et al.*, 2001).

Additionally, viruses may induce changes in the peptide repertoire presented by MHC-I. The set of presented peptides are derived from cellular proteins involved in signalling pathways initiated in response to viral infections. This has been demonstrated for Vaccinia Virus (VACV), IAV and HIV-1 infections using proteomic analysis (Hickman *et al.*, 2003; Wahl *et al.*, 2009; Spencer *et al.*, 2015). Particularly, the study conducted by Spencer *et al* showed

that peptides derived from type I interferon-inducible genes are largely presented after infection of HeLa cells with VACV (Spencer *et al.*, 2015). These changes in the peptide repertoire allow target cells to be more susceptible for NK cell recognition through activating receptors (Fadda *et al.*, 2010; Das and Khakoo, 2015).

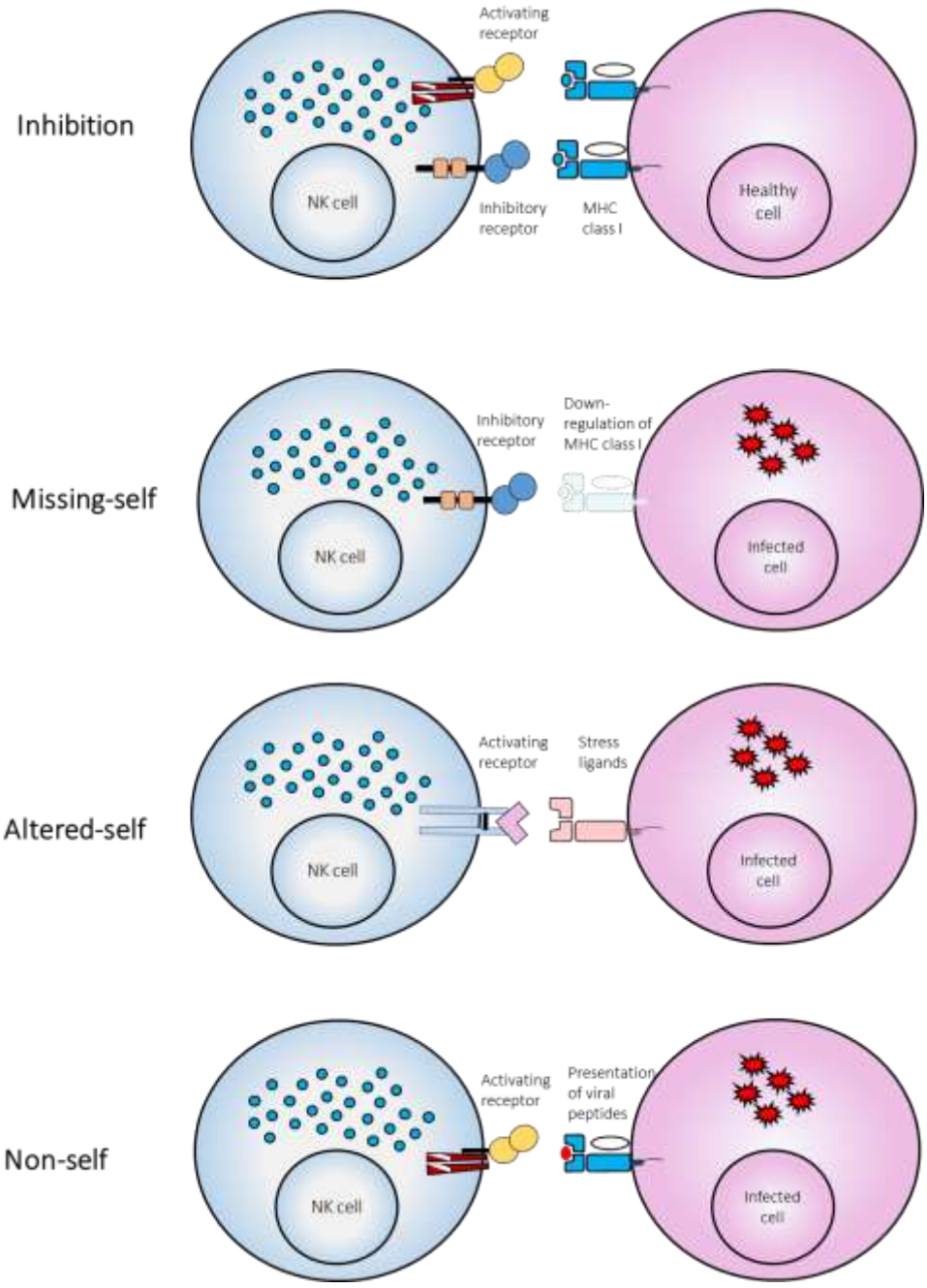

Figure 1.10 Mechanisms of NK cell inhibition and activation. The balance between inhibitory and activating signals within NK cells modulate their effector functions. The inhibitory signal predominates over the activating signal after an inhibitory KIR binds its MHC-I ligand. Disruption of the inhibitory signal due to missing expression of MHC-I results in a dominant activating signal that leads NK cell to perform their functions against target cells. Activating receptors also mediate NK cell responses through the interaction with altered ligands expressed on the surface of stressed cells or non-self ligands when recognizing viral peptides bound to MHC-I.

1.8.3 Non-self recognition

Processing of viral proteins by the immunoproteasome generates viral peptides that are loaded onto MHC-I proteins and therefore are exposed on the surface of infected cells. Viral peptides may be predominantly presented by MHC-I as was demonstrated for the measles-derived peptide KLWESPQEI bound to HLA-A*0201 (Schellens *et al.*, 2015). However, presentation of viral peptides by infected cells may have contrasting effects on NK cell recognition as they may induce either inhibitory or activating responses (Nattermann *et al.*, 2005; O'Connor *et al.*, 2006; Lunemann *et al.*, 2016; Naiyer *et al.*, 2017).

Viruses and NK cells have been in a constant evolutionary battle (Miletić, Krmpotić and Jonjić, 2013). In order to counteract NK cell recognition through missing-self, viruses encode peptides that bind inhibitory KIR, thus preventing NK cell recognition and activation. Presentation of inhibitory peptides that strongly engage inhibitory KIR has been well documented, particularly for HIV-1 **(Table 1.2)**. The effect of these peptides on NK cells is the inhibition of their effector functions. In this way, viruses are capable of evading immune detection by two mechanisms: CD8 T cells (through MHC-I down-regulation) and NK cells (through presentation of inhibitory peptides).

Nevertheless, some studies have demonstrated that certain viral peptides presented in the context of MHC-I may act as ligands for activating KIR, thereby promoting NK cell activation **(Table 1.2; Figure 1.10)**. Using KIR3DS1-CD3ζ Jurkat cell lines, O'Connor *et al* found two HIV-1-derived peptides that bind HLA-B*5701 and are recognized by KIR3DS1 (O'Connor *et al.*, 2015). However, the most compelling evidence showing functional peptide-mediated activation through activating KIR comes from the study conducted by Naiyer *et al*. These authors found three peptides encompassing all human pathogenic Flaviviruses and one HCV-derived peptide that are presented in the context of HLA-C*0102 and engage KIR2DS2 leading to strong NK cell responses (Naiyer *et al.*, 2017). Results from this work are promising as peptide-induced activation of NK cells may be exploited as a therapeutic approach against Flaviviral infections.

.

Table 1.2 Influence of MHC-I:viral peptide complexes on NK cell responses

Virus	MHC-I:peptide complex	KIR	Response	Reference
Dengue virus/ Zika virus	HLA-C*0102:IVDLMCHATF	KIR2DS2	Activation	(Naiyer *et al.*, 2017)
Cytomegalovirus	HLA-A*2402:QVDPVAALF	KIR3DL1	Inhibition	(Thananchai *et al.*, 2007)
Influenza virus	HLA-B*2705:SRYWAIRTR	KIR3DL1	Inhibition	(Stewart-Jones *et al.*, 2005)
Hepatitis C virus	HLA-C*0102:LNPSVAATL	KIR2DS2	Activation	(Naiyer *et al.*, 2017)
	HLA-C*0304:YIPLVGAPL	KIR2DL3	Inhibition	(Lunemann *et al.*, 2016)
Epstein-Barr Virus	HLA-A*0301:RLRAEAQVK	KIR3DL2	Inhibition	(Hansasuta *et al.*, 2004)
	HLA-A*1101:RLRAEAQVK	KIR3DL2	Inhibition	(Hansasuta *et al.*, 2004)
Human immunodeficiency virus	HLA-A*2402:KYKLKHIVW	KIR3DL1	Inhibition	(Thananchai *et al.*, 2007)
	HLA-A*2402:RYPLTFGW	KIR3DL1	Inhibition	(Thananchai *et al.*, 2007)
	HLA-B*2705:KRWIILGLNK	KIR3DL1	Inhibition	(Stewart-Jones *et al.*, 2005)
	HLA-B*5701:TSTLQEQIGW	KIR3DL1	Inhibition	(Fadda *et al.*, 2011)
	HLA-B*5701:ISPRTLNAW	KIR3DL1	Inhibition	(Fadda *et al.*, 2011)
	HLA-B*5701: AAVKAACWW	KIR3DS1	Activation	(O'Connor *et al.*, 2015)
	HLA-B*5701:KAAFDLSFF	KIR3DS1	Activation	(O'Connor *et al.*, 2015)
	HLA-B*5703:KAFSPEVIPMF	KIR3DL1	Inhibition	(Thananchai *et al.*, 2007)
	HLA-B*5703:KGFNPEVIPMF	KIR3DL1	Inhibition	(Thananchai *et al.*, 2007)
	HLA-C*0102:AAEWDRLHPV	KIR2DL2	Inhibition	(Fadda *et al.*, 2012)
	HLA-C*0304:YVDRFFKVL	KIR2DL3	Inhibition	(Holzemer *et al.*, 2015)
	HLA-C*0304:VHQAISPRTL	KIR2DL2, KIR2DL3	Inhibition	(van Teijlingen *et al.*, 2014)
	HLA-C*0304:KAFSPEVIPM	KIR2DL2, KIR2DL3	Inhibition	(van Teijlingen *et al.*, 2014)
	HLA-C*0304:DYVDRFFKTL	KIR2DL2, KIR2DL3	Inhibition	(van Teijlingen *et al.*, 2014)
Synthetic peptide	HLA-C*0602:SRGPVHHLL	KIR2DS1	Activation	(Chapel *et al.*, 2017)

1.9 Study of NK cell responses to viruses from the family *Flaviviridae*

1.9.1 The family *Flaviviridae*

The *Flaviviridae* are a family of positive-sense, single strand RNA viruses that comprise more than 60 members grouped into 4 genus: *Pestivirus*, *Pegivirus*, *Hepacivirus* and *Flavivirus*. Structurally, these viruses are lipid-enveloped (40-60 nm) and enclose an icosahedral nucleocapsid that surrounds the viral genome. The viral RNA contains a single open reading frame flanked by 5′ and 3′ terminal non-coding regions. Viral replication occurs in the cytoplasm where the genomic RNA serves as mRNA for the translation of a long polyprotein that is cleaved co- and post-translationally by cellular and viral proteases into structural and non-structural (NS) proteins. Structural proteins compose the viral particle whereas non-structural proteins perform different functions including viral assembly (NS2), serine protease and helicase activities (NS3 and NS4A) and RNA replication (NS5), ensuring the formation of new virions with the ability to propagate and cause disease (Simmonds *et al.*, 2017).

Viruses from *Hepacivirus* and *Flavivirus* mainly infect humans and the diseases caused by these pathogens are considered major public health issues. The most representative, medically important pathogen from the genus *Hepacivirus* is HCV whereas, from the genus *Flavivirus* is DENV, with half of the world's population being at risk of becoming infected (WHO, 2019b). Other Flaviviruses associated with human disease include Zika Virus (ZIKV), Yellow Fever Virus (YFV), West Nile Virus (WNV), Japanese Encephalitis Virus (JEV), Tick-borne Encephalitis Virus (TBEV), Louping-ill Virus (LIV), Omsk Hemorrrhagic Fever Virus (KFDV) and Powassan Encephalitis Virus (POWV) (Holbrook, 2017)

1.9.1.1 Hepatitis C Virus

Hepatitis C virus (HCV) is a hepatotropic virus that causes liver disease and is associated with the development of hepatocellular carcinoma (HCC). Transmission of HCV occurs via percutaneous contact with blood from an infected patient (WHO, 2016). Once the virus reaches the liver, envelope proteins bind cellular receptors on hepatocytes. Once

internalized, the nucleocapsid releases the viral RNA in the cytoplasm that is translated into a polyprotein cleaved into 10 individual proteins: core (C), envelope (E1 and E2), Viroporin (p7), NS2, NS3, NS4A, NS4B, NS5A and NS5B. As the viral RNA polymerase (NS5B) has no proofreading properties, nucleotide sequences among viruses are not identical. Hence, 11 HCV genotypes have been described. Genotypes 1 to 6 are the most common and are distinctively geographically distributed, with the genotype 1 being the most prevalent worldwide, followed by genotypes 3, 2 and 4 (WHO, 2016).

More than 170 million people have become infected with HCV, which constitutes an important public health issue worldwide (Petruzziello *et al.*, 2016). Individuals who develop acute HCV infection (15-45%) are usually asymptomatic and viral clearance can occur spontaneously. However, most of infected patients (55-85%) fail to eliminate the virus and establish a chronic disease, which may progress to liver fibrosis, cirrhosis and HCC. Other complications besides hepatic manifestations have also been described and include glomerulonephritis, thyroiditis, insulin resistance and diabetes (Guidotti and Chisari, 2006). The current treatment for chronic hepatitis C consists of the use of direct-acting anti-virals (DAA), which can now effectively cure HCV. To date, there is still no vaccine available for hepatitis C, therefore HCV infection continues to be an important public health issue in some regions around the world (WHO, 2016;2017).

1.9.1.2 Flaviviruses

Flavivirus is a genus of viruses that is divided according to their arthropod vectors into tick-borne or mosquito-borne viruses. Similar to HCV, binding of *Flaviviruses* to target cells requires the interaction of the envelope viral protein with cell surface receptors. Once the virus enters the cell, the RNA is translated into a polyprotein that is cleaved into capsid (C), membrane (M), envelope (E), NS1, NS2A, NS2B, NS3, NS4A, NS4B and NS5. Despite their similarity in genome structure and organization, *Flaviviruses* have profound differences in pathogenesis and tissue tropism. Overall, infections by tick-borne viruses (e.g TBEV, LIV, Omsk hemorrhagic fever OHFV, POWV) are mostly associated with neurological symptoms whereas mosquito-borne viruses (e.g DENV, ZIKV, YFV, WNV and JEV) have a broad tropism and mainly cause fever, haemorrhage as well as neurologic manifestations (Holbrook, 2017).

Among tick-borne *Flaviviruses* that infect humans, TBEV is one of the most neuropathogenic, causing more than 10000 infections annually in endemic areas of Europe

and Asia (Grabowski and Hill, 2017). Mosquito-borne viruses mainly circulate in tropical and subtropical areas around the world, being the infection by DENV (serotypes 1 to 4) one of the most important public health concerns, as around half of the world's population is currently at risk of infection. Besides, the incidence of this disease has expanded geographically due to the spreading of the mosquitoes *Aedes aegypti* and *Aedes albopictus* to more countries during the last decades (WHO, 2009; Holbrook, 2017). Other *Flaviviral* infections of global concern include ZIKV, whose recent outbreak in 2015 caused an increase in congenital neurological disorders and microcephaly in newborns (Lowe *et al.*, 2018) and WNV, which was introduced to United States in 1999 and has caused severe neurological disorders in different regions of America (Chancey *et al.*, 2015).

Individuals living in endemic areas are exposed to other circulating *Flaviviruses*, and this scenario increases the risk of developing a severe disease (Castanha *et al.*, 2017). As this group of viruses represent a high risk of morbidity and mortality in endemic regions and low-income countries, it is imperative to develop therapeutic strategies aimed to prevent or to treat *Flaviviruses*-caused infections. Many efforts have been made to develop vaccines against these viruses. The live-attenuated YFV 17D vaccine was developed in 1930 and has shown high effectivity and safety; however infection by YFV is still present in some regions of Brazil, where >700 cases were reported in 2018 (WHO, 2018b). The live-attenuated CYD-TDV dengue vaccine (Dengvaxia®) targeting the 4 serotypes of DENV is being used in highly endemic areas. This vaccine has shown to be safe and efficacious in individuals with history of a previous encounter with DENV; however individuals seronegative for DENV before vaccination have shown to be at a higher risk to develop severe forms of the disease (WHO, 2018a).

1.9.2 NK cell responses to *Flaviviridae*

As NK cells constitute the first line of cellular defence against viruses, their role in infections caused by members of the family *Flaviviridae* is being extensively studied. Although NK cells have shown to induce strong responses against these viruses *in vitro* and *in vivo*, different mechanisms have led to the impairment of NK cell functions, which allow these viruses to spread and cause disease.

The exact role of NK cells against HCV is not well understood. Although it has been described that NK cells may efficiently reduce HCV replication through over-expression of

activating receptors (Krämer *et al.*, 2012), several authors have found that NK cell functional responses are diminished during HCV infection. Thus, direct contact of NK cells with HCV-infected hepatocytes has shown to reduce their cytotoxic and cytokine production capacity; such functional alterations have also been associated with the impairment of the type I IFN signalling pathway or low cytokine activation (Miyagi *et al.*, 2010; Yoon *et al.*, 2011; Lunemann *et al.*, 2014; Serti *et al.*, 2014). Phenotypic changes of NK cells, including reduced diversity of surface receptors or down-regulation of activating NKp30 or NKG2D, have also been described (Holder *et al.*, 2013; Strunz *et al.*, 2018). These alterations in the NK receptor repertoire may result in a reduced activating signalling, leading to virus persistence and the establishment of a chronic infection.

In the context of Flaviviral infections, the relevance of NK cells against DENV (Petitdemange *et al.*, 2016; Costa *et al.*, 2017), WNV (Strauss-Albee *et al.*, 2015), JEV (Larena, Regner and Lobigs, 2013), YFV (Marquardt *et al.*, 2015) and TBEV (Blom *et al.*, 2016) has been demonstrated. Particularly, in the case of DENV infection, it has been shown that IFN type I is increased in dengue-infected individuals and suggest a major role for this cytokine in the activation of NK cells during the early stage of the disease (Becquart *et al.*, 2010). Similarly, the NK cell phenotype has shown to be modified during the febrile stage in a mouse model of dengue infection as well as in infected patients, suggesting that these cells are essential players in dengue pathogenesis (Shresta *et al.*, 2004; Keawvichit *et al.*, 2018).

A cellular mechanism that has been targeted by HCV and Flaviviruses aiming to overcome the NK cell response is the antigen processing and presentation pathway. On one hand HCV has shown to modulate MHC-I; however contrasting results suggesting up or down-regulation of surface MHC-I molecules have been reported, which makes the specific role of this virus in the expression of MHC-I and its impact in NK cell recognition unclear (Herzer *et al.*, 2003; Tardif and Siddiqui, 2003; Kang *et al.*, 2014). In contrast, the up-regulation of MHC-I by Flaviviruses has been well documented and suggests an evasion strategy developed by these viruses to avoid NK cell recognition by promoting interactions with inhibitory receptors (Lobigs, Mullbacher and Regner, 2003; Ye *et al.*, 2013; McKechnie *et al.*, 2019). In this regard, it has been described that a DENV NS1-derived peptide presented by HLA-B*57 strongly binds inhibitory KIR3DL1, thus preventing NK cell activation (Townsley *et al.*, 2016). Similarly, ZIKV-infected cells have been shown to up-regulate MHC-I and promote binding to inhibitory KIR2DL2 and LILRB1 (Glasner *et al.*, 2017). Thus, identifying mechanisms that could overcome inhibition and enhance NK cell activation against these pathogens becomes a necessity in order to find therapeutic alternatives for Flaviviral infections.

1.9.3 Current research on NK cell responses to *Flaviviridae* through the KIR/MHC-I system

The extensive polymorphism found in genes encoding KIR and MHC-I molecules results in the expression of an exceptional receptor/ligand system able to discriminate self from virus-derived peptides. Recently, the study conducted by Naiyer *et al* described that the specific interaction between an activating KIR (KIR2DS2) and *Flaviviridae*-derived peptides complexed with the HLA-C*0102 allele triggered robust cytotoxic NK cell responses against target cells (Naiyer *et al.*, 2017). The main findings from this study are summarized in the following paragraphs:

The HCV peptide LNPSVAATL is a 9-mer peptide found in the RNA helicase domain of NS3 and is conserved among HCV genotypes sharing 100% sequence identity. The only exception is genotype 5, whose sequence presents a phenylalanine replacing a leucine at P9 (LNPSVAATF). Exogenous loading of this peptide stabilized the HLA-C*0102 allele at the cell surface of TAP-deficient 721.174 cells and this complex was recognized by KIR2DS2 tetramers. Using a HCV replicon system and KIR2DS2-expressing NKL cells, these authors found that endogenous presentation of LNPSVAATL peptide in the context of HLA-C*0102 triggered KIR2DS2-mediated activation that resulted in NK cell cytotoxicity and inhibition of HCV replication. This response was specific for LNPSVAATL peptide as mutation of leucine for an aspartic acid at position 9 (L9D) abrogated such inhibition.

Similarly, the IVDLMCHATF peptide is found in the RNA helicase domain of NS3 from DENV and ZIKV. This peptide contains the “MCHAT” motif, which is highly conserved among *Flaviviruses* (61 out of 63). Exogenously loaded peptides carrying the “MCHAT” motif from DENV/ZIKV (IVDLMCHATF), YFV (VIDAMCHATL) and WNV/JEV (IVDVMCHATL) in complex with HLA-C*0102 were recognized by three KIR2DS2 allelic variants (KIR2DS2*001, KIR2DS2*007 and KIR2DS2*008), being the HLA-C*0102:IVDLMCHATF complex the one that showed the strongest binding. Functional assays using a dengue replicon system and KIR2DS2-expressing NKL cells showed that engagement of KIR2DS2 to IVDLMCHATF bound to HLA-C*0102 promoted NK cell cytotoxic functions. The results from this study indicate that the “AT” motif found in LNPSVAATL and *Flaviviral* peptides is determinant for KIR2DS2 binding. In addition, the robust NK cell responses mediated through KIR2DS2 against target cells expressing *Flaviviridae*-derived peptides bound to HLA-C*0102, could be a protective factor against

HCV and *Flaviviral* infections. Consequently, peptide-induced NK cell activation may be exploited as an anti-viral therapeutic approach.

1.10 Hypothesis and aims

The relevance of the KIR/MHC-I system in the outcome of viral infections is supported by strong scientific evidence. Understanding the mechanisms that allow viruses to modulate these interactions would help us to identify determinants that could promote potent NK cell responses against target cells. Therefore, this thesis aimed to study the NK cell response to *Flaviviridae* through the KIR/MHC-I system, with a particular emphasis on HLA-C allelic diversity and viral peptides.

The present study is based under two hypotheses: 1) HCV modulates expression of HLA-C alleles and impacts KIR2DL2/L3/S2-mediated NK cell activity, and 2) *Flaviviridae*-derived peptides presented in the context of different HLA-C allelic variants bind activating KIR2DS2 and trigger robust NK cell responses. The objectives of this study are presented as follows:

- To investigate the effect of HCV replication in the modulation of HLA-C expression and its impact in NK cell recognition through KIR2DL2/L3/S2 receptors.

- To determine the role of LNPSVAATL peptide from HCV in the induction of KIR2DS2-mediated responses in the presence of different HLA-C1 alleles (HLA-C*0304 and HLA-C*0802).

- To determine whether presentation of Flaviviral peptides in the context of HLA-C1 (HLA-C*0802) or HLA-C2 (HLA-C*0501) alleles triggers KIR2DS2-mediated NK cell activation through canonical or non-canonical interactions, respectively.

- To assess the ability of IVDLMCHATF peptide from DENV/ZIKV in the induction of NK cell specific responses through KIR2DS2.

Chapter 2 - Methodology

2.1 HCV replicon and luciferase assay

The monocistronic N17/JFH-1 subgenomic replicon is derived from the genotype 2a of HCV. This replicon lacks E1 and E2 structural proteins (ΔE1E2) and consists of a luciferase reporter gene (*Luc*), a puromycin-N-acetyltransferase (PAC) resistance gene, the structural core protein (C) and all HCV non-structural proteins (p7, NS2, NS3, NS4A, NS4B, NS5A and NS5B) (Angus *et al.*, 2012). The self-cleaving 2A peptide from foot-and-mouth disease virus (FMDV) releases *Luc* and PAC from the HCV polyprotein. Site-directed mutagenesis of P9 from the LNPSVAATL-encoding sequence, located within the RNA helicase (NS3), yielded the functional L9D mutant **(Figure 2.1)** (Naiyer *et al.*, 2017).

The HCC cell line Huh-7 carrying the wild-type (WT) HCV replicon (Huh-7 WT) or its mutant (Huh-7 L9D) were previously generated (Naiyer *et al.*, 2017). To monitor replication of both replicons within Huh-7 cells, luciferase activity was determined with the Bright-Glo™ Luciferase Assay System (Promega). Briefly, $1x10^5$ cells were mixed with 100 µl of Glo lysis buffer and incubated on shaker at room temperature for 15 min. Cell lysates were centrifuged at 17000g for 5 min and 50 µl of the lysate supernatant were mixed with 50 µl of the Bright-Glo™ luciferase assay substrate on white flat-bottom 96-well plates (Corning). Relative Luciferase Units (RLU) were measured in the Fluostar Optima microplate reader (BMG Labtech). Wells containing lysis buffer alone or lysis buffer + luciferase substrate were included as controls.

2.2 Cell lines

The Phoenix amphotropic retrovirus-packaging cell line (ATCC CRL-3213) was maintained in R10 culture medium that consists of Roswell Park Memorial Institute (RPMI) 1640 (Gibco) supplemented with 10% Foetal Bovine Serum (FBS, Sigma-Aldrich), 10000 units/ml of penicillin, 10000 µg/ml of streptomycin and 29.2 mg/ml of L-glutamine (Pen Strep; Gibco). Transfected Phoenix cells were selected with 10 µg/ml of blasticidin (Gibco).

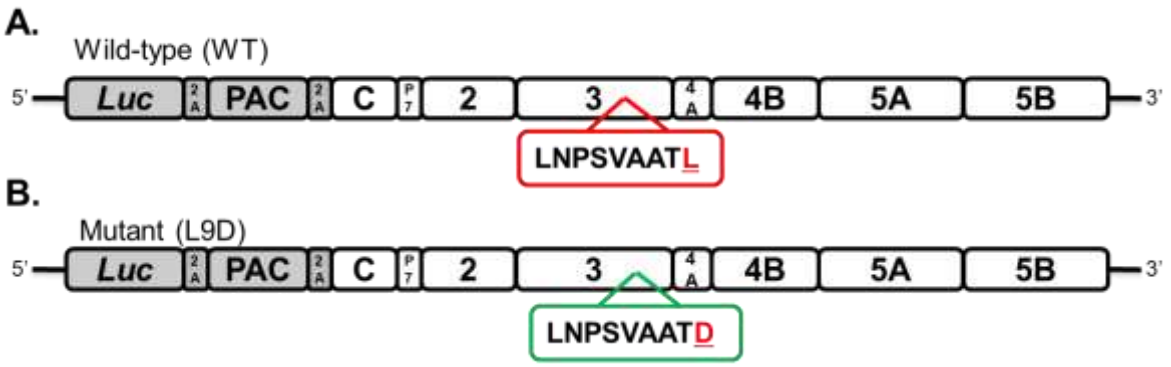

Figure 2.1 HCV N17/JFH-1 subgenomic replicon. The HCV N17/JFH-1 subgenomic replicon contains a luciferase reporter gene (Luc) and a puromycin resistance marker (PAC) replacing E1 and E2-encoding genes. **(A)** The WT HCV replicon encodes the LNPSVAATL peptide, which is located within the helicase domain of NS3. **(B)** Site-directed mutagenesis of the sequence encoding the LNPSVAATL peptide replaced a leucine for an aspartic acid at residue 9 (L9D) (Naiyer *et al.*, 2017).

The HCC cell line Huh-7 was cultured in Dulbecco's Modified Eagle's medium (DMEM, Gibco) supplemented as R10 medium (D10). Transduced Huh-7 cells were grown in the presence of 2 µg/ml of blasticidin. Huh-7 WT and Huh-7 L9D cells were selected with 2 µg/ml of puromycin (Sigma-Aldrich). Transduced replicon cells were maintained under double antibiotic selection with 2 µg/ml of puromycin and 2 µg/ml of blasticidin.

The B-lymphoblastoid MHC-I-deficient cell line 721.221 was maintained in R10. 721.221 cells expressing HLA-C*0802 or HLA-C*0501 alleles and the ones co-expressing the HSV-1-derived TAP inhibitor ICP47 (TAP-deficient) were a gift from Malcolm Sim (Sim *et al.*, 2017). These cells were cultured in Iscove's Modified Dulbecco's Medium (IMDM, Gibco) supplemented as R10 medium (I10) and selected with 0.5 mg/ml of geneticin (Life Technologies). TAP-deficient 721.221 cells were additionally selected with 0.3 µg/ml of puromycin.

721.221 cells expressing HLA-C*0802 or HLA-C*0501 and co-expressing the NS3 protein from DENV (DENV/NS3-mCherry) were grown in I10 and selected with 0.5 mg/ml of geneticin + 10 µg/ml of blasticidin. 721.221 cells transduced with the vector carrying HLA-C*0802_T2A_IVDLMCHATF were cultured in R10 and selected with 10 µg/ml of blasticidin.

The human natural killer cell leukemia (NKL) cell line (Robertson *et al.*, 1996) was grown in R10 + 100 IU/ml of recombinant human (rh) IL-2 (Tecin™). NKL cells expressing KIR2DL2 or KIR2DS2 receptors were selected with 10 µg/ml of blasticidin. All cell lines were maintained in a humidified atmosphere of 5% CO_2 at 37°C. A summary of the cell lines previously developed (Naiyer *et al.*, 2017; Sim *et al.*, 2017) and the ones generated in this study is shown in **Figure 2.2.**

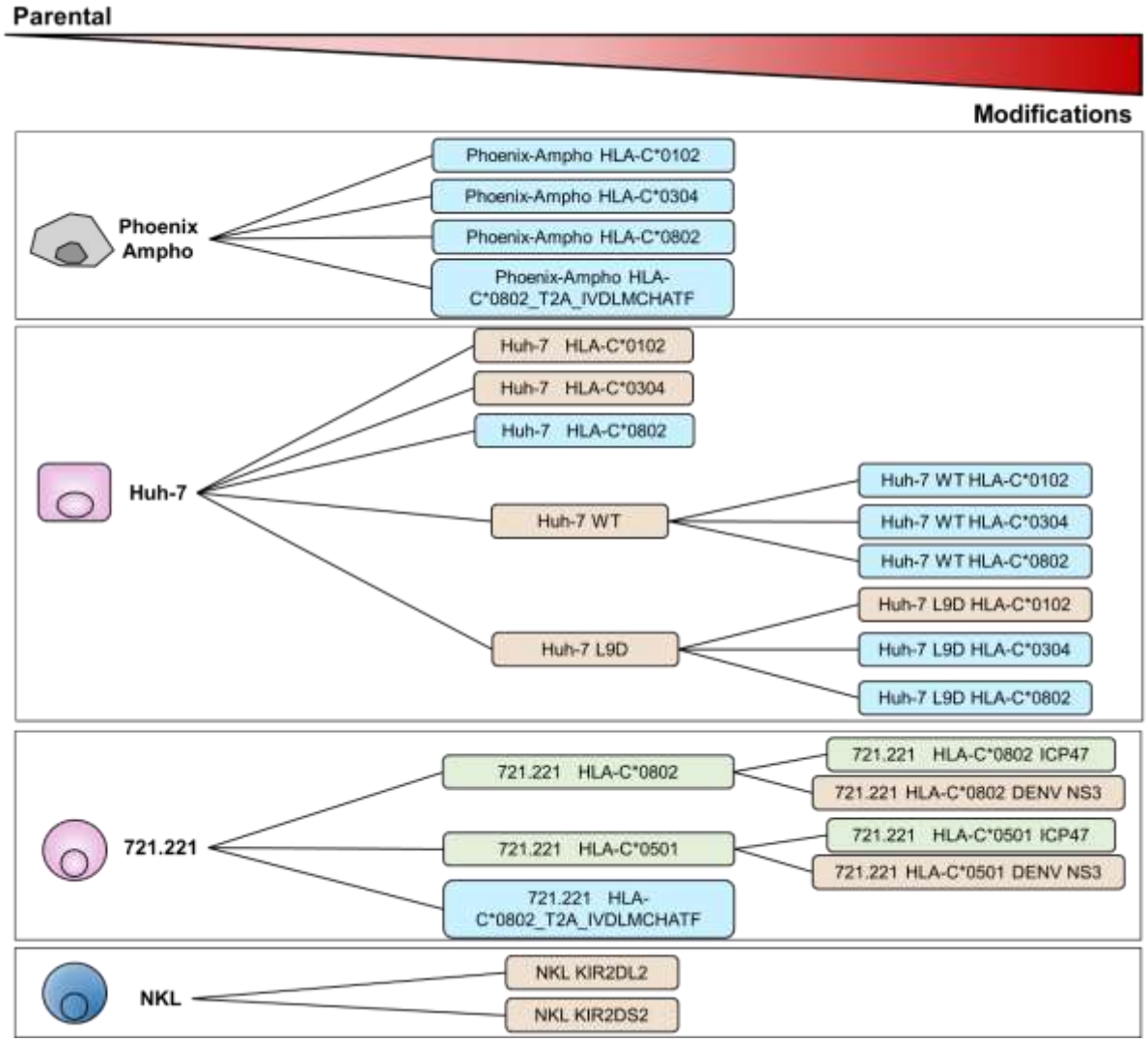

Figure 2.2 Cell lines and its derivatives. Parental Phoenix-Ampho, Huh-7, 721.221 and NKL cell lines (left) were singly (center) or doubly modified (right) using different gene delivery mechanisms, including transfection, transduction and electroporation. Cell lines in green were kindly donated by Malcolm Sim, the ones in orange were previously generated in our lab and the ones in light blue were generated in this study.

2.3 Gene delivery

2.3.1 Transfection of Phoenix-Ampho cells

Phoenix-Ampho cells were transfected with different DNA plasmids **(Table 2.1)** using the jetPRIME® transfection kit (Polyplus). Briefly, $5x10^5$ Phoenix-Ampho cells were seeded on a 6-well plate and incubated at 37°C for 24 h. Next day, 1 or 2 µg of plasmid DNA were diluted in 100 or 200 µl of jetPRIME buffer, respectively. Then, 2 or 4 µl of jetPRIME reagent were added to the corresponding tubes and incubated at room temperature for 10 min. R10 medium was replaced before the addition of the transfection mixture drop by drop into the wells. After 24 h, positive transfectants were selected with 5 µg/ml of blasticidin. On subsequent days, this concentration was increased up to 10 µg/ml.

2.3.2 Retroviral transduction of Huh-7 and 721.221 cells

Parental Huh-7, Huh-7 WT and Huh-7 L9D cells were transduced with retroviruses carrying HLA-C*0102-YFP, HLA-C*0304-YFP or HLA-C*0802 (no YFP). Twenty-for hours before transduction, blasticidin was removed from the medium of transfected Phoenix-Ampho cells. The viral supernatant from each transfected cell line was collected and filtered through a 0.22 µm membrane filter, mixed with polybrene (4 µg/ml) and incubated at room temperature for 10 min. Then, 1, 2 or 3 ml of each mixture were added into 50-60% confluent Huh-7 cells formerly seeded on 6-well plates (without puromycin in the case of replicon Huh-7 cells). Plates were centrifuged at 800g for 2h at 4°C and then incubated at 37°C. After 24h, positively transduced cells were selected with 1 µg/ml of blasticidin. Likewise, selection with puromycin was restored in replicon Huh-7 cells. Approximately two weeks after transduction, cells were washed with Versene® (EDTA) 0.02%, trypsinized with Trypsin/EDTA for 3 min (both from Lonza) and transferred to $25cm^2$ culture flasks under single (2 µg/ml of blasticidin) or double antibiotic selection (2 µg/ml of puromycin + 2 µg/ml of blasticidin).

Parental 721.221 cells were transduced with retroviruses carrying the HLA-C*0802_T2A_IVDLMCHATF construct as described above with the following modifications: one day before transduction, $1x10^6$ 721.221 cells were seeded in 6-well plates. After centrifugation, cells were incubated for 24 h and selected with 2 µg/ml of blasticidin. This concentration was increased in subsequent days to 5, 7.5 and then to 10 µg/ml. The mechanisms of transfection and retroviral transduction are shown in **Figure 2.3**.

Table 2.1 DNA plasmids for transfection of Phoenix-Ampho cells

Vector	HLA-C gene	Fluorescent proteins	Resistance gene
pIB2	HLA-C*0102	YFP	*bsr*
pIB2	HLA-C*0304	YFP	*bsr*
pIB2	HLA-C*0802	None	*bsr*
pIB2	*HLA-C*0802_T2A_IVDLMCHATF	None	*bsr*

YFP: yellow fluorescent protein
bsr: blasticidin resistance gene
* Generated in this study

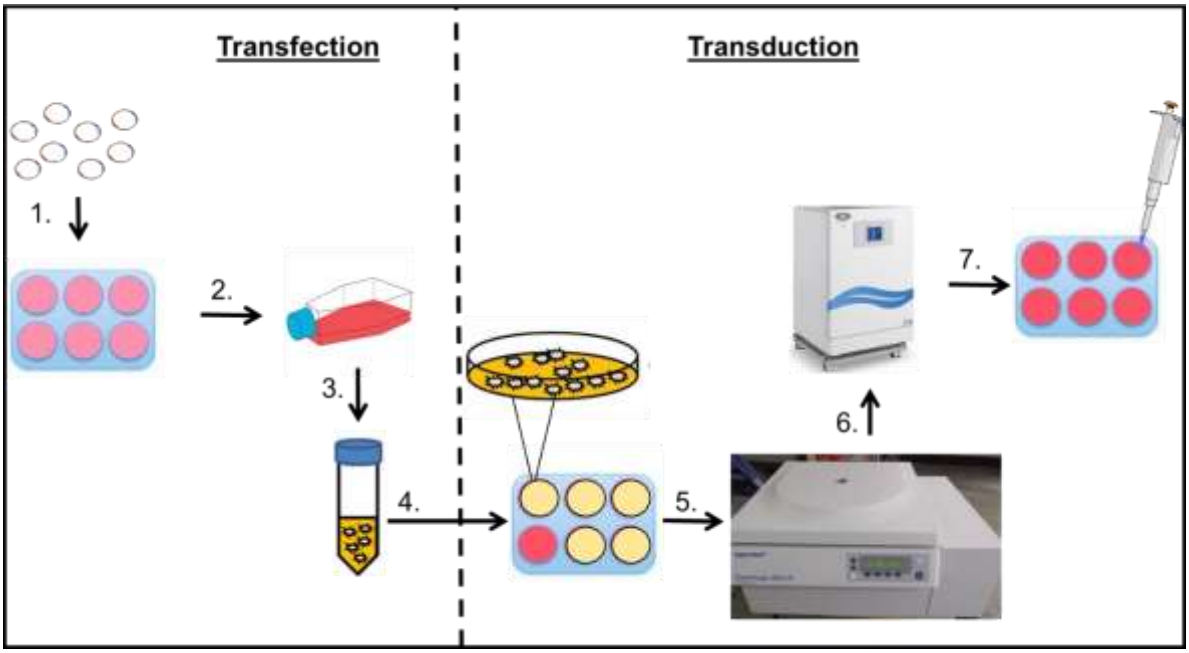

Figure 2.3 Mechanisms of transfection and retroviral transduction. Phoenix-Ampho cells were transfected with DNA plasmids carrying HLA-C genes (**1**) and transferred to T25 flasks for proliferation under antibiotic selection (**2**). The viral supernatant from transfected Phoenix cells was collected, incubated with polybrene (**3**) and added to recipient cells (**4**). Plates were centrifuged at 4°C for 2 h (**5**) and then incubated at 37°C for 24 h (**6**). Antibiotic selection was initiated next day (**7**) and transduced cells were allowed to proliferate for further 2 to 4 weeks.

2.4 Expression of fluorescent proteins

Cells expressing proteins coupled to fluorescent tags were mixed with sterile phosphate buffered solution (PBS; Lonza) and centrifuged at 300g for 5 min. The pellet was re-suspended in fresh PBS and expression of fluorescent proteins was measured in the BD Accuri™ C6 Cytometer, previous calibration with Spherotech 8-peak and 6-peak validation beads (BD Biosciences) to ensure that the data was accurate and presented minimal variability **(Figure 2.4)**.

- Expression of HLA-C*0102 or HLA-C*0304 coupled to Yellow Fluorescent Protein (YFP) in parental and replicon Huh-7 cells was measured using the FL1 channel.
- Expression of ICP47 coupled to Green Fluorescent Protein (GFP) in TAP-deficient 721.221 cells expressing HLA-C*0802 or HLA-C*0501 was detected using the FL1 channel.
- Expression of DENV NS3 protein coupled to mCherry in 721.221 cells expressing HLA-C*0802 or HLA-C*0501 was measured using the BD LSRFortessa™ Cytometer (PE-TexasRed channel).

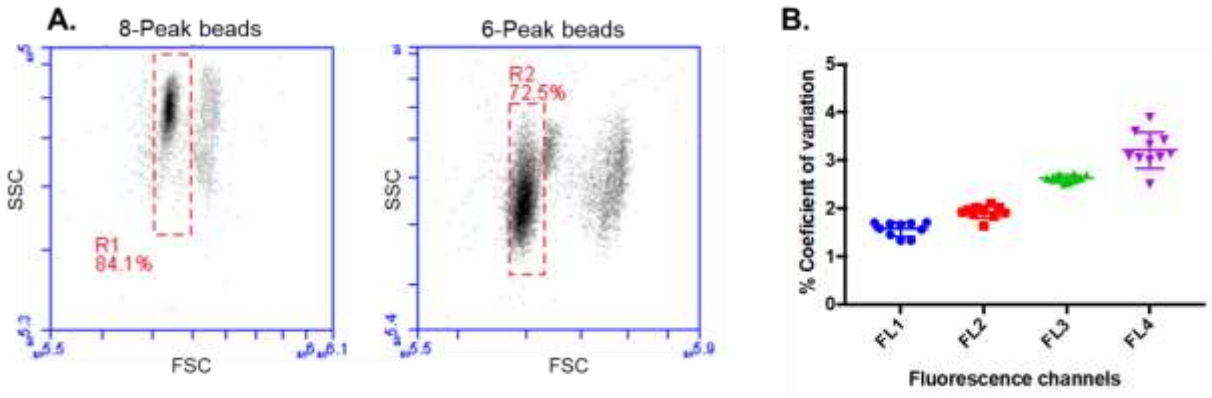

Figure 2.4 Validation of BD Accuri™ C6 Cytometer. (A) Representative plots show the main population of 8-peak and 6-peak validation beads. **(B)** Percentages of coefficient of variation for the four fluorescent channels (FL1 to FL4) over a period of one month. Values below 5% denote low variability and are a good indicator of the performance of the machine. Mean values and standard deviation (SD) of 10 independent measurements are shown. Validation of the machine with beads was performed every time before running experimental samples.

2.5 HLA-C and total MHC-I staining

Expression of HLA-C at the surface of all transduced Huh-7 and 721.221 cells was confirmed by flow cytometry. Briefly, $2x10^5$ cells were transferred to V-bottom 96-well plates and blocked with 10% human serum (Sigma) for 30 min. Cells were washed twice with FACS buffer (PBS, 1% BSA and 0.1% sodium azide) and incubated with an in-house anti-HLA-C antibody (DT9; 1.89 µg/ml) at 4°C for 30 min. Cells were washed again and incubated with the Goat Anti-Mouse IgG Alexa Fluor® 647 secondary antibody (1:6000; Catalog ab150115, Abcam) for further 30 min. Finally, cells were washed and fixed with 1% paraformaldehyde (PFA; Fisher Scientific) and analysed on the BD Accuri™ C6 Cytometer (FL4 channel), previous calibration of the instrument **(Figure 2.4)**. Non-transduced Huh-7 and 721.221 cells were used as controls.

All transduced Huh-7 cells were also stained for surface MHC-I expression. For this, Huh-7 cells were incubated with the pan-HLA class I-specific antibody (W6/32; 2.3 µg/ml) at 4°C for 1 h followed by incubation with the Goat Anti-Mouse IgG Alexa Fluor® 647 secondary antibody for further 30 min. Parental Huh-7 cells were used as controls to distinguish transduced HLA-C expression from endogenous HLA-A*11 expression.

2.6 KIR staining

To confirm expression of KIR2DL2 or KIR2DS2 receptors on transduced NKL cells, $2x10^5$ cells were incubated with an antibody that recognizes KIR2DL2, KIR2DL3 and KIR2DS2 receptors (anti-CD158b-PE; 4:100; Catalog 559785; BD Biosciences) at 4°C for 30 min. KIR2DL2 and KIR2DS2 expression was differentiated by incubating cells with an anti-1F12 antibody (1:50) that recognizes KIR2DL3 and KIR2DS2 receptors, but not KIR2DL2. Cells were washed with FACS buffer and incubated with the Goat Anti-Mouse IgG Alexa Fluor® 647 secondary antibody. Finally, cells were fixed with 1% PFA and analysed in the calibrated BD Accuri™ C6 Cytometer **(Figure 2.4)**. Non-transduced NKL cells were used as controls.

2.7 Human peripheral blood mononuclear cell isolation

Human venous blood from healthy volunteers was collected into Vacuette® blood collection tubes (Greiner Bio-One) with informed consent (Project: Immunology studies in volunteers not known to have hepatitis C virus infection, NHS). Peripheral blood mononuclear cells (PBMC) were isolated using Ficoll density gradient centrifugation. Briefly, fresh blood was diluted in PBS (1:1) and carefully layered into a 50 ml falcon tube containing 15 ml of Ficoll-Paque™ (GE Healthcare). Tubes were centrifuged at 800g at room temperature, no acceleration and no brake, for 30 min. The PBMC layer was gently removed using a Pasteur pipette and transferred to a new falcon tube containing PBS. PBMC were centrifuged at 450g for 10 min, washed twice with PBS and then re-suspended in cold freezing medium (90% FBS + 10% DMSO) for liquid nitrogen storage.

2.8 DNA extraction from PBMC

DNA was extracted from PBMC using the PureLink genomic DNA miniprep kit (Thermo Fisher Scientific). Five million PBMC were centrifuged at 17000g for 5 min and re-suspended in 200ul of PBS. Then, 20 µl of proteinase K + 20 µl of RNAse A were added to the cells, vortexed and incubated for 2 min at room temperature. For DNA binding, 200 µl of Purelink genomic lysis/binding buffer were added to the samples, briefly vortexed and incubated at 55°C for 10 min. Then, 200 µl of 96-100% of ethanol was added to the lysate, carefully placed onto a PureLink spin column and centrifuged at 17000g for 1 min. After the filtrate in the collection tube was discarded, the DNA was washed twice with 500 µl of wash buffer and the column was placed into a sterile 1.5 ml Eppendorf tube. The DNA was eluted by adding 25 µl of PureLink genomic elution buffer, followed by a quick centrifugation and addition of extra 25 µl of the elution buffer into the column having a final volume of 50 µl. The DNA concentration was quantified using NanoDrop One (Thermo Fisher Scientific) and stored at -20°C.

2.9 Genotyping of KIR genes

Genotyping of KIR genes from blood donors was performed by conventional Polymerase Chain Reaction (PCR) using the GeneAmp® PCR system 9700 version 3.12 (Applied Biosystems). Forward and reverse primers for human growth hormone 1 (GH1; internal positive control), KIR2DL2, KIR2DL3 and KIR2DS2 genes were previously reported (Gomez-Lozano and Vilches, 2002) and were synthesized by Eurofins Genomics **(Table 2.2)**. Amplification was performed in a 25 µl reaction using 200 ng of genomic DNA, forward and reverse primers for GH1 and KIR (0.5 µM), 1X green buffer, 25mM $MgCl_2$, 10mM dNTPs, and 5U/µl of Go Taq Hot Start polymerase (Promega). PCR conditions consisted of an initial denaturation at 95°C for 2 min, followed by 10 cycles at 94°C for 20 s, 65°C for 10 s and 72°C for 1min 30 s and 20 cycles at 94°C for 20 s, 61°C for 20 s and 72°C for 1min 30 s, followed by a final extension at 72°C for 10 min. Amplification products were visualized on 2% agarose gel (Fisher BioReagents) in TBE 1X (Thermo Scientific) using a Nancy-520 DNA gel stain (Sigma Aldrich). The 1 Kb DNA ladder (Biolabs) was used.

Table 2.2 Primers for KIR genotyping

Gene	Forward primer (5'-3')	Reverse primer (5'-3')	Amplicon length
GH1	CTTCCCAACCATTCCCTTA	CGGATTTCTGTTGTGTTTC	424 bp
KIR2DL2	ACTTCCTTCTGCACAGAGAA	GCCCTGCAGAGAACCTACA	1868 bp
KIR2DL3	ACAGAGAAGGGAAGTTTAAG	CCCTGCAGAGAACCTACG	1858 bp
KIR2DS2	TGCACAGAGAGGGGAAGTA	CACGCTCTCTCCTGCCAA	1775 bp

GH1: Growth hormone

2.10 Phenotyping of KIR genes

Phenotyping of KIR genes from blood donors was performed by flow cytometry using a combination of antibodies to discriminate KIR2DS2^{high} from KIR2DL2^{high} or KIR2DL2/L3^{high} NK cells (Blunt *et al.*, 2019). Briefly, 5x10^5 PBMC were transferred to V-bottom 96-well plates and blocked with 10% human serum at 4°C for 20 min. Cells were washed twice with FACS buffer and incubated with a cocktail of antibodies containing anti-CD3-PerCP (1:100; Catalog 300428; Biolegend), anti-CD56-PE-Cy7 (4:100; Catalog 318318; Biolegend), anti-CD158b-PE clone CH-L (4:100) and anti-KIR2DL3-FITC clone REA147 (10:100, Catalog 130-100-125; Miltenyi) for further 30 min. Stained PBMC were washed and analysed on the

BD FACSAria™ IIu Cytometer previous compensation of the signal overlap using BD™ Compensations beads (BD Biosciences).

2.11 NK cell isolation and fluorescent activated cell sorting (FACS)

NK cells from KIR2DL2/S2+ or KIR2DL2/L3/S2+ donors were isolated from PBMC using the human NK cell isolation kit (Miltenyi). Briefly, PBMC were mixed with sterile MACS buffer (PBS, 0.5% BSA and 2mM EDTA) and the NK cell biotin-antibody cocktail (40 µl and 10 µl per $1x10^7$ PBMC, respectively) and incubated for 5 min at 4°C. Then, MACS buffer and the NK cell microbead cocktail were added to the cell suspension (30 µl and 20 µl per $1x10^7$ PBMC, respectively), and incubated for further 10 min. NK cells were negatively separated using a LS MACS column and a MACS separator (Miltenyi), washed once with sterile PBS and re-suspended in NK MACS medium supplemented with 1% NK MACS supplement (Miltenyi), 5% human serum, 1% Pen Strep and 500 IU/ml of rhIL-2. Purified NK cells were seeded onto 24-well plates ($1x10^6$ NK cells/well) and maintained in incubation at 37°C and 5% CO_2 for 10 to 14 days. Culture medium was changed every time it turned yellow.

Fluorescent activated cell sorting (FACS) of purified NK cells was performed based on the expression of KIR2DL2, KIR2DL3 and KIR2DS2 receptors using the cocktail of antibodies previously described for KIR phenotyping. The BD FACSAria™ IIu Cytometer was used for cell sorting previous compensation of the signal overlap at high purity and high sorting efficiency (>90%). After sorting, three different NK cell subpopulations were obtained: KIR2DL2/L3/$S2^{neg}$, KIR2DL2/$L3^{high}$ and KIR2DS2^{high} NK cells. Sorted NK cells were washed once with sterile PBS, re-suspended in supplemented MACS NK medium and incubated at 37°C for NK cell functional assays (section 2.17.3).

2.12 Peptides

Synthetic peptides from HCV (LNPSVAATL), DENV/ZIKV (IVDLMCHATF), YFV (VIDAMCHATL), WNV/JEV (IVDVMCHATL), EBOV (FLSDVPVATL) and cellular peptides

(IIDKSGSTV and IVDKSGRTL) were purchased from GL Biochem (Shanghai, China) with a purity >98%. Peptides were diluted in DMSO (0.1 M and 20 mM) and stored at -80°C.

2.13 Peptide binding prediction

Binding prediction of viral peptides to HLA-C1 and HLA-C2 alleles was performed using the MHC binding predictor NetMHCPan platform version 4.0. Threshold for strong and weak binders were set on 0.5% and 2%, respectively. Binding affinity predictions were included.

2.14 Peptide loading and stabilization of HLA-C

Binding of viral peptides to HLA-C*0102, HLA-C*0802 or HLA-C*0501 alleles was confirmed by a flow cytometry-based MHC-I stabilization assay. Briefly, 721.174 or TAP-deficient cells expressing HLA-C*0802 or HLA-C*0501 were centrifuged at 300g for 5 min, re-suspended into AIM-V serum-free medium (Gibco) and seeded into round-bottom 96-well plates at a cell density of $2x10^5$/well. All peptide stocks (20 mM) were diluted 1:10 into AIM-V medium (2 mM) and serial dilution of peptides (from 200 µM to 12.5 µM) were loaded onto seeded cells, mixed and incubated at 26°C and 5% CO_2 overnight **(Figure 2.5)**. Next day, cells were washed once with FACS wash and stained for HLA-C expression as described above (section 2.5). Cells incubated without peptides were used as controls.

2.15 Tetramer staining

Binding of KIR to MHC-I:peptide complexes was evaluated using KIR tetramers. Biotinylated KIR2DL2 or KIR2DS2 were previously generated (Naiyer *et al.*, 2017) and were conjugated with 1 mg/ml of streptavidin-PE (Life Technologies) as follows: 30 µl of biotinylated KIR2DL2 or KIR2DS2 were mixed with 45 µl of streptavidin-PE and incubated on shaker at 4°C overnight. Then, 9 µl of streptavidin-PE were added to the conjugate five times every 30 min (45 µl in total). TAP-deficient 721.221 cells expressing HLA-C*0802 or HLA-C*0501 were loaded with viral peptides at a concentration of 200 µM. Next day, cells

were washed with PBS + BSA 1% and incubated with KIR2DL2-PE or KIR2DS2-PE tetramers at 4°C for 1 h **(Figure 2.5)**. Cells were washed, fixed with 1% PFA and analysed in the BD Accuri™ C6 Cytometer previous compensation of the signal overlap using compensation beads. Cells incubated without peptides were used as controls.

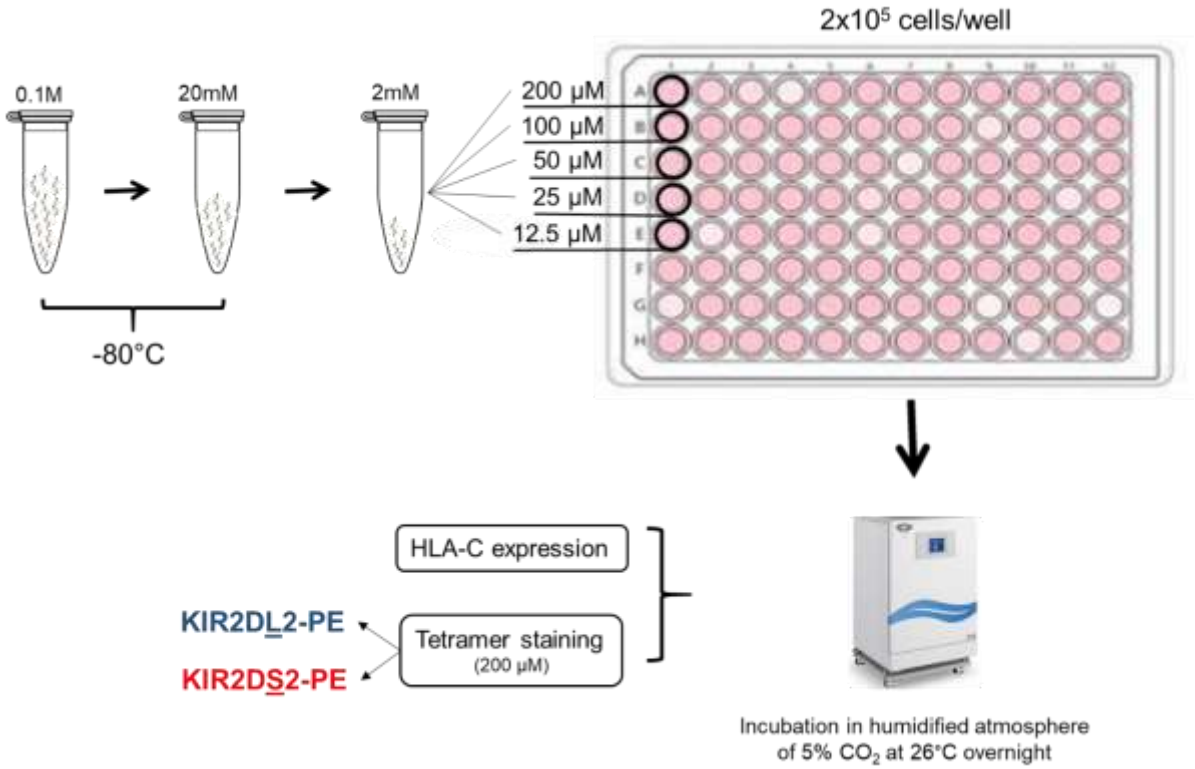

Figure 2.5 Peptide loading on TAP-deficient cells. Viral peptide stocks were serially diluted and mixed with 721.174 or TAP-deficient 721.221 cells expressing HLA-C*0802 or HLA-C*0501 alleles. Peptide-loaded cells were incubated at 26°C overnight and processed next day for HLA-C expression or staining with KIR2DL2 or KIR2DS2 tetramers coupled to PE.

2.16 Sub-cloning HLA-C*0802_T2A_IVDLMCHATF into pIB2

2.16.1 Vector synthesis

A DNA plasmid (pMK-RQ - KanR) carrying the HLA-C*0802_T2A_IVDLMCHATF sequence (1266 base pairs; bp) was synthesized by GeneArt (Invitrogen) **(Figure 2.6A)**. Upon receipt, the tube containing 5 µg of DNA plasmid was centrifuged at 300g for 5 min, re-suspended in 100 µl of distilled sterile water and incubated at 4°C overnight. Next day, DNA was re-suspended gently and stored at -20°C.

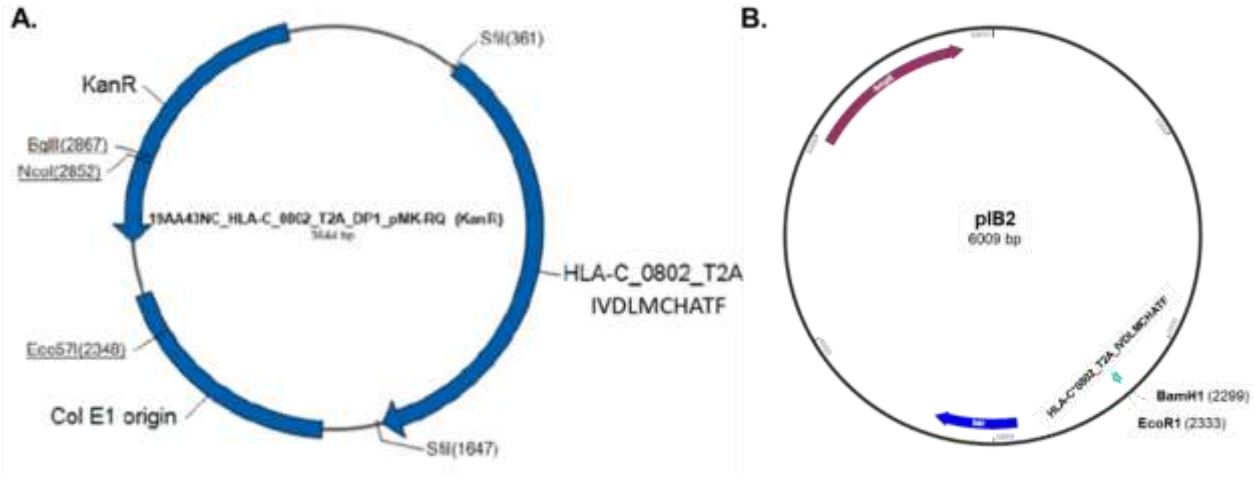

Figure 2.6 Map of donor and recipient plasmids The synthetic gene HLA-C*0802_T2A_IVDLMCHATF was cloned into a pMK-RQ donor plasmid **(A)** carrying a kanamycin resistance gene (KanR). This construct was synthesized by GeneArt and used for subcloning of HLA-C*0802_T2A_IVDLMCHATF insert into a recipient pIB2 plasmid carrying a blasticidin resistance gene) **(B)**.

2.16.2 Restriction enzyme digestion

The pMK-RQ donor plasmid carrying HLA-C*0802_T2A_IVDLMCHATF and the pIB2 recipient plasmid carrying HLA-C*0102_T2A_IVDLMCHATF **(Figure 2.6)** were digested using restriction enzymes. Digestion was performed in a 20 µl reaction using 2 µg of DNA plasmid, 1X of Cutsmart buffer, 1 µl of BamH1 HF and 1 µl of EcoR1 HF (all from BioLabs). Tubes were incubated in a 37°C water bath for 2h and then mixed with 5 µl of 5X DNA loading dye (BioLabs). Digested products were analysed on 2% agarose gel in TBE 1X using Nancy-520 DNA gel stain and visualized under UV light. The 1 Kb DNA ladder was used as a reference.

2.16.3 Gel purification

Bands corresponding to digested pIB2 recipient plasmid and HLA-C*0802_T2A_IVDLMCHATF insert were excised from the agarose gel and the DNA was purified using the QiAquick Gel Extraction kit (Qiagen). Briefly, gel slices were weighed, mixed with Buffer QG (3:1) and incubated at 50°C for 10 min, vortexed every 2 minutes.

After confirming the gel was completely dissolved, 1 gel volume of isopropanol was added to the samples and transferred to QIAquick spin columns, followed by centrifugation at 17000g for 1 min. Samples were washed with 500 µl of QG buffer, centrifuged for 1 min and then washed once with buffer PE. Finally, the DNA was eluted with 30 µl of Buffer EB and quantified using the NanoDrop One instrument.

2.16.4 DNA ligation

Digested pIB2 recipient plasmid and HLA-C*0802_T2A_IVDLMCHATF insert were ligated using the formula:

$$\text{ng Insert} = \frac{\text{Insert bp} \times 100}{\text{Vector bp}}$$

Ligation was performed in a 20 µl reaction using 1:3 and 1:5 plasmid:insert ratios, 1X T4 DNA ligase buffer and 1 µl of T4 DNA ligase (both from BioLabs). Tubes were incubated at 16°C water bath overnight. Next day, T4 DNA ligase was inactivated by incubating tubes at 65°C for 10 min and then transferred to ice. Ligated products were stored at -20°C.

2.16.5 Bacterial transformation

Ligated pIB2-HLA-C*0802_T2A_IVDLMCHATF products at 1:3 and 1:5 ratios were used to transform Escherichia coli (*E.coli*) XL2-blue ultracompetent cells (Agilent). Briefly, *E. coli* were thawed on ice for 10 min, mixed gently and transferred to 15 ml Falcon tubes. 2 µl of β-mercaptoethanol were added to the bacteria and incubated in ice for further 10 min, swirling every two minutes. Then, 50 ng of ligated products were added into the tubes and incubated on ice for 30 min. Tubes were incubated at 42°C water bath for 45 s and returned to ice for 2 min. Lysogeny Broth (LB) medium was added to the bacterial suspension and incubated in shaking incubator (225-250 rpm) at 37°C for 1 h. Bacteria were streaked onto agar plates containing 100 µg/ml of ampicillin (Fisher Scientific) and incubated at 37°C overnight.

Next day, single colonies were picked from agar plates and placed into 15 ml Falcon tubes containing 5 ml of LB medium + 100 µg/ml of ampicillin. Tubes were incubated in shaking incubator (225-250 rpm) at 37°C for further 12-18 h. Glycerol stocks were made using 50% glycerol and stored at -80°C.

2.16.6 Plasmid DNA extraction

DNA extraction from bacteria was performed using the GeneJET Plasmid Miniprep kit (Thermo Fisher Scientific). Briefly, bacteria were centrifuged at 3000g for 15 min and the pellet was mixed with 250 µl of re-suspension solution. Then, 250 µl of lysis buffer were added, followed by 350 µl of neutralization solution and centrifugation at 17000g for 5 min. The supernatant was transferred to a GeneJET spin column and washed twice with 500 µl of wash buffer, followed by a quick centrifugation at 17000g for 1 min. The column was placed into an Eppendorf tube and DNA was eluted using 50 µl of elution buffer. The DNA concentration was quantified using NanoDrop One and sent for DNA sequencing using pIB2 specific primers flanking the inserted sequence (Source BioScience).

2.17 NK cell functional assays

2.17.1 Inhibition of viral replication assay

The ability of NK cells to inhibit HCV replicon replication was determined by measuring the luciferase activity of transduced replicon Huh-7 cells after co-culture with NKL cells expressing KIR2DL2 (NKL-2DL2) or KIR2DS2 (NKL-2DS2) receptors. Briefly, transduced replicon Huh-7 cells were trypsinized, re-suspended in R10 medium, seeded on flat-bottom 96-well plates ($1x10^4$ cells/well) and incubated overnight at 37°C. Next day, untransduced NKL cells, NKL-2DL2 and NKL-2DS2 cells were centrifuged at 300g for 5 min and re-suspended in fresh R10 + rhIL-2. Co-culture of effector (E) and target (T) cells was performed in triplicates at 0.1:1, ratio and incubated at 37°C. After 24 h, plates were centrifuged at 800g for 5 min and a luciferase assay was carried out as described above (section 2.1). Non-transduced replicon cells were used as controls.

2.17.2 Cytotoxicity assay

Killing of target cells by NKL-2DL2 or NKL-2DS2 cells was evaluated by flow cytometry using a Live/Dead dye. First, parental 721.221 cells and its derivatives (except TAP-deficient cells) were labelled with the Cell Trace™ Far Red Cell Proliferation Kit (Life Technologies) and incubated at 37°C for 20 min. Then, five volumes of R10 were added to the labelled cells, incubated for further 5 min and centrifuged at 800g for 5 min. Target cells were seeded on round-bottom 96-well plates ($6x10^4$ cells/well) and mixed with untransduced NKL, NKL-2DL2 or NKL-2DS2 cells at 20:1 or 10:1 E:T ratios in a final volume of 100 µl. Target and effector cells were incubated at 37°C for 4 hours and then transferred to V-bottom 96-well plates for washing with PBS. Cells were re-suspended with the Live/Dead™ Fixable Red Dead Cell stain (Life Technologies) and incubated at room temperature for 30 min. Finally, cells were washed, fixed with 1% PFA and analysed using the BD Accuri™ C6 Cytometer using the gating strategy shown in **Figure 2.7**. Labelled target cells incubated without effector cells were used as controls.

2.17.3 LAMP-1 degranulation assay

Degranulation of NK cells to target cells was evaluated by detecting surface expression of CD107a. PBMC from KIR2DL2/S2+ or KIR2DL2/L3/S2+ donors were thawed, re-suspended in R10 + 1 ng/ml of IL-15 (R & D Systems) and incubated at 37°C overnight. Next day, PBMC were re-suspended in fresh R10 + CD107a-eF660 antibody (1:175; Fisher Scientific) and seeded into round-bottom 96-well plates at a cell density of $3x10^5$ cells/well. Target cells were mixed with PBMC at 10:1 and 5:1 E:T ratios in a final volume of 100 µl with some modifications for the following target cells:

- Huh-7 cells and its derivatives were seeded into 96-well plates the day before to allow cell attachment.
- TAP-deficient 721.221 cells were loaded with peptides the day before as described in section 2.14 and incubated with PBMC in the presence of peptides at 26°C.

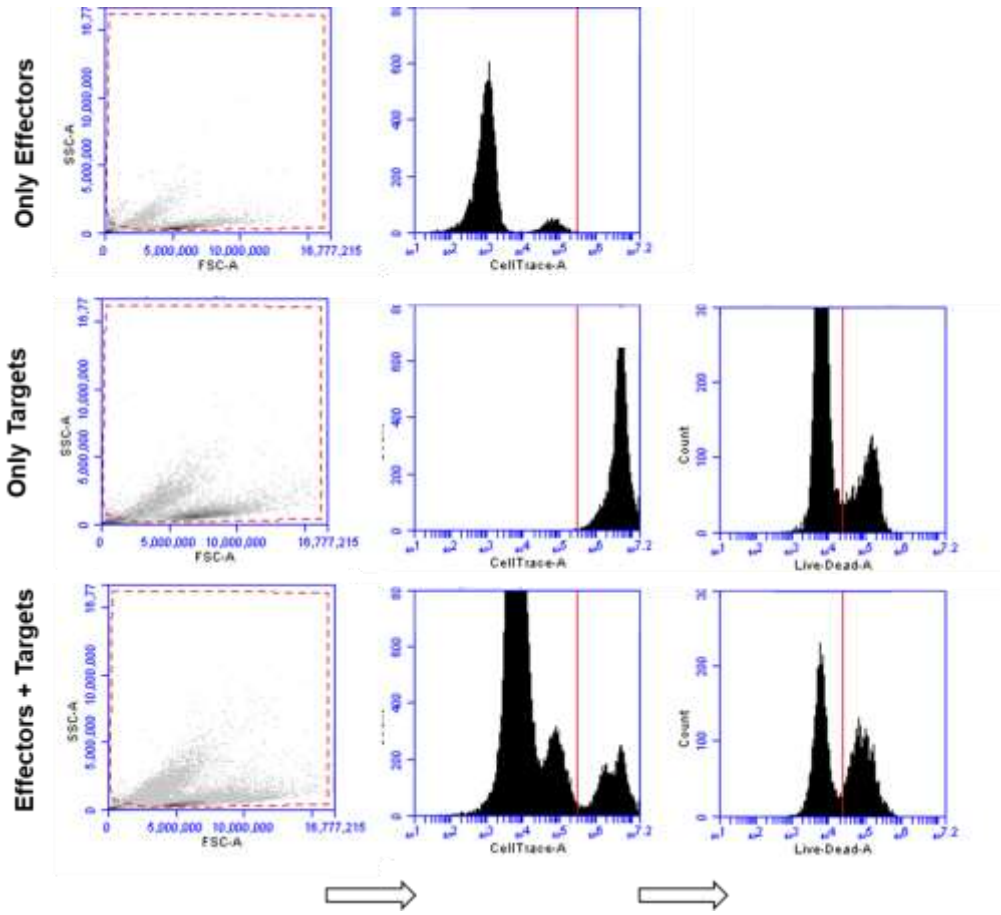

Figure 2.7 Gating strategy for cytotoxicity assay. Target and effector cells were gated on FSC/SSC plots. Target cells labelled with CellTrace fluorescent dye were visible in FL4 channel. Live/Dead cells (FL2 channel) were gated on CellTrace+ cells.

After 1 h incubation, Golgi stop (BD Biosciences) was added into the co-culture (6 µg/ml) and plates were incubated at 37°C for further 3 h. Cells were transferred to V-bottom 96-well plates, washed once with FACS wash and blocked with 10% human serum for 20 min. Cells were washed again and were incubated with a cocktail of antibodies containing anti-CD3-PerCP (1:100), anti-CD56-PE-Cy7 (4:100), anti-CD158b-PE clone CH-L (4:100) and anti-KIR2DL3-FITC clone REA147 (10:100) at 4°C for 30 min. Cells were washed and analysed in the BD FACSAria^{TM} IIu Cytometer previous compensation of the signal overlap using compensations beads. Analysis was performed using the FlowJo software version 10.6.0.

Primary NK cells sorted by high expression of KIR2DL2/L3 or KIR2DS2 receptors were used to determine NK cell degranulation to 721.221 cells and its derivatives (except TAP-deficient cells) as described above. For staining, anti-CD158b-PE clone CH-L (4:100) and anti-KIR2DL3-FITC clone REA147 (10:100) antibodies were used. The gating strategy for

total PBMC and sorted NK cells is shown in **Figure 2.8**. Effector cells incubated without target cells were used as controls.

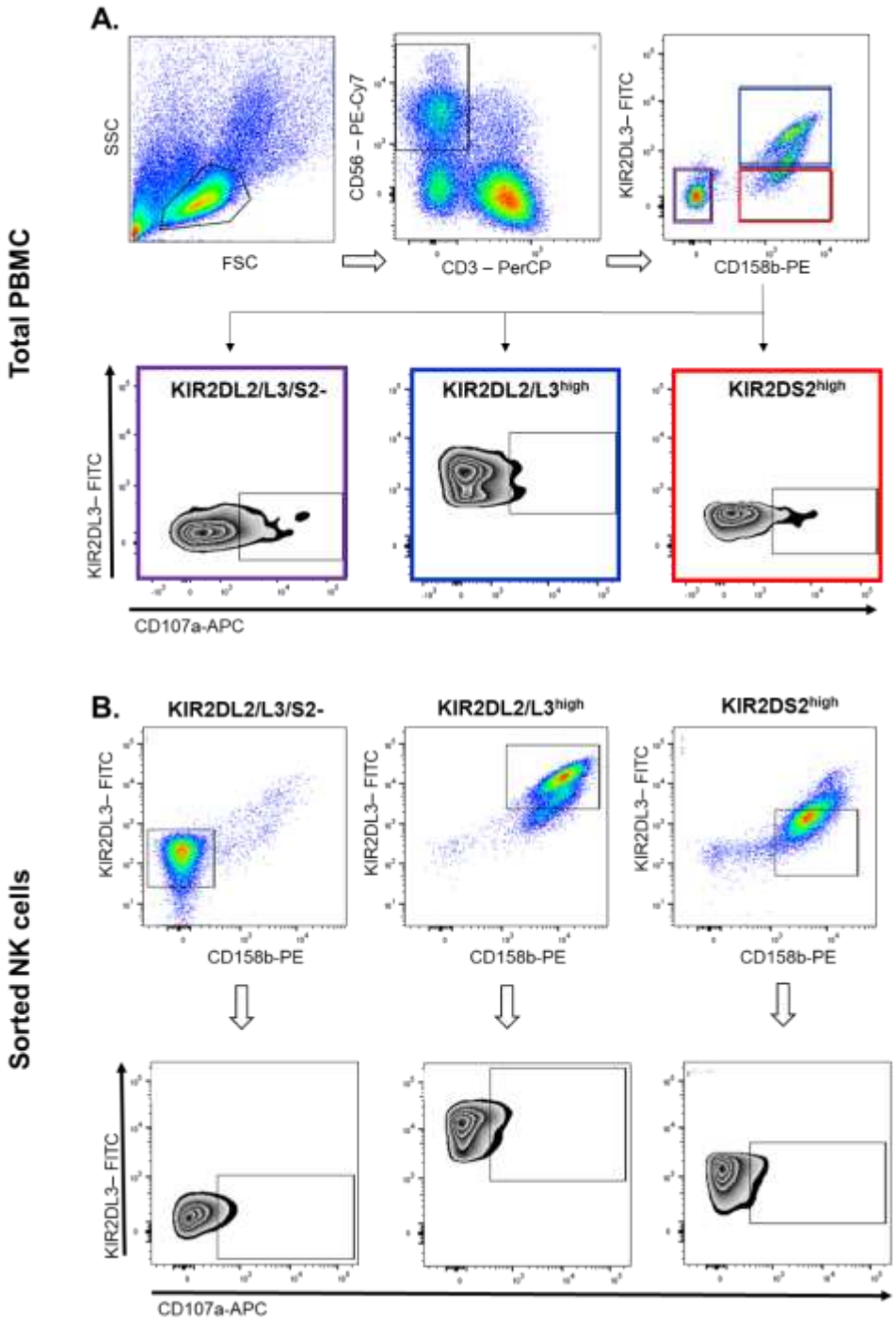

Figure 2.8 **Gating strategy for LAMP-1 degranulation assay. (A).** Lymphocytes were gated on FSC/SSC plots. NK cells were gated from lymphocytes using anti-CD3-PerCP and CD56-PECy7 antibodies (CD3- CD56+). KIR2DL2/L3/S2^{neg} (purple) KIR2DL2/L3^{high} (blue) and KIR2DS2^{high} (red) NK cell subpopulations were defined using anti-CD158b-PE (clone CH-L) and anti-KIR2DL3-FITC (clone REA147) antibodies. CD107a+ NK cells were gated on each NK cell subpopulation. (**B).** NK cells were previously sorted based on the expression of KIR2DL2/L3 and KIR2DS2 receptors. CD107a+ NK cells were gated on each individual NK cell subpopulation.

2.18 Statistical analysis

To determine whether variables had a normal distribution, Shapiro-wilk and D'Agostino & Pearson normality tests were carried out. The null hypothesis, which states that the population is normally distributed was rejected with a p value <0.05. For normally distributed data, differences between groups were determined using paired or unpaired t-test, as appropriate and results are presented as mean +/- standard deviation (SD). Conversely, non-parametric Mann-Whitney or Wilcoxon tests were used to test differences of data that did not follow a normal distribution. For this datasets, median and interquartile range were used. Differences for multiple comparison were determined using a Kruskal-Wallis test and Dunn's correction.

Results were considered statistically significant with p values <0.05. All statistical analyses were performed using GraphPad Prism Software Version 7 and 8.2.1 (2017 and 2019, respectively).

Chapter 3 - Natural Killer cell reactivity to Hepatitis C virus

3.1 Introduction

In the course of a viral infection, (NK) cells play a major role in the early recognition of viruses and in the modulation of adaptive responses. NK cell functions are determined by the balance between inhibitory or activating signals that occur after engagement of NK cell receptors with their ligands. A dominant activating signal induces NK cell cytotoxicity or cytokine production, resulting in elimination of virus-infected cells (Cooper, Fehniger and Caligiuri, 2001; Vivier *et al.*, 2011). Nevertheless, in the context of viral infections caused by Herpesviruses, IAV or HCV, NK cells may show a reduced functional capacity due to viral factors that enhance their inhibitory state or interfere with the activating signalling (Mao *et al.*, 2009; Yoon *et al.*, 2011; De Pelsmaeker *et al.*, 2018).

In the context of HCV infection, defective NK cell functions against chronically infected cells are associated with virus persistence. These defects include a reduced capacity in the production of cytokines (Miyagi *et al.*, 2010; Rogalska-Taranta *et al.*, 2015) and an impaired interaction with other components of the immune system such as complement or other immune cells (Kim *et al.*, 2014; Serti *et al.*, 2014). Some of the mechanisms behind the altered functionality of NK cells have been associated with the expression of structural or non-structural HCV proteins that affect surface expression of NK cell receptors (Holder *et al.*, 2013; Yang *et al.*, 2017). Recently, it was described that the NK cell receptor repertoire is altered in individuals chronically infected with HCV, limiting their phenotypic diversity (Strunz *et al.*, 2018).

One family of NK cell receptors are the KIR family, which recognize MHC-I:peptide complexes on target cells and perform either inhibitory or activating functions. As genes encoding KIR and MHC-I are highly polymorphic, certain receptor/ligand interactions have been associated with susceptibility or resistance to HCV infection. For instance, the KIR2DL2/KIR2DL2-HLA-C1C2 genotype has shown to be correlated with HCV chronicity whereas homozygosity for KIR2DL3/HLA-C1 is associated with resolution of the infection (Khakoo *et al.*, 2004; Knapp *et al.*, 2010; Vidal-Castineira *et al.*, 2010). This indicates that

genetic factors positively or negatively influence NK cell responses to HCV and highlights the need for the identification of MHC-I alleles that could mediate protective effects in specific populations.

Besides the contribution of KIR and MHC-I polymorphism, the role of peptides bound to MHC-I in modulating NK cell responses is being increasingly recognized. Recently, the immunopeptidome of Huh-7 cells co-expressing the N17/JFH-1 HCV subgenomic replicon and the HLA-C*0102 allele has been revealed as part of an ongoing study in our laboratory. Preliminary data has shown that HCV induces changes in the peptide repertoire selecting peptides that in general inhibit NK cell functions (Mbiribindi, 2016; Mbiribindi *et al.*, 2019). Similarly, the study conducted by Nattermann *et al* showed that an HCV core-derived peptide stabilizes HLA-E and mediates inhibition of NK cells through interaction with CD94/NKG2A (Nattermann *et al.*, 2005). Thus, peptides derived from either structural or non-structural HCV proteins mediating binding to inhibitory receptors could be a mechanism by which NK cell responses are diminished in HCV infection.

In the search of viral peptides that could promote virus clearance through the anti-viral activity of NK cells, Naiyer *et al* identified a HCV NS3-derived peptide (LNPSVAATL) that in complex with HLA-C*0102 is specifically recognized by KIR2DS2 triggering an activating signal within NK cells and resulting in target cell death (Naiyer *et al.*, 2017). Huh-7 cells expressing the N17/JFH-1 HCV subgenomic replicon and endogenously presenting LNPSVAATL peptide in the context of HLA-C*0102 specifically activated KIR2DS2-expressing NKL cells leading to a strong inhibition of viral replication. This effect was abrogated when P9 of LNPSVAATL peptide within the replicon was mutated by site-directed mutagenesis (L9D). Therefore, a central role for this viral peptide in the induction of KIR2DS2-mediated NK cell activation has been suggested.

Given the fact that MHC-I allelic polymorphism and virus-derived peptides are key determinants in the modulation of NK cell responses to HCV, the present study aimed to investigate the effect of HCV replication in Huh-7 cells expressing different HLA-C1 alleles (HLA-C*__0102__, HLA-C*__0304__ and HLA-C*__0802__) and the impact on NK cell functions. By using the wild-type and mutant replicon system described by Naiyer *et al*, this chapter also aimed to determine whether LNPSVAATL peptide bound to other HLA-C1 alleles besides HLA-C*__0102__ (HLA-C*__0304__ and HLA-C*__0802__) is relevant for KIR2DS2 recognition and induction of NK cell activity.

3.2 Generation of Huh-7 cell lines supporting HCV replication and presenting viral peptides in the context of HLA-C1 alleles

Genotyping of the HCC cell line Huh-7 has revealed that these cells normally express HLA-A*11, HLA-B*54 and HLA-C*01; however surface levels of HLA-B and HLA-C are reduced (Kurokohchi *et al.*, 1996). In order to generate target cells supporting HCV replication and endogenously presenting HCV-derived peptides in the context of HLA-C1 alleles, Huh-7 cells expressing the WT replicon (Huh-7 WT) or its L9D mutant (Huh-7 L9D) were retrovirally transduced with HLA-C*__0102__, HLA-C*__0304__ or HLA-C*__0802__ alleles.

As a first stage, retroviral-packaging Phoenix-Ampho cells were transfected with DNA plasmids carrying HLA-C*__0102__-YFP, HLA-C*__0304__-YFP or HLA-C*__0802__ (no YFP). After two weeks under antibiotic selection (blasticidin), Phoenix cells transfected with plasmids carrying the YFP tag were examined under fluorescence microscope. A moderate fluorescent emission was observed in both cell lines compared to the non-transfected control, which suggests that the DNA vectors were successfully delivered into Phoenix cells **(Figure 3.1)**. Transfected cells were incubated for longer time under antibiotic selection in order to obtain stable cell lines.

The next step consisted of retroviral transduction of Huh-7 WT or Huh-7 L9D cells using the viral supernatant from Phoenix cells transfected with HLA-C*__0102__-YFP, HLA-C*__0304__-YFP or HLA-C*__0802__ constructs. As controls, parental non-replicon Huh-7 cells expressing the corresponding alleles were also generated. The factors influencing the success of this method included cell confluency, concentration of the cationic polymer, start point for selection and concentration of both selectable antibiotics (puromycin and blasticidin), among others.

3.2.1 Non-replicon cells

Retroviral transduction of Huh-7 cells with HLA-C*__0102__-YFP or HLA-C*__0304__-YFP had been previously performed in our lab. Huh-7 cells expressing HLA-C*__0802__ (no YFP) were generated in this study. Expression of surface and total HLA-C was measured in the three

cell lines and compared to their parental cells (Huh-7). Surface HLA-C expression was determined using the anti-HLA-C antibody DT9 whereas total HLA-C expression was assessed by measuring the expression of YFP (except in cells transduced with HLA-C*0802).

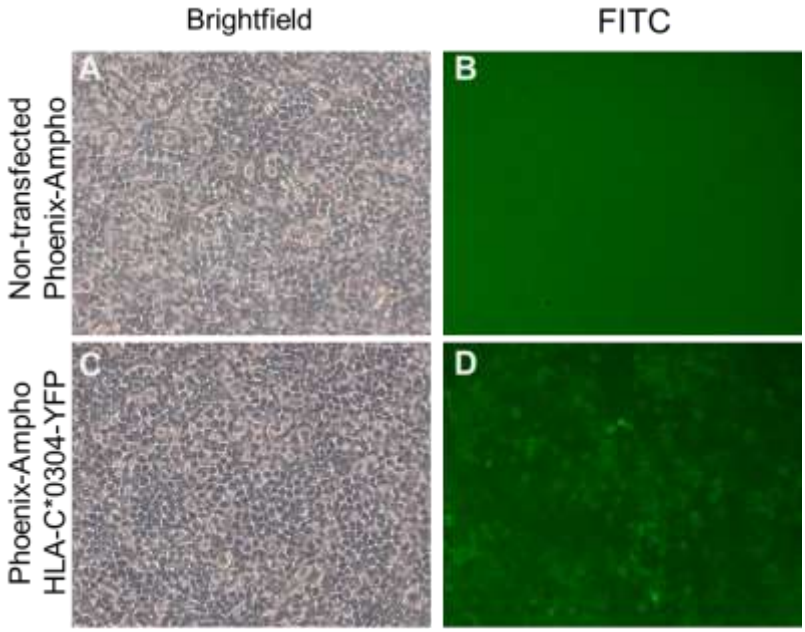

Figure 3.1 Transfection of Phoenix-Ampho cells with HLA-C1 alleles. Phoenix-Ampho cells were transfected with plasmids carrying HLA-C***0102**-YFP, HLA-C***0304**-YFP, or HLA-C***0802** (no YFP). YFP-tagged transfected Phoenix cells were examined under light **(A,C)** and fluorescence microscope **(B,D)**. The same field is shown under normal light (Brightfield) and fluorescent light (FITC channel) for each cell line. Only images for HLA-C***0304**-YFP are shown. Magnification 40X.

Surface HLA-C expression was significantly increased in the three transduced cell lines compared to non-transduced Huh-7 cells (MFI: 2132 vs 9555 for HLA-C***0102**, 7322 for HLA-C***0304** and 6797 for HLA-C***0802**; $p<0.0001$ for each comparison; **Figure 3.2A**). Regarding total HLA-C expression, Huh-7 cells transduced with HLA-C***0102** or HLA-C***0304** showed high MFI values that were statistically significant compared to non-transduced controls (MFI: 13935 vs 83700 and 65700, respectively $p<0.0001$ for each comparison; **Figure 3.2B**).

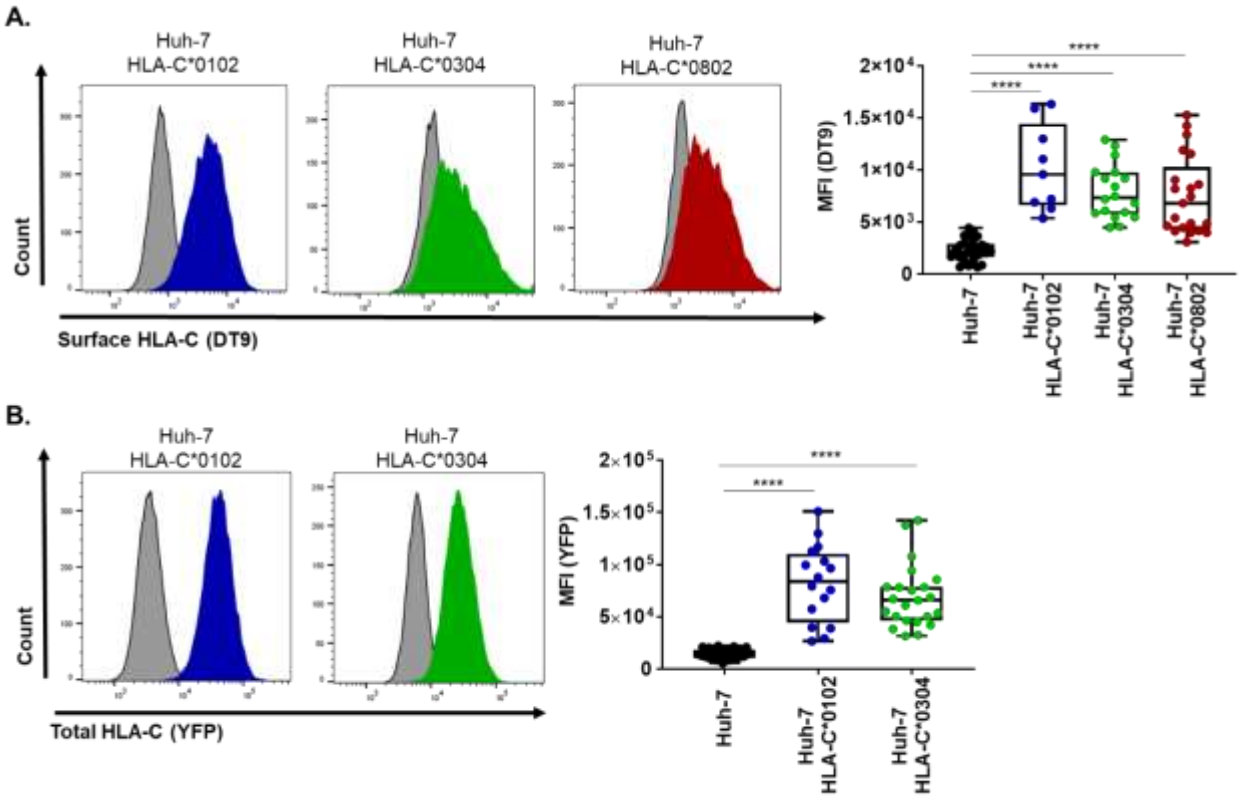

Figure 3.2 Expression of surface and total HLA-C on non-replicon Huh-7 cells transduced with HLA-C1 alleles. Expression of surface **(A)** and total HLA-C **(B)** in non-replicon Huh-7 cells transduced with HLA-C***0102**-YFP (blue), HLA-C***0304**-YFP (green) or HLA-C***0802** (no YFP; red) compared to their parental cell line (grey). Box and whiskers plots show Mean Fluorescence Intensities (MFI) values of surface **(A)** and total HLA-C **(B)** expression for the corresponding cell lines. Each dot represents a single measurement. Median and interquartile range of at least ten independent experiments are shown (n=10-22). Differences were determined with the unpaired t-test. Comparison of total HLA-C between Huh-7 and Huh-7 HLA-C*0304 cells was performed using a Mann-Whitney test as the latter did not follow a normal distribution. P value **** <0.0001.

3.2.2 Replicon cells

3.2.2.1 Huh-7 cells carrying the WT replicon

Huh-7 WT cells expressing HLA-C***0102**-YFP, HLA-C***0304**-YFP or HLA-C***0802** (no YFP) were generated in this study. Luciferase activity – which is an indirect measure of HCV replicon replication – as well as expression of surface (DT9) and total HLA-C (YFP) were measured in the three cell lines and compared to their parental cells (Huh-7 WT).

Luciferase activity of the three newly generated cell lines was reduced compared to their parental cell line ($p<0.0001$ for HLA-C*__0102__ and HLA-C*__0304__; $p=0.0066$ for HLA-C*__0802__). Despite this decline, luciferase units still remained significantly above non-replicon controls with no less than $1x10^3$ units for HLA-C*__0102__ ($p=0.0002$) and $1x10^4$ units for HLA-C*__0304__ and HLA-C*__0802__-expressing cells ($p<0.0001$ for each comparison; **Figure 3.3A**). Evaluation of replicon replication over time showed a gradual reduction in the luciferase activity of replicon cells, suggesting that Huh-7 cells were unable to support sustained replication of the HCV replicon **(Figure 3.3A)**.

Expression of surface HLA-C was significantly increased on the three transduced cell lines compared to their parental cell line (MFI: 2045 vs 5378 for HLA-C*__0102__, 4487 for HLA-C*__0304__ and 3905 for HLA-C*__0802__; $p<0.0001$ and $p=0.0001$, respectively; **Figure 3.3B**). Similarly, expression of total HLA-C was significantly increased in Huh-7 WT cells transduced with HLA-C*__0102__ or HLA-C*__0304__ compared to non-transduced Huh-7 WT cells (MFI: 18029 vs 97938 and 124028, respectively; $p<0.0001$ for each comparison; **Figure 3.3C**).

3.2.2.2 Huh-7 cells carrying the L9D mutant replicon

Retroviral transduction of Huh-7 L9D cells with HLA-C*__0102__-YFP had been previously performed in our laboratory. Huh-7 L9D cells expressing HLA-C*__0304__-YFP or HLA-C*__0802__ (no YFP) were generated in this study. Luciferase activity and expression of surface (DT9) and total HLA-C (YFP) were measured in the three cell lines and compared to their parental cell line (Huh-7 L9D).

The luciferase activity of the three cell lines was reduced compared to parental cells. This difference was statistically significant for Huh-7 L9D cells expressing the HLA-C*__0102__ and HLA-C*__0802__ alleles ($p<0.0001$ for each comparison), but not for those expressing HLA-C*__0304__ ($p=0.1687$; **Figure 3.4A**). Of notice, Huh-7 L9D cells expressing HLA-C*__0304__ was the most stable cell line amongst newly generated Huh-7 cell lines. As with the WT replicon, Huh-7 L9D cells did not support high replication levels over time **(Figure 3.4A)**.

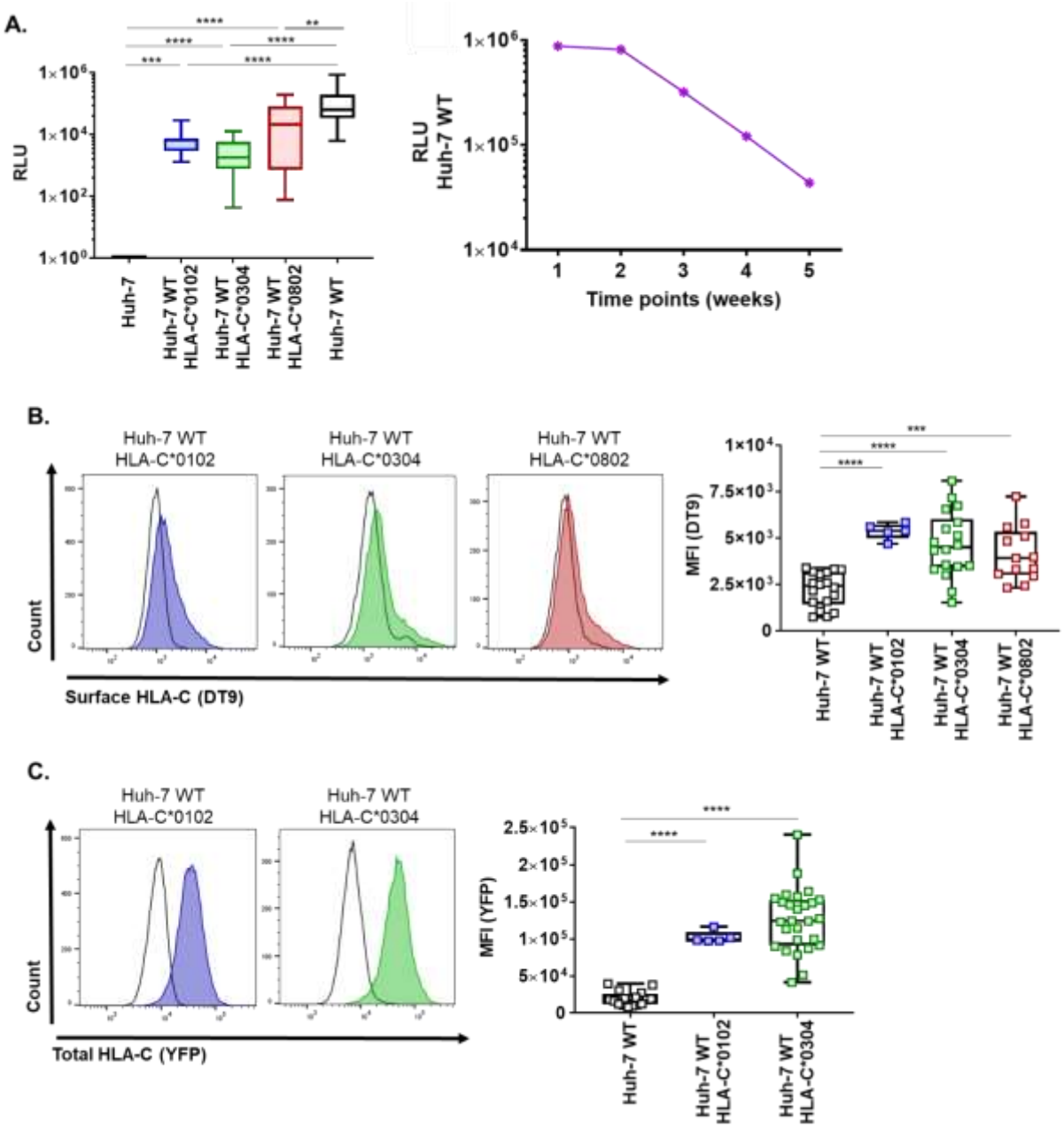

Figure 3.3 Luciferase activity and expression of surface and total HLA-C of Huh-7 WT cells transduced with HLA-C1 alleles. (A) Luciferase activity of Huh-7 WT cells transduced with HLA-C***0102**-YFP (blue), HLA-C***0304**-YFP (green) or HLA-C***0802** (no YFP; red) compared to their parental cell line (white). Box and whiskers plot (left) shows relative luciferase units (RLU). The line chart (right) shows the replication of the WT replicon over a period of 5 weeks. Expression of surface **(B)** and total HLA-C **(C)** on Huh-7 cells co-expressing the WT replicon and HLA-C1 alleles compared to their parental cell line. Box and whiskers plots show MFI values of surface **(B)** and total HLA-C **(C)** expression for the corresponding cell lines. Each dot represents a single measurement. Median and interquartile range of at least five independent experiments are shown (n=5-27). Differences were determined with the unpaired t-test. Comparison of luciferase activity among cell lines and of total HLA-C between Huh-7 WT HLA-C*0102 and its parental cell line was performed using a Mann-Whitney test as those did not follow a normal distribution. P value ** <0.01, *** <0.001, **** <0.0001.

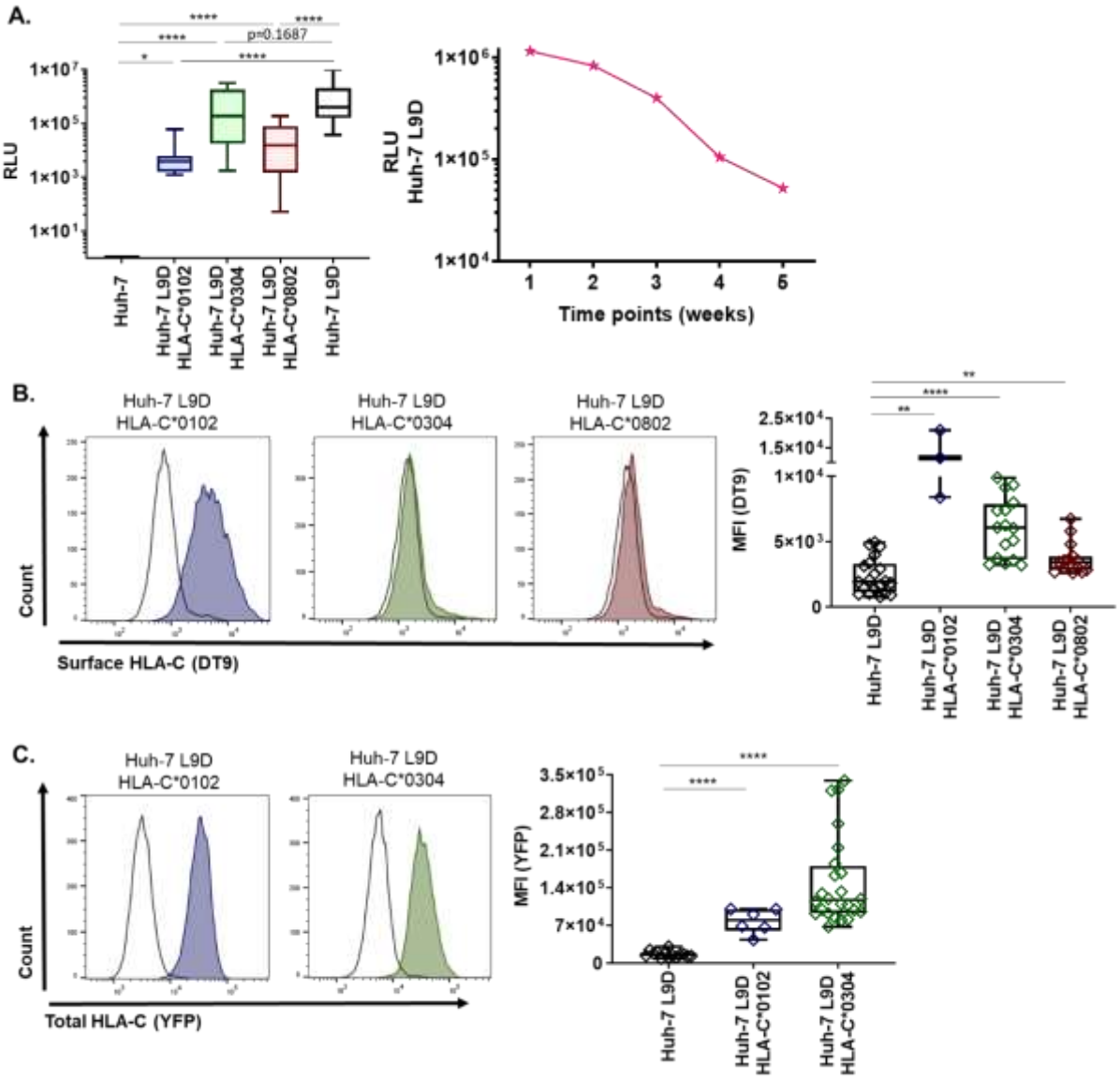

Figure 3.4 Luciferase activity and expression of surface and total HLA-C of Huh-7 L9D cells transduced with HLA-C1 alleles.Luciferase activity of Huh-7 L9D cells transduced with HLA-C*__0102__-YFP (blue), HLA-C*__0304__-YFP (green) or HLA-C*__0802__ (no YFP; red) compared to their parental cell line (white). Box and whiskers plot (left) shows RLU. The line chart (right) shows the replication of the L9D replicon over a period of 5 weeks. Expression of surface **(B)** and total HLA-C **(C)** on Huh-7 cells co-expressing the mutant replicon and HLA-C1 alleles compared to their parental cell line. Box and whiskers plots show MFI values of surface **(B)** and total HLA-C **(C)** expression for the corresponding cell lines. Each dot represents a single measurement. Median and interquartile range of at least three independent experiments are shown (n=3-22). Differences were determined with the Mann-Whitney test. Comparison of total HLA-C between Huh-7 L9D HLA-C*0102 and its parental cell line was performed using an unpaired t-test as both followed a normal distribution. P value ns=non-significant, * <0.05, ** <0.01, **** <0.0001.

Surface HLA-C expression on Huh-7 L9D cells transduced with HLA-C*__0102__, HLA-C*__0304__ or HLA-C*__0802__ alleles was significantly increased compared to cells expressing the mutant replicon alone (MFI: 1952 vs 11564, 6066 and 3449; p=0.0011, p<0.0001 and p=0.0044; respectively; **Figure 3.4B**). Likewise, Total HLA-C expression in cells transduced with HLA-C*__0102__ or HLA-C*__0304__ was significantly increased compared to its parental cell line (MFI: 15655 vs 79991 and 117266, respectively; p<0.0001 for each comparison; **Figure 3.4C**).

Altogether, these results confirm the successful generation of stable Huh-7 cell lines co-expressing WT or L9D replicons and different HLA-C1 alleles. As both replicons were unable to achieve long-term stable replication within Huh-7 cells, the luciferase activity was constantly monitored and only cells expressing >1x10^4 RLU were used for further experiments.

3.3 The HCV replicon preferentially down-regulates surface expression of HLA-C

To determine whether HCV replicon replication modulates the expression of HLA-C alleles, replicon and non-replicon cell lines were compared in terms of surface (DT9) or total HLA-C (YFP) as well as surface MHC-I expression (W6/32). Of note, Huh-7 L9D cells expressing HLA-C*__0102__ were not taken into account in the following analysis as this cell line showed considerably reduced luciferase units over time and less than 3 measurements could be obtained.

First, to assess whether HCV replicon affects the expression of HLA-C at the cell membrane, surface expression of HLA-C alleles was compared in replicon vs non-replicon cells. Surface HLA-C expression of newly generated replicon cells (WT and L9D) was significantly reduced compared to non-replicon cells expressing either HLA-C*__0102__ (MFI: 9555 vs 5378; p=0.0070), HLA-__C*0304__ (MFI: 7322 vs 4487 or 6066; p=0.0009 and p=0.0368, respectively) or HLA-C*__0802__ alleles (MFI: 6797 vs 3173 or 3449; p=0.0001 and p<0.0001, respectively; **Figure 3.5A-C**). As both HCV replicons have been shown to be actively replicating within transduced cell lines, these data suggest a role for virus replication in surface down-regulation of HLA-C molecules.

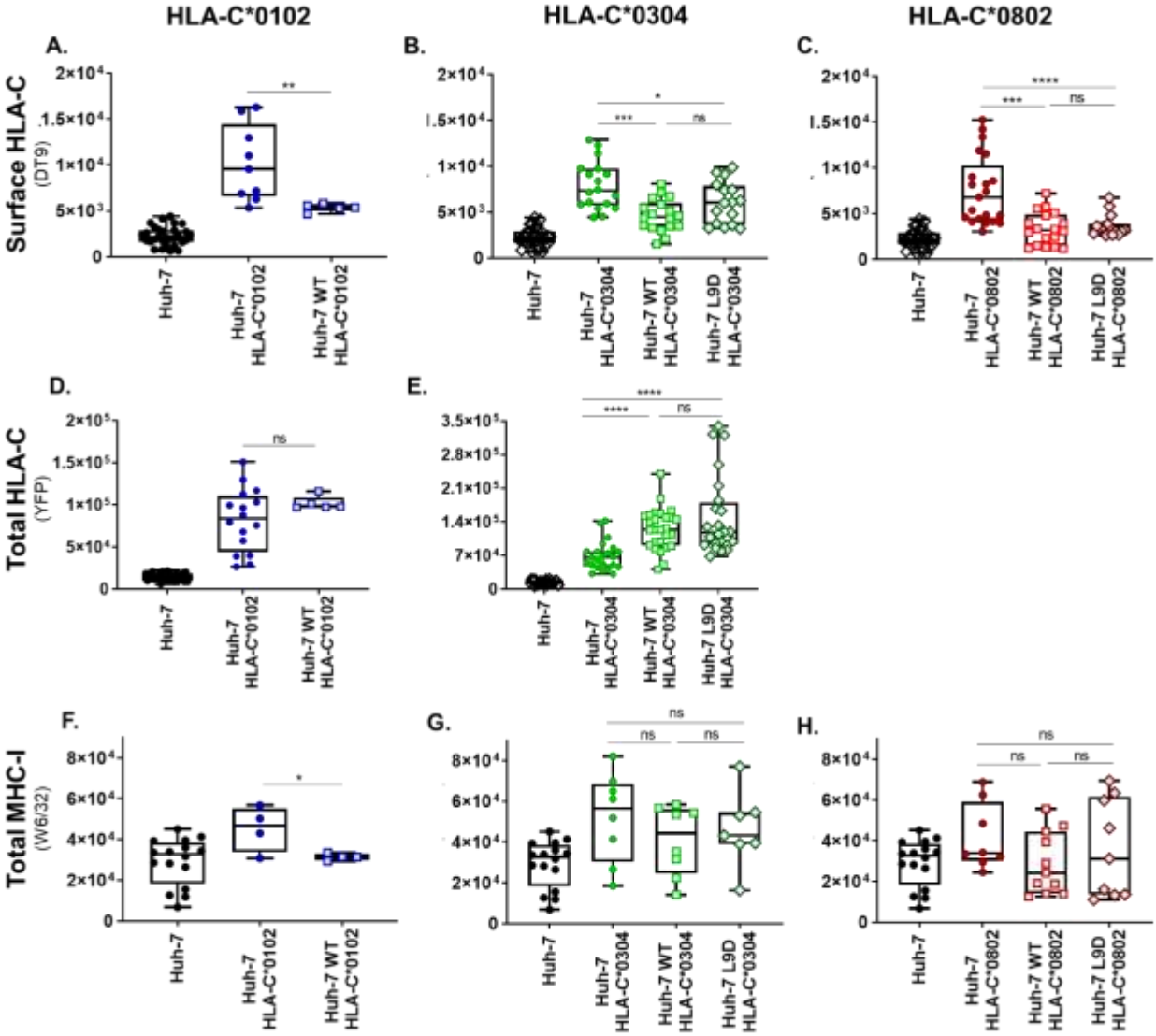

Figure 3.5 Expression of surface HLA-C, total HLA-C and surface MHC-I on non-replicon and replicon cells transduced with HLA-C1 alleles. Expression of surface HLA-C **(A)** total HLA-C **(B)** and surface MHC-I **(C)** on Huh-7 WT or Huh-7 L9D cells transduced with HLA-C*__0102__-YFP (left), HLA-C*__0304__-YFP (middle) or HLA-C*__0802__ (no YFP; right) compared to non-replicon cells expressing the same allele. Box and whiskers plots show MFI values of surface HLA-C **(A-C),** total HLA-C **(D-E)** and surface MHC-I expression **(F-H)** for the corresponding cell lines. Each dot represents a single measurement. Median and interquartile ranges of at least four independent experiments are shown (n=4-22). Differences were determined with the unpaired t-test. Differences among normal variables were determined with the unpaired t-test whereas those that did not follow a normal distribution were analysed using a Mann-Whitney test. P value ns=non-significant, * <0.05, ** <0.01, *** <0.001, **** <0.0001.

Then, to determine whether reduced levels of surface HLA-C were associated with intracellular accumulation of these molecules, total HLA-C expression was compared in replicon vs non-replicon cells. Interestingly, unlike surface HLA-C expression, levels of total HLA-C were significantly increased on cells co-expressing either the WT or L9D replicon and HLA-C*__0304__ compared to their corresponding non-replicon controls (MFI: 56034 vs 108812 or 115485; p<0.0001 for each comparison; **Figure 3.5E**). A trend towards an increase was also seen in Huh-7 WT cells expressing the HLA-C*__0102__ allele; however, these differences did not reach statistical significance (MFI: 83700 vs 97938; p=0.2748; **Figure 3.5D**). Together, these results strongly suggest that HLA-C molecules are being synthesized within replicon cells but are retained intracellularly and therefore are unable to reach the cell membrane. HCV-induced intracellular accumulation of MHC-I molecules within the ER has been previously reported (Tardif and Siddiqui, 2003).

Finally, to assess the effect of HCV replicons in the modulation of HLA-A (HLA-A11) at the cell membrane, surface expression of MHC-I was determined using the pan-HLA class I-specific antibody W6/32. Overall, there was a slight reduction of MHC-I expression in replicon cells expressing either of the three HLA-C1 alleles compared to non-replicon controls expressing the corresponding allele. These differences were not statistically significant for any of the WT or L9D cells tested (MFI: 46687 vs 31440, p=0.0658 for HLA-C*__0102__; MFI: 56509 vs 44379 or 43200; p=0.2701 and p=0.5827 for HLA-C*__0304;__ MFI: 33881 vs 24251 or 31171, p=0.0982 and p=0.7523 for HLA-C*__0802__, respectively; **Figure 3.5F-H**). This suggests that surface levels of HLA-A11 are not affected by HCV replication and its expression could compensate down-regulated HLA-C molecules at the cell surface.

To understand more deeply the relation between HLA-C and HLA-A11, the ratio between surface HLA-C and surface MHC-I expression was calculated. As shown in **Figure 3.6**, HLA-C/MHC-I ratio was significantly reduced for WT and L9D replicon cells compared to their corresponding controls expressing HLA-C*__0102__ (0.2870/0.1898; p=0.01), HLA-C*__0304__ (0.1291/0.1026 and 0.1291/0.0910; p=0.0486 and p=0.0401, respectively) or HLA-C*__0802__ (0.1807/0.0956 and 0.1807/0.0876; p=0.0002 and p<0.0001, respectively; **Figure 3.6**). Thus, HCV seems to mediate a preferential down-regulation of HLA-C, but not of HLA-A11.

Taken together, these results suggest that productive replication of HCV prevents expression of HLA-C molecules at the surface of Huh-7 cells leading to their intracellular accumulation. This phenomenon could have an impact in the recognition of virus-infected cells by NK cells expressing receptors specific for those ligands.

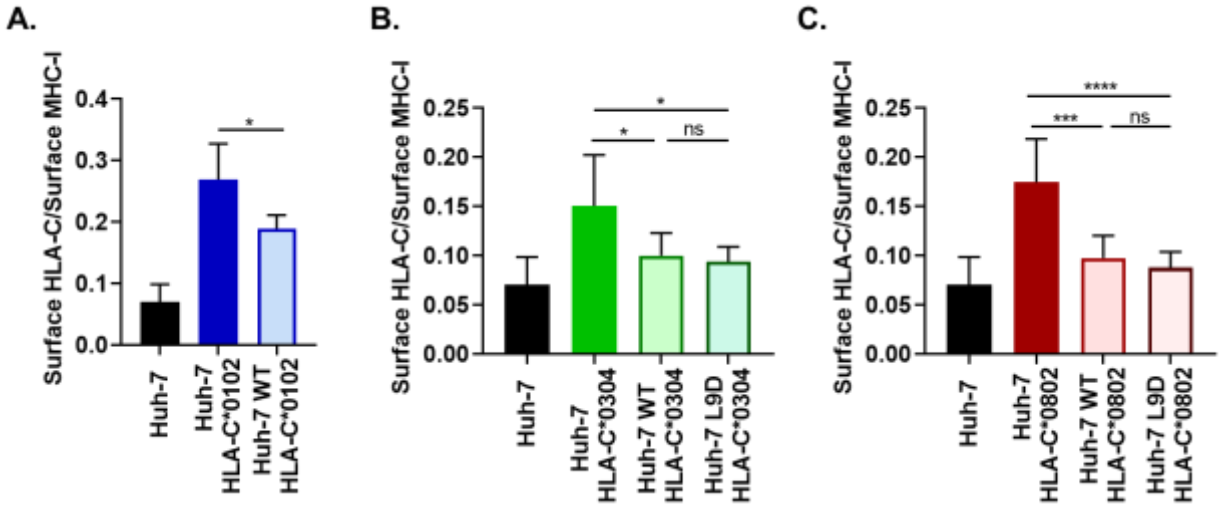

Figure 3.6 Relation of surface HLA-C and MHC-I of non-replicon and replicon cells transduced with HLA-C1 alleles. The relation between surface HLA-C and MHC-I of non-replicon and replicon cells transduced with HLA-C***0102**-YFP **(A)**, HLA-C***0304**-YFP **(B)** or HLA-C***0802 (C)** was determined by calculating the ratio between MFI of surface HLA-C and surface MHC-I. Mean values and SD are shown of at least three independent experiments are shown (n=3-5). Differences among normal variables were determined with the unpaired t-test whereas those that did not follow a normal distribution were analysed using a Mann-Whitney test. P value ns=non-significant, * <0.05, *** <0.001, **** <0.0001.

3.4 Down-regulation of HLA-C1 alleles renders HCV replicon-expressing cells susceptible to NK cell attack

Inhibitory and activating KIR differ in their mechanisms of target cell recognition. On one hand, down-regulation of inhibitory KIR ligands has shown to promote NK cell activation through missing-self whereas, on the other hand, presentation of viral epitopes triggers NK cell responses through activating KIR (Stewart *et al.*, 2005b; Raulet, 2006). To investigate the relevance of HCV-mediated HLA-C down-modulation on NK cell activity through KIR2DL2/S2, as a first stage, a co-culture system using primary NK cells expressing KIR2DL2/L3/S2 receptors and Huh-7 cells co-expressing the HCV replicon (WT) and HLA-C1 ligands was optimized.

For this, PBMC from healthy volunteers were isolated and tested for KIR2DL2/L3/S2 phenotyping using a multi-colour flow cytometry-based panel developed by our group (Blunt *et al.*, 2019). This panel allowed to identify three different CD3- CD56+ NK cell subsets in individuals with KIR2DL2/S2 homozygous or KIR2DL2/L3/S2 heterozygous genotypes, two of them with relatively high expression of those receptors: 1) KIR2DL2/L3/S2^{neg}, 2) KIR2DL2^{high} or KIR2DL2/L3^{high}, respectively and 3) KIR2DS2^{high} **(Figure 3.7A)**. Even though the KIR2DS2^{high} subset may contain a mixed population of NK cells expressing KIR2DL2/L3, the inhibitory effect is much less pronounced (Blunt *et al.*, 2019). The NK cell phenotype for each donor was confirmed by KIR genotyping **(Figure 3.7B)** (Gomez-Lozano and Vilches, 2002).

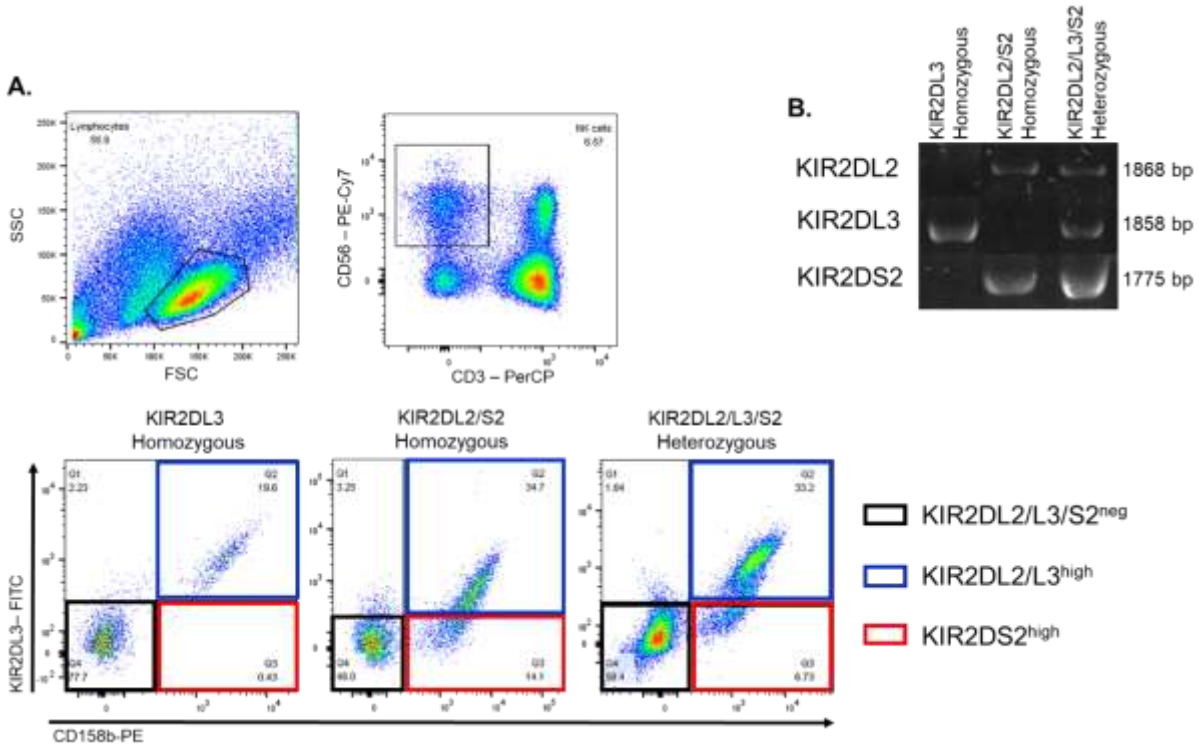

Figure 3.7 Multi-colour flow cytometry panel to discriminate KIR2DL2 from KIR2DS2 in primary NK cells. A. FSC/SSC plot show the population of lymphocytes from PBMC of healthy volunteers. NK cells were identified using anti-CD3-PerCP and CD56-PECy7 antibodies (CD3-CD56+). Three NK cell subsets were discriminated using anti-CD158b-PE (clone CH-L) and anti-KIR2DL3-FITC (clone REA147) antibodies: KIR2DL2/L3/S2^{neg} (black square) KIR2DL2/L3^{high} (blue square) and KIR2DS2^{high} (red square). Plots for KIR2DL3 homozygous, KIR2DL2/S2 homozygous and KIR2DL2/L3/S2 heterozygous donors are shown. **B.** NK cell phenotype was confirmed by KIR genotyping using specific primers for KIR2DL2, KIR2DL3 and KIR2DS2.

Once KIR phenotype and genotype was confirmed, PBMC from KIR2DL2/S2 homozygous (n=2-3) or KIR2DL2/L3/S2 heterozygous donors (n=5-6) were used as effector cells in degranulation assays against different Huh-7 WT cells at 5:1 ratio. As no differences between homozygous and heterozygous donors have been noticed, the data from both types of donors were pooled. The degranulation profile of KIR2DL2/L3/S2^{neg}, KIR2DL2/L3^{high} and KIR2DS2^{high} NK cell subpopulations was analysed. The gating strategy for LAMP-1 degranulation assay is shown in **Figure 2.8**.

The KIR2DL2/L3/S2^{neg} NK cell subpopulation showed significantly high levels of CD107a to Huh-7 WT HLA-C***0102** cells compared to cells expressing the HLA-C***0102** allele alone (p=0.0173; **Figure 3.8A**). This finding would suggest that other KIR receptors could be involved in the recognition of HLA-C***0102**-expressing replicon cells, possibly KIR2DS4, which has shown to bind HLA-C*0102 alleles (Graef *et al.*, 2009). KIR2DL2/L3/S2^{neg} NK cell activation through KIR-independent mechanisms could also be suggested. On the other hand, this NK cell subset did not showed statistically significant levels of degranulation against replicon cells expressing either HLA-C***0304** or HLA-C***0802** compared to their corresponding non-replicon controls **(Figure 3.8B,C)**.

Overall, the percentages of CD107a from KIR2DL2/L3^{high} or KIR2DS2^{high} NK cells were significantly increased against Huh-7 WT cells expressing either of the HLA-C1 alleles compared to their corresponding non-replicon controls (p=0.0017 and p=0.0039 for HLA-C***0102**; p=0.0146 and p=0.0029 for HLA-C***0304**; p=0.0295 and p=0.0466 for HLA-C***0802**, respectively; **Figure 3.8A-C**). This suggests that replicon-expressing cells with a down-regulated expression of HLA-C1 alleles are susceptible to be recognized by NK cells through KIR2DL2/L3 and KIR2DS2 receptors.

3.5 LNPSVAATL peptide is not associated with KIR2DS2-mediated recognition of HCV replicon cells expressing HLA-C1 alleles

To investigate whether activation of the KIR2DS2^{high} NK cell subset against different Huh-7 WT targets was the result of endogenous presentation of LNPSVAATL peptide by HLA-C1 alleles, Huh-7 cells carrying the WT or L9D replicons alone or co-expressing HLA-C***0304** or HLA-C***0802** alleles were co-cultured with PBMC from KIR2DL2/S2 homozygous (n=2)

or KIR2DL2/L3/S2 heterozygous donors (n=4-6) at 5:1 ratio. The degranulation profile of KIR2DL2/L3/S2^{neg}, KIR2DL2/L3^{high} and KIR2DS2^{high} NK cells was analysed and compared to each other

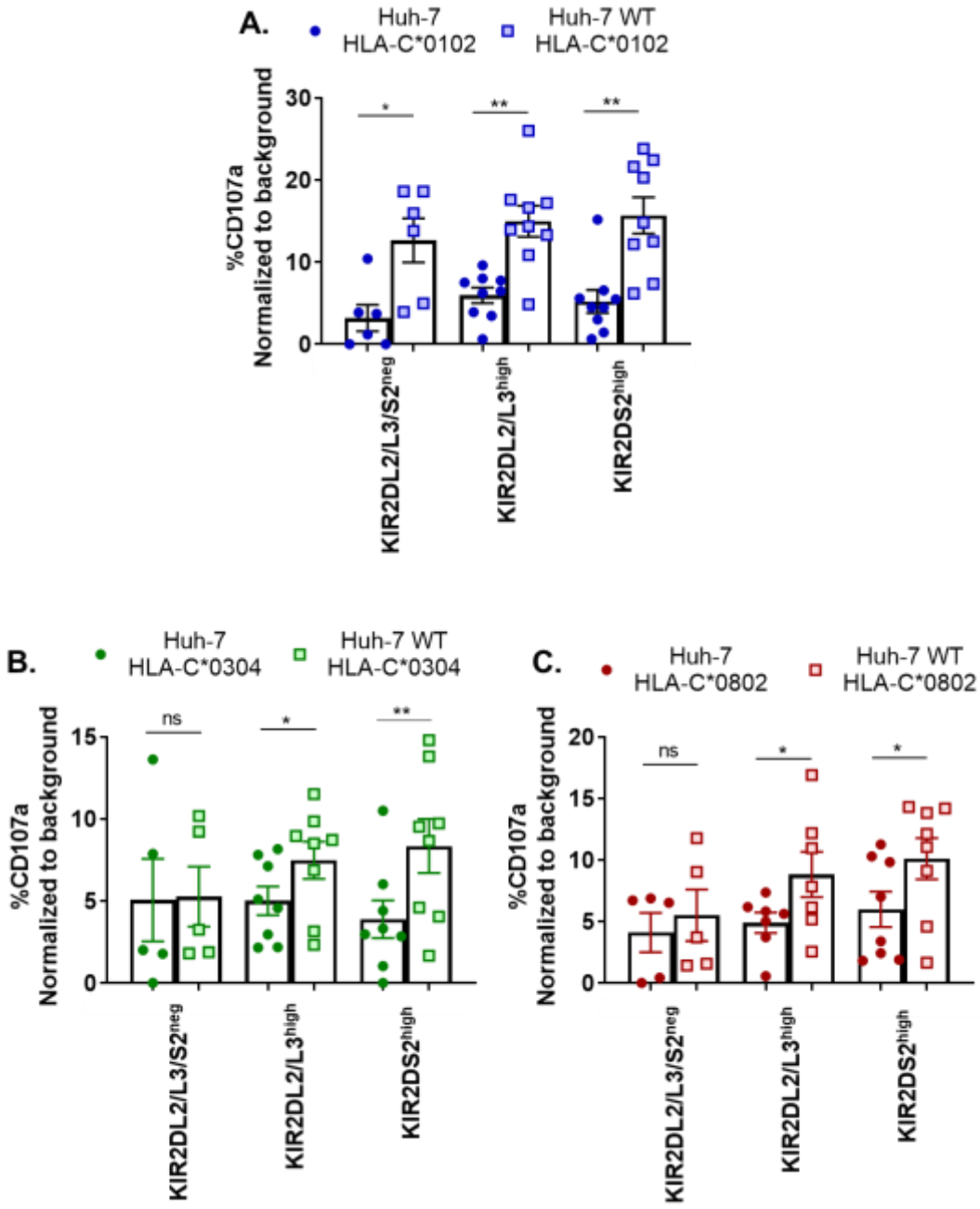

Figure 3.8 Degranulation of PBMC-derived NK cells to Huh-7 WT cells transduced with HLA-C1 alleles. Scatter dot plots show the percentage of CD107a expression of KIR2DL2/L3/S2^{neg}, KIR2DL2/L3^{high} and KIR2DS2^{high} NK cell subsets against Huh-7 WT cells or non-replicon controls transduced with HLA-C***0102 (A)**, HLA-C***0304 (C)** or HLA-C***0802 (E)** at 5:1 ratio. CD107a from the No target control was subtracted. Mean values and SD of at least five independent experiments are shown (n=5-8). Differences were determined with a paired t-test. P value ns=non-significant, * <0.05, ** <0.01.

Degranulation levels between KIR2DL2/L3^{high} and KIR2DS2^{high} NK cells were similar against cells expressing the WT replicon alone (CD107a: 11% vs 10.8%; p=0.8922; **Figure 3.9A**). Conversely, the KIR2DS2^{high} NK cell subset showed a trend towards a stronger degranulation against replicon cells co-expressing either HLA-C***0304** or HLA-C***0802**; however those differences were not statistically significant (CD107a: 7.5% vs 8.3%; p=0.4207 and CD107a: 8.8% vs 10.1%; p=0.4271, respectively; **Figure 3.9B,C**).

Similarly, degranulation of KIR2DL2/L3^{high} and KIR2DS2^{high} NK cells were equivalent to each other against Huh-7 cells harbouring the mutant replicon alone (CD107a: 8.7% vs 8.6%; p=0.9693; **Figure 3.9D**) or the ones co-expressing HLA-C***0304** (CD107a: 9.9% vs 9.6%; p=0.8583) or HLA-C***0802** alleles (CD107a: 7.7% vs 8.4%; p=0.5466; **Figure 3.9E,F**). These data suggest that, in the presence of HLA-C***0304** or HLA-C***0802** alleles, LNPSVAATL peptide does not mediate activation of KIR2DS2-expressing NK cells.

3.6 KIR2DS2 mediates inhibition of HCV replication in cells expressing HLA-C1 alleles independently of LNPSVAATL peptide

To evaluate more in depth the role of LNPSVAATL peptide in terms of target cell recognition, a co-culture system to assess inhibition of viral replication in Huh-7 WT or Huh-7 L9D cells expressing individual HLA-C1 alleles by effector cells expressing individual KIR receptors had been optimized in our laboratory. These effector cells consist of the human natural killer cell leukaemia cell line (NKL) that was previously characterized by Robertson *et al* (Robertson *et al.*, 1996). The NKL cell line does not normally express KIR receptors on their surface, therefore transduction of NKL cells with plasmids carrying genes encoding inhibitory KIR2DL2 (NKL-2DL2) or activating KIR2DS2 receptors (NKL-2DS2) was previously performed (Naiyer *et al.*, 2017).

.

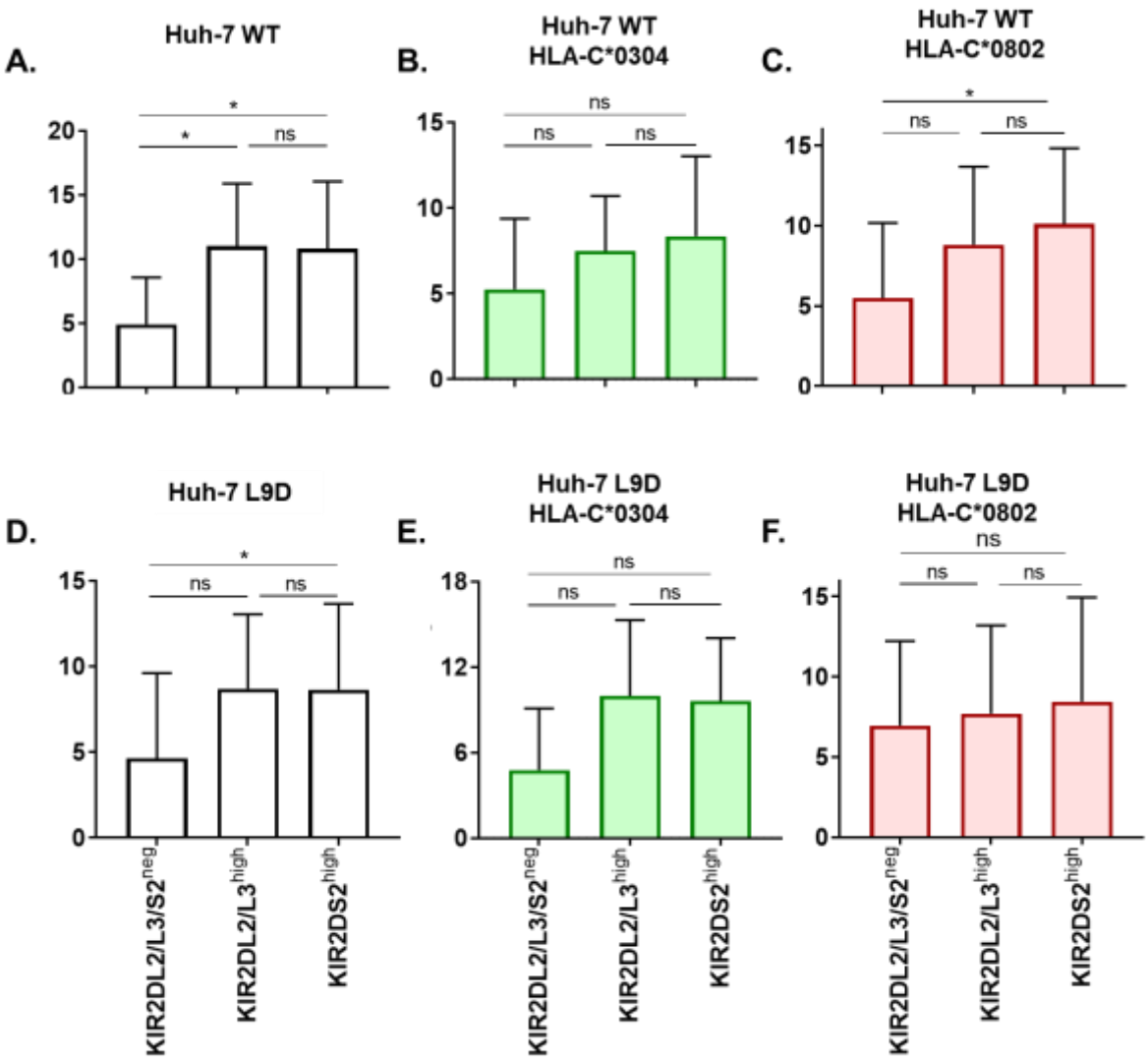

Figure 3.9 Degranulation of PBMC-derived NK cells to Huh-7 WT or Huh-7 L9D cells transduced with HLA-C1 alleles. Bar plots show the percentage of CD107a expression of KIR2DL2/L3/S2^{neg}, KIR2DL2/L3^{high} and KIR2DS2^{high} NK cell subsets against Huh-7 cells expressing the WT **(A)** or L9D replicon **(D)** and the ones transduced with HLA-C***0304 (B,E)** or HLA-C***0802 (C,F)** at 5:1 ratio. CD107a from the No target control was subtracted. Mean values and SD of at least five independent experiments are shown (n=5-8). Differences were determined with a paired t-test. P value ns=non-significant, * <0.05.

As a first step, KIR receptor expression at the surface of NKL-2DL2 or NKL-2DS2 cells was assessed by flow cytometry. Both cell lines were positive for anti-CD158b-PE staining compared to parental NKL cells (p=0.0030 for NKL-2DL2 and p=0.0015 for NKL-2DS2), with the fluorescence being significantly brighter for NKL-2DL2 cells (p=0.0055; **Figure 3.10A**). To precisely confirm the expression of KIR2DL2 or KIR2DS2, these cells were stained with anti-1F12, an antibody that recognizes KIR2DL3/S2, but not KIR2DL2 (David *et al.*, 2009). As expected, only NKL-2DS2 cells showed an increased binding to 1F12

(Figure 3.10B), which confirms the correct expression of KIR at the surface of the corresponding NKL cell lines.

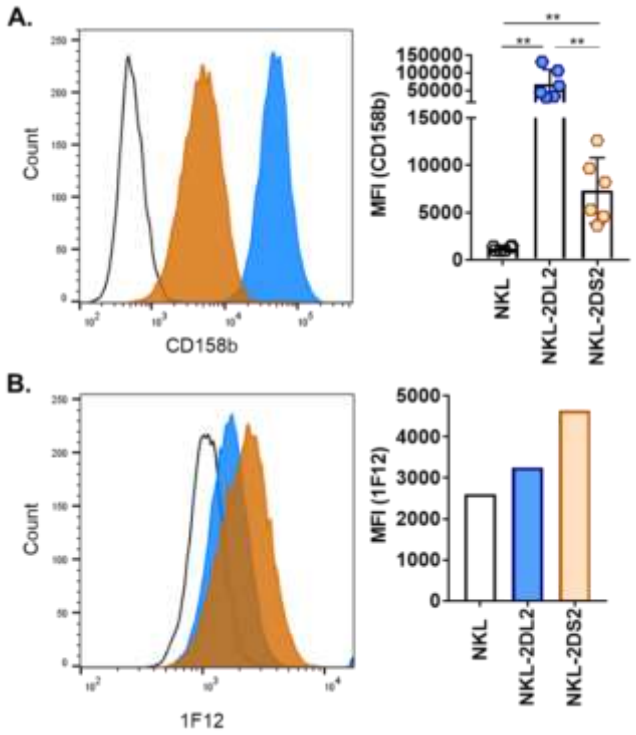

Figure 3.10 Expression of KIR2DL2 or KIR2DS2 receptors by transduced NKL cell lines. NKL cells had been previously transduced with individual KIR2DL2 or KIR2DS2-encoding genes. NKL cell lines were tested for KIR receptor expression using CD158b, which recognizes KIR2DL2/L3/S2 **(A)**, or 1F12, which binds KIR2DL3/S2, but not KIR2DL2 **(B)**. Bar plots show MFI of CD158b **(A)** or 1F12 expression **(B)** of non-transduced NKL (white), NKL-2DL2 (blue) or NKL-2DS2 (orange) cell lines. Mean values and SD of six independent experiments are shown in **A** whereas values from only one experiment are shown in **B**.

The next step included the co co-culture of target and effectors cells at 0.1:1 ratio and the subsequent assessment of the NKL-mediated inhibition of viral replication. As targets, Huh-7 cells co-expressing the WT or L9D replicon and HLA-C*__0304__ or HLA-C*__0802__ alleles were used. As effectors, parental NKL, NKL-2DL2 or NKL-2DS2 cells were used.

For Huh-7 cells expressing the WT replicon alone, the percentage of inhibition of viral replication did not differ after co-culture with NKL-2DL2 or NKL-2DS2 cells, although a slight increase with NKL-2DS2 cells was evident; however, it was not statistically significant (p=0.1898; **Figure 3.11A**). NKL-2DS2 cells showed a more robust response to Huh-7 cells co-expressing the WT replicon and HLA-C*__0304__ or HLA-C*__0802__ alleles as compared to that

from NKL-2DL2 cells. This difference was statistically significant for both alleles (p=0.0320 for HLA-C*0304 and p=0.0188 for HLA-C*0802; **Figure 3.11B,C**).

Similar findings were observed for cells expressing the mutant HCV replicon alone as NKL-2DL2 and NKL-2DS2 cells inhibited viral replication at a similar extent, with this effect being slightly increased for NKL-2DS2 cells (p=0.1958; **Figure 3.11D**). Similar to WT replicon, NKL-2DS2 cells induced a strong inhibition of HCV replication in cells co-expressing the L9D mutant and HLA-C*0304 or HLA-C*0802 alleles (p=0.0093 and p=0.0122, respectively; **Figure 3.11E,F**) as compared to NKL-2DL2 cells. As mutation of LNPSVAATL peptide did not have a differential effect in KIR2DS2-mediated NK cell activation, it is suggested that engagement of KIR2DS2 with HLA-C*0304 or HLA-C*0802 alleles is independent of this viral peptide

.

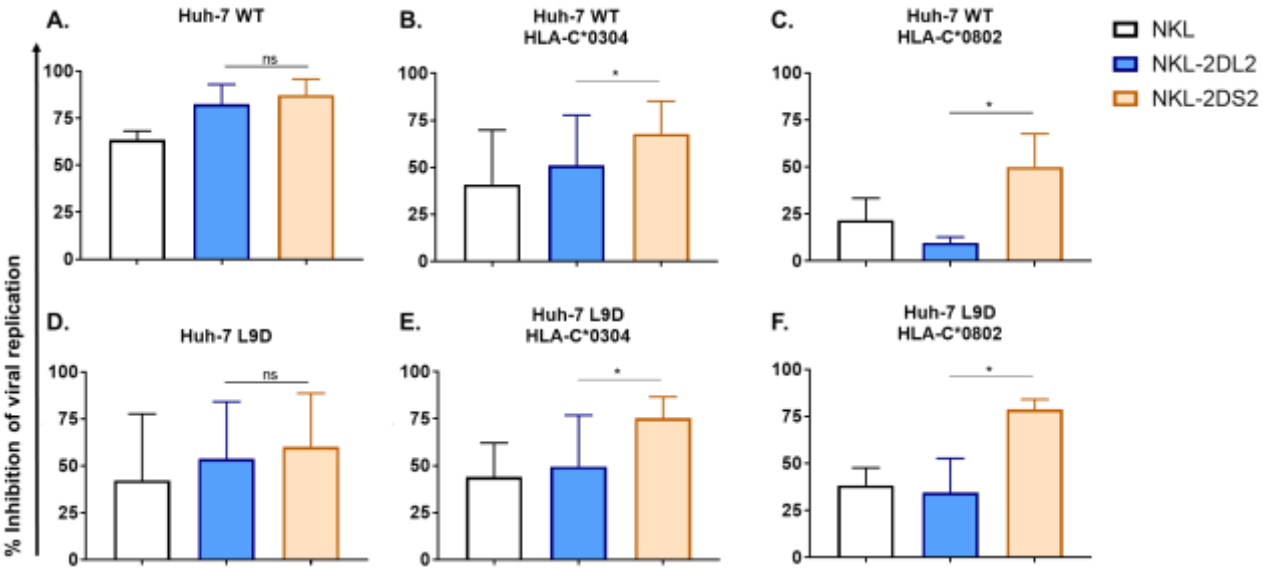

Figure 3.11 Inhibition of viral replication by NKL cell lines. Huh-7 WT (top panel) or Huh-7 L9D cells (bottom panel) transduced with HLA-C*0304 or HLA-C*0802 were co-cultured with non-transduced NKL (white), NKL-2DL2 (blue) or NKL-2DS2 cells (orange) at 0.1:1 ratio. After 24h, the inhibition of viral replication was assessed by measuring the reduction in luciferase activity. The percentage of inhibition of viral replication was calculated. Mean values and SD of at least three independent experiments are shown (n=3-5). Differences were determined with the Paired t-test. P value ns=non-significant * <0.05.

Taken together, these results suggest that NK cells activation against replicon cells expressing HLA-C*0304 or HLA-C*0802 alleles is mainly mediated through KIR2DS2 and that LNPSVAATL peptide is not required to induce such responses**.** Therefore it can be assumed that other HCV-derived peptides in complex with these alleles could be recognized by KIR2DS2 and together be able to induce NK cell anti-viral responses.

3.7 *In silico* analysis suggests that the binding specificity of LNPSVAATL peptide is restricted to the HLA-C*0102 allele

Binding of self and non-self peptides to HLA-C1 or C2 alleles is determined by anchor residues within the peptide sequence. LNPSVAATL is a 9-mer peptide that carries a polar amino acid at P2 (asparagine), non-polar residues at P3 (proline) and P9 (leucine), and additionally, contains the KIR2DS2-binding motif “AT” at P7 and P8. Peptide motifs of HLA-C alleles have been recently revealed and showed that HLA-C***0102** is the only HLA-C allele displaying a preference for proline at P3 and leucine at the C-terminus of 9-mer and 10-mer peptides (Di Marco *et al.*, 2017), suggesting a unique binding specificity of this viral peptide.

To determine whether LNPSVAATL peptide is likely to bind other HLA-C1 or C2 alleles, peptide binding prediction was performed using NetMHCpan. This software calculates the binding level of peptides based on the rank percentages of the binding affinity, which is predicted according to a set of natural eluted peptides (Jurtz *et al.*, 2017). Strikingly, the rank value of LNPSVAATL peptide to different HLA-C1 and C2 alleles was higher than the threshold for weak binders determined by the NetMHCPan software and therefore was categorized as non-binder **(Table 3.1)**.

Table 3.1 Binding prediction of LNPSVAATL peptide to HLA-C1 and C2 alleles

Group	Allele	Binding affinity (nM)	% Rank	Binding level
HLA-C1	HLA-C*0102	**7019.7**	**1.0991**	**WB**
	HLA-C*0304	5000.8	4.1482	NB
	HLA-C*0702	4163.7	2.5442	NB
	HLA-C*0802	18249.5	3.8459	NB
	HLA-C*1202	4299.1	4.4511	NB
	HLA-C*1402	1223.6	2.7151	NB
	HLA-C*1601	2570.8	4.5145	NB
HLA-C2	HLA-C*0202	6489.5	5.5153	NB
	HLA-C*0401	19020.8	3.4838	NB
	HLA-C*0501	15159.1	5.2211	NB
	HLA-C*0602	8469.5	3.1256	NB
	HLA-C*1502	9635.9	7.9933	NB
	HLA-C*1701	14447.5	5.6540	NB
	HLA-C*1801	21805	3.0128	NB

Threshold for strong binders = 0.5%
Threshold for weak binders = 2.0%
SB= Strong binder; WB= Weak binder; NB = Non-binder
WB and SB are shown in bold

To validate these results *in vitro*, a peptide stabilization assay using TAP-deficient cell lines expressing one representative allele from each HLA-C group was carried out. Thus, 721.221 cells co-expressing ICP47-GFP and HLA-C***0802** (C1) or HLA-C***0501** (C2) alleles were used. Infected cell protein 47 (ICP47) is a protein from HSV-1/2 that blocks TAP function and prevents loading of peptides onto MHC-I; consequently, expression of these molecules at the cell surface is reduced (Neumann *et al.*, 1997). The TAP-deficient 721.174 cell line – which synthesizes HLA-C***0102** but is unable to load endogenous peptides – was used as positive control (Young *et al.*, 1998). These cell lines are suitable for exogenous peptide loading as they promote formation and stabilization of MHC-I:peptide complexes that reach the cell surface (Luft *et al.*, 2001).

As shown in **Figure 3.12**, LNPSVAATL peptide stabilized surface expression of the HLA-C***0102** allele, even at very low concentrations; however, it was unable to stabilize HLA-C***0802** or HLA-C***0501** alleles. These results are consistent with the binding prediction data and suggest that binding of this viral peptide is restricted to the HLA-C***0102** allele.

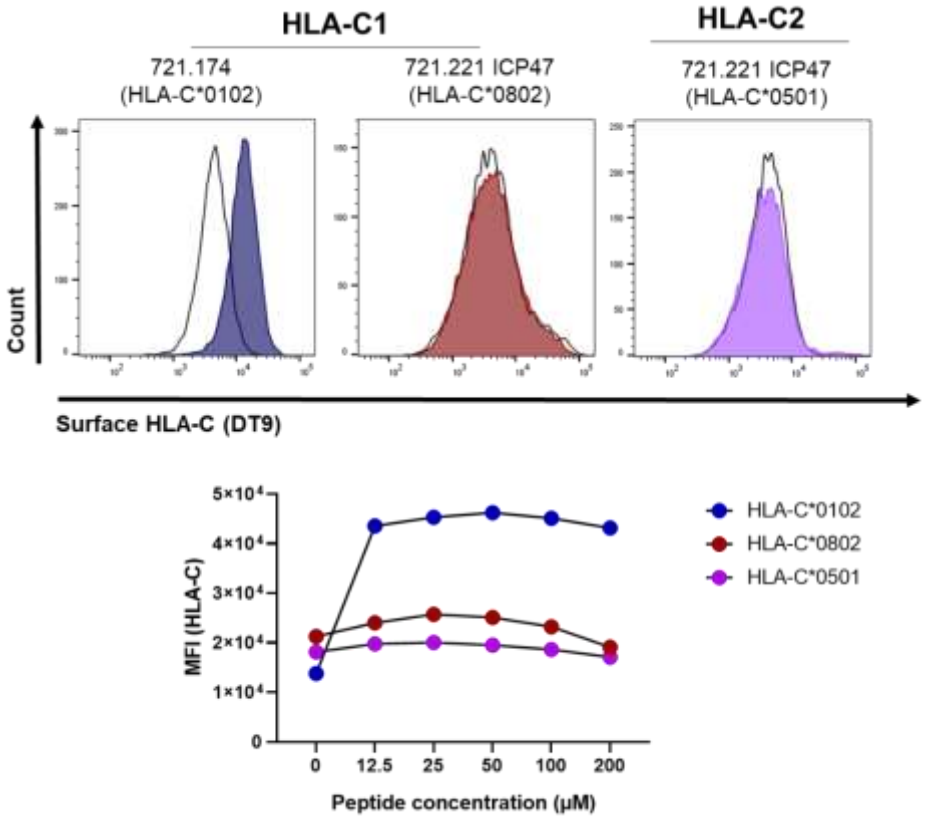

Figure 3.12 MHC-I stabilization on LNPSVAATL-loaded TAP-deficient 721.174 or 721.221 cells. TAP-deficient 721.174 (blue) or 721.221 cells expressing HLA-C***0802** (red) or HLA-C***0501** alleles (purple) were loaded with increasing concentrations of LNPSVAATL peptide at 26°C and then stained for surface HLA-C expression. The stabilization curve for each allele is shown. Flow cytometry plots show the corresponding cell lines loaded with 200 μM of LNPSVAATL peptide compared to the no peptide control (white).

3.8 Peptides from HCV structural and non-structural proteins are potential binders to HLA-C1 alleles and KIR2DS2

The above results showed that KIR2DS2 mediated a strong NK cell activation against replicon cells expressing HLA-C*__0304__ or HLA-C*__0802__, suggesting that these alleles may be presenting endogenous HCV-derived peptides and together, serve as cognate ligands for this activating receptor. In an attempt to identify HCV-derived peptides likely to bind those HLA-C1 alleles and engage KIR2DS2, an *in silico* analysis was performed using NetMHCpan.

Initially, the HCV genotype 1b polyprotein (PubMed Reference AAL55821.1) was screened for the identification of potential peptide binders to HLA-C*__0304__ or HLA-C*__0802__ alleles of 8 to 11 amino acids length. Naiyer *et al* previously showed that a peptide variant carrying the "AW" motif at P7 and P8 in complex with HLA-C*__0304__ was recognized by KIR2DS2 tetramers (Naiyer *et al.*, 2017). Therefore, peptides with the "AW" as well as the "AT" motif at those positions were included in the search as potential KIR2DS2 binders.

Three 9-mer peptides carrying the "AT" motif and located within structural and non-structural proteins were identified **(Figure 3.13; Table 3.2)**. HTTRGLATL (E2) and YLVAYQATV (NS3) peptides were predicted to bind HLA-C*__0304__ with a strong and weak affinity, respectively **(Table 3.2)**. The HLA-C*__0304__ allele has shown to have a preference for small residues at P2 and leucine at P9, which makes the HTTRGLATL peptide a potential candidate epitope likely to engage KIR2DS2 (Di Marco *et al.*, 2017). No HCV-derived peptides carrying the AW motif at P7 and P8 were identified.

Table 3.2 Binding prediction of HCV-derived peptides to HLA-C*0304 and HLA-C*0802

Peptide sequence	HCV Protein	Predicted allele	Binding affinity (nM)	% Rank	Binding level
HTTRGL**AT**L	E2 (10-18)	HLA-C*0304 HLA-C*0802	121.2 6394.1	0.4090 0.8312	SB WB
YLVAYQ**AT**V	NS3 (559-567)	HLA-C*0304 HLA-C*0802	182.7 6159.2	0.5309 0.7933	WB WB
AVDSGT**AT**A	NS5A (435-443)	HLA-C*0802	2784.3	0.3171	SB

Threshold for strong binders = 0.5%
Threshold for weak binders = 2.0%
SB= Strong binder; WB= Weak binder

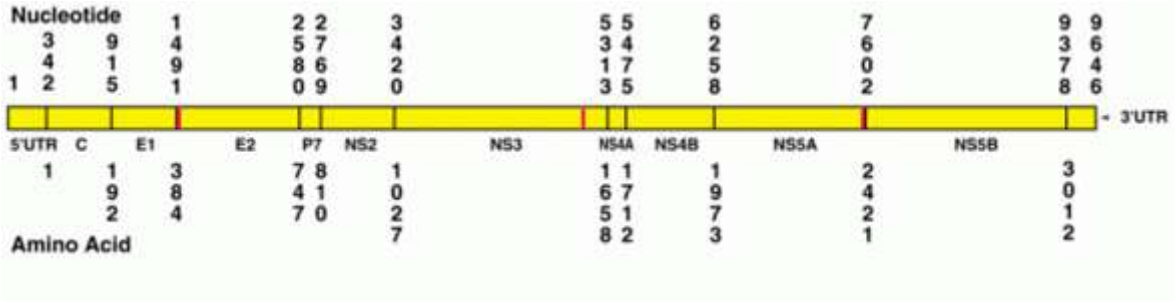

Figure 3.13 Location of HCV-derived peptides predicted to bind HLA-C1 alleles. Map of the HCV genome/polyprotein showing the location of HTTRGLATL, YLVAYQATV and AVDSGTATA peptides within E2, NS3 and NS5A proteins, respectively. The exact positions of the three peptides are shown as red bars. The diagram was taken from Los Alamos HCV sequence database.

Similarly, HTTRGLATL, YLVAYQATV and AVDSGTATA (NS5A) peptides were predicted to bind HLA-C*__0802__. The E2 and NS3-derived peptides showed rank percentages above 0.5% and were categorized as weak binders whereas the NS5A-derived peptide displayed the lowest rank value among this set of peptides and was predicted to be a strong binder **(Table 3.2)**. Interestingly, peptide specificities of HLA-C*__0802__ include small residues at P2, acidic residues at P3 and hydrophobic amino acids at P9 (Di Marco *et al.*, 2017). The AVDSGTATA peptide meet all these requirements and together with HLA-C*0802 constitute a potential ligand for KIR2DS2.

3.9 Discussion

The central role of NK cells in the early control of viral infections is well recognized. The wide array of germline-encoded, non-rearranged surface receptors that NK cells express, enables them to respond to viruses in a highly specific manner (Jamil and Khakoo, 2011). In particular, the extreme diversity of the family of KIR receptors and their MHC-I ligands contribute to augment such specificity. Currently, it is known that specific KIR/MHC-I combinations impact the outcome of infectious diseases, including HCV infection, either to make the host susceptible or resistant to the disease (Rajagopalan and Long, 2005; Rajalingam, 2011). For this reason, these receptor/ligand interactions have become a major subject of interest in NK cell research.

This chapter focused on studying the reactivity of NK cells to HCV through the KIR/MHC-I system. For this purpose, two paths were explored: First, the effect of HCV replication in

the modulation of different HLA-C1 ligands and its impact in NK cell recognition through KIR2DL2/L3/S2 receptors; and second, the ability of LNPSVAATL peptide in the induction of KIR2DS2-mediated NK cell activation in the presence of different HLA-C1 alleles. Overall, the methodological approach to address both aims required the optimization of a co-culture system using NKL cells or PBMC-derived NK cells as effectors and cells co-expressing the N17/JFH-1 subgenomic HCV replicon (or the L9D mutant) and single HLA-C1 alleles (HLA-C*__0102__, HLA-C*__0304__ or HLA-C*__0802__) as targets. The reasoning behind the selection of these alleles was their affinity to the KIR2DS2 inhibitory counterpart (KIR2DL2/L3) as well as their potential relevance in the outcome of viral infections (Knapp *et al.*, 2010; van Teijlingen *et al.*, 2014; Saunders *et al.*, 2015; Naiyer *et al.*, 2017; Sim *et al.*, 2017). As a result, HCC Huh-7 cells supporting HCV replication and able to present endogenously-processed viral peptides in the context of different HLA-C1 alleles to KIR-expressing NK cells were generated.

The use of HCV replicons that efficiently replicate within hepatic cell lines is suitable for the study of different intracellular mechanisms that occur within hepatocytes during HCV infection (Blight, McKeating and Rice, 2002). As infectious HCV strains are unable to display productive and long-term replication *in vitro*, subgenomic replicons lacking structural proteins are commonly used, as non-structural proteins are sufficient to ensure synthesis of viral RNA. The monocistronic N17/JFH1 HCV subgenomic replicon and its L9D mutant used in this study were unable to maintain a stable replication pattern over time; however this issue has been previously described in genotype 2a-derived replicons (Targett-Adams and McLauchlan, 2005; Angus *et al.*, 2012). Therefore, improved subgenomic or full-length replicons with high replication efficiencies in a wide variety of cell lines are required in order to count with a reliable system for the study of HCV biology *in vitro* (Blight, McKeating and Rice, 2002)

Analysis of newly generated target cells suggested that HCV replication prevents traffic of newly synthesized HLA-C molecules towards the cell membrane, and as a consequence, they accumulate intracellularly. Modulation of MHC-I molecules by HCV is controversial as contradictory results demonstrating up-regulation or down-regulation of these molecules at the surface of liver cell lines have been reported. On one hand, Herzer *et al* showed that the HCV core protein promotes over-expression of MHC-I on HepG2 cells (Herzer *et al.*, 2003) whereas Tardif and Siddiqui have shown that a genotype 1b HCV replicon induces down-regulation of MHC-I by reducing protein glycosylation, which results in ER stress and intracellular accumulation of unfolded MHC-I (Tardif, Mori and Siddiqui, 2002; Tardif and Siddiqui, 2003). Similarly, by using hepatic tissue samples from HCV-infected individuals,

Valli de Re *et al* found down-regulation of proteins associated with peptide loading and MHC-I maturation in the ER (De Re *et al.*, 2008). Results from this chapter are consistent with those of Tardif and Siddiqui and suggest that HCV has evolved mechanisms to disturb the antigen processing and presentation machinery and, as a result, prevent trafficking of antigen-presenting molecules towards the cell membrane.

The preferential down-regulation of HLA-C over HLA-A*11 is an interesting finding that could be thought as an evasion strategy developed by HCV. This mechanism of preferential down-regulation of MHC-I molecules has been described for HIV-1, as the Nef protein has shown to preferentially reduce expression of HLA-A and HLA-B by binding to their cytoplasmic tails and facilitating protein degradation (Schafer *et al.*, 2015). Similarly, US2 and US11 proteins from HCMV only target certain HLA-A and HLA-B alleles, leaving HLA-C and HLA-E available for interaction with inhibitory NK cell receptors (Llano *et al.*, 2003). These strategies allow viruses to remain undetected from the two arms of the immune system leading to viral propagation and persistence.

The relevance of HCV-induced down-regulation of HLA-C1 alleles lies on the implications that this phenomenon may have for immune recognition. Down-regulation of MHC-I at the cell surface has been employed by viruses to avoid attack from immune cells. This strategy would prevent recognition by T CD8+ lymphocytes; however, a different scenario occurs with NK cells as they are capable of recognizing and killing cells with an altered expression of these molecules through the missing-self mechanism (Raulet, 2006). Degranulation of PBMC-derived NK cells with high expression of inhibitory KIR2DL2 or KIR2DL2/L3 to replicon cells with down-regulated expression of HLA-C1 ligands was high; however, NKL-2DL2 cells did not have a similar response against the same targets. These contrasting results could be associated with high donor variability or the difficulty to specifically discriminate KIR2DL2/L3 from KIR2DS2 in our cytometry panel. The generation of KIR2DL2+ or KIR2DS2+ NK clones would be a suitable experimental approach to overcome these issues.

Conversely, the mechanisms by which activating KIR recognize virus-infected cells differ from those of inhibitory KIR. Despite ligands for activating KIR receptors are not well defined, some insights have been recently provided and suggest that these receptors engage viral epitopes presented by MHC-I (O'Connor *et al.*, 2015; Chapel *et al.*, 2017; Naiyer *et al.*, 2017). This chapter showed strong anti-viral responses from the NKL-2DS2 cell line against targets co-expressing either the WT or L9D HCV replicons and HLA-C1 alleles, suggesting that LNPSVAATL peptide is not relevant for KIR2DS2 recognition of

target cells in the presence of HLA-C*__0304__ or HLA-C*__0802__ alleles. Thus, results from the present study complement those of Naiyer *et al* and confirm that KIR2DS2 recognition of LNPSVAATL peptide is allele-specific. As the peptidome of HCV has shown to dominate in replicon-expressing cells (Mbiribindi, 2016), other viral epitopes from core or non-structural HCV proteins presented by HLA-C*__0304__ or HLA-C*__0802__ alleles could serve as ligands for KIR2DS2 leading to the induction of robust NK cell responses.

Recognition of HCV-derived peptides in the context of HLA-C1 alleles has been demonstrated by other authors for inhibitory KIR. In this regard, Lunemann *et al* have shown that the core-derived 9-mer peptide YIPLVGAPL in complex with HLA-C*__0304__ strongly binds KIR2DL3 and prevents NK cell activation whereas Cheent *et al* showed that the HCV core peptide YLLPRRGPRL binds HLA-E and together with MHC-I leader peptides inhibit NKG2A+ NK cells (Cheent *et al.*, 2013; Lunemann *et al.*, 2016). This evidence suggests that HCV has been continuously evolving immune evasion mechanisms to impair NK cell functions and emphasize the need for identification of ligands that promote anti-viral NK cell responses either indirectly through non-strong interactions with inhibitory KIR or directly, by engaging activating KIR. Indeed, the *in silico* binding prediction analysis identified three viral peptides derived from structural and non-structural proteins likely to bind HLA-C*__0304__ or HLA-C*__0802__ alleles as well as KIR2DS2. Their ability to stabilize these alleles and to induce NK cell activation through KIR2DS2 needs to be determined *in vitro* by performing MHC-I stabilization and functional assays.

In summary, this is the first study to demonstrate a HCV-induced and preferential down-modulation of HLA-C molecules. Furthermore, it has been suggested that HLA-C alleles presenting HCV epitopes may be ligands for KIR2DS2. Due to the extensive allelic diversity of HLA-C, it is imperative to search for peptides across multiple viruses and with a broader specificity for HLA-C alleles that could have therapeutic relevance.

Chapter 4 - Recognition of viral peptides by NK cells through canonical or non-canonical interactions

4.1 Introduction

One of the mechanisms to alert NK cells from an ongoing viral infection involves the interaction between KIR receptors and MHC-I:peptide complexes. Classical MHC-I molecules (HLA-A, -B, -C) binding virus-derived peptides have shown to serve as ligands for inhibitory or activating KIR and thus, modulate NK cell responses. Particularly, HLA-C and its interaction with the group of KIR2D receptors plays an essential role in NK cell-mediated immunity (Blais, Dong and Rowland-Jones, 2011).

The HLA-C molecule displays unique features that distinguish it from the other two classical HLA-A and HLA-B. First, HLA-C is the most recently evolved MHC-I molecule and its C1+C2 epitopes are highly specialized for KIR2D receptors (Pohla *et al.*, 1989; Older Aguilar *et al.*, 2010; Moesta and Parham, 2012; Anderson, 2018). Structurally, HLA-C displays a reduced polymorphism in the peptide-binding groove due to the presence of conserved residues in its α1 and α2 domains (Pohla *et al.*, 1989). This has an impact in the number of peptides that can be accommodated, and therefore, this molecule present a restricted set of self-peptides (Neisig, Melief and Neefjes, 1998). In addition, expression of HLA-C at the cell surface is 15-35% lower than that of HLA-A and HLA-B. This phenomenon has been explained by different factors including low levels of mRNA, reduced assembly of heavy chains with β2-microglobulin and a prolonged association with TAP (Blais, Dong and Rowland-Jones, 2011).

Despite allelic diversity of HLA-C being the lowest among classical MHC-I molecules, the number of reported alleles (5140) is of great relevance (Robinson *et al.*, 2015). All HLA-C alleles belong to either of the 14 HLA-C allotypes described so far, which are allocated into HLA-C1 or C2 groups. Thus, HLA-C1 group (Ser^{77}/Asn^{80}) includes C*01, C*03, C*07, C*08, C*12, C*14 and C*16 allotypes and canonically bind KIR2DL2, KIR2DL3 and KIR2DS2. On the other hand, group C2 (Asn^{77}/Lys^{80}) contains C*02, C*04, C*05, C*06, C*15, C*17 and C*18 allotypes that interact with KIR2DL1 and KIR2DS1. Correspondingly, the KIR

molecule contains specific residues that determine the specificity to HLA-C (Winter and Long, 1997). Besides canonical interactions with HLA-C1 alleles, inhibitory KIR2DL2 and KIR2DL3 have shown to have a certain degree of cross-reactivity with HLA-C2 alleles, leading to inhibition of NK cell functions (Moesta and Parham, 2012). Conversely, cross-reactivity of KIR2DL1 to HLA-C1 alleles is less common. In both cases, non-canonical interactions seem to be determined by the bound peptide (Sim *et al.*, 2017).

Recently, peptide-binding motifs of multiple HLA-C1 and C2 alleles were elucidated using mass spectrometry (Di Marco *et al.*, 2017). Overall, these motifs are characterized by the presence of variable anchor residues at P2 and P3 and hydrophobic or aromatic residues at the C-terminus. Particularly, the motifs for HLA-C*0802 (C1) and HLA-C*0501 (C2) – two alleles that share high sequence homology – were almost identical and showed a preference for small amino acids at P2, acidic residues at P3 and non-polar residues at the C-terminus of different length peptides **(Figure 4.1A)** (Rasmussen *et al.*, 2014; Di Marco *et al.*, 2017). Using a panel of self-peptides eluted from HLA-C*0501 able to stabilize both, HLA-C*0501 and HLA-C*0802, Sim *et al* studied how the bound peptide influences binding to inhibitory KIR2D receptors. These authors found that most self-peptides facilitated the establishment of canonical interactions, with the binding of KIR2DL2/L3 to HLA-C*0802 being more peptide selective than that of KIR2DL1 to HLA-C*0501. Conversely, only a limited number of peptides promoted cross-reactive associations, thereby implying that peptide sequence dictates binding to KIR receptors (Sim *et al.*, 2017).

The contribution of virus-derived peptide sequences to canonical or cross-reactive binding to inhibitory KIR has also been described (Sim *et al.*, 2017). However, little is known about the influence of viral peptides in binding to activating KIR receptors and the modulation of NK cell responses to pathogens. Our group recently reported that peptides derived from *Flaviviridae* contain a conserved “MCHAT” sequence, with the “AT” motif being specific for KIR2DS2 binding. By using the HLA-C*0802/HLA-C*0501 system, this chapter aimed to identify viral peptides that, in complex with these molecules, are able to induce NK cell activation through canonical or non-canonical interactions with KIR2DS2, respectively.

4.2 Viral peptides are predicted to bind HLA-C*0802 (C1) and HLA-C*0501 (C2) alleles

A set of five viral peptides including four *Flaviviridae*-derived peptides and one ebolavirus (EBOV) peptide were used in this study. The ebolavirus peptide is a 10-mer (FLSDVPVATL) derived from the RNA-dependent RNA polymerase whereas the *Flaviviridae*-derived peptides are located within the helicase domain of NS3 proteins from HCV (LNPSVAATL; $NS3_{228-236}$), DENV/ZIKV (IVDLMCHATF; $NS3_{256-265}$ and $NS3_{255-264}$, respectively), YFV (VIDAMCHATL; $NS3_{255-264}$) and WNV/JEV (IVDVMCHATL; $NS3_{255-264}$). Unlike LNPSVAATL, *Flaviviridae*-derived peptides are 10-mers that share a highly conserved sequence "MCHAT" from P5 to P9 (Naiyer *et al.*, 2017). All peptides contain the "AT" KIR2DS2-binding motif immediately preceding the C-terminus **(Figure 4.1B)**.

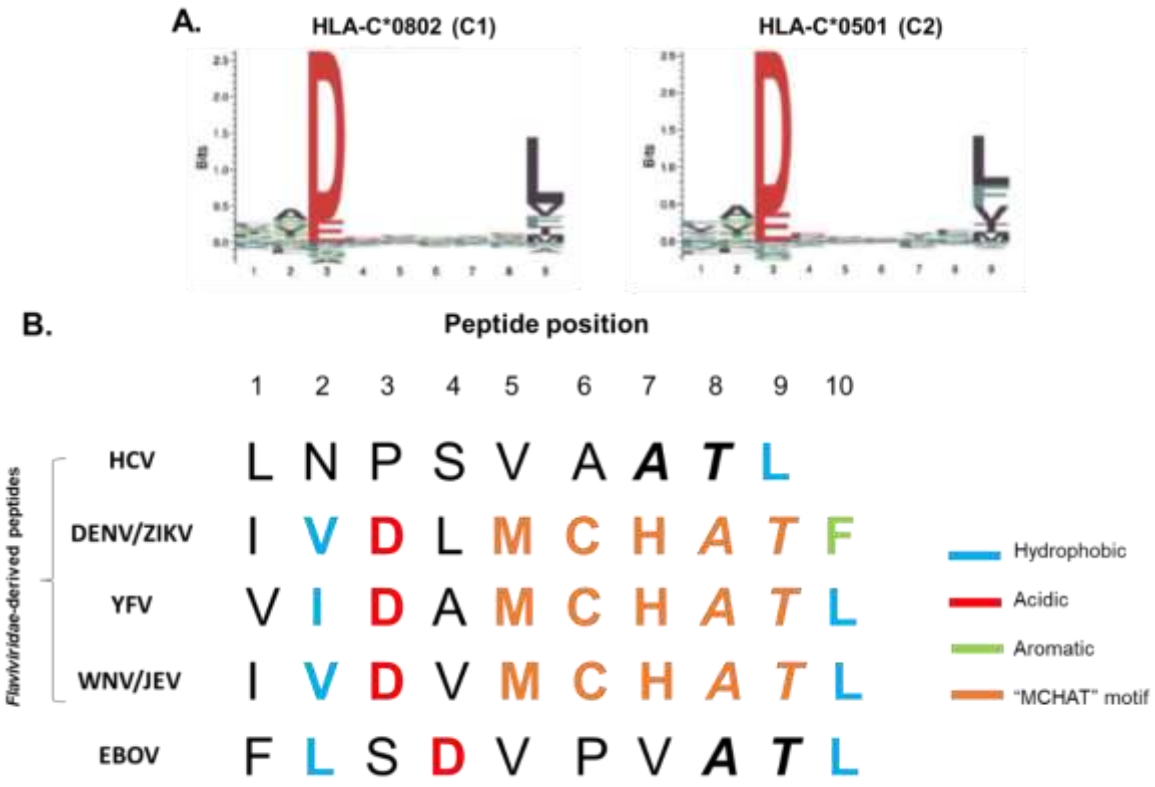

Figure 4.1 Peptide-binding motifs and viral peptides. (A) The peptide-binding motifs from the structurally similar HLA-C*0802 (C1) and HLA-C*0501 (C2) alleles were previously described. Figure adapted from Di Marco *et al* and originally published by the Journal of Immunology (Di Marco *et al.*, 2017). **(B)** The sequence of five viral peptides (one 9-mer and four 10-mer) used in this study share the "AT" binding motif for KIR2DS2.

The viral peptide sequences had the peptide-binding motifs previously described for HLA-C*0802 and HLA-C*0501 **(Figure 4.1B)**. Thus, Flaviviral peptides sharing the “MCHAT” motif carry small hydrophobic anchors at P2 (valine or isoleucine) and a negatively charged anchor at P3 (aspartic acid in all). The C-terminus of these peptides presented hydrophobic residues (phenylalanine or leucine). Similarly, the EBOV peptide carries a small hydrophobic amino acid at P2 and P10 (leucine); however, the acidic residue is present at P4 instead P3. There was no match of the LNPSVAATL anchor residues to the binding motif of both HLA-C alleles.

Binding prediction of viral peptides to HLA-C*0802 and HLA-C*0501 alleles was performed using NetMHCPan **(Table 4.1)** (Jurtz *et al.*, 2017). Two cellular peptides previously reported to stabilize both HLA-C alleles were used as positive controls (Sim *et al.*, 2017). These peptides, eluted from HLA-C*0501 are derived from AP-3 complex subunit mu-1 (*IIDKSGSTV*) and methionine synthase (*IVDKSGRTL*) and, as expected, are predicted to bind both HLA-C alleles. From the set of viral peptides, three out of five peptides (V**ID**AMCHAT**L**, I**VD**VMCHAT**L** and F**LS**DVPVAT**L**) were predicted to be strong binders to both HLA-C alleles. The I**VD**LMCHAT**F** peptide showed rank values close to the specified threshold value (0.6734% and 0.5041% for HLA-C*0802 and HLA-C*0501, respectively) and therefore is categorized as a weak binder to both alleles. L**NP**SVAAT**L** peptide is not predicted to bind either of the two HLA-C molecules. These data indicate that all 10-mer viral peptides from this set are likely to bind both HLA-C alleles and could be potential ligands for KIR2DS2.

4.3 Viral peptides stabilize HLA-C*0802 and HLA-C*0501 molecules at the surface of TAP-deficient 721.221 cells

Binding of viral peptides to HLA-C*0802 or HLA-C*0501 alleles was tested *in vitro* by a peptide stabilization assay using 721.221 cells co-expressing ICP47-GFP and either of the HLA-C alleles.

Table 4.1 Binding prediction of viral peptides to HLA-C*0802 and HLA-C*0501 alleles

	Peptide sequence	Protein	Origin	Predicted binding affinity					
				HLA-C*0802 (C1)			HLA-C*0501 (C2)		
				Binding affinity (nM)	% Rank	Binding level	Binding affinity (nM)	% Rank	Binding level
Control peptides	IIDKSGSTV	AP-3 complex subunit mu-1	Cellular peptide	363.5	0.0392	SB	99.5	0.0521	SB
	IVDKSGRTL	Methyonine synthase	Cellular peptide	246.8	0.0273	SB	118.9	0.0639	SB
Viral peptides	LNPSVAATL	NS3 RNA helicase domain genotypes 1-4 and 6-7	Hepatitis C Virus	18249.5	3.8459	NB	15159.1	5.2211	NB
	IVDLMCHATF	NS3 RNA helicase domain	Dengue Virus / Zika Virus	5374.3	0.6734	WB	1590.1	0.5041	WB
	VIDAMCHATL	NS3 RNA helicase domain	Yellow Fever Virus	3327.7	0.3895	SB	954.1	0.3318	SB
	IVDVMCHATL	NS3 RNA helicase domain	West Nile Virus / Japanese Encephalitis Virus	2664.6	0.2995	SB	794.7	0.2839	SB
	FLSDVPVATL	RNA-dependent RNA polymerase	Tai Forest ebolavirus	420.1	0.0488	SB	93.5	0.0485	SB

Threshold for strong binders = 0.5%
Threshold for weak binders = 2.0%
SB= Strong binder; WB= Weak binder; NB = Non-binder

Initially, to confirm whether TAP-deficient cell lines down-regulated surface expression of HLA-C*0802 or HLA-C*0501 due to the effector functions of ICP47, expression of both, ICP47-GFP and HLA-C was measured by flow cytometry. Both TAP-deficient cell lines showed expression of ICP47 as indicated by the GFP fluorescence, with the levels of this protein being significantly higher in cells co-expressing HLA-C*0501 ($p<0.0001$**; Figure 4.2A**). Consequently, down-regulation of HLA-C at the cell surface was more evident in cells co-expressing HLA-C*0501 compared to HLA-C*0802 **(Figure 4.2B)**, indicating that ICP47 is efficiently blocking TAP on HLA-C*0501-expressing cells. Even though HLA-C expression is significantly reduced in TAP-deficient cells expressing HLA-C*0802 compared to its parental cell line ($p<0.0001$), these levels were much higher than TAP-deficient cells expressing HLA-C*0501 ($p<0.0001$; **Figure 4.2B**).

To circumvent this issue, concentration of the selectable antibiotic for ICP47 (puromycin) was titrated, and ICP47 and HLA-C levels from HLA-C*0802-expressing cells were measured again. **Figure 4.2C** shows that increasing concentrations of puromycin gradually improved ICP47 expression and at the same time, reduced HLA-C at the cell surface. As higher concentrations of puromycin affected cell viability, this cell line was selected with up to 2 µg/ml of puromycin for further experiments.

After confirming adequate blocking of TAP in both cell lines, control and viral peptides were exogenously loaded onto these cells. Exogenous loading of control peptides resulted in high levels of surface HLA-C expression compared to cells without peptides **(Figure 4.3A)**. At a concentration of 200 µM, *IVDKSGRTL* showed higher affinity to HLA-C*0802 whereas the same was true for *IIDKSGSTV* and HLA-C*0501 **(Figure 4.3B,C)**.

Similarly, all viral peptides (except L**NP**SVAAT**L**) stabilized expression of both HLA-C alleles **(Figure 4.3A)**. Particularly, for HLA-C*0802-expressing cells, V**ID**AMCHAT**L**, I**VD**VMCHAT**L** and F**LS**DVPVAT**L** stabilized HLA-C expression to a similar extent whereas it was slightly reduced for I**VD**LMCHAT**F** peptide **(Figure 4.3B)**. Regarding HLA-C*0501-expressing cells, I**VD**VMCHAT**L** and I**VD**LMCHAT**F** promoted the highest HLA-C expression, followed by F**LS**DVPVAT**L** and V**ID**AMCHAT**L (Figure 4.3C)**. Overall, HLA-C stabilization was increased for TAP-deficient cells expressing HLA-C*0501 compared to the ones expressing HLA-C*0802. However, this may be due to lower levels of ICP47 in HLA-C*0802-expressing cells rather than a preferential peptide binding to HLA-C*0501. These data are consistent with the binding prediction results generated by the NetMHCpan tool and confirm that 4 out of 5 viral peptides from this set are able to form stable complexes

with HLA-C1 and C2 alleles, and reach the cell membrane to become available for interaction with NK cells, potentially through KIR2DS2.

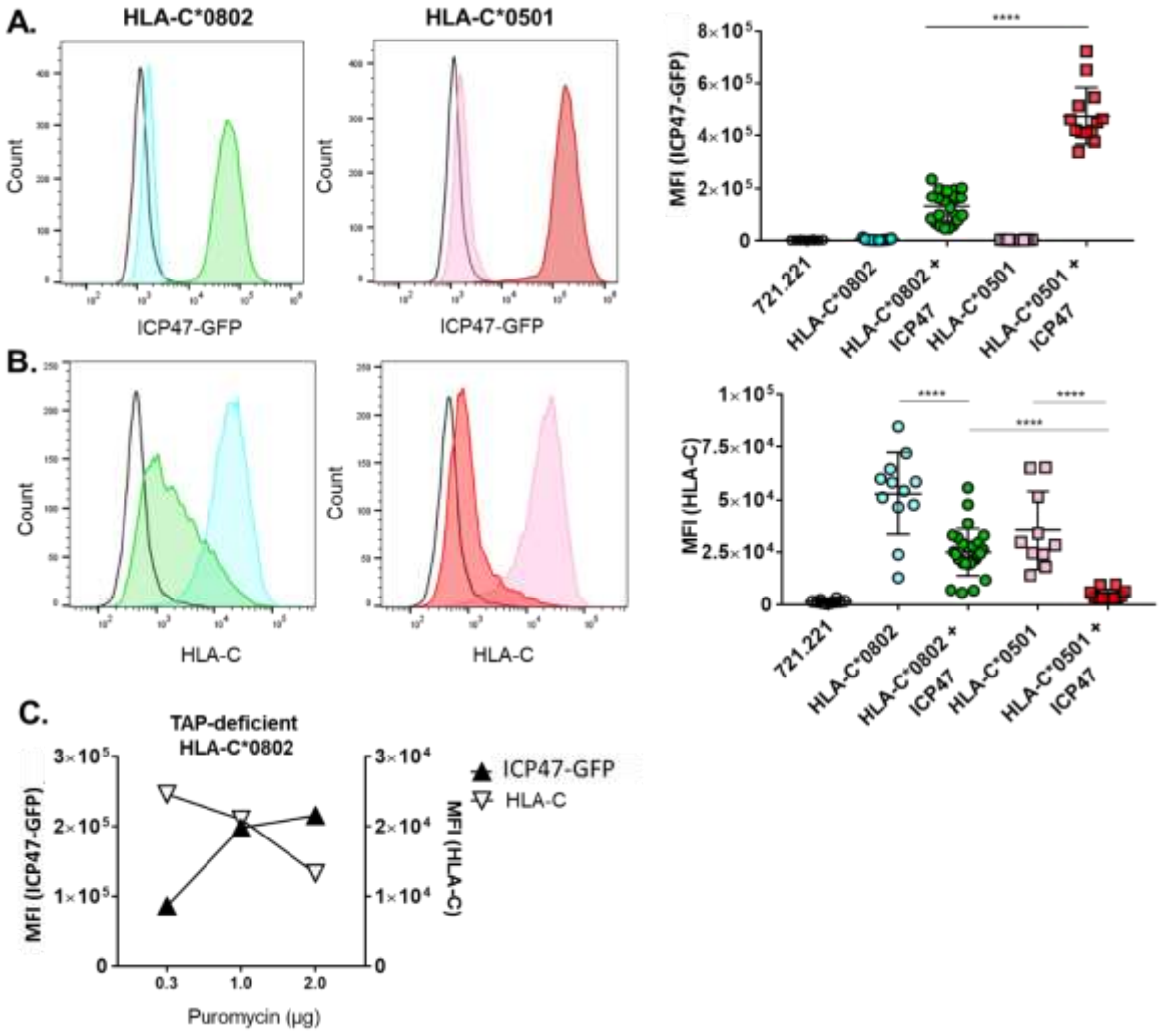

Figure 4.2 TAP blocking and HLA-C down-regulation on 721.221 cells. Expression of ICP47-GFP **(A)** and HLA-C **(B)** on TAP-deficient 721.221 cells expressing HLA-C*0802 or HLA-C*0501 alleles was determined by flow cytometry and compared to its parental cell line. **(C)** Titration of antibiotic selection on HLA-C*0802-expressing cells. Each dot represents one measurement. Mean values and SD of at least six independent experiments are shown (n=6-12). Differences were determined using an unpaired t-test. P value **** <0.0001.

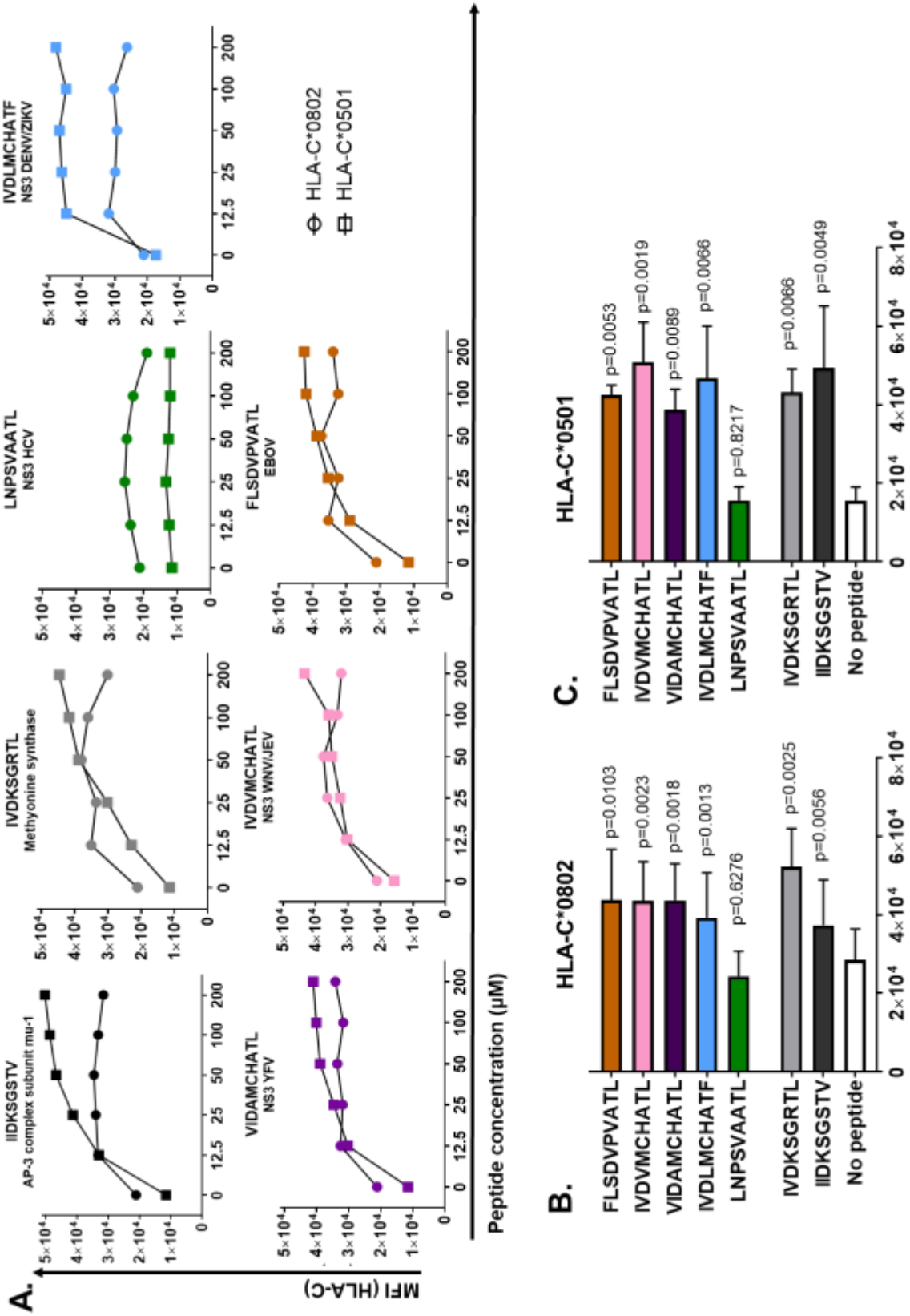
A.
IIDKSGSTV
AP-3 complex subunit mu-1
IVDKSGRTL
Methyonine synthase
LNPSVAATL
NS3 HCV
IVDLMCHATF
NS3 DENV/ZIKV
VIDAMCHATL
NS3 YFV
IVDVMCHATL
NS3 WNV/JEV
FLSDVPVATL
EBOV
HLA-C*0802
HLA-C*0501
MFI (HLA-C)
Peptide concentration (μM)
B.
HLA-C*0802
FLSDVPVATL
IVDVMCHATL
VIDAMCHATL
IVDLMCHATF
LNPSVAATL
IVDKSGRTL
IIDKSGSTV
No peptide
p=0.0103
p=0.0023
p=0.0018
p=0.0013
p=0.6276
p=0.0025
p=0.0056
MFI (HLA-C)
C.
HLA-C*0501
FLSDVPVATL
IVDVMCHATL
VIDAMCHATL
IVDLMCHATF
LNPSVAATL
IVDKSGRTL
IIDKSGSTV
No peptide
p=0.0053
p=0.0019
p=0.0089
p=0.0066
p=0.8217
p=0.0066
p=0.0049
MFI (HLA-C)

Figure 4.3 MHC-I stabilization on peptide-loaded TAP-deficient 721.221 cells. (A) TAP-deficient 721.221 cells expressing HLA-C*0802 or HLA-C*0501 alleles were loaded with increasing concentrations of control or viral peptides at 26ºC and then stained for HLA-C expression. **(B,C)** Bar plots show the MFI of cells expressing HLA-C*0802 **(B)** or HLA-C*0501 **(C)** loaded with no peptide or 200 μM of control or viral peptides. The mean and SD of at least three independent experiments are shown (n=3-5). Differences with the no peptide control were determined using a paired t test. The p value for each peptide is shown.

4.4 The KIR2DS2 tetramer strongly binds IVDLMCHATF peptide in complex with HLA-C*0802 and HLA-C*0501 alleles

To evaluate whether KIR2DS2 canonically binds HLA-C*0802:peptide or whether it cross-reacts with HLA-C*0501:peptide complexes, staining using fluorescent KIR tetramers was carried out. Biotinylated tetramers for KIR2DS2 and its inhibitory counterpart KIR2DL2 were conjugated to Streptavidin-PE and were used as probes against TAP-deficient cells exogenously loaded with control and viral peptides.

For HLA-C*0802-expressing cells, L**NP**SVAAT**L** peptide served as negative control and *IVDKSGRTL* peptide was selected as positive control as this peptide in complex with HLA-C*0802 has been shown to canonically bind KIR2DL2 with strong affinity (Sim *et al.*, 2017). Overall, KIR2DL2-PE binding to the no peptide control showed a high background **(Figure 4.4A)**. This can be explained by low levels of ICP47 on this cell line, which allows endogenous peptides to be presented at the cell surface and act as cognate ligands for KIR2DL2. Despite this background, binding to *IVDKSGRTL* was increased and statistically significant (>4-fold; p<0.0004; **Figure 4.4A,C**). All viral peptides complexed to HLA-C*0802 showed a certain degree of binding to KIR2DL2-PE compared to the no peptide control (~2-fold), being statistically significant only for cells loaded with I**VD**LMCHAT**F** peptide (p=0.0103; **Figure 4.4A,C**).

Staining with KIR2DS2-PE showed a reduced non-specific binding to the *IVDKSGRTL* peptide (2 fold; **Figure 4.4B,C**). Among viral peptides, KIR2DS2-PE binding had a 4-fold increase to I**VD**VMCHAT**L** peptide with a p value close to the margin of statistical significance (p=0.0501). Remarkably, KIR2DS2-PE tetramer strongly recognized the I**VD**LMCHAT**F** peptide bound to HLA-C*0802, with a much larger fold increase (20-fold) compared to the no peptide control (p=0.0023; **Figure 4.4B.C**).

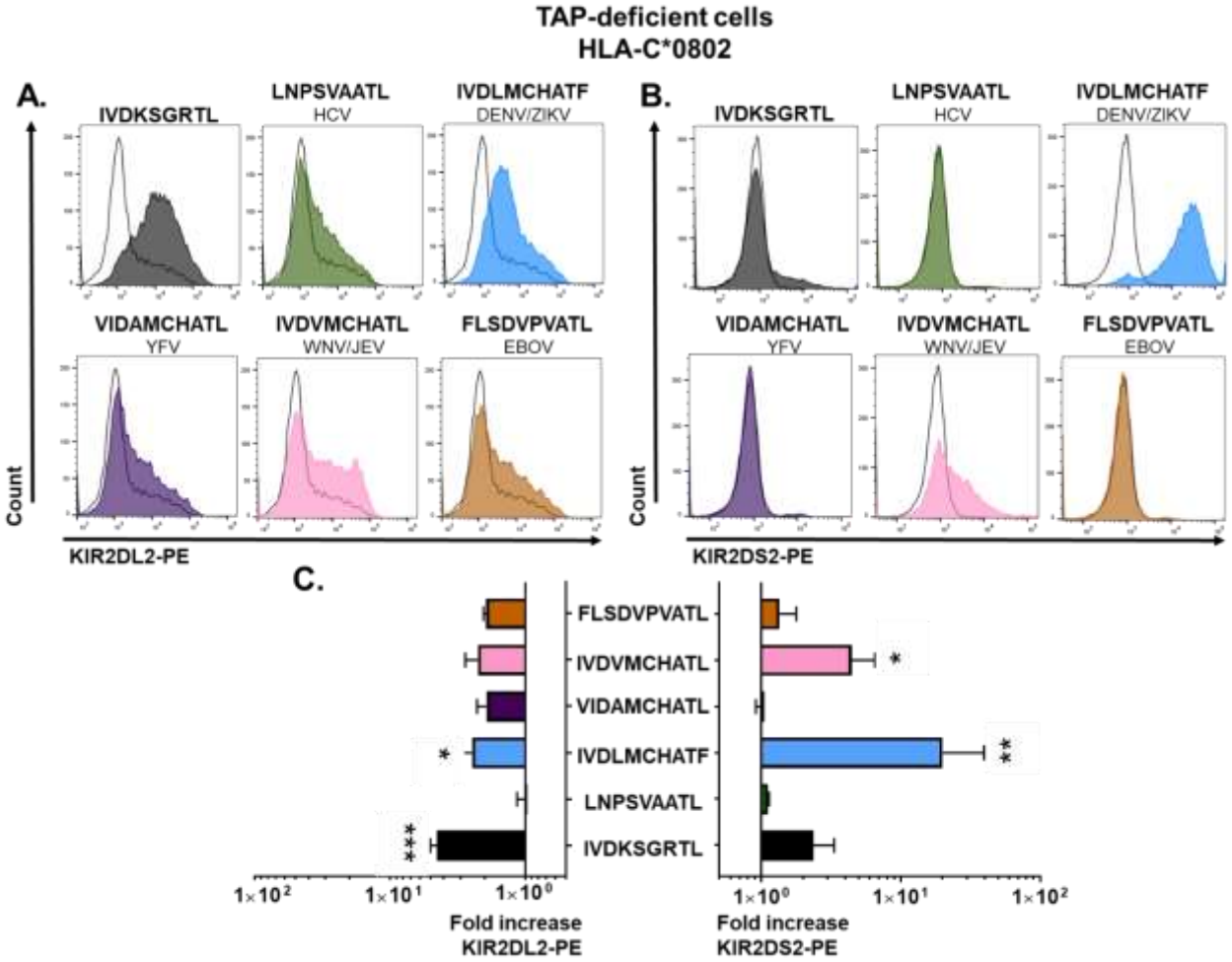

Figure 4.4 KIR tetramer binding to HLA-C*0802 and viral peptides. (A,B) TAP-deficient 721.221 cells expressing HLA-C*0802 were loaded with no peptide or 200 µM of control or viral peptides at 26°C and then stained with fluorescent KIR2DL2 **(A)** or KIR2DS2 **(B)** tetramers. **(C)** Bar plots show the fold change in the MFI of KIR2DL2 (left) or KIR2DS2 (right) tetramers. The mean and SD of at least three independent experiments are shown (n=3-6). Differences were determined using a Kruskal-Wallis test and Dunn's test for multiple comparisons. P value * <0.05, ** <0.01, *** <0.001.

Regarding HLA-C*0501-expressing cells, L**NP**SVAAT**L** peptide served as negative control and *IIDKSGSTV* was selected as positive control, as this peptide in complex with HLA-C*0501 is known to confer strong cross-reactive binding to KIR2DL2 (Sim *et al.*, 2017). As expected, *IIDKSGSTV* was strongly recognized by KIR2DL2-PE (>12-fold; p=0.0002). Similarly to HLA-C*0802-expressing cells, KIR2DL2-PE cross-reacted with viral peptides in complex with HLA-C*0501 at a low extent (~2-fold) and at a slightly greater extent to I**VD**LMCHAT**F** peptide (6-fold; p=0.0088; **Figure 4.5A,C**). Staining with KIR2DS2-PE showed a significantly augmented binding to I**VD**LMCHAT**F** peptide with a 28-fold increase compared to the no peptide control (p=0.0076, **Figure 4.5B,C**). Although there was some binding to I**VD**VMCHAT**L** peptide, this did not reach statistical significance (p=0.7351).

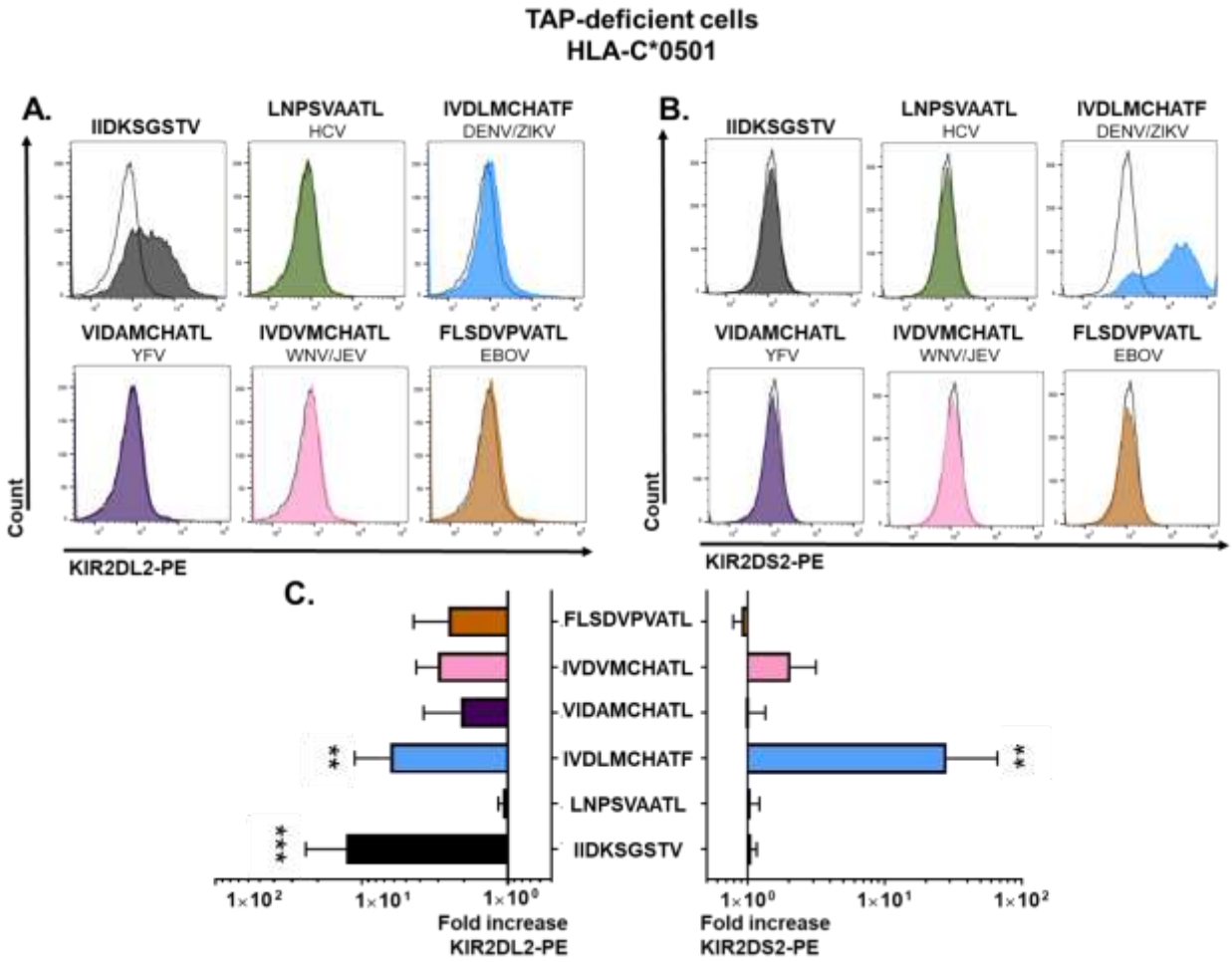

Figure 4.5 KIR tetramer binding to HLA-C*0501 and viral peptides. (A,B) TAP-deficient 721.221 cells expressing HLA-C*0501 were loaded with no peptide or 200 μM of control or viral peptides at 26ºC and then stained with fluorescent KIR2DL2 **(A)** or KIR2DS2 **(B)** tetramers. **(C)** Bar plots show the fold change in the MFI of KIR2DL2 (left) or KIR2DS2 (right) tetramers. The mean and SD of at least three independent experiments are shown (n=3-6). Differences were determined using a Kruskal-Wallis test and Dunn's test for multiple comparisons. P value ** <0.01, *** <0.001.

Taken together, these results strongly suggest that I**VD**LMCHAT**F** peptide from DENV/ZIKV and I**VD**VMCHAT**L** peptide from WNV/JEV bound to HLA-C*0802 may be cognate ligands for activating KIR2DS2, whereas I**VD**LMCHAT**F** peptide bound to HLA-C*0501 may cross-react with this activating receptor. Binding of KIR2DL2-PE to I**VD**LMCHAT**F** peptide presented by both HLA-C alleles was also evident, which may suggest a dual role for this viral peptide in the modulation of NK cell responses.

4.5 Exogenous IVDLMCHATF peptide induce weak degranulation in the KIR2DS2^{high} NK cell subset

To determine whether binding of KIR tetramers to Flaviviral peptides is functionally relevant, TAP-deficient cells expressing HLA-C*0802 or HLA-C*0501 alleles were exogenously loaded with control (*IIDKSGSTV* for HLA-C*0501 and *IVDKSGRTL* for HLA-C*0802), I**VD**LMCHAT**F**, V**ID**AMCHAT**L** or I**VD**VMCHAT**L** peptides and then incubated with total PBMC from KIR2DL2/L3/S2 heterozygous donors (n=5-6) in the presence of the correspondent peptides at 10:1 and 5:1 E:T ratios. Degranulation of KIR2DL2/L3/S2^{neg}, KIR2DL2/L3^{high} and KIR2DS2^{high} NK cell subpopulations to peptide-loaded cells was measured using the combination of antibodies previously described (Blunt *et al.*, 2019) **(Figure 4.6A and 4.7A)**.

For HLA-C*0802-expressing cells, the no peptide control triggered the highest CD107a expression in all three NK cell subpopulations **(Figure 4.6B,C)**. KIR2DL2/L3/S2^{neg} NK cells degranulated to *IVDKSGRTL*, V**ID**AMCHAT**L** and I**VD**VMCHAT**L** peptides to a similar extent at both E:T ratios. Particularly, I**VD**LMCHAT**F** peptide induced low levels of CD107a in this NK cell subset with a statistically significant difference compared to the control peptide at 10:1 ratio (p=0.0255). Of note, the three Flaviviral peptides inhibited NK cell degranulation of KIR2DL2/L3^{high} NK cells at levels close to the obtained by cognate *IVDKSGRTL* peptide at both E:T ratios, although it was significantly increased against I**VD**LMCHAT**F**-loaded cells at 5:1 ratio (p=0.0150; **Figure 4.6B,C**).

On the other hand, levels of CD107a expression in the KIR2DS2^{high} NK cell subpopulation were higher to HLA-C*0802-expressing cells loaded with I**VD**VMCHAT**L** (Median: 21.92%), I**VD**LMCHAT**F** (Median: 17.31%), *IVDKSGRTL* (Median: 13.43%) and V**ID**AMCHAT**L** (Median: 7.92%) at 5:1 ratio **(Figure 4.6C)**. At 10:1 ratio, the percentage of CD107a to *IVDKSGRTL* peptide was slightly higher than to Flaviviral peptides (Median 14.59% compared to 12.81% for I**VD**VMCHAT**L**, 11.31% for I**VD**LMCHAT**F** and 5.74% for V**ID**AMCHAT**L**). This may be due to a non-specific recognition of the control peptide by KIR2DS2^{high} NK cells as observed with the KIR2DS2-PE tetramer. No statistically significant differences were found between control and viral peptides for this NK cell subset at any E:T ratio **(Figure 4.6C)**.

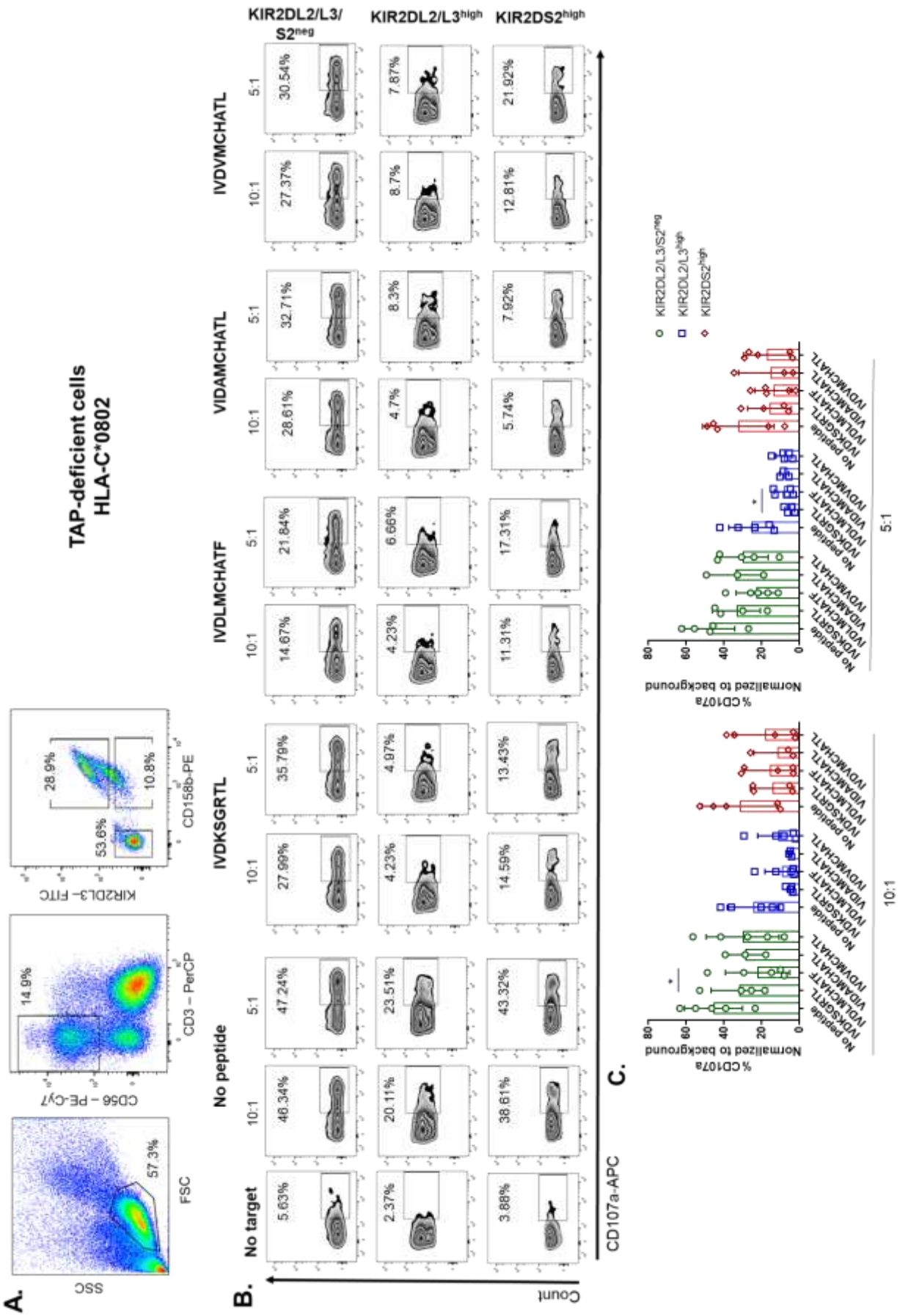
TAP-deficient cells
HLA-C*0802
A.
SSC
FSC
57.3%
CD56 – PE-Cy7
CD3 – PerCP
14.9%
KIR2DL3– FITC
CD158b-PE
28.9%
53.6%
10.8%
B.
No target
No peptide
IVDKSGRTL
IVDLMCHATF
VIDAMCHATL
IVDVMCHATL
KIR2DL2/L3/S2neg
KIR2DL2/L3high
KIR2DS2high
10:1
5:1
5.63%
48.34%
47.24%
27.99%
35.78%
14.67%
21.84%
28.61%
32.71%
27.37%
30.54%
2.37%
20.11%
23.51%
4.23%
4.97%
4.23%
6.66%
4.7%
8.3%
8.7%
7.87%
3.88%
38.61%
43.32%
14.59%
13.43%
11.31%
17.31%
5.74%
7.92%
12.81%
21.92%
Count
CD107a-APC
C.
KIR2DL2/L3/S2neg
KIR2DL2/L3high
KIR2DS2high
% CD107a
Normalized to background
No peptide
IVDKSGRTL
IVDLMCHATF
VIDAMCHATL
IVDVMCHATL
10:1
5:1

Figure 4.6 Degranulation of NK cells to Flaviviral peptides bound to HLA-C*0802. (A) Flow cytometry plots show KIR2DL2/L3/S2^{neg}, KIR2DL2/L3^{high} and KIR2DS2^{high} NK cell subsets gated on CD3- CD56+ NK cells from total PBMC. Percentages of each cell population are shown. **(B)** TAP-deficient 721.221 cells expressing HLA-C*0802 were loaded with no peptide or 200 μM of control or Flaviviral peptides at 26^{o}C and used as targets in a degranulation assay to total PBMC from KIR2DL2/L3/S2 heterozygous donors at 10:1 and 5:1 ratios. A representative experiment from one donor is shown. **(C)** Box and whiskers plots show the mean and SD of five independent experiments. Each dot represents one donor. CD107a from the No target control was subtracted. Differences were determined using a paired t test. P value * <0.05.

The inability of Flaviviral peptides to induce NK cell activation through KIR2DS2 in this assay contrasts with the results from the tetramer staining, in which a strong binding of KIR2DS2 to I**VD**LMCHAT**F**, and to a lesser extent to I**VD**VMCHAT**L** peptide, was observed **(Figure 4.4)**. The low ICP47 levels in this cell line could explain the lack of KIR2DS2-mediated responses to Flaviviral peptides.

Similarly to HLA-C*0802, HLA-C*0501-expressing cells without peptides induced the highest degranulation levels in all three NK cell subpopulations **(Figure 4.7B,C)**. CD107a expression on KIR2DL2/L3/S2^{neg} NK cells to *IIKDSGSTV* and Flaviviral peptides was slightly reduced, with statistically significant differences for the I**VD**VMCHAT**L** at 5:1 ratio (p=0.0155) and I**VD**LMCHAT**F** peptide at 10:1 and 5:1 ratios (p=0.0148 and p=0.0154, respectively). This suggest that other KIR receptors may interact with these peptides presented by HLA-C*0501 (i.e KIR2DL1) leading to NK cell inhibition.

Degranulation of KIR2DL2/L3^{high} NK cells to *IIKDSGSTV* peptide was reduced compared to the no peptide control at both ratios; however such inhibition was less marked compared to HLA-C*0802, the cognate ligand for KIR2DL2/L3 receptors **(Figure 4.6B)**. Degranulation of this NK cell subset to Flaviviral peptides was also inhibited compared to the no peptide control, but was significantly increased to the three viral peptides compared to *IIKDSGSTV* at both E:T ratios (I**VD**LMCHAT**F**: p=0.0642 and p=0.0273; V**ID**AMCHAT**L**: p=0.0106 and p=0.0189; I**VD**VMCHAT**L**: p=0.0088 and p=0.0035; respectively; **Figure 4.7B,C**).

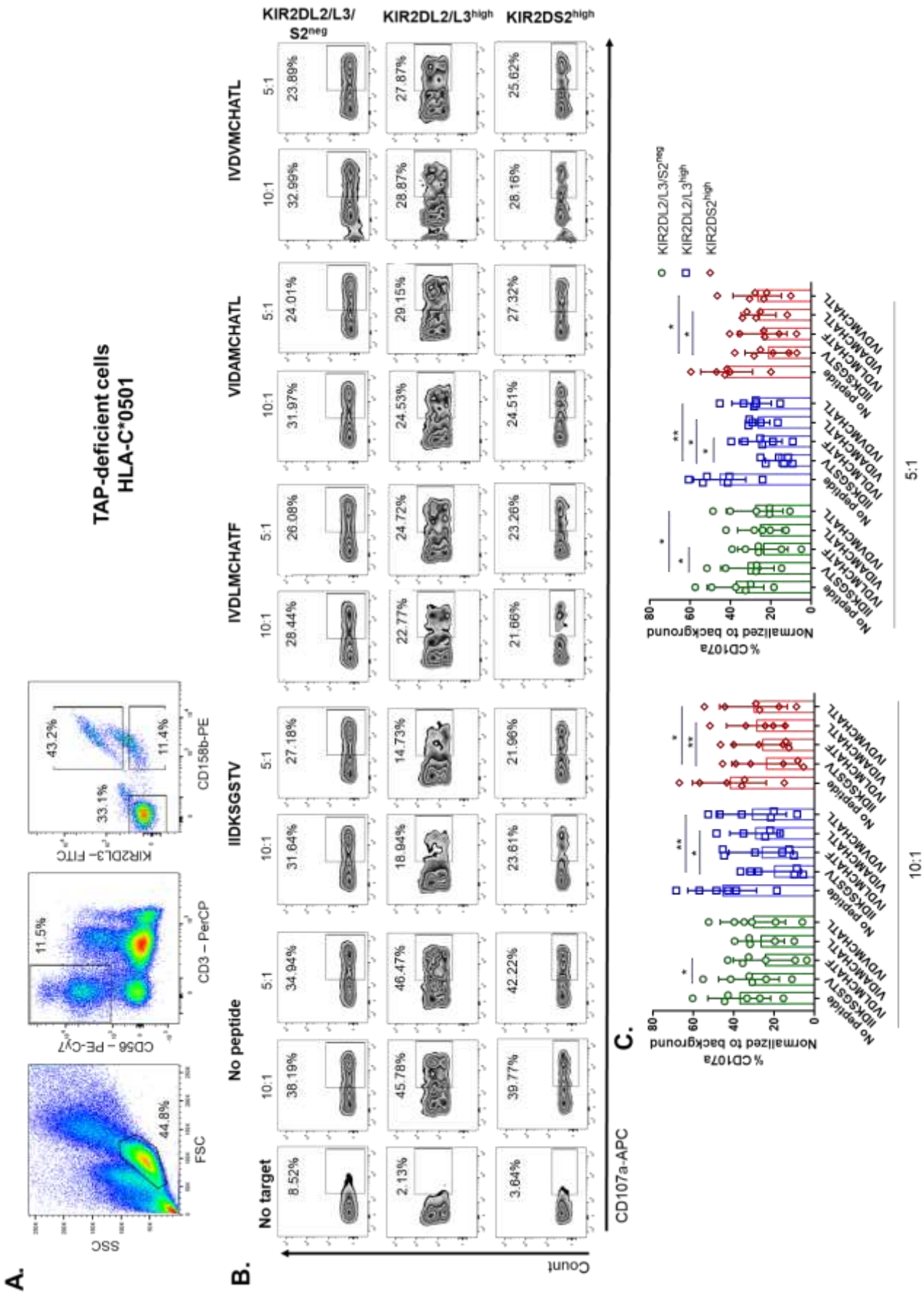
A.
TAP-deficient cells
HLA-C*0501
SSC
FSC
44.8%
CD56 – PE-CY7
CD3 – PerCP
11.5%
KIR2DL3 – FITC
CD158b-PE
33.1%
43.2%
11.4%
B.
No peptide
IIDKSGSTV
IVDLMCHATF
VIDAMCHATL
IVDVMCHATL
No target
10:1
5:1
KIR2DL2/L3/S2neg
KIR2DL2/L3high
KIR2DS2high
8.52%
38.19%
34.94%
2.13%
45.78%
46.47%
3.64%
39.77%
42.22%
31.64%
27.18%
18.94%
14.73%
23.61%
21.86%
28.44%
26.08%
22.77%
24.72%
21.66%
23.26%
31.97%
24.01%
24.53%
29.15%
24.51%
27.32%
32.99%
23.89%
28.87%
27.87%
28.16%
25.62%
Count
CD107a-APC
C.
% CD107a
Normalized to background
No peptide
IIDKSGSTV
IVDLMCHATF
VIDAMCHATL
IVDVMCHATL
KIR2DL2/L3/S2neg
KIR2DL2/L3high
KIR2DS2high
10:1
5:1

Figure 4.7 Degranulation of NK cells to Flaviviral peptides bound to HLA-C*0501. (A) Flow cytometry plots show KIR2DL2/L3/S2^{neg}, KIR2DL2/L3^{high} and KIR2DS2^{high} NK cell subsets gated on CD3- CD56+ NK cells from total PBMC. Percentages of each cell population are shown. **(B)** TAP-deficient 721.221 cells expressing HLA-C*0501 were loaded with no peptide or 200 μM of control or Flaviviral peptides at 26ºC and used as targets in a degranulation assay to total PBMC from KIR2DL2/L3/S2 heterozygous donors at 10:1 and 5:1 ratios. A representative experiment from one donor is shown **(C)** Box and whiskers plots show the mean and SD of five independent experiments. Each dot represents one donor. CD107a from the No target control was subtracted. Differences were determined using a paired t test. P value * <0.05, ** <0.01.

Degranulation levels of KIR2DS2^{high} NK cells to HLA-C*0501-expressing cells loaded with Flaviviral peptides were slightly increased at 5:1 ratio (Median 27.32% for V**ID**AMCHAT**L**, 25.62% for I**VD**VMCHAT**L** and 23.26% for I**VD**LMCHAT**F** compared to 21.96% for *IIDKSGSTV*). Such increase was maintained to I**VD**VMCHAT**L** and V**ID**AMCHAT**L** peptides at 10:1 ratio (Median 28.16% and 24.51%, respectively) whereas it was stable to I**VD**LMCHAT**F** peptide (Median: 21.66%; **Figure 4.7B,C**). As with HLA-C*0802, no statistically significant differences were found between control and I**VD**LMCHAT**F** peptide; however those differences yielded significant results for V**ID**AMCHAT**L** (p=0.0079 at 10:1 and p=0.0239 at 5:1 ratios) and I**VD**VMCHAT**L** peptides (p=0.0348 at 10:1 and p=0.0253 at 5:1 ratios; **Figure 4.7B,C**). These results are not consistent with the tetramer binding as I**VD**LMCHAT**F** peptide bound to HLA-C*0501 was strongly recognized by KIR2DS2.

The reasons that could explain lack of consistency between the tetramer staining and this assay include donor variability, low levels of ICP47 on HLA-C*0802-expressing cells, unstable presentation of exogenous peptides and co-expression of inhibitory KIR2DL2 by the KIR2DS2^{high} NK cell subset as described by Blunt et al (Blunt *et al.*, 2019). To circumvent this issue, an improved co-culture system consisting of target and effector cells stably expressing MHC-I:peptide complexes and KIR receptors, respectively, was established. Given the fact that I**VD**LMCHAT**F** peptide from DENV/ZIKV bound to HLA-C*0802 and HLA-C*0501 was strongly recognized by KIR2DS2-PE tetramer and when bound to HLA-C*0102 has shown to specifically induce NK cell activity through KIR2DS2 (Naiyer *et al.*, 2017), this peptide was selected for further experiments.

4.6 Generation of a co-culture system using endogenously presented peptides

To determine the effect of I**VD**LMCHAT**F** peptide from DENV/ZIKV in the induction of NK cell responses through canonical or cross-reactive interactions with KIR2DS2, target cells stably presenting endogenously processed viral peptides were co-cultured with NKL cells stably expressing KIR2DL2 or KIR2DS2 receptors or with purified primary NK cells. This improved co-culture system closely resembles endogenous presentation of peptides through MHC-I to NK cells occurring *in vivo*.

4.6.1 Target cells

TAP-competent 721.221 cells expressing HLA-C*0802 or HLA-C*0501 alleles had been electroporated in our laboratory with a DNA plasmid carrying the NS3 protein from DENV coupled to a mCherry fluorescent tag. The helicase domain of the DENV/NS3 protein carries the I**VD**LMCHAT**F** peptide. Endogenous processing of this viral protein allows these cells to present I**VD**LMCHAT**F** peptide in the context of HLA-C*0802 or HLA-C*0501 alleles.

To confirm stable expression of DENV/NS3 protein and HLA-C alleles, mCherry fluorescence and HLA-C expression were measured by flow cytometry. As expected, mCherry was increased in both target cells electroporated with DENV/NS3; however it was significantly higher in those expressing the HLA-C*0501 allele ($p=0.0250$; **Figure 4.8A,B**). Regarding HLA-C expression, this molecule was significantly increased in both cell lines expressing DENV/NS3 compared to their corresponding parental cells ($p=0.0312$ for HLA-C*0802 and $p=0.0382$ for HLA-C*0501; **Figure 4.8C,D**), suggesting that DENV/NS3 might be involved in up-regulation of MHC-I as a mechanism to evade immune recognition.

4.6.2 Effector cells

As effector cells, two different sources of NK cells were used. The first one consisted of the NKL cell line previously transduced with genes encoding KIR2DL2 or KIR2DS2 receptors. As described in chapter 3, these generated cell lines stably express those receptors and

have been used elsewhere (Naiyer *et al.*, 2017; Blunt *et al.*, 2019). The second one consisted of primary NK cells isolated from PBMC from KIR2DL2/S2 homozygous or KIR2DL2/L3/S2 heterozygous donors that were subsequently sorted based on the expression of those receptors.

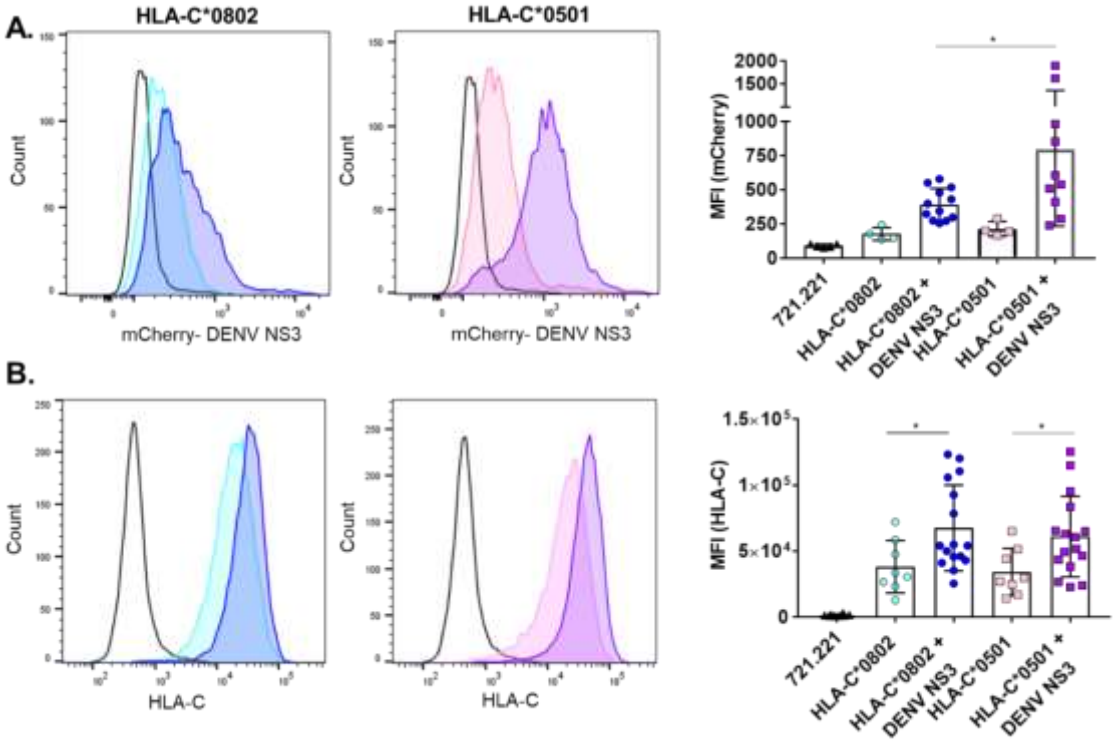

Figure 4.8 Generation of target cells endogenously presenting DENV/NS3-derived peptides. Expression of DENV/NS3-mCherry **(A)** and HLA-C **(B)** on 721.221 cells expressing HLA-C*0802 or HLA-C*0501 alleles was measured by flow cytometry and compared to its parental cell line. Each dot represents one measurement. Mean values and SD of at least 4 independent experiments are shown (n=4-16). Differences were determined using an unpaired t test. Comparison of HLA-C between cells expressing HLA-C*0802 or the ones co-expressing HLA-C*0802 and DENV NS3 was performed using a Mann-Whitney test as the latter did not follow a normal distribution. P value * <0.05.

In order to enrich primary NK cell subpopulations, NK cells were isolated from PBMC and cultured in an optimized cell culture medium with high concentration of rhIL-2 to promote NK cell expansion. First, to monitor NK cell growth and viability, purified NK cells from five donors were counted at day 0, 7 and 15 of incubation and cell viability was determined using trypan blue. NK cell growth was evident at day 7 for all donors and continued to increase at day 15 **(Figure 4.9A)**. Likewise, NK cell viability was >90% and maintained high over time **(Figure 4.9B)**. Approximately at day 15 of incubation, NK cells were sorted based on the expression of KIR2DL2/L3 and KIR2DS2 receptors using the combination of antibodies previously described (Blunt *et al.*, 2019) **(Figure 4.9C)**. Between $0.5x10^6$ and $1x10^6$ sorted

KIR2DL2/L3/S2^{neg}, KIR2DL2/L3^{high} and KIR2DS2^{high} NK cells were expanded in the same culture medium + rhIL-2 and were further used for functional assays.

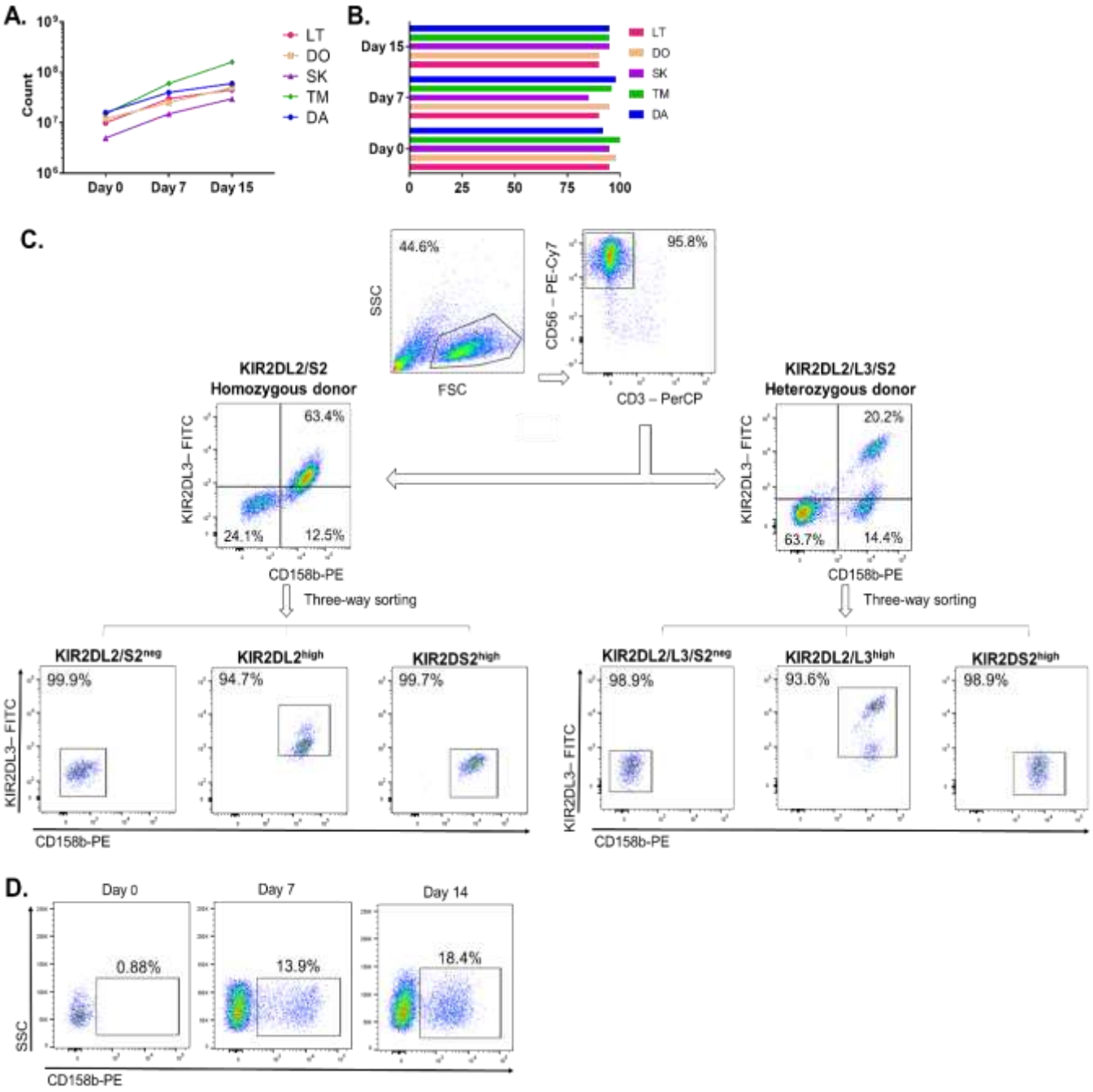

Figure 4.9 Generation of enriched effector cells using Fluorescent Activated Cell Sorting (FACS). (A,B) NK cells from five donors were isolated from PBMC and grown in supplemented NK MACS culture medium + rhIL-2 for two weeks. NK cell expansion **(A)** and cell viability **(B)** were determined. **(C)** Gating strategy for three-way sorting of CD3- CD56+ NK cells from KIR2DL2/S2 homozygous or KIR2DL2/L3/S2 heterozygous donors. Percentages of each cell population are shown. **(D)** Flow cytometry plots show acquisition of KIR receptors (CD158b) on the KIR2DL2/L3/S2^{neg} NK cell subset over time.

Surprisingly, it became evident that the KIR2DL2/L3/S2^{neg} subset started to gradually increase the percentage of KIR2DL2/L3/S2 positive NK cells **(Figure 4.9D)**, consistent with an *in vitro* differentiation of immature KIR negative NK cells into a more mature phenotype. This modulation of the KIR repertoire has been previously documented and is explained by the presence of high amounts of rhIL-2 (Gays *et al.*, 2005; de Rham *et al.*, 2007). Due to these findings, sorted NK cells were cultured for up to one week before using them for functional assays.

4.7 KIR2DS2 specifically mediates killing of HLA-C*0802-expressing cells endogenously presenting DENV/NS3-derived peptides

In an attempt to determine whether endogenous presentation of I**VD**LMCHAT**F** peptide bound to HLA-C*0802 or HLA-C*0501 could activate NK cells through canonical or cross-reactive interactions with KIR2DS2, respectively, target cells expressing DENV/NS3 were co-cultured with NKL cells expressing KIR2DL2 or KIR2DS2 receptors. Specific cytotoxicity of NKL cells to target cells was determined by flow cytometry. The gating strategy for this assay is shown in chapter 2 **(Figure 2.7)**.

As shown in **Figure 4.10**, cytotoxic activity of untransduced NKL cells to HLA-C*0802 cells expressing DENV/NS3 was slightly increased compared to its parental cell line at both E:T ratios, however this difference was not statistically significant (p=0.4834 for 20:1 and p=0.3743 for 10:1). As expected, NKL cells expressing KIR2DL2 mediated inhibition of target cell lysis. Such inhibition tended to be more evident to cells expressing HLA-C*0802 alone at 10:1 ratio (p=0.1047; **Figure 4.10C**). As the KIR2DL2-PE tetramer had shown binding to HLA-C*0802:I**VD**LMCHAT**F** complex, this suggests that the canonical interaction of KIR2DL2 with HLA-C*0802:I**VD**LMCHAT**F** complex might antagonize NK cell inhibition.

Unlike NKL and NKL-2DL2 cells, NKL cells bearing activating KIR2DS2 killed target cells expressing HLA-C*0802 and DENV/NS3 at a greater extent compared to cells expressing HLA-C*0802 alone. Such specific cytotoxicity of NKL-2DS2 cells was consistent and statistically significant at 20:1 and 10:1 ratios (p=0.0087 and p=0.0039, respectively; **Figure 4.10**).

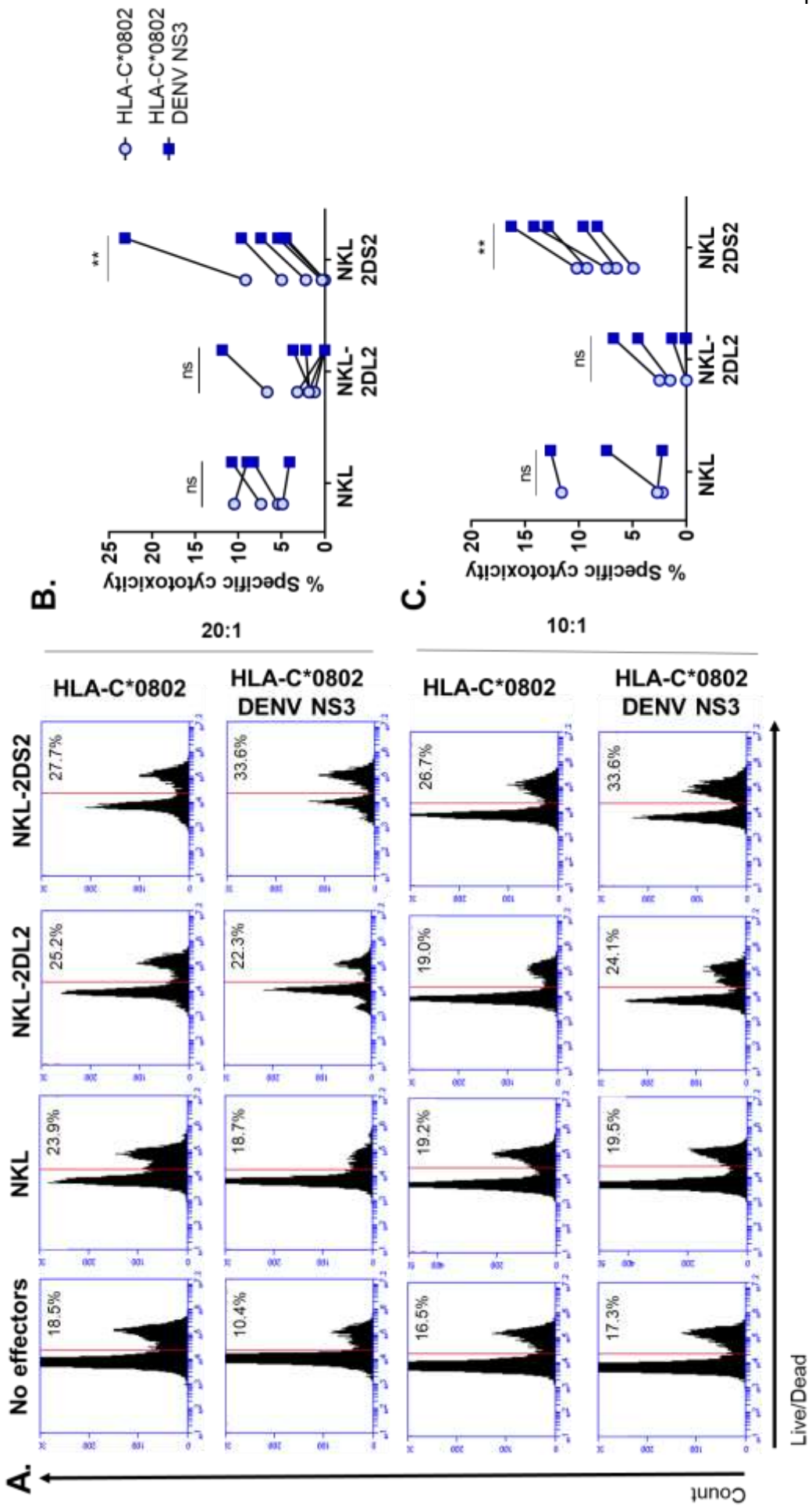
A.
Count
Live/Dead
No effectors
NKL
NKL-2DL2
NKL-2DS2
HLA-C*0802
HLA-C*0802 DENV NS3
18.5%
10.4%
23.9%
18.7%
25.2%
22.3%
27.7%
33.6%
16.5%
17.3%
19.2%
19.5%
19.0%
24.1%
26.7%
33.6%
B.
20:1
% Specific cytotoxicity
ns
ns
**
NKL
NKL-2DL2
NKL-2DS2
C.
10:1
HLA-C*0802
HLA-C*0802 DENV NS3

Figure 4.10 Killing of target cells presenting DENV/NS3-derived peptides bound to HLA-C*0802 by NKL cell lines. (A) 721.221 cells expressing HLA-C*0802 or co-expressing DENV/NS3 were co-cultured with NKL cell expressing KIR2DL2 or KIR2DS2 receptors at 20:1 and 10:1 ratios and then stained with a Live/Dead dye. A representative experiment is shown. **(B,C)** Line charts show the mean and SD of at least five independent experiments at 20:1 **(B)** and 10:1 **(C)** ratios (n=3-5). The percentage of dead cells from the No effector control was subtracted. Differences were determined using a paired t test. ns= non-significant; P value ** <0.01.

These results indicate that DENV/NS3-derived peptides presented in the context of HLA-C*0802 induce specific KIR2DS2-mediated killing of target cells. Given the strong binding of KIR2DS2-PE tetramer to I**VD**LMCHAT**F** peptide, it is extremely likely that this peptide in complex with HLA-C*0802 canonically binds KIR2DS2 and triggers NK cell activation, resulting in target cell death.

A different scenario was seen for HLA-C*0501-expressing cells after co-culture with NKL cell lines **(Figure 4.11)**. First, target cells expressing HLA-C*0501 alone and the ones co-expressing DENV/NS3 were killed to a similar extent by untransduced NKL cells, with a slight, non-significant reduction to HLA-C*0501 DENV/NS3 cells at 10:1 ratio (p=0.5344; **Figure 4.11C**). Target cell lysis was inhibited by NKL-2DL2 cells, with such inhibitory effect tending to be more noticeable on target cells co-expressing HLA-C*0501 and DENV/NS3 **(Figure 4.11B)**. These results indicate that endogenous peptides presented by HLA-C*0501 mediate cross-reactive interactions with KIR2DL2. Likewise, it could be suggested that cross-reactivity of KIR2DL2 with HLA-C*0501:I**VD**LMCHAT**F** complex presents a stronger affinity than that of HLA-C*0802:I**VD**LMCHAT**F**, as observed with the KIR2DL2-PE tetramer staining **(Figure 4.4 and 4.5)**. Thus, I**VD**LMCHAT**F** in complex with HLA-C*0501 would act as an inhibitory peptide that prevents NK cell activation through KIR2DL2.

Finally, despite KIR2DS2-PE tetramer strongly cross-reacted with HLA-C*0501:I**VD**LMCHAT**F** complex, cells co-expressing HLA-C*0501 and DENV/NS3 did not induce any specific activation of KIR2DS2-expressing NKL cells. In fact, there was a slight reduction in levels of specific cytotoxicity to these target cells compared to its parental cell line at both E:T ratios **(Figure 4.11)**. Although such reduction was not statistically significant (p=0.6945 for 20:1 and p=0.3185 for 10:1), this suggests that non-canonical binding of HLA-C*0501:I**VD**LMCHAT**F** complex to KIR2DS2 is not sufficient to induce the threshold needed for NK cell activation.

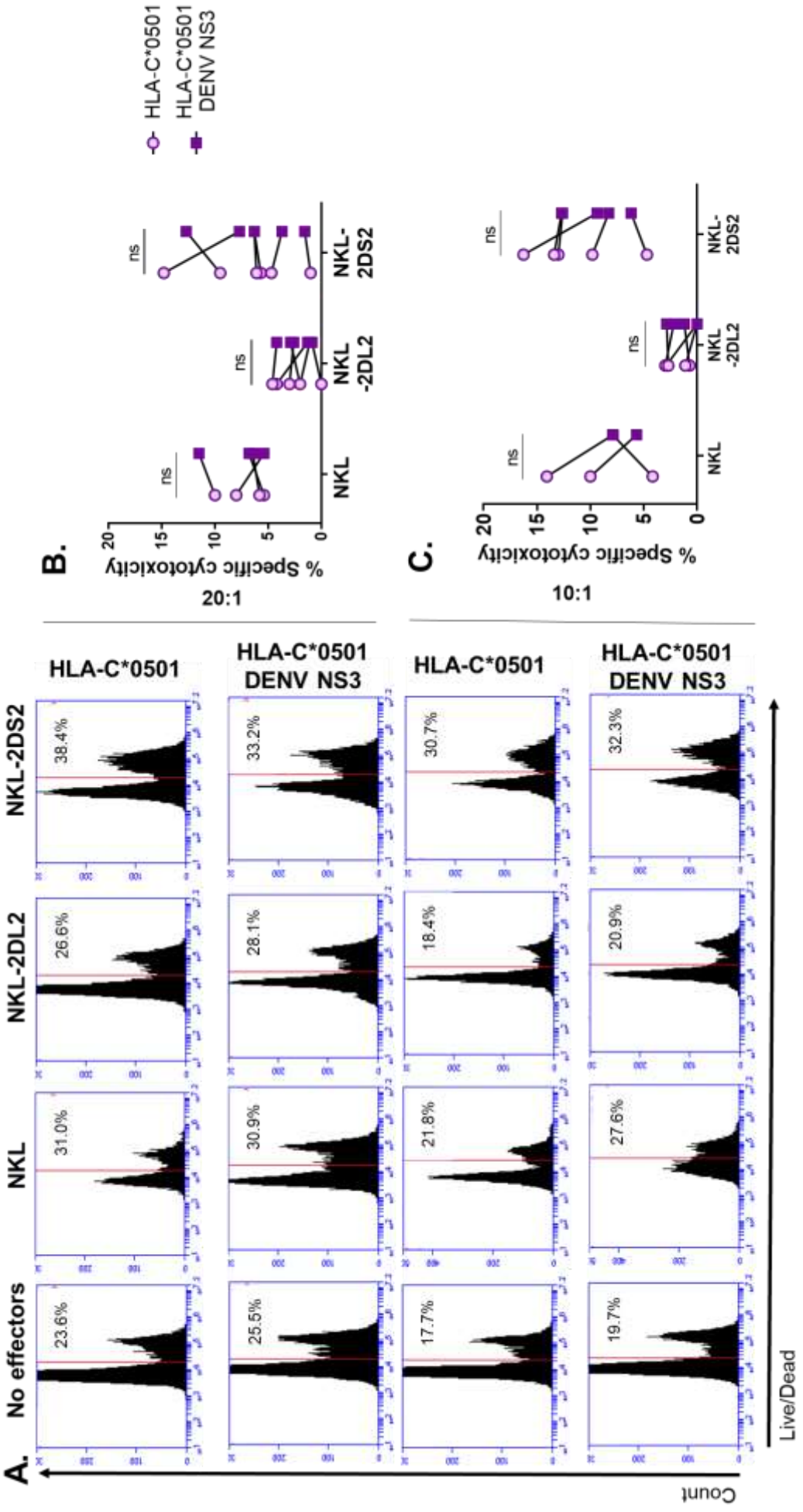
A.
No effectors
NKL
NKL-2DL2
NKL-2DS2
HLA-C*0501
HLA-C*0501 DENV NS3
23.6%
31.0%
26.6%
38.4%
25.5%
30.9%
28.1%
33.2%
17.7%
21.8%
18.4%
30.7%
19.7%
27.6%
20.9%
32.3%
Count
Live/Dead
B.
20:1
% Specific cytotoxicity
ns
NKL
NKL-2DL2
NKL-2DS2
HLA-C*0501
HLA-C*0501 DENV NS3
C.
10:1

Figure 4.11 Killing of target cells presenting DENV/NS3-derived peptides bound to HLA-C*0501 by NKL cell lines. (A) 721.221 cells expressing HLA-C*0501 or co-expressing DENV/NS3 were co-cultured with NKL cell expressing KIR2DL2 or KIR2DS2 receptors at 20:1 and 10:1 ratios and then stained with a Live/Dead dye. A representative experiment is shown. **(B,C)** Line charts show the mean and SD of at least three independent experiments at 20:1 **(B)** and 10:1 **(C)** ratios (n=3-6). The percentage of dead cells from the No effector control was subtracted. Differences were determined using a paired t test. ns= non-significant.

4.8 KIR2DS2^{high} NK cells specifically degranulate in response to target cells expressing HLA-C*0802 and DENV/NS3

To evaluate whether primary NK cells expressing KIR2DS2 mediate NK cell responses to cells endogenously presenting I**VD**LMCHAT**F** peptide bound to HLA-C*0802 or HLA-C*0501, target cells expressing DENV/NS3 were co-cultured with primary NK cells from KIR2DL2/S2 homozygous (n=1) or KIR2DL2/L3/S2 heterozygous donors (n=6), previously sorted based on the expression of those receptors. Then, a degranulation assay was performed and CD107a expression was detected by flow cytometry. The gating strategy for this assay is shown in chapter 2 **(Figure 2.8)**

Degranulation of KIR2DL2/L3/S2^{neg} NK cells to HLA-C*0802 expressing DENV/NS3 was moderately increased compared to cells expressing HLA-C*0802 alone. Although this increase was noticeable at both E:T ratios, it was close to statistical significance only at 5:1 ratio (p=0.0625; **Figure 4.12A,B**). This indicates that other NK cell receptors besides KIR2DL2/L3/S2 could have a role in NK cell activation to DENV/NS3.

Both target cells inhibited KIR2DL2/L3^{high} NK cell degranulation at comparable levels (p=0.5000 for 10:1and p=0.2500 for 5:1), which indicates that presentation of DENV/NS3-derived peptides do not make a difference in NK cell inhibitory functions. Similarly to the cytotoxicity assay, KIR2DS2^{high} NK cells specifically degranulated in response to HLA-C*0802 presenting DENV/NS3 peptides at 10:1 and 5:1 ratios, but not the ones expressing HLA-C*0802 alone (p=0.0156 and 0.0125, respectively; **Figure 4.12**). These results confirm that HLA-C*0802 presenting DENV/NS3-derived peptides – among which the I**VD**LMCHAT**F** peptide is included – specifically induce an activating NK cell response through canonical interactions with KIR2DS2.

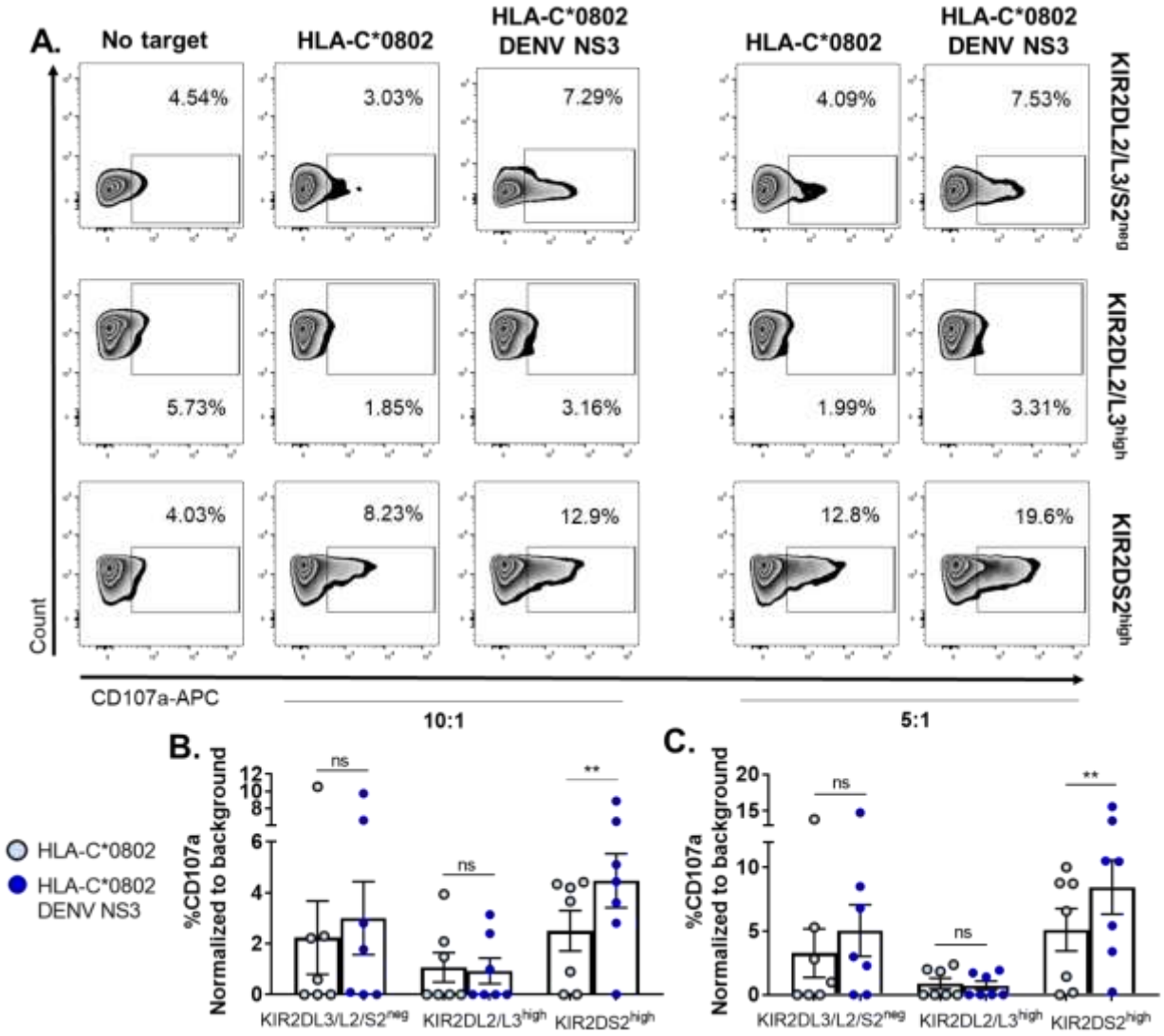

Figure 4.12 Degranulation of sorted NK cells to DENV/NS3-derived peptides bound to HLA-C*0802. (A) 721.221 cells expressing HLA-C*0802 or co-expressing DENV/NS3 were used as targets in a degranulation assay to sorted KIR2DL2/L3/S2^{neg}, KIR2DL2/L3^{high} and KIR2DS2^{high} NK cells at 10:1 and 5:1 ratios. A representative experiment from one donor is shown **(B,C)** Scatter dot plots show the mean and SD of seven independent experiments. CD107a from the No target control was subtracted. Each dot represents one donor. Differences were determined using a paired t test. ns= non-significant; P value ** <0.01.

For HLA-C*0501-expressing cells, the KIR2DL2/L3/S2^{neg} NK cell subpopulation expressed CD107a to HLA-C*0501 alone and HLA-C*0501 expressing DENV/NS3 at similar levels at both E:T ratios. Interestingly, KIR2DL2/L3^{high} NK cells were more inhibited in response to HLA-C*0501 expressing DENV/NS3, and even though this difference was not statistically significant at 10:1 ratio (p=0.2500), the p value was close to the significance threshold at 5:1 ratio (p=0.0625). These results correlate with the findings from the cytotoxicity assay and suggest that IVDLMCHATF peptide bound to HLA-C*0501 may cross-react with KIR2DL2/L3 and act as an inhibitory peptide.

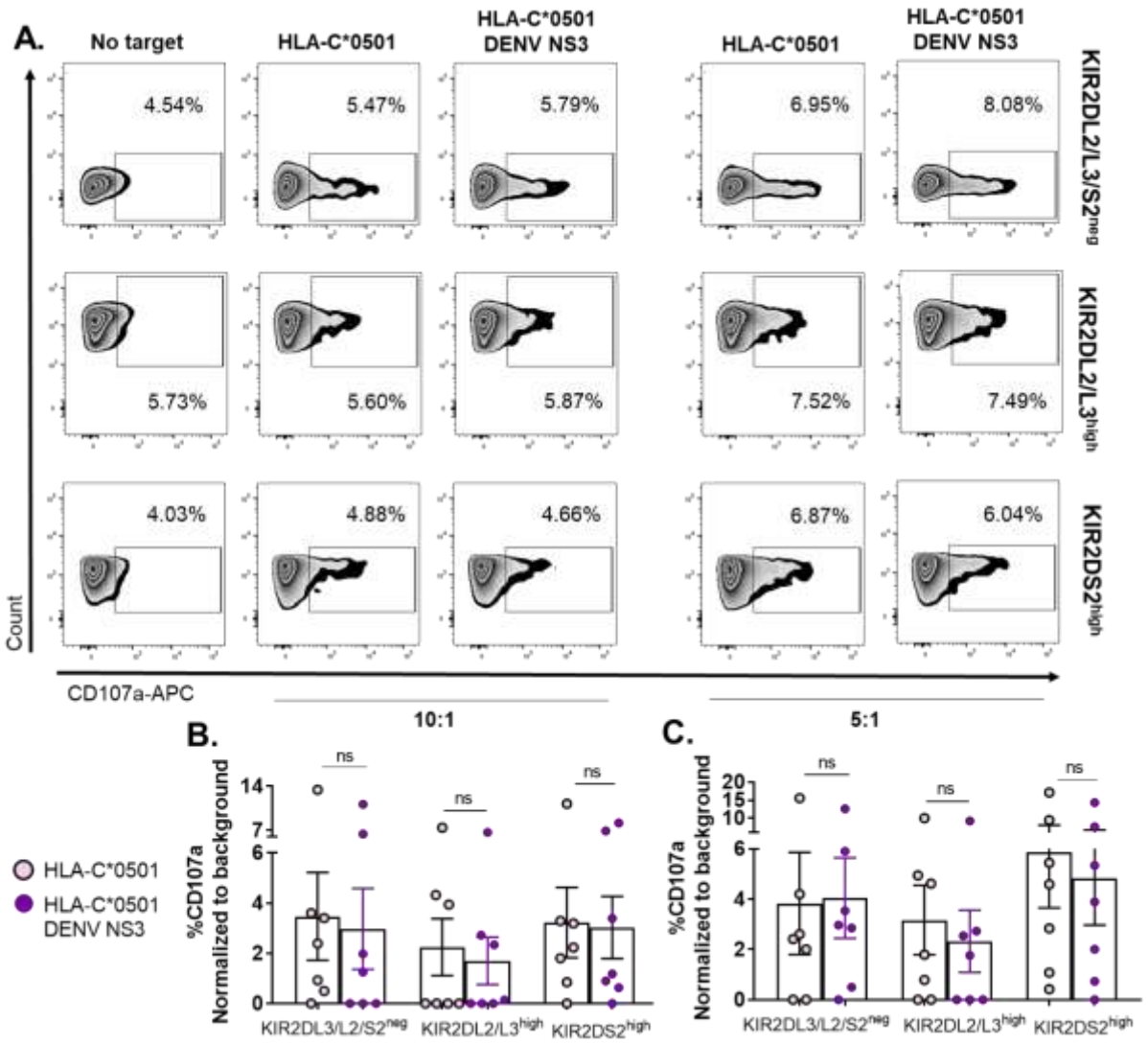

Figure 4.13 Degranulation of sorted NK cells to DENV/NS3-derived peptides bound to HLA-C*0501. (A) 721.221 cells expressing HLA-C*0501 or co-expressing DENV/NS3 were used as targets in a degranulation assay to sorted KIR2DL2/L3/S2^{neg}, KIR2DL2/L3^{high} and KIR2DS2^{high} NK cells at 10:1 and 5:1 ratios. A representative experiment from one donor is shown **(B,C)** Scatter dot plots show the mean and SD from seven independent experiments. CD107a from the No target control was subtracted. Each dot represents one donor. Differences were determined using a paired t test. ns= non-significant.

Finally, KIR2DS2^{high} NK cells had a reduced degranulation to cells expressing HLA-C*0501 and DENV/NS3 at both E:T ratios as observed in the cytotoxicity assay. This difference was not statistically significant (p=0.5625 for 10:1 and p=0.5496 for 5:1); however it reinforces the hypothesis of a possible role for I**VD**LMCHAT**F** as a potential inhibitory peptide when bound to HLA-C*0501 allele. The role of other mechanisms of NK cell recognition cannot be excluded.

4.9 Discussion

The influence of NK cell functions in the clinical outcome of viral infections is largely determined by receptor/ligand interactions that regulate the balance of signals for their inhibition or activation. Interactions that are particularly relevant for NK cell activity involve KIR2D receptors that bind HLA-C ligands (Blais, Dong and Rowland-Jones, 2011). Even though both molecules show extreme diversity, the presence of certain HLA-C1/C2 alleles have been found to be associated with either susceptibility or resistance to viral infections, including HLTV-1, HCV (both C1), HSV-2 (C2) and HIV-1 (C1/C2) (Lekstrom-Himes *et al.*, 1999; Jeffery *et al.*, 2000; Khakoo *et al.*, 2004; Leslie *et al.*, 2010). Thus, allelic diversity of HLA-C ligands and their receptors fine-tune NK cell responses to viruses.

Besides the interaction between KIR and HLA-C alleles, the role of the bound peptide in modulating the overall NK cell response has gained more attention. Specific residues or combinations of residues within the peptide sequence have been shown to modify the interaction with the receptor (Fadda *et al.*, 2011; Fadda *et al.*, 2012; Sim *et al.*, 2017). Particularly, amino acids at P7 and P8 of peptides may either enhance or disrupt interactions with inhibitory or activating KIR, and such events depend on their structural properties including molecular size and electric charge. The relevance of those residues is such, that they are able to modify the original receptor specificity. In this regard, it has been described that peptides carrying arginine at P7 bound to HLA-C*0802 promote canonical inhibition to KIR2DL2/L3 and cross-reactive inhibition to KIR2DL1 (Sim *et al.*, 2017). Similarly, peptides carrying a tryptophan at P8 bound to HLA-C*0501 have been found to activate NK cells through interaction with KIR2DS4 (Sim *et al.*, 2019). Thus, the peptide sequence selectively dictates canonical or cross-reactive binding to KIR.

This chapter focused on the search of viral peptides that in complex with HLA-C1 or C2 alleles could be able to engage activating KIR2DS2 through canonical or non-canonical interactions, respectively. To achieve this, a set of five viral peptides (4 *Flaviviridae* and 1 ebolavirus) containing the AT-binding motif at P7 and P8 and forming stable complexes with HLA-C*0802 and HLA-C*0501 were identified. Both alleles were selected as representative from each HLA-C group due to their high structural homology (99.5%) and identical peptide-binding motifs (Rasmussen *et al.*, 2014; Di Marco *et al.*, 2017). In addition, distribution of both alleles frequencies is worldwide, with the HLA-C*0802 allele being more prevalent in Pakistan and England whereas the HLA-C*0501 allele is mainly found in European countries (Italy, France and Spain) and India (Gonzalez-Galarza *et al.*, 2015). These

characteristics make the HLA-C*0802/HLA-C*0501 system a reliable approach to compare KIR binding to HLA-C1/C2 groups and to study interactions with KIR receptors that could be of high relevance in specific populations.

As a first step, in order to evaluate the ability of viral peptides to engage KIR2DS2, stable HLA-C:peptide complexes at the cell surface of TAP-deficient cells were used as ligands for KIR2DS2 tetramers. Two out of five viral peptides (I**VD**LMCHAT**F** and I**VD**VMCHAT**L**) bound to HLA-C*0802 and HLA-C*0501 showed canonical and cross-reactive interactions with KIR2DS2 tetramers, being I**VD**LMCHAT**F** from DENV/ZIKV the peptide that promoted the strongest binding. Both peptide sequences only differ at two positions: P4 and P10. As the C-terminus of 9-mer and 10-mer peptides is thought to determine KIR binding, it is likely that P10 plays a role in the interaction with the receptor.

The relevance of the C-terminus from the peptide in mediating engagement to KIR has been well described. Particularly, the C-terminus ends of the 9-mer self-peptide LSSPVTKSF and the 10-mer HIV-1-derived peptide TSTLQEQIGW presented by HLA-B*5701 have shown to promote binding to D1 and D2 domains from KIR3DL1 (Vivian *et al.*, 2011; Pymm *et al.*, 2017). Mutational analysis have specifically shown that phenylalanine and histidine at P8 promote KIR3DL1 binding whereas small non-polar residues such as alanine and leucine abrogate it (O'Connor *et al.*, 2014). This evidence suggests that phenylalanine at P10 from the 10-mer I**VD**LMCHAT**F** peptide may be a key residue that mediates binding to KIR2DS2.

Despite strong engagement of I**VD**LMCHAT**F** peptide to KIR2DS2 tetramer, degranulation of KIR2DS2^{high} NK cells to this peptide exogenously loaded onto HLA-C*0802 or HLA-C*0501-expressing cells was low. These weak NK cell responses can be attributed to factors related to the co-culture system, either the target or effector cells. First, from the effector cell front, the KIR2DS2^{high} NK cell subset is relatively small compared to the other NK cell subsets (~10% from CD3- CD56+ NK cells) and besides, this subpopulation co-expresses KIR2DL2/L3 receptors (Blunt *et al.*, 2019). Thus, inhibitory KIR in the KIR2DS2^{high} NK cell subset could interact with cellular peptides presented by HLA-C*0802 or HLA-C*0501 alleles and favour the balance of signals towards inhibition.

From the target cell front, the inability of ICP47 to efficiently block TAP in HLA-C*0802-expressing cells together with the moderate affinity of I**VD**LMCHAT**F** peptide to this allele may suggest that self-peptides with higher affinities than that of I**VD**LMCHAT**F** peptide could have been presented by this cell line. These complexes could have been recognized

by KIR2DL2/L3 receptors co-expressed by KIR2DS2^{high} NK cells, thus preventing NK cell activation. Likewise, peptide loading of TAP-deficient cells requires uptake and intracellular loading of peptides onto newly synthesized MHC-I molecules at low temperatures (26^{o}C); however these are not as stable as TAP-competent cells at 37^{o}C (De Silva *et al.*, 1999). The study conducted by Stroobant *et al* showed that a tumour peptide exogenously loaded onto HLA-B*4402-expressing cells was unable to stimulate cytotoxic T lymphocytes (CTL); however endogenous presentation of this peptide triggered antigen-specific responses from CTL (Stroobant *et al.*, 2012), suggesting the latter as a more reliable approach.

As a strategy to mimic the antigen presentation process that occurs within cells, an improved co-culture system using endogenously presented peptides to NKL cells expressing single receptors or to enriched primary NK cells was generated. *In vitro* systems for endogenous presentation of viral peptides use cells stably expressing virus replicons or individual proteins that are processed intracellularly in order to generate viral peptides able to bind MHC-I molecules. Naiyer *et al* previously showed that HEK cells stably expressing a DENV replicon and the HLA-C*0102 allele were strongly killed by KIR2DS2-expressing NK cells; however this effect was not seen against replicon cells expressing HLA-C*0304 (Naiyer *et al.*, 2017). Such specific KIR2DS2-mediated NK cell responses were attributed to recognition of I**VD**LMCHAT**F** peptide endogenously presented by HLA-C*0102.

To determine more closely whether I**VD**LMCHAT**F** peptide endogenously presented by HLA-C*0802 or HLA-C*0501 could mediate NK cells activation through canonical or non-canonical binding with KIR2DS2, HLA-C-expressing 721.221 cells electroporated with the NS3 protein from DENV were used. This non-structural protein has two domains: an N-terminal serine protease domain and a C-terminus helicase domain, and is involved in polyprotein processing and viral replication (Simmonds *et al.*, 2017). The I**VD**LMCHAT**F** peptide (256-265) carrying the highly conserved “MCHAT” motif is thought to play a crucial role in the helicase functions of NS3 during viral replication (Khan *et al.*, 2008; Naiyer *et al.*, 2017).

Flow cytometry analysis of target cells expressing DENV/NS3 showed an increased HLA-C expression compared to their parental cell line. Up-regulation of MHC-I after *Flavivirus* infection of cells has been previously reported (Mullbacher and Lobigs, 1995; Ye *et al.*, 2013; McKechnie *et al.*, 2019). Similarly, cell lines stably expressing self-replicating subgenomic DENV replicons have shown an increased expression of MHC-I and reduced susceptibility to NK cell killing, suggesting that non-structural DENV proteins may mediate mechanisms for viral evasion of NK cell responses (Mullbacher and Lobigs, 1995;

Hershkovitz *et al.*, 2008). Results from the present study are consistent with a role for DENV NS3 protein in the up-regulation of HLA-C alleles; however, the molecular mechanisms for this assumption need to be determined in detail.

Functional responses of NK cells to target cells endogenously presenting DENV/NS3-derived peptides were tested by using a NKL cell line expressing KIR2DS2 or purified primary NK cells from healthy volunteers. Remarkably, target cells expressing HLA-C*0802 and DENV NS3 were efficiently killed by KIR2DS2-expressing NKL cells. These targets also induced a strong degranulation response from primary KIR2DS2^{high} NK cells suggesting that the balance of signals within NK cells shifted in favour of an activation state. These results indicate that DENV/NS3 is intracellularly processed into peptides (including I**VD**LMCHAT**F** peptide), which are presented by HLA-C*0802 at the cell surface. HLA-C*0802:peptide complexes canonically engage KIR2DS2 and trigger NK cell activation that results in degranulation and target cell lysis. Although this effect could have been mediated by I**VD**LMCHAT**F** peptide, the role of other DENV/NS3-derived peptides cannot be excluded.

Conversely, DENV/NS3 and HLA-C*0501-expressing cells did not induce any specific response from KIR2DS2-expressing NKL cells or primary KIR2DS2^{high} NK cells. The strong KIR2DS2 tetramer staining and the lack of induction of KIR2DS2-mediated NK cell responses might be explained by the lack of an intracellular signal that overcome the activation threshold. The activating signals within NK cells are characterized by the clustering of activating receptors at the cell surface, which together trigger an intracellular cascade of phosphorylation leading to NK cell activation (Oszmiana *et al.*, 2016).

Similarly to these results, Stewart *et al* showed that TAP-deficient RMA-S cells expressing HLA-C*0401 and exogenously loaded with QYDDAVYK peptide canonically engaged KIR2DS1 tetramers. Despite tetramer binding, HLA-C:peptide complexes failed to activate KIR2DS1+ NK clones (cytotoxicity and IFNγ production) (Stewart *et al.*, 2005b). This indicates that NK cell receptor expression is complex and the presence of other non-KIR receptor (i.e CD94/NKG2A) could also account for the lack of a cross-reactive response from KIR2DS2-expressing NK cells to DENV/NS3-derived peptides presented by cells with up-regulated expression of HLA-C*0501. Similarly, presentation of high affinity viral peptides with inhibitory properties is a possible scenario.

In summary, this chapter showed that DENV/NS3-derived peptides induce NK cell effector functions through canonical binding to KIR2DS2 and suggest that I**VD**LMCHAT**F** is the peptide mediating such effect. The ability of this conserved peptide to bind multiple HLA-C1 alleles make it an attractive target in the development of NK-cell based therapeutic strategies against flaviviral infections.

Chapter 5 - Peptide-specific activation of NK cells through KIR2DS2

5.1 Introduction

The ability of NK cells to discriminate healthy from abnormal cells is based on the intimate interactions between the wide array of cell surface receptors with their ligands and the balance of positive and negative signals that emerge from such associations (Borhis and Khakoo, 2011). In the specific case of KIR receptors and MHC-I ligands, the small peptide fragments bound to MHC-I are essential mediators of this system as they may facilitate or abrogate the interaction of both molecules, thereby influencing NK cell immune responses (Stewart *et al.*, 2005a; Long *et al.*, 2013).

In the context of viral infections, presentation of virus-derived peptides to NK cells may result in inhibition or activation of their effector functions. The modulation of these interactions depends on the relative abundance of the peptides and their affinity to both, the MHC-I molecule and the KIR receptor (Cassidy *et al.*, 2015; Boulanger *et al.*, 2018). Binding affinity to the MHC-I molecule is largely determined by anchor residues within the peptide sequence, which define peptide binding specificities and correlate with expression of MHC-I:peptide ligands at the cell surface. It has been described that low and high-affinity peptides compete for the MHC-I binding site; hence, presentation of peptides that have high affinity for the MHC-I molecule are more stable than low-affinity peptides, which are displaced by tapasin within the ER (Luft *et al.*, 2001; Praveen *et al.*, 2010; Kelly and Trowsdale, 2017).

Likewise, binding affinity of MHC-I:peptide complexes to KIR receptors influences the overall response and accounts for the differential effects on NK cells. For instance, several studies have described that viruses are capable of mutating their epitopes and present peptides that increase the affinity of the MHC-I molecule to inhibitory KIR, thus evading NK cell recognition (Alter *et al.*, 2011; Colantonio *et al.*, 2011; Holzemer *et al.*, 2015; Schafer *et al.*, 2015). Conversely, certain peptides presented by MHC-I molecules that bind inhibitory KIR with lower affinity may antagonise the inhibitory effect leading to NK cell activation (Fadda *et al.*, 2010; Cassidy, Cheent and Khakoo, 2014; Mbiribindi *et al.*, 2019). Finally, some viral peptides have shown the ability to directly engage activating KIR and thereby

shift the balance of signals towards a state of activation (Stewart *et al.*, 2005a; O'Connor *et al.*, 2015; Chapel *et al.*, 2017; Naiyer *et al.*, 2017). Thus, depending on the affinity to either inhibitory or activating KIR, the peptide repertoire in virally infected cells may be able to activate NK cells, which would be beneficial for the host in the recognition and elimination of viruses.

Our group recently identified a peptide derived from DENV and ZIKV (IVDLMCHATF) that in complex with HLA-C*0102 strongly engaged activating KIR2DS2 leading to NK cell activation and killing of target cells (Naiyer *et al.*, 2017). The experimental approach consisted on the design of a new method to co-express HLA-C*0102 and IVDLMCHATF peptide within the same cell. For this, a DNA plasmid carrying the Kozak sequence, the HLA-C*0102 allele, the T2A self-cleaving peptide from Thosea asigna virus (TaV), the E3/19K ER-targeting sequence from Adenovirus and the IVDLMCHATF peptide-encoding sequence was generated. This novel mechanism of endogenous peptide presentation has shown to be a successful approach for the induction of NK cell responses (Naiyer *et al.*, 2017).

The evidence from Chapter 4 suggested that DENV/NS3-derived peptides in complex with the HLA-C*0802 allele are cognate ligands for activating KIR2DS2 and promote NK cell activation. By using the methodological strategy developed by Naiyer *et al*, the aim of this chapter was to confirm whether IVDLMCHATF peptide endogenously presented by HLA-C*0802 could be sufficient to activate NK cells through the specific interaction with activating KIR2DS2.

5.2 A cloning strategy to generate a pIB-2 plasmid carrying the HLA-C*0802 allele and IVDLMCHATF peptide

The retroviral vector pIB2 (6009 bp) carrying the HLA-C*0102_T2A_IVDLMCHATF insert (1266 bp) has been previously reported (Borhis *et al.*, 2013; Naiyer *et al.*, 2017). In this study, the HLA-C*0102 gene sequence (PubMed Reference D50852.1) was replaced by HLA-C*0802 (PubMed Reference M84173.1) and sent for gene synthesis. A DNA donor plasmid (pMK-RQ – KanR) carrying the Kozak sequence, followed by the HLA-C*0802 gene, the T2A self-cleaving sequence, the E3/19K ER-targeting sequence, the IVDLMCHATF peptide-encoding sequence and a termination codon was received. This insert (hereafter referred as *HLA-C*0802_T2A_IVDLMCHATF*) was flanked by two

restriction sites: BamH1 (5') and EcoR1 (3'), and maintained the same total size of 1266 bp **(Table 5.1; Figure 5.1, Appendix A)**.

Table 5.1 Synthetic HLA-C*0802_T2A_IVDLMCHATF insert

DNA sequence	Origin	Length (bp)	Reference/PubMed accession number
Kozak consensus sequence	Vertebrate	9	(Kozak, 1987)
HLA-C*0802 gene	Human	1098	M84173.1
T2A self-cleaving peptide	Thosea asigna virus	63	Liu (Liu *et al.*, 2017)
E3/19K ER-signal sequence	Adenovirus	51	J01917.1 (Anderson *et al.*, 1991)
IVDLMCHATF peptide-encoding sequence	Dengue virus (DENV1-4) Zika Virus	30	DENV-1: U60585.1 DENV-2: U60587.1 DENV-3: U09270.1 DENV-4: U09483.1 ZIKV: AY632535.2
Termination codon	Human	3	

In order to generate 721.221 cells co-expressing HLA-C*0802 and IVDLMCHATF peptide, sub-cloning of the *HLA-C*0802_T2A_IVDLMCHATF* insert into the retroviral vector pIB2 was carried out. To achieve this, the pMK-RQ donor plasmid carrying the *HLA-C*0802_T2A_IVDLMCHATF* insert together with the pIB2 recipient plasmid carrying the HLA-C*0102_T2A_IVDLMCHATF insert were digested using BamH1 and EcoR1 restriction enzymes **(Figure 5.2)**. The bands corresponding to the pIB2 vector and the *HLA-C*0802_T2A_IVDLMCHATF* insert were purified from the gel and then ligated following directional cloning **(Figure 5.2)**. Subsequently, the products of the ligation reaction were used to transform ultra competent *E. coli* bacteria. Several bacterial clones were allowed to grow and then each clone was harvested individually and lysed in order to purify plasmid DNA.

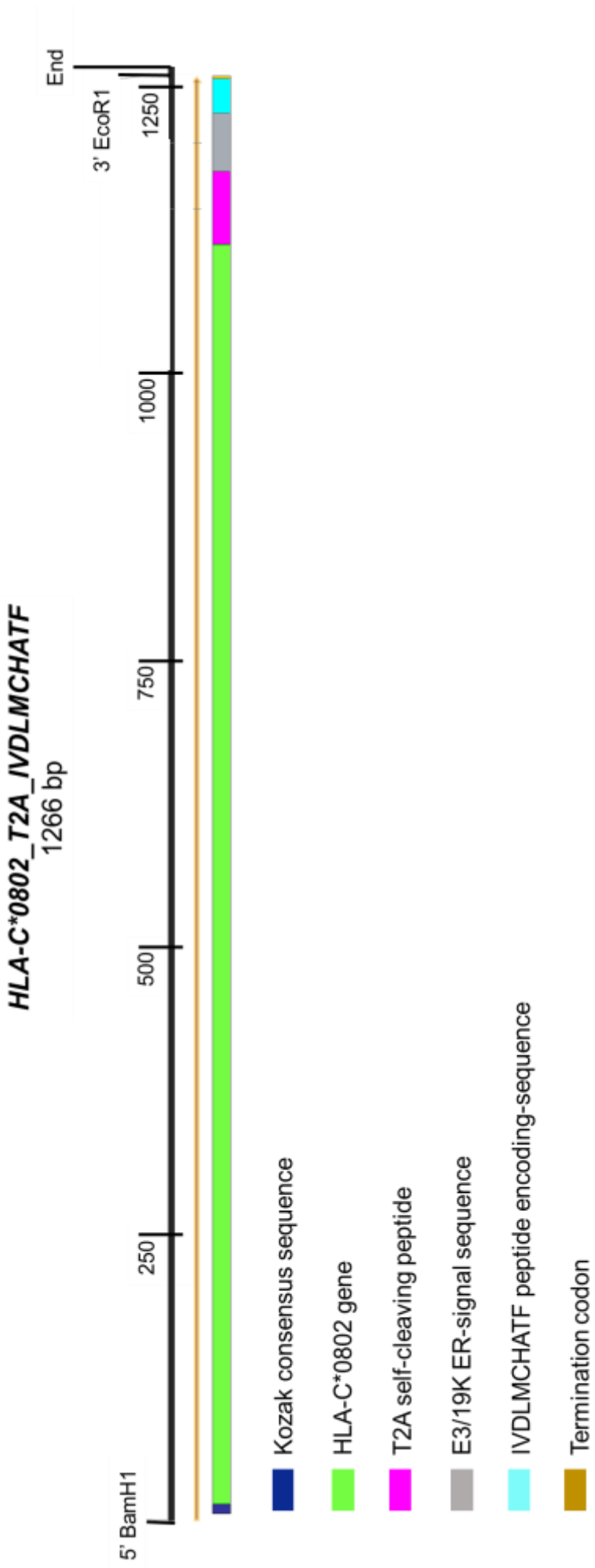
HLA-C*0802_T2A_IVDLMCHATF
1266 bp
5' BamH1
250
500
750
1000
3' EcoR1
1250
End
Kozak consensus sequence
HLA-C*0802 gene
T2A self-cleaving peptide
E3/19K ER-signal sequence
IVDLMCHATF peptide encoding-sequence
Termination codon

Figure 5.1 Synthetic HLA-C*0802_T2A_IVDLMCHATF insert. The *HLA-C*0802_T2A_IVDLMCHATF* insert (1266 bp) was synthesized by GeneArt. The insert contains (from 5' to 3'): the BamH1 restriction site, the Kozak sequence (dark blue), the HLA-C*0802 gene (green), the T2A self-cleaving peptide (pink), the E3/19K ER signal sequence (grey), the IVDLMCHATF peptide-encoding sequence (aqua blue), a termination codon (orange) and the EcoR1 restriction site. The figure was drawn to scale using the SnapGene software.

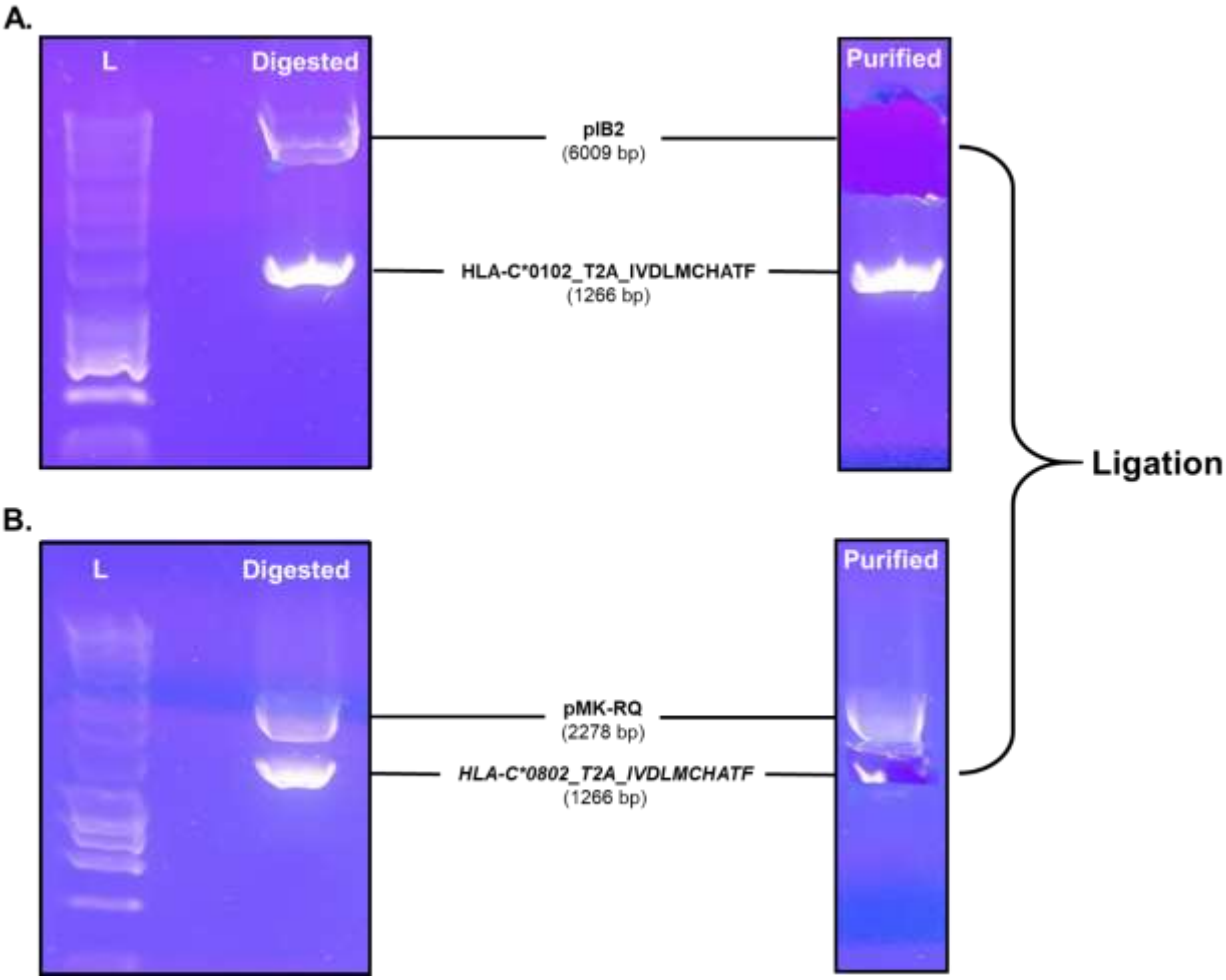

Figure 5.2 Sub-cloning HLA-C*0802_T2A_IVDLMCHATF insert into pIB2. Restriction enzyme digestion of pIB2 recipient plasmid carrying the HLA-C*0102_T2A_IVDLMCHATF insert **(A)** and pMK-RQ – KanR donor plasmid carrying the *HLA-C*0802_T2A_IVDLMCHATF* insert **(B)** was performed using BamH1 and EcoR1 enzymes. Digested products were analysed on agarose gel and visualized under UV light. Digested pIB2 **(A)** and *HLA-C*0802_T2A_IVDLMCHATF* insert **(B)** were excised from the agarose gel and DNA was purified and ligated overnight. L= DNA Ladder

Successful sub-cloning of the *HLA-C*0802_T2A_IVDLMCHATF* insert into the pIB2 vector was confirmed in three bacterial clones (3, A and H) by digesting purified plasmid DNA with BamH1 and EcoR1 enzymes as well as by DNA sequencing using pIB2 specific primers. Restriction enzyme digestion of clones 3, A and H showed two DNA fragments with the

expected sizes corresponding to the pIB2 vector (6009 bp) and the *HLA-C*0802_T2A_IVDLMCHATF* insert (1266 bp; **Figure 5.3A**). Similarly, the sequences retrieved from DNA sequencing of the three bacterial clones were aligned with the reference sequence sent for gene synthesis and showed a 100% identity **(Figure 5.3B)**. This confirms the successful generation of the pIB2 *HLA-C*0802_T2A_IVDLMCHATF* construct.

5.3 Generation of target cells endogenously presenting IVDLMCHATF peptide in the context of HLA-C*0802

In order to generate a cell line expressing HLA-C*0802 and endogenously presenting the IVDLMCHATF peptide, Phoenix-Ampho cells were transfected with the pIB2 *HLA-C*0802_T2A_IVDLMCHATF* construct (clone 3). Then, the viral supernatant from transfected Phoenix-Ampho cells was collected to perform retroviral transduction of the MHC-I-deficient 721.221 cell line.

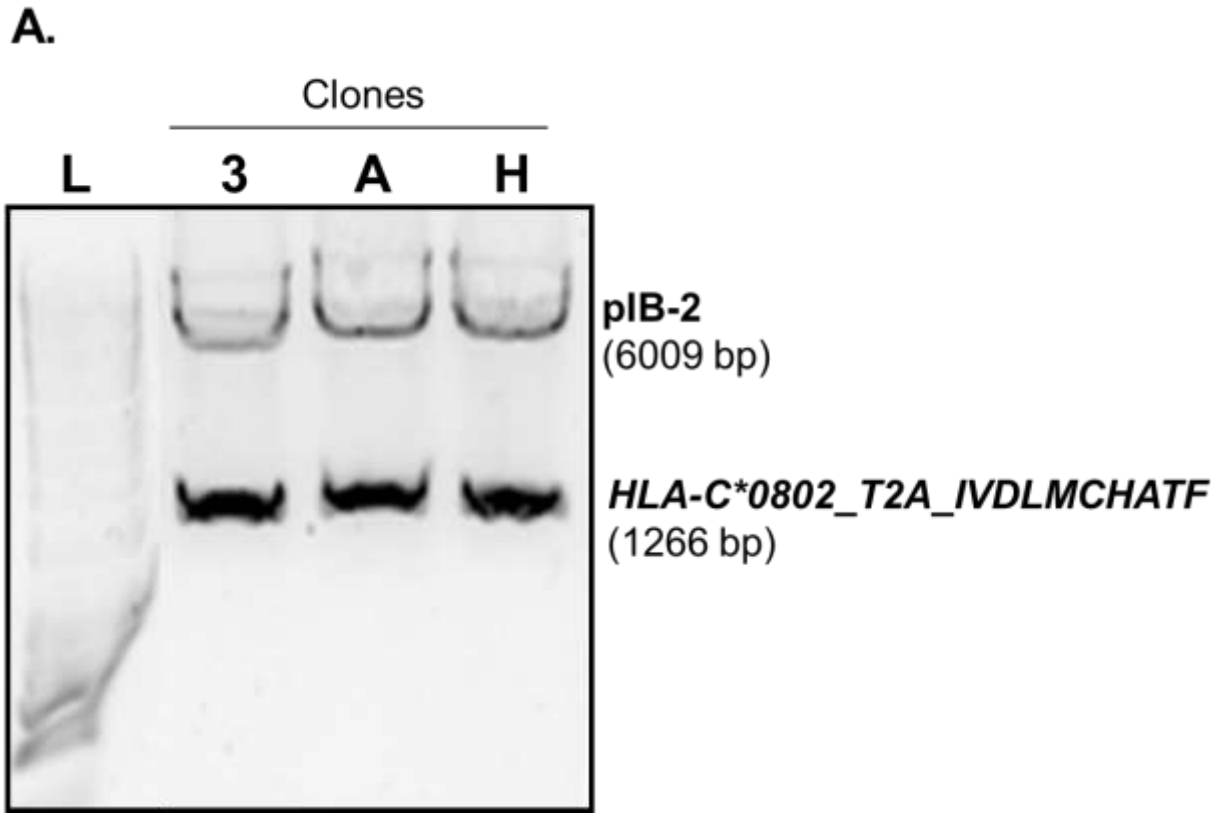

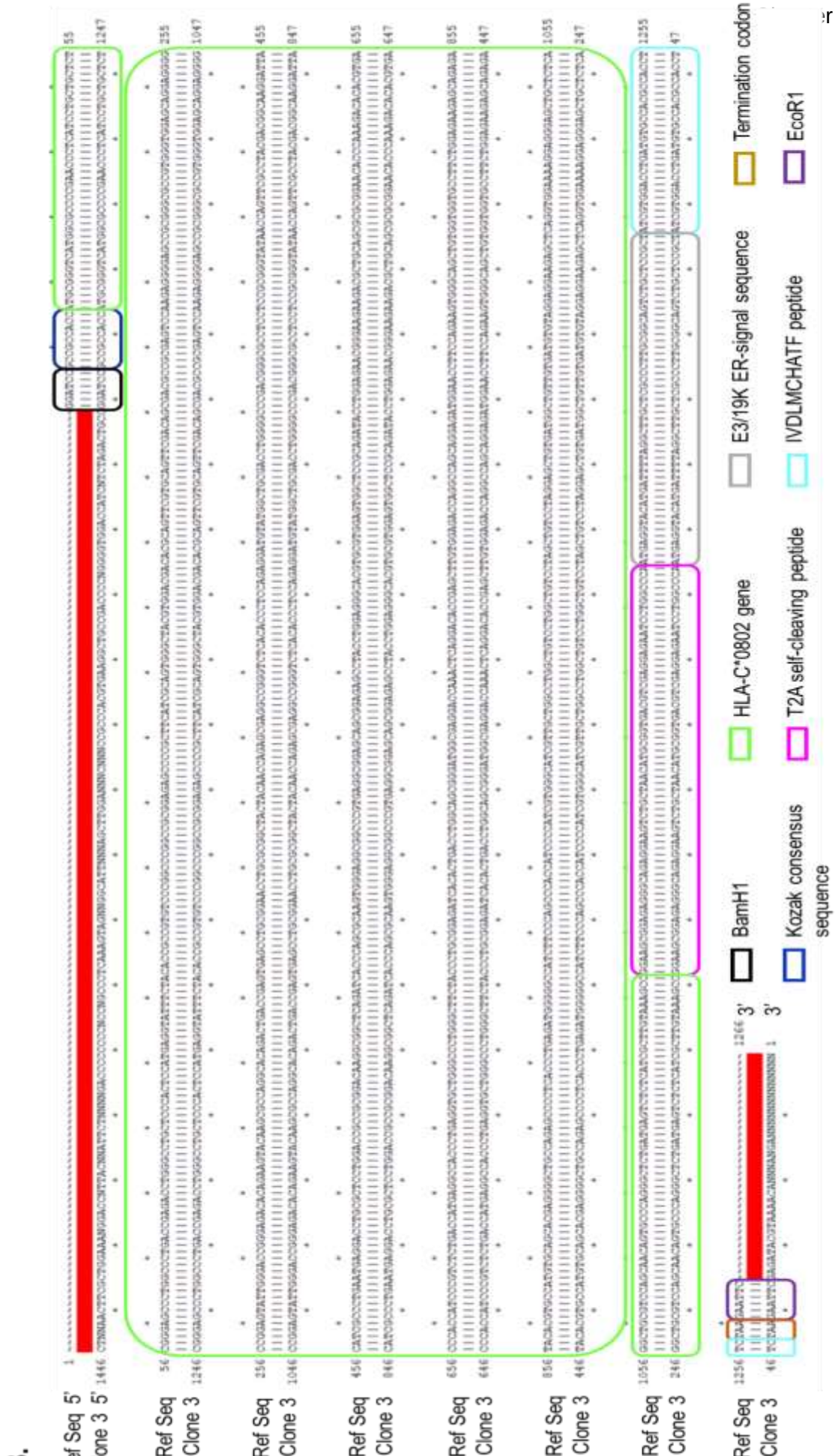
B.
Ref Seq 5'
Clone 3 5'
Ref Seq
Clone 3
BamH1
HLA-C*0802 gene
E3/19K ER-signal sequence
Termination codon
Kozak consensus sequence
T2A self-cleaving peptide
IVDLMCHATF peptide
EcoR1

Figure 5.3 pIB2 HLA-C*0802_T2A_IVDLMCHATF construct. (A) Restriction digestion of pIB2 *HLA-C*0802_T2A_IVDLMCHATF* construct from three different bacterial clones (3, A and H). **(B)** Sequence alignment of *HLA-C*0802_T2A_IVDLMCHATF* insert using the reference sequence used for gene synthesis (Ref Seq) and the sequence derived from DNA sequencing for one of the bacterial clones (Clone 3). Individual DNA sequences within the insert are highlighted. Sequences were aligned in the Plasmid Editor software.

Following retroviral transduction, 721.221 cells were maintained in culture conditions for about two weeks with increasing concentrations of the blasticidin selectable marker (5, 7.5 and 10 µg/ml) and further tested for HLA-C expression by flow cytometry. As shown in **Figure 5.4A**, HLA-C fluorescence was brighter in cells cultured with the highest concentration of blasticidin. Hence, transduced cells were allowed to grow under high antibiotic selection for further two weeks and HLA-C expression was measured again. Newly generated cells showed significantly high MFI compared to the parental 721.221 cell line ($p=0.0098$); however these values were significantly reduced compared to cells expressing HLA-C*0802 alone ($p=0.0095$; **Figure 5.4B**). Therefore, these cells were maintained under high antibiotic selection for longer before using them as targets in cytotoxicity and degranulation assays.

These results confirm the efficient incorporation of the pIB2 *HLA-C*0802_T2A_IVDLMCHATF* construct by 721.221 cells, which followed a series of intracellular processes including integration, translation, ER translocation, sequence cleavage, peptide loading and, finally, the transport of HLA-C*0802 molecules in complex with IVDLMCHATF peptide to the cell membrane.

5.4 Target cells endogenously presenting IVDLMCHATF peptide in the context of HLA-C*0802 are killed by KIR2DS2-expressing NKL cells

Target cells expressing *HLA-C*0802_T2A_IVDLMCHATF* or HLA-C*0802 alone were co-cultured with NKL cells or the ones expressing KIR2DL2 or KIR2DS2 receptors. Then, a cytotoxicity assay was carried out. The gating strategy for this assay is shown in Chapter 2 **(Figure 2.7)**.

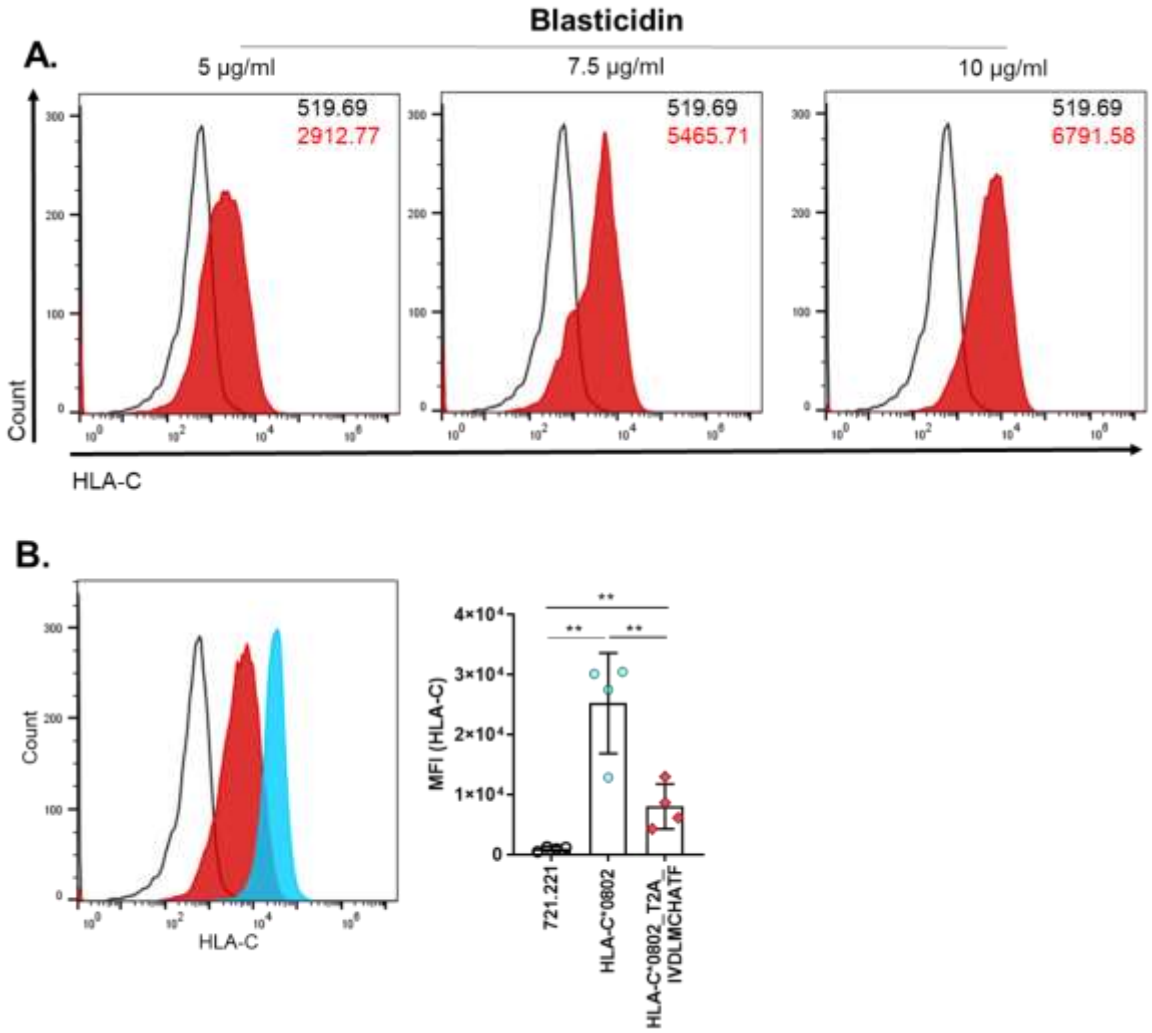

Figure 5.4 Generation of target cells expressing HLA-C*0802_T2A_IVDLMCHATF. (A) 721.221 cells transduced with the pIB2 *HLA-C*0802_T2A_IVDLMCHATF* construct were grown under increasing concentrations of blasticidin and tested for HLA-C expression. MFI for parental (black) and newly generated cell lines (red) are shown. **(B)** After longer time under antibiotic selection, HLA-C expression of transduced cells (red) was measured again and compared to parental 721.221 cells (white) and cells expressing HLA-C*0802 alone (blue). Dot plot shows the MFI of HLA-C expression for the corresponding cell lines. Mean and SD of four independent experiments are shown. Differences were determined using an unpaired t test. P value ** <0.01.

Cytotoxic activity of NKL cells against cells expressing *HLA-C*0802_T2A_IVDLMCHATF* tended to increase compared to the ones expressing HLA-C*0802 alone; however this augment was not statistically significant at any E:T ratio (p=0.0917 and p=0.1300 for 10:1 and 5:1 ratios, respectively; **Figure 5.5**). NKL-2DL2 cells killed both target cell lines at a similar extent, with this effect being slightly increased to cells expressing HLA-C*0802 alone. As with NKL cells, these differences were not statistically significant at any ratio (p=0.1250 and p=0.7500 for 10:1 and 5:1 ratios, respectively; **Figure 5.5**).

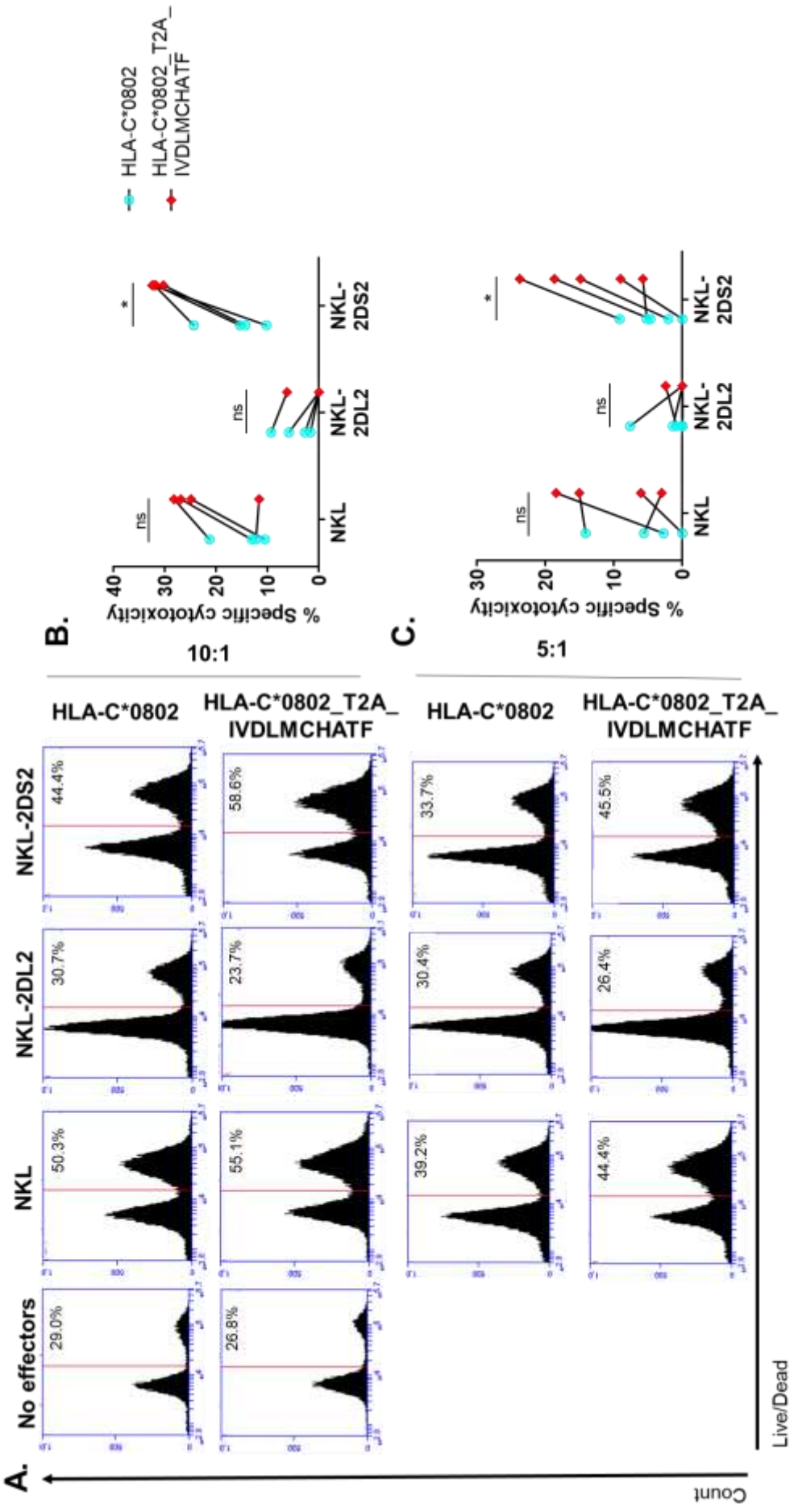
A.
HLA-C*0802
HLA-C*0802_T2A_ IVDLMCHATF
HLA-C*0802
HLA-C*0802_T2A_ IVDLMCHATF
NKL-2DS2
NKL-2DL2
NKL
No effectors
29.0%
26.8%
50.3%
55.1%
30.7%
23.7%
44.4%
58.6%
39.2%
44.4%
30.4%
26.4%
33.7%
45.5%
Count
Live/Dead
B.
10:1
% Specific cytotoxicity
ns
ns
*
NKL
NKL-2DL2
NKL-2DS2
C.
5:1
% Specific cytotoxicity
ns
ns
*
NKL
NKL-2DL2
NKL-2DS2
HLA-C*0802
HLA-C*0802_T2A_ IVDLMCHATF

Figure 5.5 Cytotoxic activity of NKL cell lines to HLA-C*0802-expressing cells endogenously presenting IVDLMCHATF peptide. (A) 721.221 cells expressing HLA-C*0802 alone or the pIB2 *HLA-C*0802_T2A_IVDLMCHATF* construct were co-cultured with NKL cell expressing KIR2DL2 or KIR2DS2 receptors at 10:1 and 5:1 ratios and then stained with a Live/Dead dye. Cytometry plots from a representative experiment are shown. **(B,C)** Line charts show the mean and SD of at least four independent experiments at 10:1 **(B)** and 5:1 **(C)** ratios (n=4-5). The percentage of dead cells from the No effector control was subtracted. Differences were determined using a paired t test. ns= non-significant; P value * <0.05.

Conversely, NKL-2DS2 showed a sustained and increase cytotoxic activity against cells expressing *HLA-C*0802_T2A_IVDLMCHATF*. This increase was evident at both E:T ratios and was statistically significant compared to cells expressing HLA-C*0802 alone (p=0.0138 and p=0.0169 for 10:1 and 5:1 ratios, respectively; **Figure 5.5**). These data indicate that this Flaviviral peptide bound to HLA-C*0802 engages KIR2DS2 in a specific manner and triggers NK cell activation that leads to target cell death.

5.5 IVDLMCHATF peptide endogenously presented by HLA-C*0802 specifically triggers a strong degranulation of KIR2DS2^{high} NK cells

To confirm the specific activation of KIR2DS2-expressing cells to the HLA-C*0802:IVDLMCHATF complex, primary NK cells from KIR2DL2/S2 homozygous (n=1) or KIR2DL2/L3/S2 heterozygous donors (n=3) were sorted based on the expression of those receptors (Blunt *et al.*, 2019) and expanded *in vitro* before using them in degranulation assays. As targets, 721.221 cells expressing *HLA-C*0802_T2A_IVDLMCHATF* were used and compared to cells expressing HLA-C*0802 alone or those co-expressing HLA-C*0802 and DENV/NS3. The gating strategy for this assay is shown in Chapter 2 **(Figure 2.8)**.

Degranulation of KIR2DL2/L3/S2^{neg} NK cells against 721.221 cells expressing *HLA-C*0802_T2A_IVDLMCHATF* did not differ compared to cells expressing HLA-C*0802 alone (p=0.7757 and p=0.4006 for 10:1 and 5:1 ratios, respectively) or the ones co-expressing HLA-C*0802 and DENV/NS3 (p=0.2003 and p=0.4596 for 10:1 and 5:1 ratios, respectively; **Figure 5.6**).

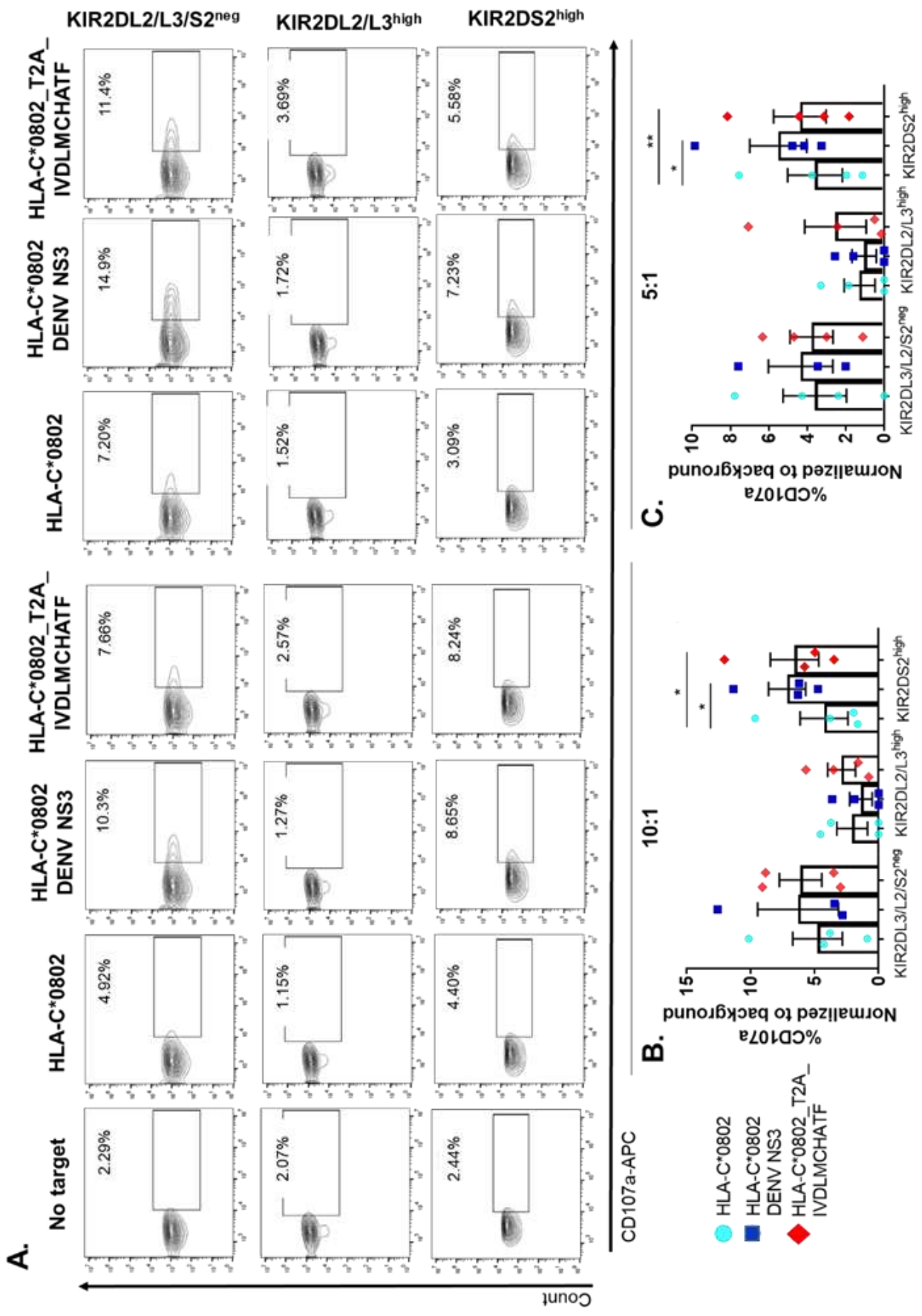
A.
KIR2DL2/L3/S2neg
KIR2DL2/L3high
KIR2DS2high
HLA-C*0802_T2A_IVDLMCHATF
HLA-C*0802 DENV NS3
HLA-C*0802
No target
2.29%
4.92%
10.3%
7.66%
11.4%
2.07%
1.15%
1.27%
2.57%
3.69%
2.44%
4.40%
8.65%
8.24%
5.58%
7.20%
14.9%
1.52%
1.72%
3.09%
7.23%
Count
CD107a-APC
B.
10:1
%CD107a Normalized to background
KIR2DL3/L2/S2neg
KIR2DL2/L3high
KIR2DS2high
C.
5:1
HLA-C*0802
HLA-C*0802 DENV NS3
HLA-C*0802_T2A_IVDLMCHATF

Figure 5.6 Degranulation of sorted primary NK cells to HLA-C*0802-expressing cells endogenously presenting IVDLMCHATF peptide (A) 721.221 cells expressing HLA-C*0802 alone (light blue), the ones co-expressing DENV/NS3 (dark blue) and newly transduced cells expressing pIB2 *HLA-C*0802_T2A_IVDLMCHATF* construct (red) were used as targets in a degranulation assay to sorted KIR2DL2/L3/S2^{neg}, KIR2DL2/L3^{high} and KIR2DS2^{high} NK cell subsets at 10:1 and 5:1 ratios. A representative experiment from one donor is shown. **(B,C)** Scatter dot plots show the mean and SD of four independent experiments at 10:1 **(B)** and 5:1 **(C)** ratios. Percentage of CD107a from the No target control was subtracted. Each dot represents one donor. Differences were determined using a paired t test. P value * <0.05; ** <0.01.

Regarding cells with high expression of inhibitory KIR2DL2/L3, it was observed that the percentage of CD107a against *HLA-C*0802_T2A_IVDLMCHATF*-expressing cells was marginally increased compared with cells only expressing HLA-C*0802 or those co-expressing HLA-C*0802 and DENV/NS3. No statistically significant results were obtained from these comparisons (to HLA-C*0802: p=0.2350 for 10:1 ratio and p=0.1214 for 5:1 ratio; to HLA-C*0802 and DENV/NS3: p=0.2356 for 10:1 and p=0.1660 for 5:1 ratio; **Figure 5.6**).

Finally, NK cells with high expression of KIR2DS2 showed increased CD107a levels after co-culture with 721.221 cells expressing *HLA-C*0802_T2A_IVDLMCHATF* compared with cells expressing HLA-C*0802 alone, with differences being statistically significant at both E:T ratios (p=0.0097 and p=0.0268 for 10:1 and 5:1 ratios, respectively). No differences were seen in degranulation levels between cells expressing *HLA-C*0802_T2A_IVDLMCHATF* and those co-expressing HLA-C*0802 and DENV/NS3 (p=0.0942 and p=0.5134 for 10:1 and 5:1 ratios, respectively; **Figure 5.6**). These results confirm that IVDLMCHATF peptide bound to HLA-C*0802 specifically interacts with KIR2DS2, triggering a positive signal within NK cells and resulting in a strong degranulation response.

5.6 The IVLDMCHATF peptide is likely to have a broad HLA-C specificity

The ability of the IVDLMCHATF peptide to bind multiple HLA-C alleles suggest that, unlike LNPSVAATL, this peptide has a broader specificity for HLA-C1 and HLA-C2 allelic variants. To predict whether other HLA-C alleles are likely to present IVDLMCHATF peptide to NK cells, HLA-C1 and HLA-C2 alleles present in the largest numbers of worldwide populations

were selected from the allelefrequencies.net database for subsequent *in silico* peptide binding analysis using NetMHCpan (Gonzalez-Galarza *et al.*, 2015; Jurtz *et al.*, 2017).

Besides HLA-C*0102 and HLA-C*0802, IVDLMCHATF peptide is predicted to bind one additional HLA-C1 allele (HLA-C*0103). Although HLA-C*0103 allele is present in less populations compared to HLA-C*0102, its frequency is the second largest among HLA-C*01 alleles **(Table 5.2)**.

Table 5.2 Binding prediction of IVDLMCHATF peptide to HLA-C1 and C2 alleles

Group	Allotype	Allele	Number of populations presenting the allele	Binding affinity (nM)	% Rank	Binding level
HLA-C1	HLA-C*01	HLA-C*0102	214	**10123.9**	**1.9461**	**WB**
		HLA-C*0103	42	**15781.2**	**1.1101**	**WB**
	HLA-C*03	HLA-C*0303	221	7344.5	5.5408	NB
		HLA-C*0304	197	7344.5	5.5408	NB
	HLA-C*07	HLA-C*0701	193	21962.8	14.2431	NB
		HLA-C*0702	235	13634.3	9.6270	NB
	HLA-C*08	HLA-C*0801	151	7282.6	2.3797	NB
		HLA-C*0802	162	**5374.3**	**0.6734**	**WB**
	HLA-C*12	HLA-C*1202	196	5497.1	5.6016	NB
		HLA-C*1203	197	4845.1	8.0172	NB
	HLA-C*14	HLA-C*1402	164	4724.1	7.5043	NB
		HLA-C*1403	92	4724.1	7.5043	NB
	HLA-C*16	HLA-C*1601	158	2569.2	4.5125	NB
		HLA-C*1602	142	2902.4	2.7804	NB
HLA-C2	HLA-C02	HLA-C*0202	149	5066.6	4.2195	NB
		HLA-C*0210	43	5066.6	4.2195	NB
	HLA-C*04	HLA-C*0401	230	**10284.8**	**0.8000**	**WB**
		HLA-C*0403	108	**3879.6**	**0.3760**	**SB**
	HLA-C*05	HLA-C*0501	176	**1590.1**	**0.5041**	**WB**
		HLA-C*0509	13	**1590.1**	**0.5041**	**WB**
	HLA-C*06	HLA-C*0602	226	26225.5	18.7346	NB
		HLA-C*0617	17	26225.5	18.7346	NB
	HLA-C*15	HLA-C*1502	198	8862.3	7.3570	NB
		HLA-C*1505	131	8412.1	5.1841	NB
	HLA-C*17	HLA-C*1701	144	9677.5	3.3109	NB
		HLA-C*1703	21	9677.5	3.3109	NB
	HLA-C*18	HLA-C*1801	72	**18253.9**	**1.6695**	**WB**
		HLA-C*1802	7	**18253.9**	**1.6695**	**WB**

Threshold for strong binders = 0.5%
Threshold for weak binders = 2.0%
SB= Strong binder; WB= Weak binder; NB = Non-binder
WB and SB are shown in bold

On the other hand, besides HLA-C*0501, IVDLMCHATF peptide is likely to bind five additional HLA-C2 alleles (HLA-C*0401, HLA-C*0403, HLA-C*0509, HLA-C*1801 and HLA-C*1802). The prediction analysis showed that this peptide is a potential weak binder to most

of the alleles, with the exception of HLA-C*0403, whose rank percentage was below 0.5% and therefore is likely to be a strong binder **(Table 5.2)**. These results suggest that IVDLMCHATF peptide has a broad binding specificity for HLA-C molecules, which could favour its interaction with a wider range of KIR receptors (i.e KIR2DL1/KIR2DS1, KIR2DS4, KIR2DS5).

5.7 The KIR2DS2/HLA-C1 combination may be selected in regions with endemic Flaviviruses

The above results and those of Naiyer *et al* have shown the ability of IVDLMCHATF peptide and other Flaviviral peptides carrying the “MCHAT” motif to bind multiple HLA-C1 alleles and to establish canonical interactions with KIR2DS2, which results in the induction of robust NK cell responses against target cells. As KIR/MHC-I combinations have shown to impact disease outcomes, our results suggest that KIR2DS2/HLA-C1 interactions could be protective factors against Flaviviruses. In order to gain an insight into the clinical relevance of our findings, an *in silico* approach analysing KIR2DS2/HLA-C1 frequencies in regions where these Flaviviruses circulate was performed.

First, a search of the geographical distribution of DENV, ZIKV, WNV and JEV was collected from updated bulletins (July-September 2019) provided by the Centre for Disease Control and Prevention (CDC), the European Centre for Disease Control and Prevention (ECDC) and the World Health Organization (WHO). Then, frequencies of KIR2DS2 as well as of IVDLMCHATF-binding alleles (HLA-C*0102/HLA-C*0802) in populations from countries with circulation of Flaviviruses, were retrieved from the allelefrequencies.net database (Gonzalez-Galarza *et al.*, 2015). Frequency values for KIR2DS2 are shown as the percentages of individuals that have the gene whereas HLA-C frequencies are displayed in decimals. Due to the fact that most of the populations with a reported frequency of KIR2DS2 do not display a reported frequency of HLA-C alleles and vice versa, the data was examined according to the country of origin. As most of the selected countries showed reports from multiple populations, the lowest and highest frequencies from populations with the same ethnic background are shown.

5.7.1 Dengue Virus and Zika Virus

According to the WHO, Dengue virus (DENV) and Zika virus (ZIKV) mainly circulate in tropical and subtropical countries from Latin American and Asian countries (WHO, 2019b;a). To date, confirmed cases of DENV or ZIKV infection have been reported from different worldwide regions including the Americas, Western Pacific, South East Asia and Africa. In the case of DENV infection, Brazil is the country with the highest reported number of confirmed cases (about 2 million), followed by Philippines, Vietnam, Nicaragua, Mexico, Malaysia, Colombia, Thailand and Honduras. For ZIKV infection, the number of reported cases is reduced compared to DENV and is limited to countries from the Latin and Central America region such as Brazil, Panama, Guatemala and Bolivia **(Table 5.3)**.

The co-circulation of DENV and ZIKV across Brazil began in 2015 and continue until today (Estofolete *et al.*, 2019). In Brazilian populations, the percentage of individuals carrying KIR2DS2 is variable, ranging from 20% in the Brazilian Guarani Kaiowa population up to 67.3% in the Brazil Rondonia Karitiana population **(Table 5.3)**. High frequencies of KIR2DS2 (above 50%) have also been found in 13 other Brazilian populations from all over the country (Gonzalez-Galarza *et al.*, 2015). Unfortunately, none of the populations with relatively high KIR2DS2 frequency displayed data for HLA-C allele frequencies. Only low frequencies (below 0.1) of HLA-C*0102 (Brazil Terena 0.0240 and Brazil Mixed 0.0320) or HLA-C*0802 alleles (Brazil Mixed 0.0750), have been reported **(Table 5.3)**. As Brazil is the country with the most reported cases of DENV and ZIKV infection, the need for KIR/MHC-I genetic association studies in these populations would be important in order to understand the potential of Flaviviruses to drive the selection of KIR.

Some countries with the highest number of reported cases of DENV after Brazil have populations displaying higher frequencies of the HLA-C*0102 allele (above 0.1). These countries include Mexico (Mexico Chihuahua Tarahumara 0.1360 and Mexico Hidalgo Mezquital Valley Otomi 0.1042), Malaysia (Malaysia Peninsular Chinese 0.1753), Vietnam (Vietnam Hanoi Kinh pop 2 0.1650) and Thailand (Thailand 0.1160). From these populations, only the Vietnam Hanoi Kinh population has reports of KIR2DS2 frequency from two studies performed at different time points (36.4% and 41%; **Table 5.3**). Although these values are moderate, it is suggested that individuals from this population may carry the KIR2DS2/HLA-C*0102 combination. Regarding the other countries, KIR2DS2 frequencies were variable, ranging from 34 - 63% in Mexico, 35 - 44% in Thailand and 43.3% in Malaysia **(Table 5.3)**. As the ethnic origins of the populations with reported

frequencies of KIR2DS2 or HLA-C*0102 are similar (Amerindian in Mexico, Oriental in Thailand and Austronesian in Malaysia), it could be assumed that individuals with these backgrounds may carry both genes.

Table 5.3 KIR2DS2 and HLA-C1 frequencies in countries with high circulation of DENV or ZIKV

Region	Country	Flaviviruses		KIR2DS2 frequency	HLA-C1 frequency	
		DENV[a]	ZIKV[b]		HLA-C*0102	HLA-C*0802
Americas	Brazil	1958031	19020	0.137 – 0.673	0.0240 – 0.0320	0.0750
	Nicaragua	109084	NA	NA	0.0861	0.0320 – 0.0476
	Mexico	100510	877	0.34 – 0.636	0.0300 – 0.1360	0.0070 – 0.0406
	Colombia	87174	857	NA	0.1138 – 0.5096	0.0385 – 0.0492
	Honduras	75122	NA	NA	NA	NA
	Panama	3250	2752	0.474	NA	NA
	Guatemala	25738	2300	NA	NA	NA
	Bolivia	8779	1736	NA	NA	NA
	Peru	8864	984	NA	NA	NA
	Cuba	1542	873	0.529	NA	NA
	El Salvador	17869	481	NA	NA	NA
	Costa Rica	5164	431	0.49	0.0200 – 0.1520	0.0040 – 0.0540
	United States	530	34	0.373 – 0.54	0.0002 – 0.2050	0.0006 – 0.0640
Western Pacific	Philippines	208917	NA	NA	0.0100	NA
	Vietnam	124751	NA	0.364 – 0.41	0.1650	NA
	Malaysia	96300	NA	0.433	0.0442 – 0.1753	NA
	Papua New Guinea	NA	NA	0.64 – 0.909	0.0710 – 0.3020	NA
	China	788	NA	0.72 – 0.417	0.0260 – 0.2940	0.0018 – 0.0100
	Japan	NA	NA	0.85 – 0.16	0.1480 – 0.2010	0.0003
South East Asia	Thailand	85520	NA	0.35 – 0.44	0.1160	NA
	India	NA	NA	0.27 – 0.75	0.0190 – 0.0820	0.0010
	Indonesia	NA	NA	0.36 – 0.63	NA	NA
Africa	Reunion	17902	NA	0.53	NA	NA
	Tanzania	2919	NA	NA	NA	NA
	Côte d'Ivoire	302	NA	NA	NA	NA

a, b Number of cases reported in 2019
NA= data no available

5.7.2 West Nile Virus and Japanese Encephalitis Virus

West Nile Virus (WNV) is distributed in different worldwide regions including Africa, Europe, the Middle East, North America and West Asia, whereas Japanese Encephalitis Virus (JEV) is limited to the Western Pacific and Asia regions (CDC, 2019; WHO, 2019c). Most of the cases of WNV infection this year have been reported in United States, followed by European countries such as Greece, Romania, Italy and Hungary **(Table 5.4)**. In the case of JEV,

there is no information about the number of cases reported so far, but a recent bulletin from the CDC described that this virus is currently widespread across Western Pacific and South East Asian countries **(Table 5.4)**.

The initial outbreaks of WNV infection in United States in 1999 were followed by a high distribution of WNV in this country (Chancey *et al.*, 2015; WHO, 2019c). Frequencies of HLA-C*0102 or HLA-C*0802 in United States are highly variable as the allelefrequencies.net database contains data of multiple populations from different ethnic backgrounds, with the Polynesian, Oriental and Asian ethnicities within this country being the ones with the highest HLA-C*0102 frequencies (ranging from 0.1291 to 0.2050). Conversely, high KIR2DS2 frequencies included populations of Hispanic or Caucasoid ethnicities (ranging from 50 to 54%). Regarding European countries, frequencies of HLA-C1 alleles are generally low whereas KIR2DS2 frequencies are ~50% **(Table 5.4)**.

Analysis of KIR2DS2 frequencies in JEV endemic regions showed a high frequency of KIR2DS2 in Papua New Guinea Irian Jaya (64%) and Papua New Guinea Nasioi (90.9%) populations, both of them with a Melanesian ethnicity **(Table 5.4)**. Several populations having the same ethnic origin had also high frequencies of HLA-C*0102 ranging from 0.0710 to 0.3020, suggesting that Melanesians are likely to have high frequencies of both, HLA-C*0102 and KIR2DS2.

Table 5.4 KIR2DS2 and HLA-C1 frequencies in countries with high circulation of WNV and JEV

Region	Country	Flaviviruses		KIR2DS2 frequency	HLA-C1 frequency	
		WNV[a]	JEV[b]		HLA-C*0102	HLA-C*0802
Americas	United States	468		0.373 – 0.54	0.0002 – 0.2050	0.0006 – 0.0640
Europe	Greece	194		0.54	0.0301 – 0.0363	0.0060 – 0.0219
	Romania	51		0.476	0.0397	0.0255
	Italy	28		0.45 – 0.53	0.0200 – 0.0330	0.0220 – 0.0500
	Hungary	18		NA	NA	NA
Western Pacific	Philippines		Widespread	NA	0.0100	NA
	Vietnam		Widespread	0.364 – 0.41	0.1650	NA
	Malaysia		Widespread	0.433	0.0442 – 0.1753	NA
	Papua New Guinea		Widespread	0.64 – 0.909	0.0710 – 0.3020	NA
	China		All provinces except Xinjiang and Qinghai	0.72 – 0.417	0.0260 – 0.2940	0.0018 – 0.0100
	Japan		All islands	0.85 – 0.16	0.1480 – 0.2010	0.0003
South East Asia	Thailand		Widespread	0.35 – 0.44	0.1160	NA
	India		Northern and Southern India	0.27 – 0.75	0.0190 – 0.0820	0.0010
	Indonesia		Widespread	0.36 – 0.63	NA	NA

a, Number of cases reported in 2019
b Affected areas per country
NA= data no available

Finally, we identified worldwide populations with high or low frequencies of KIR2DS2, HLA-C*0102 or HLA-C*0802 alleles in an attempt to correlate those variables with the circulation of Flaviviruses. KIR2DS2 and HLA-C*0102 are mostly found in populations from Asian and Western Pacific countries, some of them with high circulation of DENV and JEV such as Papua New Guinea, Australia and India (Ganeshkumar *et al.*, 2018; Luang-Suarkia *et al.*, 2018; CDC, 2019; van den Hurk *et al.*, 2019). Frequencies of HLA-C*0802 are generally low; however this allele is mainly present in regions that have reported dengue infection cases such as Pakistan (Yousaf M *et al.*, 2018) but also in regions with low circulation of Flaviviruses such as European countries **(Figure 5.7)**.

The highest HLA-C*0102 frequency was found in a Colombian population (0.5096), the highest HLA-C*0802 is present in a Pakistani population (0.1320), whereas the highest percentage of individuals carrying KIR2DS2 was present in a Papua New Guinean population (90.9%) **(Figure 5.7; Table 5.3 and 5.4)**. Although the background ethnicities from these populations are different (Amerindian, Asian and Melanesian, respectively), a recent study suggested that Amerindians from Colombia may be related with natives from Pacific Islander groups, including populations from Papua New Guinea (Arnaiz-Villena *et al.*, 2018). As both regions are endemic for DENV infection and Papua New Guinea is also endemic for JEV (Moore *et al.*, 2017; Luang-Suarkia *et al.*, 2018), it could be suggested that pathogen-driven evolutionary forces may select the KIR2DS2/HLA-C*0102 combination in individuals from the same ethnic origin exposed to these pathogens.

Overall, although these results did not allow us to establish solid associations between the presence of KIR2DS2/HLA-C1 and circulation of Flaviviruses in specific populations, this reflects the need to conduct disease association studies in order to identify the influence of the KIR/MHC-I system in the susceptibility or protection against Flaviviral infections in endemic areas as well as to understand the pathogen-driven evolution of KIR.

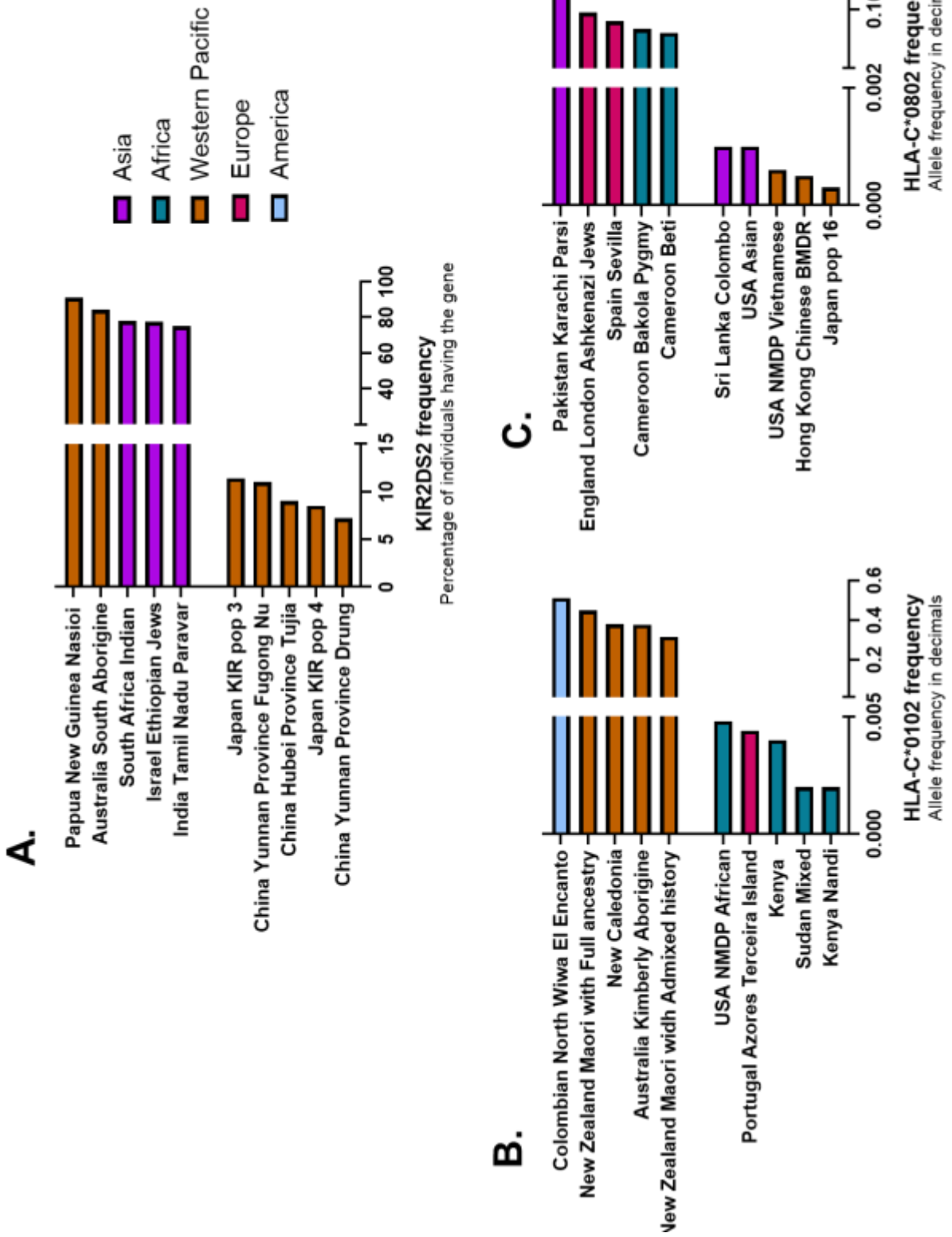
A.
Asia
Africa
Western Pacific
Europe
America
Papua New Guinea Nasioi
Australia South Aborigine
South Africa Indian
Israel Ethiopian Jews
India Tamil Nadu Paravar
Japan KIR pop 3
China Yunnan Province Fugong Nu
China Hubei Province Tujia
Japan KIR pop 4
China Yunnan Province Drung
0 5 10 15 40 60 80 100
KIR2DS2 frequency
Percentage of individuals having the gene
B.
Colombian North Wiwa El Encanto
New Zealand Maori with Full ancestry
New Caledonia
Australia Kimberly Aboriginе
New Zealand Maori widh Admixed history
USA NMDP African
Portugal Azores Terceira Island
Kenya
Sudan Mixed
Kenya Nandi
0.000 0.005 0.2 0.4 0.6
HLA-C*0102 frequency
Allele frequency in decimals
C.
Pakistan Karachi Parsi
England London Ashkenazi Jews
Spain Sevilla
Cameroon Bakola Pygmy
Cameroon Beti
Sri Lanka Colombo
USA Asian
USA NMDP Vietnamese
Hong Kong Chinese BMDR
Japan pop 16
0.000 0.002 0.10 0.15
HLA-C*0802 frequency
Allele frequency in decimals

Figure 5.7 Highest and lowest frequencies of KIR2DS2, HLA-C*0102 or HLA-C*0802 alleles in worldwide populations. The five populations displaying the highest (top) or lowest frequencies of KIR2DS2 **(A)**, HLA-C*0102 **(B)** or HLA-C*0802 **(C)** from worldwide regions (Western Pacific, Africa, Asia, America, Europe) were retrieved from the allelefrequencies.net database. The names of the populations, as displayed in the database, are shown.

5.8 Discussion

The modulation of NK cell functions through specific peptides bound to MHC-I molecules is currently a matter of active research. Understanding how a particular peptide sequence facilitate or hinder receptor/ligand interactions is imperative in order to gain a deeper insight into the complex interplay between NK cells and their targets, and the implications on disease. Particularly, a 10-mer peptide (IVDLMCHATF) derived from the NS3 protein of DENV and ZIKV – two of the more pathogenic Flaviviruses in tropical and sub-tropical countries – has shown a potent effect in the induction of KIR2DS2-mediated NK cell responses when bound to the HLA-C*0102 allele (Naiyer *et al.*, 2017). As the level of allelic diversity at the HLA-C locus is exceptional, the search of other allelic variants that could present this Flaviviral peptide to NK cells and induce their activation becomes necessary.

The preceding chapter showed that exogenous presentation of IVDLMCHATF peptide by HLA-C*0802 was canonically recognized by KIR2DS2 tetramers. Additionally, endogenous presentation of DENV/NS3-derived peptides by the same allele specifically promoted increased degranulation and a strong cytotoxic activity of KIR2DS2-expressing NK cells. This effect could be due to the presentation of IVDLMCHATF peptide by HLA-C*0802; however other DENV/NS3-derived peptides could have been involved. Therefore, to elucidate precisely the role of IVDLMCHATF peptide in the induction of NK cell effector functions, this chapter aimed to investigate whether endogenous presentation of this Flaviviral peptide by HLA-C*0802 promoted robust NK cells responses through the interaction with activating KIR2DS2.

The methodological approach consisted of a cloning strategy to promote the expression of multiple DNA sequences from a single vector to generate cell lines co-expressing HLA-C*0802 and IVDLMCHATF peptide. In addition to those sequences, the synthetic insert generated in this study contained: 1) the Kozak consensus sequence that facilitated the initiation of the translation process (Kozak, 1987); 2) the T2A-self cleaving peptide from TaV

to separate the HLA-C*0802 gene and IVDLMCHATF peptide and; 3) the E3/19K ER signal sequence for ER translocation. The reason behind the selection of T2A was its high cleavage efficiency over other self-cleavage sequences such as E2A from equine rhinitis A virus (ERAV) and F2A from FMDV, which has been demonstrated *in vitro* and *in vivo* (Daniels *et al.*, 2014; Liu *et al.*, 2017). Regarding the selection of E3/19K, it has been shown that peptides containing this sequence are efficiently translocated into the ER to subsequently associate with MHC-I molecules (Anderson *et al.*, 1991). Therefore, by using this novel method, it is possible to generate cell lines that mimic natural endogenous presentation of a specific viral peptide. Previous work has confirmed that this is an efficient strategy in the induction of NK cell activation (Naiyer *et al.*, 2017).

Cell lines stably expressing the insert of interest were used as targets in cytotoxicity and degranulation assays using the NKL cell line and primary NK cells, respectively. Results from these functional experiments demonstrated that IVDLMCHATF peptide in complex with the HLA-C*0802 allele specifically induced a consistent and sustained activation of NKL cells expressing KIR2DS2 and primary NK cells with high expression of this receptor, but not the ones expressing the inhibitory counterpart or the ones negative for both receptors. Thereby, it is possible to confirm that besides HLA-C*0102, IVDLMCHATF peptide in complex with HLA-C*0802 allele is also a cognate ligand for KIR2DS2 receptors leading to NK cell activation and killing of target cells.

Several studies have identified specific peptide sequences derived from different viruses able to interact with KIR receptors. Although most of these studies have reported viral peptides and their interaction with inhibitory KIR (Fadda *et al.*, 2011; Fadda *et al.*, 2012; van Teijlingen *et al.*, 2014; Townsley *et al.*, 2016; Sim *et al.*, 2017), some authors have investigated the effect of peptides in NK cells through activating KIR. Thus, O'connor *et al* found that two HIV-1-derived peptides AAVKAACWW ($Pol_{839-847}$) and KAAFDLSFF (Nef_{82-90}) in complex with HLA-B*5701 promoted activation of the KIR3DS1-CD3ζ Jurkat cell line (O'Connor *et al.*, 2015). Likewise, van der Ploeg *et al* found that HCMV-infected fibroblasts were specifically recognized by primary KIR2DS1+ NK cells and attributed this effect to the presentation of HCMV-derived peptides (van der Ploeg *et al.*, 2017). This evidence, in conjunction with the results from the present study confirm a role for viral peptides in the induction of NK cell responses through activating KIR.

The fact that MHC-I molecules display a peptide-dependent binding to KIR indicates that naturally occurring as well as synthetic peptide sequences derived from peptide libraries can have a great impact in the generation of NK cell activation. In this regard, Chapel *et al*

identified the synthetic peptide SRGPVHHLL, that when presented in the context of HLA-C*0602, engaged KIR2DS1 and induced cytotoxic responses from KIR2DS1+ NK clones (Chapel *et al.*, 2017). This evidence highlights the need for the identification of either natural or synthetic peptides with activating functions that could be relevant in the induction of NK cell responses against a specific target.

Particularly, the relevance of IVDLMCHATF viral peptide in the activation of NK cells is related to its degree of conservation and the implications that can be derived from this phenomenon. The fact that IVDLMCHATF peptide is present in ZIKV and all the four serotypes of DENV, together with the evidence that the “MCHAT” motif is highly conserved among Flaviviruses leads to think that the helicase region of NS3 encoding this sequence may be determinant in RNA replication and is unable to mutate (Frick and Lam, 2006; Naiyer *et al.*, 2017). The evidence to support this came from the analysis of the crystal structures of several Flaviviral NS3 helicases showing the IVDLMCHATF epitope contacting the viral RNA (Naiyer *et al.*, 2017). Thus, presentation of conserved regions of viral proteins to NK cells gives an advantage to the host, as viruses would be unable to mutate these epitopes and therefore would be difficult for them to avoid recognition by NK cells.

The significance of the findings presented in this Chapter and those of Naiyer *et al* in a clinical context need to be determined. As a mechanism to approach such scenario, the *in silico* analysis suggested that selective evolutionary forces may maintain high frequencies of KIR2DS2 and HLA-C1 alleles in worldwide populations with a related ethnicity. As few interpretations could be made from this analysis due to the lack of KIR2DS2 and HLA-C frequency data within the same population, we suggest that disease association studies need to be carried out in these populations in order to identify protective factors that could result in the design of new anti-viral therapeutic alternatives.

In summary, there is evidence that a highly conserved Flaviviral peptide derived from the NS3 protein of DENV and ZIKV binds multiple HLA-C1 alleles (HLA-C*0102, HLA-C*0501 and HLA-C*0802) and two of these complexes are cognate ligands for activating KIR2DS2. Identifying peptide sequences that strengthen binding to activating KIR would be ideal in order to search for potential candidates that could lead to the development of peptide-based vaccines able to induce effective NK cell responses.

Chapter 6 - General Discussion

The prominent contribution of NK cells in the recognition and elimination of viruses during the innate immune response is widely accepted. The complex interplay between NK cells and viruses is seen as a constant evolutionary battle that has imposed a reciprocal selective pressure, forcing them to mutually adapt in order to reach an equilibrium (Vossen *et al.*, 2002). Hence, NK cells have evolved mechanisms to protect the host from the infection whereas viruses have developed strategies to counteract and escape the anti-viral NK cell response. This type of co-evolutionary arms race maintains a balance between opposing forces that favour the preservation of the pathogen and the host (Miletić, Krmpotić and Jonjić, 2013; Carrillo-Bustamante, Kesmir and de Boer, 2015).

The interaction between NK cells with healthy or virus-infected cells depends on a series of molecular associations that regulate cellular functions towards an inhibitory or activation state, respectively (Saunders *et al.*, 2015). Cell-cell interactions through KIR and MHC-I – one of the most important receptor/ligand systems in innate immunity due to their extensive polymorphism – have shown to be advantageous to the host due to their extensive diversity that favours rapid adaptation to evolving viruses (Carrillo-Bustamante, Kesmir and de Boer, 2015). Despite their distant chromosomal locations, it has been demonstrated that KIR and MHC-I co-evolve in order to select specific receptor/ligand combinations that could become beneficial to the host and detrimental to the virus (Single *et al.*, 2007; Gendzekhadze *et al.*, 2009).

To overcome the protective host immune response, viruses have been continuously evolving mechanisms that undermine NK cell functional capacity. Some of these processes favour the balance of signals towards strong inhibition, whereas others interfere with their activation functions (Ma, Li and Kuang, 2016). Particularly, viruses from the family *Flaviviridae* have shown to induce a differential modulation of MHC-I expression that impact their interaction with inhibitory or activating KIR, with consequences that could favour either the host or the virus (Lobigs, Mullbacher and Regner, 2003; Ye *et al.*, 2013). As members of this family currently affect populations from different geographic regions worldwide and, in some cases, represent a major threat to human health (Bhatt *et al.*, 2013; Chancey *et al.*, 2015; Petruzziello *et al.*, 2016), it is imperative to understand the cellular and molecular mechanisms underlying the NK cell – virus interactions in order to exploit them for the benefit of human health.

This thesis aimed to identify molecular determinants from the KIR/MHC-I interaction that could promote robust NK cell responses against different targets expressing epitopes from viruses belonging to the family *Flaviviridae*. Overall, the methodological approach combined molecular biological techniques in order to generate *in vitro* co-culture systems resembling protein processing and endogenous presentation of viral peptides to NK cells. Viral peptides were derived either from a virus replicon (HCV), a non-structural viral protein (NS3 from DENV) or single peptides (HCV, DENV, ZIKV, YFV, WNV and JEV) and presented in the context of different HLA-C alleles to either NKL cell lines or primary NK cells expressing inhibitory KIR2DL2/L3 or activating KIR2DS2 receptors. As the mechanisms employed by NK cells to recognize and kill virus-infected cells vary according to the nature of the KIR molecule (inhibitory or activating), relevant results for each type of receptors are discussed.

6.1 Inhibitory KIR2DL2/L3 and missing-self recognition

Besides their essential role in NK cell education and induction of self-tolerance, inhibitory KIR receptors mediate recognition and lysis of virus-infected cells with reduced expression of MHC-I (Anfossi *et al.*, 2006; Raulet, 2006). Lack of engagement between inhibitory KIR and MHC-I prevents the generation of the inhibitory signal within NK cells, which results in a dominant activation that triggers NK cell functions. This mechanism of missing-self recognition complements CD8+ T cell-mediated cytotoxicity as viruses downregulating MHC-I expression remain undetected by this subset of T lymphocytes, but are susceptible to NK cell killing through inhibitory KIR (Bern *et al.*, 2019).

Interestingly, members of the family *Flaviviridae* have shown a differential modulation of MHC-I molecules, with viruses from the genus Flavivirus mediating MHC-I up-regulation whereas viruses from Hepacivirus being mainly associated with MHC-I down-regulation (Lobigs, Mullbacher and Regner, 2003; Tardif and Siddiqui, 2003). Results from Chapter 3 demonstrated that a genotype 2a-derived HCV replicon down-modulated surface expression of multiple HLA-C1 alleles. This is the first description of HCV-induced locus specific down-regulation and suggests that, in a clinical context, HCV-infected cells could be susceptible to NK cell-mediated attack by KIR2DL2/L3 receptors through the missing-self mechanism. The fact that NK cell functional capacity is undermined in HCV-infected individuals leads us to think that other NK cell receptors could be associated with the altered response against this virus (Yoon *et al.*, 2011; Holder *et al.*, 2013).

Recognition and elimination of virus-infected cells through missing-self is relevant because viruses have evolved mechanisms to manipulate inhibitory signalling. As mentioned above, Flaviviruses have been shown to induce up-regulation of MHC-I and thereby remain hidden from NK cell attack. The mechanisms behind this modulation of MHC-I expression include a transcriptional activation involving NF-κB and an increased amount of peptide availability in the ER, which would promote a more efficient traffic of MHC-I:peptide complexes to the cell surface. As a result, reduced NK cell-mediated cytotoxicity of Flavivirus-infected cells has been observed, which makes this an effective mechanism to maintain NK cell inhibition (Momburg, Mullbacher and Lobigs, 2001; Kesson, Cheng and King, 2002; Hershkovitz *et al.*, 2008; Yossef *et al.*, 2012; Glasner *et al.*, 2017; McKechnie *et al.*, 2019). In Chapter 4, it was showed that the NS3 protein from DENV induced up-regulation of HLA-C1 and C2 alleles. This allows to suggest the hypothesis that the DENV helicase alone is sufficient to induce up-regulation of HLA-C molecules as a mechanism of this virus to enhance NK cell inhibition leading to its dissemination and persistence.

However, it is not only the increased MHC-I expression, but also the strength of the inhibitory signal what determines the outcome of the inhibitory KIR/MHC-I interaction. Different viruses have been shown to modify the peptide repertoire presented by infected cells through MHC-I, even within hours post-infection; with virus-derived peptides as well as inflammation-related peptides being presented at the cell surface (Wahl *et al.*, 2010; Croft *et al.*, 2013; Schellens *et al.*, 2015; Spencer *et al.*, 2015; Ternette *et al.*, 2016). Immune pressure generated by NK cells has forced viruses to adapt and select peptides that strongly engage inhibitory KIR, with consequences for disease pathogenesis. (Achdout, Manaster and Mandelboim, 2008; Holzemer *et al.*, 2015; Lunemann *et al.*, 2016; Townsley *et al.*, 2016). Conversely, the rapid evolution and adaptation of the KIR/MHC-I system could select antagonistic peptides with the ability to disrupt inhibitory signals in order to trigger NK cell activation (Fadda *et al.*, 2010; Borhis *et al.*, 2013; Cassidy *et al.*, 2015; Mbiribindi *et al.*, 2019). In the particular case of KIR2DL2 and KIR2DL3, it has been demonstrated that NK cells expressing KIR2DL3 are more sensitive to changes in the peptide repertoire, which suggests that viral peptides with antagonistic properties that weakly interact with KIR2DL3+ NK cells could be selected by the host in order to induce protection against disease (Cassidy *et al.*, 2015).

Overall, this evidence emphasizes the major role of inhibitory KIR in the effective control of viral infections; hence haplotype A, which mainly comprises inhibitory KIR, has been suggested to be specialized in fighting pathogens (Parham and Moffett, 2013). However, NK cells integrate signal from both, inhibitory and activating receptors in order to optimally

protect the host (Long *et al.*, 2013). As a matter of fact, inhibitory KIR may enhance the functions of activating KIR as has been suggested for KIR3DL1 and KIR3DS1 during HIV-1 infection (Pelak *et al.*, 2011), which means that, together, these receptors impact disease outcomes.

6.2 Activating KIR2DS2 and recognition of viral peptides

Induction of NK cell effector functions through activating KIR is achieved upon their engagement with surface ligands on infected cells that results in the delivery of positive signals. Even though inhibitory and activating KIR share high sequence homology in their extracellular domains, the MHC-I ligands for inhibitory KIR bind with less affinity to their activating counterpart. Therefore, ligands for activating receptors are poorly defined (Bottino *et al.*, 2005; Borhis and Khakoo, 2011). Over the last years, there has been increasing evidence demonstrating that viral epitopes in complex with MHC-I are able to specifically bind activating KIR leading to NK cell activation and target cell death (O'Connor *et al.*, 2015; Chapel *et al.*, 2017; Naiyer *et al.*, 2017; van der Ploeg *et al.*, 2017). Therefore, many efforts have been made to specifically identify optimal KIR/MHC-I/peptide combinations capable of triggering a robust activating signal within NK cells that could be exploited in a therapeutic scenario.

Results from Chapter 3 showed that LNPSVAATL peptide from HCV is unable to bind other HLA-C1 alleles besides HLA-C*0102, which makes the HLA-C*0102:LNPSVAATL complex, and its interaction with KIR2DS2, a highly specific combination that could be relevant in populations with high frequencies of both, the ligand and the receptor. On the other hand, Chapter 5 showed that the combination of KIR2DS2, the HLA-C*0802 allele and the IVDLMCHATF peptide from DENV/ZIKV had the ability to induce a strong and sustained NK cell degranulation and cytotoxic response to target cells. The implications of this novel finding are of major relevance as it is reported for the first time that a viral peptide – which is highly conserved among Flaviviruses – binds multiple HLA-C alleles and favour canonical interactions with KIR2DS2. From these results and those of Naiyer *et al*, it can be assumed that these KIR/MHC-I/peptide combinations could be beneficial in populations exhibiting high frequencies of KIR2DS2 and HLA-C*0102/HLA-C*0802, from regions where ZIKV and/or any of the four serotypes of DENV circulate (Gonzalez-Galarza *et al.*, 2015). Likewise, the high degree of conservation of the MCHAT motif within Flaviviruses leads us to think that other members of this family, besides DENV and ZIKV, are likely to be

susceptible to the NK cell anti-viral response through KIR2DS2, which would have a positive impact in the early immune control of these pathogens.

The influence of KIR2DS2 and/or HLA-C1 in the outcome of infections caused by *Flaviviridae* viruses differs according to the populations studied. In the case of HCV, KIR2DS2-HLA-C1 has shown to be a protective factor in the UK Caucasian population; however such interaction has been associated with susceptibility to chronic HCV infection in Polish and Brazilian individuals (de Vasconcelos *et al.*, 2013; Kusnierczyk *et al.*, 2015; Naiyer *et al.*, 2017). Regarding Flaviviruses, the few reports assessing KIR2DS2 and HLA-C1 alleles alone, or in combination, have been unable to demonstrate a clear effect in the outcome of dengue (Beltrame *et al.*, 2013; Petitdemange *et al.*, 2014) or WNV infection (Lanteri *et al.*, 2011; Spiroski *et al.*, 2013). Lack of consistency and robustness amongst these studies could be explained by small sample sizes, population stratification or low resolution typing (Alter *et al.*, 2017). Therefore, high throughput, high-resolution disease association studies in populations at risk would be needed in order to precisely define the potential protective effect of the KIR/MHC-I combinations reported in this thesis and by Naiyer *et al* against these pathogenic viruses.

This thesis also confirmed that HCV and DENV/NS3-derived peptides (besides the ones mentioned above) bind different HLA-C1 alleles and canonically interact with KIR2DS2. Even though the precise peptide sequences mediating NK cell activation were not elucidated, some potential binders were identified. The fact that viral peptides from non-structural proteins could be selected for antigen presentation suggests a mechanism from the host to target residues from viral proteins with key roles in viral replication. Particularly, it has been described that helicases from RNA viruses – whose function is to catalyse the separation of double-stranded RNA – play essential roles in multiple processes such as RNA replication, transcription, translation, genome translocation, regulation of RNA-protein interactions, polyprotein processing and viral assembly (Borowski *et al.*, 2002; Frick and Lam, 2006; Papageorgiou *et al.*, 2016). As random mutations in this protein would be detrimental for the virus, specific protein regions are preserved in order to ensure viral fitness and survival (Khan *et al.*, 2008).

Despite the fact RNA viruses exist as viral quasispecies, with naturally occurring mutations continuously taking place, a certain degree of sequence conservation can be found throughout the viral genome (Frick and Lam, 2006; Presloid and Novella, 2015; Papageorgiou *et al.*, 2016). Particularly, the study conducted by Khan *et al* in 2008 identified conserved sequences of DENV1-4 isolates reported from worldwide regions at different

time points. The most conserved sequences between 9 and 22 amino acids length were found in NS5 (n=17), followed by NS3 (n=12), NS1 (n=7), NS4 (n=6) and E (n=2), many of them with high immunological significance (Khan *et al.*, 2008). Interestingly, in the same study, one of the conserved sequences – identified as a T-cell determinant – carries the "MCHAT" motif, suggesting that this particular region has being conserved across multiple DENV isolates from different geographic areas. This, together with the fact that "MCHAT" motif is highly conserved among Flaviviruses strongly suggest that this sequence plays a key role in virus fitness and survival and has been a strong selective force driving the evolution of KIR. Recognition of conserved residues from rapidly mutating viruses could be an exceptional adaptive mechanism used by the host that counterbalances viral evasion.

In conclusion, this thesis showed that viruses from the family *Flaviviridae* modulate NK cell activity through the KIR/MHC-I system and this maintains the balance in the evolutionary arms race between host and virus. The ability of *Flaviviridae*-derived peptides to activate NK cells through activating KIR2DS2 could be exploited as a potential anti-viral therapy in order to combat these pathogens. Viral peptides able to promote robust NK cell effector functions represent attractive candidates for vaccine development.

6.3 Future directions

The *in vitro* system used in this study allowed to identify viral peptides that, bound to specific HLA-C alleles, are able to bind KIR2DS2 leading to a robust NK cell activation against target cells. The next stage will assess the relevance of the HLA-C*0802:IVDLMCHATF complex *in vivo* and the characterization of activated KIR2DS2+ NK cells using a KIR transgenic mouse model. Similarly, previous work in our lab has showed that a DNA vaccine based on HLA-C*0102 and IVDLMCHATF peptide activates NK cells and induces anti-tumour responses. Therefore, HLA-C*0802 and IVDLMCHATF peptide could also be employed as a vaccine strategy in a tumour mouse model, which could be effective for cancer immunotherapy.

Binding of IVDLMCHATF peptide to the HLA-C*0501 (C2) allele was demonstrated in this study. Whether this complex is a cognate ligand for inhibitory KIR2DL1 or activating KIR2DS1 and whether such interactions positively or negatively impact NK cell responses remain to be elucidated. The combination of two commercial antibodies to discriminate KIR2DL1 and KIR2DS1 in flow cytometry assays has been previously tested in our

laboratory and could be used to assess NK cell activation against HLA-C*0501-expressing cells exogenously or endogenously presenting IVDLMCHATF peptide. The generation of KIR2DL1+ or KIR2DS1+ NK clones could give a better insight in the precise role of these receptors in the modulation of NK cell functions.

The *in silico* analysis of the HCV genome allowed to identify peptide sequences carrying the KIR2DS2-binding motif that are likely to bind HLA-C1 alleles. Likewise, IVDLMCHATF peptide was predicted to strongly bind HLA-C*0403. The relevance of these HLA-C:peptide complexes could be tested *in vitro* following the methodology optimized in this study.

Finally, it would be ideal to confirm through disease association studies the protective effect of the KIR2DS2/HLA-C*0102 or KIR2DS2/HLA-C*0802 combinations in a cohort of dengue-infected individuals.

Appendix A - Protein sequences HLA-C*0802 and IVDLMCHATF peptide

Protein alignment HLA-C*0802

Sequence ID: AAA59687.1 Length: 366 Number of Matches: 1

See 4 more title(s)

Range 1: 1 to 366 GenPept Graphics

Score	Expect	Method	Identities	Positives	Gaps
759 bits(1959)	0.0	Compositional matrix adjust.	366/366(100%)	366/366(100%)	0/366(0%)

```
RefSeq      1   MRVMAPRTLILLLSGALALTETWACSHSMRYFYTAVSRPGRGEPRFIAVGYVDDTQFVQF  60
                MRVMAPRTLILLLSGALALTETWACSHSMRYFYTAVSRPGRGEPRFIAVGYVDDTQFVQF
AAA59687.1  1   MRVMAPRTLILLLSGALALTETWACSHSMRYFYTAVSRPGRGEPRFIAVGYVDDTQFVQF  60

RefSeq     61   DSDAASPRGEPRAPWVEQEGPEYWDRETQKYKRQAQTDRVSLRNLRGYYNQSEAGSHTLQ  120
                DSDAASPRGEPRAPWVEQEGPEYWDRETQKYKRQAQTDRVSLRNLRGYYNQSEAGSHTLQ
AAA59687.1  61   DSDAASPRGEPRAPWVEQEGPEYWDRETQKYKRQAQTDRVSLRNLRGYYNQSEAGSHTLQ  120

RefSeq     121  RMYGCDLGPDGRLLRGYNQFAYDGKDYIALNEDLRSWTAADKAAQITQRKWEAAREAEQR  180
                RMYGCDLGPDGRLLRGYNQFAYDGKDYIALNEDLRSWTAADKAAQITQRKWEAAREAEQR
AAA59687.1  121  RMYGCDLGPDGRLLRGYNQFAYDGKDYIALNEDLRSWTAADKAAQITQRKWEAAREAEQR  180

RefSeq     181  RAYLEGTCVEWLRRYLENGKKTLQRAEHPKTHVTHHPVSDHEATLRCWALGFYPAEITLT  240
                RAYLEGTCVEWLRRYLENGKKTLQRAEHPKTHVTHHPVSDHEATLRCWALGFYPAEITLT
AAA59687.1  181  RAYLEGTCVEWLRRYLENGKKTLQRAEHPKTHVTHHPVSDHEATLRCWALGFYPAEITLT  240

RefSeq     241  WQRDGEDQTQDTELVETRPAGDGTFQKWAAVVVPSGEEQRYTCHVQHEGLPEPLTLRWGP  300
                WQRDGEDQTQDTELVETRPAGDGTFQKWAAVVVPSGEEQRYTCHVQHEGLPEPLTLRWGP
AAA59687.1  241  WQRDGEDQTQDTELVETRPAGDGTFQKWAAVVVPSGEEQRYTCHVQHEGLPEPLTLRWGP  300

RefSeq     301  SSQPTIPIVGIVAGLAVLAVLAVLGAVMAVVMCRRKSSGGKGGSCSQAASSNSAQGSDES  360
                SSQPTIPIVGIVAGLAVLAVLAVLGAVMAVVMCRRKSSGGKGGSCSQAASSNSAQGSDES
AAA59687.1  301  SSQPTIPIVGIVAGLAVLAVLAVLGAVMAVVMCRRKSSGGKGGSCSQAASSNSAQGSDES  360

RefSeq     361  LIACKA  366
                LIACKA
AAA59687.1  361  LIACKA  366
```

Appendix A

IVDLMCHATF peptide in DENV1-4 and ZIKV

nonstructural protein NS3, partial [Dengue virus 1]

GenBank: AAB03618.1

GenPept Identical Proteins Graphics

>AAB03618.1 nonstructural protein NS3, partial [Dengue virus 1]
VNREGKIVGLYGNGVVTTSGTYVSAIAQAKASQEGPLPEIEDEVFKKRNLTIMDLHPGSGKTRRYLPAIV
REAIKRNVRTLILAPTRVVASEMAEALRGMPIRYQTTAVKSEHTGREIVDLMCHATFTMRLLSPVRVPNY
NMI

nonstructural protein NS3, partial [Dengue virus 2]

GenBank: AAB03620.1

GenPept Identical Proteins Graphics

>AAB03620.1 nonstructural protein NS3, partial [Dengue virus 2]
IVDKKGKVVGLYGNGVVTRSGTYVSAIAQTEKSIEDNPEIEDDIFRKKRLTIMDLHPGAGKTKRYLPAIV
REAIKRGLRTLILAPTRVVAAEMEEALRGLPIRYQTPAIRAEHTGREIVDLMCHATFTMRLLSPVRVPNY
NLI

nonstructural protein NS3, partial [Dengue virus 3]

GenBank: AAA68492.1

GenPept Identical Proteins Graphics

>AAA68492.1 nonstructural protein NS3, partial [Dengue virus 3]
KVVGLYGNGVVTKNGGYVSGIAQTNAEPDGPTPELEEEMFKKRNLTIMDLHPGSGKTRKYLPAIVREAIK
RRLRTLILAPTRVVAAEMEEALKGLPIRYQTTATKSEHTGREIVDLMCHATFTMRLLSPVRV

nonstructural protein NS3, partial [Dengue virus 4]

GenBank: AAA18247.1

GenPept Identical Proteins Graphics

>AAA18247.1 nonstructural protein NS3, partial [Dengue virus 4]
RKGKVIGLYGNGVVTKSGDYVSAITQAERTGEPDYEVDEDIFRKKRLTIMDLHPGAGKTKRILPSIVREA
LKRRLRTLILAPTRVVAAEMEEALRGLPIRYQTPAVKSEHTGREIVDLMCHATFTTRLLSSTRVPNYNLI

NS3 protein, partial [Zika virus]

GenBank: AHL16750.1

GenPept Identical Proteins Graphics

>AHL16750.1 NS3 protein, partial [Zika virus]
NGVVIKNGSYVSAITQGKREEETPVECFEPSMLRKKQLTVLDLHPGAGKTRRVLPEIVREAIKKRLRTVI
LAPTRVVAAEMEEALRGLPVRYMTTAVNVTHSGTEIVDLMCHATFTSRLLQPIRVPNYNLYIMDEAHFTD
PSSIAARGYISTRVEMGEAAAIFMTATPPGTRDAFPDSNSPIMDTEVEVPERAWSSGFDWVTDHSGKTIW
FVPSVRNGNEIAACLTKAGKRVIQLSRKTFETEFQKTKNQEWDFVIT

Bibliography

1. Abbas Abul, L.A., Pober Jordan (2014) *Cellular and molecular immunology*.

2. Abel, A.M. *et al.* (2018) 'Natural Killer Cells: Development, Maturation, and Clinical Utilization', *Front Immunol*, 9, p. 1869.

3. Abendroth, A. *et al.* (2001) 'Varicella-zoster virus retains major histocompatibility complex class I proteins in the Golgi compartment of infected cells', *J Virol*, 75(10), pp. 4878-88.

4. Achdout, H., Manaster, I. and Mandelboim, O. (2008) 'Influenza virus infection augments NK cell inhibition through reorganization of major histocompatibility complex class I proteins', *J Virol*, 82(16), pp. 8030-7.

5. Ahn, K. *et al.* (1997) 'The ER-luminal domain of the HCMV glycoprotein US6 inhibits peptide translocation by TAP', *Immunity*, 6(5), pp. 613-21.

6. Alagarasu, K. *et al.* (2015) 'Profile of killer cell immunoglobulin-like receptor and its human leucocyte antigen ligands in dengue-infected patients from Western India', *Int J Immunogenet*, 42(6), pp. 432-8.

7. Ali, A.K. *et al.* (2016) 'NK Cell-Specific Gata3 Ablation Identifies the Maturation Program Required for Bone Marrow Exit and Control of Proliferation', *J Immunol*, 196(4), pp. 1753-67.

8. Alter, G. *et al.* (2011) 'HIV-1 adaptation to NK-cell-mediated immune pressure', *Nature*, 476(7358), pp. 96-100.

9. Alter, I. *et al.* (2017) 'HLA class I haplotype diversity is consistent with selection for frequent existing haplotypes', *PLoS Comput Biol*, 13(8), p. e1005693.

10. Anderson, K. *et al.* (1991) 'Endogenously synthesized peptide with an endoplasmic reticulum signal sequence sensitizes antigen processing mutant cells to class I-restricted cell-mediated lysis', *J Exp Med*, 174(2), pp. 489-92.

11. Anderson, S.K. (2018) 'Molecular evolution of elements controlling HLA-C expression: Adaptation to a role as a killer-cell immunoglobulin-like receptor ligand regulating natural killer cell function', *HLA*, 92(5), pp. 271-278.

12. Anfossi, N. *et al.* (2006) 'Human NK cell education by inhibitory receptors for MHC class I', *Immunity*, 25(2), pp. 331-42.

13. Angelo, L.S. *et al.* (2015) 'Practical NK cell phenotyping and variability in healthy adults', *Immunol Res*, 62(3), pp. 341-56.

14. Angus, A.G. *et al.* (2012) 'Conserved glycine 33 residue in flexible domain I of hepatitis C virus core protein is critical for virus infectivity', *J Virol*, 86(2), pp. 679-90.

15. Apps, R. *et al.* (2007) 'A homodimeric complex of HLA-G on normal trophoblast cells modulates antigen-presenting cells via LILRB1', *Eur J Immunol*, 37(7), pp. 1924-37.

16. Arnaiz-Villena, A. *et al.* (2018) 'Study of Colombia North Wiwa El Encanto Amerindians HLA- genes: Pacific Islanders relatedness', *Hum Immunol*, 79(7), pp. 530-531.

17. Bastidas-Legarda, L.Y. and Khakoo, S.I. (2018) 'Conserved and variable natural killer cell receptors: diverse approaches to viral infections', *Immunology*.

18. Becknell, B. and Caligiuri, M.A. (2005) 'Interleukin-2, interleukin-15, and their roles in human natural killer cells', *Adv Immunol*, 86, pp. 209-39.

19. Becquart, P. *et al.* (2010) 'Acute dengue virus 2 infection in Gabonese patients is associated with an early innate immune response, including strong interferon alpha production', *BMC Infect Dis*, 10, p. 356.

20. Beltrame, L.M. *et al.* (2013) 'Influence of KIR genes and their HLA ligands in susceptibility to dengue in a population from southern Brazil', *Tissue Antigens*, 82(6), pp. 397-404.

21. Bern, M.D. *et al.* (2019) 'Inducible down-regulation of MHC class I results in natural killer cell tolerance', *J Exp Med*, 216(1), pp. 99-116.

22. Bernardini, G., Gismondi, A. and Santoni, A. (2012) 'Chemokines and NK cells: regulators of development, trafficking and functions', *Immunol Lett*, 145(1-2), pp. 39-46.

23. Bhatt, S. *et al.* (2013) 'The global distribution and burden of dengue', *Nature*, 496(7446), pp. 504-7.

24. Billadeau, D.D. and Leibson, P.J. (2002) 'ITAMs versus ITIMs: striking a balance during cell regulation', *J Clin Invest*, 109(2), pp. 161-8.

25. Blais, M.E., Dong, T. and Rowland-Jones, S. (2011) 'HLA-C as a mediator of natural killer and T-cell activation: spectator or key player?', *Immunology*, 133(1), pp. 1-7.

26. Blight, K.J., McKeating, J.A. and Rice, C.M. (2002) 'Highly permissive cell lines for subgenomic and genomic hepatitis C virus RNA replication', *J Virol*, 76(24), pp. 13001-14.

27. Blokhuis, J.H. *et al.* (2017) 'KIR2DS5 allotypes that recognize the C2 epitope of HLA-C are common among Africans and absent from Europeans', *Immun Inflamm Dis*, 5(4), pp. 461-468.

28. Blom, K. *et al.* (2016) 'NK Cell Responses to Human Tick-Borne Encephalitis Virus Infection', *J Immunol*, 197(7), pp. 2762-71.

29. Blunt, M.D. *et al.* (2019) 'A novel antibody combination to identify KIR2DS2(high) natural killer cells in KIR2DL3/L2/S2 heterozygous donors', *HLA*, 93(1), pp. 32-35.

30. Bonagura, V.R. *et al.* (2010) 'Activating killer cell immunoglobulin-like receptors 3DS1 and 2DS1 protect against developing the severe form of recurrent respiratory papillomatosis', *Hum Immunol*, 71(2), pp. 212-9.

31. Borhis, G. *et al.* (2013) 'A peptide antagonist disrupts NK cell inhibitory synapse formation', *J Immunol*, 190(6), pp. 2924-30.

32. Borhis, G. and Khakoo, S.I. (2011) 'NK cell receptors: evolution and diversity'.

33. Borowski, P. *et al.* (2002) 'NTPase/helicase of Flaviviridae: inhibitors and inhibition of the enzyme', *Acta Biochim Pol*, 49(3), pp. 597-614.

34. Bottino, C. *et al.* (2005) 'Cellular ligands of activating NK receptors', *Trends Immunol*, 26(4), pp. 221-6.

35. Bottino, C. *et al.* (2000) 'Identification and molecular characterization of a natural mutant of the p50.2/KIR2DS2 activating NK receptor that fails to mediate NK cell triggering', *Eur J Immunol*, 30(12), pp. 3569-74.

36. Boulanger, D.S.M. *et al.* (2018) 'A Mechanistic Model for Predicting Cell Surface Presentation of Competing Peptides by MHC Class I Molecules', *Front Immunol*, 9, p. 1538.

37. Boyington, J.C., Brooks, A.G. and Sun, P.D. (2001) 'Structure of killer cell immunoglobulin-like receptors and their recognition of the class I MHC molecules', *Immunol Rev*, 181, pp. 66-78.

38. Boyington, J.C. *et al.* (2000) 'Crystal structure of an NK cell immunoglobulin-like receptor in complex with its class I MHC ligand', *Nature*, 405(6786), pp. 537-43.

39. Brodin, P. *et al.* (2015) 'Variation in the human immune system is largely driven by non-heritable influences', *Cell*, 160(1-2), pp. 37-47.

40. Brodin, P., Karre, K. and Hoglund, P. (2009) 'NK cell education: not an on-off switch but a tunable rheostat', *Trends Immunol*, 30(4), pp. 143-9.

41. Budagian, V. *et al.* (2006) 'IL-15/IL-15 receptor biology: a guided tour through an expanding universe', *Cytokine Growth Factor Rev*, 17(4), pp. 259-80.

42. Campbell, K.S. and Purdy, A.K. (2011) 'Structure/function of human killer cell immunoglobulin-like receptors: lessons from polymorphisms, evolution, crystal structures and mutations', *Immunology*, 132(3), pp. 315-25.

43. Carotta, S. *et al.* (2011) 'Identification of the earliest NK-cell precursor in the mouse BM', *Blood*, 117(20), pp. 5449-52.

44. Carrillo-Bustamante, P., Kesmir, C. and de Boer, R.J. (2015) 'A Coevolutionary Arms Race between Hosts and Viruses Drives Polymorphism and Polygenicity of NK Cell Receptors', *Mol Biol Evol*, 32(8), pp. 2149-60.

45. Carrington, M. and Norman, P.J. (2003) *The KIR gene cluster*.

46. Carrington, M. *et al.* (2005) 'Hierarchy of resistance to cervical neoplasia mediated by combinations of killer immunoglobulin-like receptor and human leukocyte antigen loci', *J Exp Med*, 201(7), pp. 1069-75.

47. Cassidy, S. *et al.* (2015) 'Peptide selectivity discriminates NK cells from KIR2DL2- and KIR2DL3-positive individuals', in *Eur J Immunol*. Hoboken, pp. 492-500.

48. Cassidy, S.A., Cheent, K.S. and Khakoo, S.I. (2014) 'Effects of Peptide on NK cell-mediated MHC I recognition', *Front Immunol*, 5, p. 133.

49. Castanha, P.M.S. *et al.* (2017) 'Dengue Virus-Specific Antibodies Enhance Brazilian Zika Virus Infection', *J Infect Dis*, 215(5), pp. 781-785.

50. CDC (2019) *Japanese Encephalitis*. Available at: https://wwwnc.cdc.gov/travel/yellowbook/2020/travel-related-infectious-diseases/japanese-encephalitis (Accessed: September).

51. Chancey, C. *et al.* (2015) 'The global ecology and epidemiology of West Nile virus', *Biomed Res Int*, 2015, p. 376230.

52. Chapel, A. *et al.* (2017) 'Peptide-specific engagement of the activating NK cell receptor KIR2DS1', *Sci Rep*, 7(1), p. 2414.

53. Cheent, K.S. *et al.* (2013) 'Synergistic inhibition of natural killer cells by the nonsignaling molecule CD94', *Proc Natl Acad Sci U S A*, 110(42), pp. 16981-6.

54. Chua, H.L., Serov, Y. and Brahmi, Z. (2004) 'Regulation of FasL expression in natural killer cells', *Hum Immunol*, 65(4), pp. 317-27.

55. Cohnen, A. *et al.* (2013) 'Surface CD107a/LAMP-1 protects natural killer cells from degranulation-associated damage', *Blood*, 122(8), pp. 1411-8.

56. Colantonio, A.D. *et al.* (2011) 'KIR polymorphisms modulate peptide-dependent binding to an MHC class I ligand with a Bw6 motif', *PLoS Pathog*, 7(3), p. e1001316.

57. Colucci, F. and Di Santo, J.P. (2000) 'The receptor tyrosine kinase c-kit provides a critical signal for survival, expansion, and maturation of mouse natural killer cells', *Blood*, 95(3), pp. 984-91.

58. Cooper, M.A., Fehniger, T.A. and Caligiuri, M.A. (2001) 'The biology of human natural killer-cell subsets', *Trends Immunol*, 22(11), pp. 633-40.

59. Costa, V.V. *et al.* (2017) 'Dengue Virus-Infected Dendritic Cells, but Not Monocytes, Activate Natural Killer Cells through a Contact-Dependent Mechanism Involving Adhesion Molecules', *MBio*, 8(4).

60. Croft, N.P. *et al.* (2013) 'Kinetics of antigen expression and epitope presentation during virus infection', *PLoS Pathog*, 9(1), p. e1003129.

61. Daniels, R.W. *et al.* (2014) 'Expression of multiple transgenes from a single construct using viral 2A peptides in Drosophila', *PLoS One*, 9(6), p. e100637.

62. Dantuma, N.P., Sharipo, A. and Masucci, M.G. (2002) 'Avoiding proteasomal processing: the case of EBNA1', *Curr Top Microbiol Immunol*, 269, pp. 23-36.

63. Das, J. and Khakoo, S.I. (2015) 'NK cells: tuned by peptide?', *Immunol Rev*, 267(1), pp. 214-27.

64. David, G. *et al.* (2009) 'Discrimination between the main activating and inhibitory killer cell immunoglobulin-like receptor positive natural killer cell subsets using newly characterized monoclonal antibodies', *Immunology*, 128(2), pp. 172-84.

65. De Pelsmaeker, S. *et al.* (2018) 'Herpesvirus Evasion of Natural Killer Cells', *J Virol*, 92(11).

66. De Re, V. *et al.* (2008) 'HCV inhibits antigen processing and presentation and induces oxidative stress response in gastric mucosa', *Proteomics Clin Appl*, 2(9), pp. 1290-9.

67. de Rham, C. *et al.* (2007) 'The proinflammatory cytokines IL-2, IL-15 and IL-21 modulate the repertoire of mature human natural killer cell receptors', *Arthritis Res Ther*, 9(6), p. R125.

68. de Saint Basile, G., Menasche, G. and Fischer, A. (2010) 'Molecular mechanisms of biogenesis and exocytosis of cytotoxic granules', *Nat Rev Immunol*, 10(8), pp. 568-79.

69. De Silva, A.D. *et al.* (1999) 'Thermolabile H-2Kb molecules expressed by transporter associated with antigen processing-deficient RMA-S cells are occupied by low-affinity peptides', *J Immunol*, 163(8), pp. 4413-20.

70. de Vasconcelos, J.M. *et al.* (2013) 'Association of killer cell immunoglobulin-like receptor polymorphisms with chronic hepatitis C and responses to therapy in Brazil', *Genet Mol Biol*, 36(1), pp. 22-7.

71. Di Bona, D. *et al.* (2014) 'HLA and killer cell immunoglobulin-like receptors influence the natural course of CMV infection', *J Infect Dis*, 210(7), pp. 1083-9.

72. Di Marco, M. *et al.* (2017) 'Unveiling the Peptide Motifs of HLA-C and HLA-G from Naturally Presented Peptides and Generation of Binding Prediction Matrices', *J Immunol*, 199(8), pp. 2639-2651.

73. Diefenbach, A. *et al.* (2001) 'Rae1 and H60 ligands of the NKG2D receptor stimulate tumour immunity', *Nature*, 413(6852), pp. 165-71.

74. Dong, G. *et al.* (2009) 'Insights into MHC class I peptide loading from the structure of the tapasin-ERp57 thiol oxidoreductase heterodimer', *Immunity*, 30(1), pp. 21-32.

75. Elliott, J.M. and Yokoyama, W.M. (2011) 'Unifying concepts of MHC-dependent natural killer cell education', *Trends Immunol*, 32(8), pp. 364-72.

76. Enard, D. *et al.* (2016) 'Viruses are a dominant driver of protein adaptation in mammals', *Elife*, 5.

77. Estefania, E. *et al.* (2007) 'Influence of KIR gene diversity on the course of HSV-1 infection: resistance to the disease is associated with the absence of KIR2DL2 and KIR2DS2', *Tissue Antigens*, 70(1), pp. 34-41.

78. Estofolete, C.F. *et al.* (2019) 'Co-infection between Zika and different Dengue serotypes during DENV outbreak in Brazil', *J Infect Public Health*, 12(2), pp. 178-181.

79. Fadda, L. *et al.* (2010) 'Peptide antagonism as a mechanism for NK cell activation', *Proc Natl Acad Sci U S A*, 107(22), pp. 10160-5.

80. Fadda, L. *et al.* (2012) 'HLA-Cw*0102-restricted HIV-1 p24 epitope variants can modulate the binding of the inhibitory KIR2DL2 receptor and primary NK cell function', *PLoS Pathog*, 8(7), p. e1002805.

81. Fadda, L. *et al.* (2011) 'Common HIV-1 peptide variants mediate differential binding of KIR3DL1 to HLA-Bw4 molecules', *J Virol*, 85(12), pp. 5970-4.

82. Fan, Q.R., Long, E.O. and Wiley, D.C. (2001) 'Crystal structure of the human natural killer cell inhibitory receptor KIR2DL1-HLA-Cw4 complex', *Nat Immunol*, 2(5), pp. 452-60.

83. Fernandez, N.C. *et al.* (2005) 'A subset of natural killer cells achieves self-tolerance without expressing inhibitory receptors specific for self-MHC molecules', *Blood*, 105(11), pp. 4416-23.

84. Freud, A.G. *et al.* (2005) 'A human CD34(+) subset resides in lymph nodes and differentiates into CD56bright natural killer cells', *Immunity*, 22(3), pp. 295-304.

85. Freud, A.G. *et al.* (2006) 'Evidence for discrete stages of human natural killer cell differentiation in vivo', in *J Exp Med*. pp. 1033-43.

86. Freud, A.G., Yu, J. and Caligiuri, M.A. (2014) 'Human natural killer cell development in secondary lymphoid tissues', *Semin Immunol*, 26(2), pp. 132-7.

87. Frick, D.N. and Lam, A.M. (2006) 'Understanding helicases as a means of virus control', *Curr Pharm Des*, 12(11), pp. 1315-38.

88. Früh, K. *et al.* (1995) 'A viral inhibitor of peptide transporters for antigen presentation', *Nature*, 375(6530), pp. 415-8.

89. Ganeshkumar, P. *et al.* (2018) 'Dengue infection in India: A systematic review and meta-analysis', *PLoS Negl Trop Dis*, 12(7), p. e0006618.

90. Garcia-Beltran, W.F. *et al.* (2016) 'Open conformers of HLA-F are high-affinity ligands of the activating NK-cell receptor KIR3DS1', *Nat Immunol*, 17(9), pp. 1067-74.

91. Gascoyne, D.M. *et al.* (2009) 'The basic leucine zipper transcription factor E4BP4 is essential for natural killer cell development', *Nat Immunol*, 10(10), pp. 1118-24.

92. Gasser, S. and Raulet, D.H. (2006) 'Activation and self-tolerance of natural killer cells', *Immunol Rev*, 214, pp. 130-42.

93. Gays, F. *et al.* (2005) 'Multiple cytokines regulate the NK gene complex-encoded receptor repertoire of mature NK cells and T cells', *J Immunol*, 175(5), pp. 2938-47.

94. Gendzekhadze, K. *et al.* (2009) 'Co-evolution of KIR2DL3 with HLA-C in a human population retaining minimal essential diversity of KIR and HLA class I ligands', *Proc Natl Acad Sci U S A*, 106(44), pp. 18692-7.

95. Gilbert, M.J. *et al.* (1996) 'Cytomegalovirus selectively blocks antigen processing and presentation of its immediate-early gene product', *Nature*, 383(6602), pp. 720-2.

96. Glasner, A. *et al.* (2017) 'Zika Virus Escapes NK Cell Detection by Upregulating Major Histocompatibility Complex Class I Molecules', *J Virol*, 91(22).

97. Gomez-Lozano, N. and Vilches, C. (2002) 'Genotyping of human killer-cell immunoglobulin-like receptor genes by polymerase chain reaction with sequence-specific primers: an update', *Tissue Antigens*, 59(3), pp. 184-93.

98. Gonzalez-Galarza, F.F. *et al.* (2015) 'Allele frequency net 2015 update: new features for HLA epitopes, KIR and disease and HLA adverse drug reaction associations', *Nucleic Acids Res*, 43(Database issue), pp. D784-8.

99. Goodridge, J.P. *et al.* (2019) 'Remodeling of secretory lysosomes during education tunes functional potential in NK cells', *Nat Commun*, 10(1), p. 514.

100. Grabowski, J.M. and Hill, C.A. (2017) 'A Roadmap for Tick-Borne Flavivirus Research in the "Omics" Era', *Front Cell Infect Microbiol*, 7, p. 519.

101. Graef, T. *et al.* (2009) 'KIR2DS4 is a product of gene conversion with KIR3DL2 that introduced specificity for HLA-A*11 while diminishing avidity for HLA-C', *J Exp Med*, 206(11), pp. 2557-72.

102. Guia, S. *et al.* (2011) 'Confinement of activating receptors at the plasma membrane controls natural killer cell tolerance', *Sci Signal*, 4(167), p. ra21.

103. Guidotti, L.G. and Chisari, F.V. (2006) 'Immunobiology and pathogenesis of viral hepatitis', *Annu Rev Pathol*, 1, pp. 23-61.

104. Gumá, M. *et al.* (2004) 'Imprint of human cytomegalovirus infection on the NK cell receptor repertoire', *Blood*, 104(12), pp. 3664-71.

105. Hansasuta, P. *et al.* (2004) 'Recognition of HLA-A3 and HLA-A11 by KIR3DL2 is peptide-specific', *Eur J Immunol*, 34(6), pp. 1673-9.

106. He, Y. and Tian, Z. (2017) 'NK cell education via nonclassical MHC and non-MHC ligands', *Cell Mol Immunol*, 14(4), pp. 321-330.

107. Hernandez-Ramirez, D. *et al.* (2015) 'Association of KIR3DL1/S1 and HLA-Bw4 with CD4 T cell counts in HIV-infected Mexican mestizos', *Immunogenetics*, 67(8), pp. 413-24.

108. Hershkovitz, O. *et al.* (2008) 'Dengue virus replicon expressing the nonstructural proteins suffices to enhance membrane expression of HLA class I and inhibit lysis by human NK cells', *J Virol*, 82(15), pp. 7666-76.

109. Herzer, K. *et al.* (2003) 'Upregulation of major histocompatibility complex class I on liver cells by hepatitis C virus core protein via p53 and TAP1 impairs natural killer cell cytotoxicity', *J Virol*, 77(15), pp. 8299-309.

110. Hewitt, E.W. (2003) 'The MHC class I antigen presentation pathway: strategies for viral immune evasion', *Immunology*, 110(2), pp. 163-9.

111. Hickman, H.D. *et al.* (2003) 'Cutting edge: class I presentation of host peptides following HIV infection', *J Immunol*, 171(1), pp. 22-6.

112. Holbrook, M.R. (2017) 'Historical Perspectives on Flavivirus Research', *Viruses*, 9(5).

113. Holder, K.A. *et al.* (2013) 'Hepatitis C virus-infected cells downregulate NKp30 and inhibit ex vivo NK cell functions', *J Immunol*, 191(6), pp. 3308-18.

114. Holzemer, A. *et al.* (2015) 'Selection of an HLA-C*03:04-Restricted HIV-1 p24 Gag Sequence Variant Is Associated with Viral Escape from KIR2DL3+ Natural

Killer Cells: Data from an Observational Cohort in South Africa', *PLoS Med*, 12(11), p. e1001900; discussion e1001900.

115. Horowitz, A. *et al.* (2013) 'Genetic and environmental determinants of human NK cell diversity revealed by mass cytometry', *Sci Transl Med*, 5(208), p. 208ra145.

116. Hsu, K.C. *et al.* (2002) 'Killer Ig-like receptor haplotype analysis by gene content: evidence for genomic diversity with a minimum of six basic framework haplotypes, each with multiple subsets', *J Immunol*, 169(9), pp. 5118-29.

117. Hudson, A.W., Howley, P.M. and Ploegh, H.L. (2001) 'A human herpesvirus 7 glycoprotein, U21, diverts major histocompatibility complex class I molecules to lysosomes', *J Virol*, 75(24), pp. 12347-58.

118. Ito, M. *et al.* (2006) 'Killer cell lectin-like receptor G1 binds three members of the classical cadherin family to inhibit NK cell cytotoxicity', *J Exp Med*, 203(2), pp. 289-95.

119. Ivarsson, M.A. *et al.* (2013) 'Differentiation and functional regulation of human fetal NK cells', *J Clin Invest*, 123(9), pp. 3889-901.

120. Jamil, K.M. and Khakoo, S.I. (2011) 'KIR/HLA interactions and pathogen immunity', *J Biomed Biotechnol*, 2011, p. 298348.

121. Janeway, C.A., Travers, P. and M, W. (2001) *Immunobiology: The Immune System in Health and Disease*. 5th edition edn. New York.

122. Jeffery, K.J. *et al.* (2000) 'The influence of HLA class I alleles and heterozygosity on the outcome of human T cell lymphotropic virus type I infection', *J Immunol*, 165(12), pp. 7278-84.

123. Jennes, W. *et al.* (2006) 'Cutting edge: resistance to HIV-1 infection among African female sex workers is associated with inhibitory KIR in the absence of their HLA ligands', *J Immunol*, 177(10), pp. 6588-92.

124. Joncker, N.T. *et al.* (2009) 'NK cell responsiveness is tuned commensurate with the number of inhibitory receptors for self-MHC class I: the rheostat model', *J Immunol*, 182(8), pp. 4572-80.

125. Jones, T.R. *et al.* (1996) 'Human cytomegalovirus US3 impairs transport and maturation of major histocompatibility complex class I heavy chains', *Proc Natl Acad Sci U S A*, 93(21), pp. 11327-33.

126. Jurtz, V. *et al.* (2017) 'NetMHCpan-4.0: Improved Peptide-MHC Class I Interaction Predictions Integrating Eluted Ligand and Peptide Binding Affinity Data', *J Immunol*, 199(9), pp. 3360-3368.

127. Kang, W. *et al.* (2014) 'Hepatitis C virus attenuates interferon-induced major histocompatibility complex class I expression and decreases CD8+ T cell effector functions', *Gastroenterology*, 146(5), pp. 1351-60.e1-4.

128. Keating, S.E. *et al.* (2016) 'Metabolic Reprogramming Supports IFN-gamma Production by CD56bright NK Cells', *J Immunol*, 196(6), pp. 2552-60.

129. Keawvichit, R. *et al.* (2018) 'Differences in activation and tissue homing markers of natural killer cell subsets during acute dengue infection', *Immunology*, 153(4), pp. 455-465.

130. Kelley, J., Walter, L. and Trowsdale, J. (2005) 'Comparative genomics of natural killer cell receptor gene clusters', *PLoS Genet*, 1(2), pp. 129-39.

131. Kelly, A. and Trowsdale, J. (2017) 'Introduction: MHC/KIR and governance of specificity', *Immunogenetics*, 69(8-9), pp. 481-488.

132. Kelly, J.M. *et al.* (2004) 'Granzyme M mediates a novel form of perforin-dependent cell death', *J Biol Chem*, 279(21), pp. 22236-42.

133. Kesson, A.M., Cheng, Y. and King, N.J. (2002) 'Regulation of immune recognition molecules by flavivirus, West Nile', *Viral Immunol*, 15(2), pp. 273-83.

134. Khakoo, S.I. *et al.* (2002) 'The D0 domain of KIR3D acts as a major histocompatibility complex class I binding enhancer', *J Exp Med*, 196(7), pp. 911-21.

135. Khakoo, S.I. *et al.* (2004) 'HLA and NK cell inhibitory receptor genes in resolving hepatitis C virus infection', *Science*, 305(5685), pp. 872-4.

136. Khan, A.M. *et al.* (2008) 'Conservation and variability of dengue virus proteins: implications for vaccine design', *PLoS Negl Trop Dis*, 2(8), p. e272.

137. Kiessling, R., Klein, E. and Wigzell, H. (1975) '"Natural" killer cells in the mouse. I. Cytotoxic cells with specificity for mouse Moloney leukemia cells. Specificity and distribution according to genotype', *Eur J Immunol*, 5(2), pp. 112-7.

138. Kikuchi-Maki, A., Catina, T.L. and Campbell, K.S. (2005) 'Cutting edge: KIR2DL4 transduces signals into human NK cells through association with the Fc receptor gamma protein', *J Immunol*, 174(7), pp. 3859-63.

139. Kim, H. *et al.* (2014) 'Hepatitis C virus impairs natural killer cell-mediated augmentation of complement synthesis', *J Virol*, 88(5), pp. 2564-71.

140. Knapp, S. *et al.* (2010) 'Consistent beneficial effects of killer cell immunoglobulin-like receptor 2DL3 and group 1 human leukocyte antigen-C following exposure to hepatitis C virus', *Hepatology*, 51(4), pp. 1168-75.

141. Knox, J.J. *et al.* (2016) 'Corrigendum: Characterization of T-bet and Eomes in Peripheral Human Immune Cells', *Front Immunol*, 7, p. 337.

142. Kozak, M. (1987) 'An analysis of 5'-noncoding sequences from 699 vertebrate messenger RNAs', *Nucleic Acids Res*, 15(20), pp. 8125-48.

143. Krämer, B. *et al.* (2012) 'Natural killer p46High expression defines a natural killer cell subset that is potentially involved in control of hepatitis C virus replication and modulation of liver fibrosis', *Hepatology*, 56(4), pp. 1201-13.

144. Krzewski, K. *et al.* (2013) 'LAMP1/CD107a is required for efficient perforin delivery to lytic granules and NK-cell cytotoxicity', *Blood*, 121(23), pp. 4672-83.

145. Kulkarni, S., Martin, M.P. and Carrington, M. (2008) 'The Yin and Yang of HLA and KIR in human disease', *Semin Immunol*, 20(6), pp. 343-52.

146. Kurokohchi, K. *et al.* (1996) 'Expression of HLA class I molecules and the transporter associated with antigen processing in hepatocellular carcinoma', *Hepatology*, 23(5), pp. 1181-8.

147. Kusnierczyk, P. *et al.* (2015) 'Contribution of genes for killer cell immunoglobulin-like receptors (KIR) to the susceptibility to chronic hepatitis C virus infection and to viremia', *Hum Immunol*, 76(2-3), pp. 102-8.

148. Lanier, L.L. *et al.* (1991) 'Molecular and functional analysis of human natural killer cell-associated neural cell adhesion molecule (N-CAM/CD56)', *J Immunol*, 146(12), pp. 4421-6.

149. Lanier, L.L. *et al.* (1983) 'Subpopulations of human natural killer cells defined by expression of the Leu-7 (HNK-1) and Leu-11 (NK-15) antigens', *J Immunol*, 131(4), pp. 1789-96.

150. Lanteri, M.C. *et al.* (2011) 'Association between HLA class I and class II alleles and the outcome of West Nile virus infection: an exploratory study', *PLoS One*, 6(8), p. e22948.

151. Larena, M., Regner, M. and Lobigs, M. (2013) 'Cytolytic effector pathways and IFN-gamma help protect against Japanese encephalitis', *Eur J Immunol*, 43(7), pp. 1789-98.

152. Lee, K.M. *et al.* (2006) 'Requirement of homotypic NK-cell interactions through 2B4(CD244)/CD48 in the generation of NK effector functions', *Blood*, 107(8), pp. 3181-8.

153. Lekstrom-Himes, J.A. *et al.* (1999) 'Association of major histocompatibility complex determinants with the development of symptomatic and asymptomatic genital herpes simplex virus type 2 infections', *J Infect Dis*, 179(5), pp. 1077-85.

154. Leslie, A. *et al.* (2010) 'Additive contribution of HLA class I alleles in the immune control of HIV-1 infection', *J Virol*, 84(19), pp. 9879-88.

155. Li, P. *et al.* (2010) 'Granzyme B is recovered by natural killer cells via clathrin-dependent endocytosis', *Cell Mol Life Sci*, 67(18), pp. 3197-208.

156. Li, X.C. and Raghavan, M. (2010) 'Structure and function of major histocompatibility complex class I antigens', *Curr Opin Organ Transplant*, 15(4), pp. 499-504.

157. Liu, J. *et al.* (2014) 'Activating killer cell immunoglobulin-like receptor 2DS2 binds to HLA-A*11', *Proc Natl Acad Sci U S A*, 111(7), pp. 2662-7.

158. Liu, Z. *et al.* (2017) 'Systematic comparison of 2A peptides for cloning multi-genes in a polycistronic vector', *Sci Rep*, 7(1), p. 2193.

159. Llano, M. *et al.* (2003) 'Differential effects of US2, US6 and US11 human cytomegalovirus proteins on HLA class Ia and HLA-E expression: impact on target susceptibility to NK cell subsets', *Eur J Immunol*, 33(10), pp. 2744-54.

160. Lobigs, M., Mullbacher, A. and Regner, M. (2003) 'MHC class I up-regulation by flaviviruses: Immune interaction with unknown advantage to host or pathogen', *Immunol Cell Biol*, 81(3), pp. 217-23.

161. Long, E.O. *et al.* (2013) 'Controlling natural killer cell responses: integration of signals for activation and inhibition', *Annu Rev Immunol*, 31, pp. 227-58.

162. Lopez, J.A. *et al.* (2012) 'Protecting a serial killer: pathways for perforin trafficking and self-defence ensure sequential target cell death', *Trends Immunol*, 33(8), pp. 406-12.

163. Lowe, R. *et al.* (2018) 'The Zika Virus Epidemic in Brazil: From Discovery to Future Implications', *Int J Environ Res Public Health*, 15(1).

164. Luang-Suarkia, D. *et al.* (2018) 'Hyperendemic dengue transmission and identification of a locally evolved DENV-3 lineage, Papua New Guinea 2007-2010', *PLoS Negl Trop Dis*, 12(3), p. e0006254.

165. Luft, T. *et al.* (2001) 'Exogenous peptides presented by transporter associated with antigen processing (TAP)-deficient and TAP-competent cells: intracellular loading and kinetics of presentation', *J Immunol*, 167(5), pp. 2529-37.

166. Lunemann, S. *et al.* (2014) 'Compromised function of natural killer cells in acute and chronic viral hepatitis', *J Infect Dis*, 209(9), pp. 1362-73.

167. Lunemann, S. *et al.* (2016) 'Sequence variations in HCV core-derived epitopes alter binding of KIR2DL3 to HLA-C *03:04 and modulate NK cell function', *J Hepatol*, 65(2), pp. 252-8.

168. Lunemann, S. *et al.* (2018) 'Interactions Between KIR3DS1 and HLA-F Activate Natural Killer Cells to Control HCV Replication in Cell Culture', *Gastroenterology*.

169. Lyman, S.D. and Jacobsen, S.E. (1998) 'c-kit ligand and Flt3 ligand: stem/progenitor cell factors with overlapping yet distinct activities', *Blood*, 91(4), pp. 1101-34.

170. Ma, Y., Li, X. and Kuang, E. (2016) 'Viral Evasion of Natural Killer Cell Activation', *Viruses*, 8(4), p. 95.

171. MacFarlane, A.W. and Campbell, K.S. (2006) 'Signal transduction in natural killer cells', *Curr Top Microbiol Immunol*, 298, pp. 23-57.

172. Mangino, M. *et al.* (2017) 'Innate and adaptive immune traits are differentially affected by genetic and environmental factors', *Nat Commun*, 8, p. 13850.

173. Mao, H. *et al.* (2009) 'Influenza virus directly infects human natural killer cells and induces cell apoptosis', *J Virol*, 83(18), pp. 9215-22.

174. Marquardt, N. *et al.* (2015) 'The Human NK Cell Response to Yellow Fever Virus 17D Is Primarily Governed by NK Cell Differentiation Independently of NK Cell Education', *J Immunol*, 195(7), pp. 3262-72.

175. Martín-Fontecha, A. *et al.* (2004) 'Induced recruitment of NK cells to lymph nodes provides IFN-gamma for T(H)1 priming', *Nat Immunol*, 5(12), pp. 1260-5.

176. Martin, M.P. *et al.* (2018) 'Killer cell immunoglobulin-like receptor 3DL1 variation modifies HLA-B*57 protection against HIV-1', *J Clin Invest*.

177. Mbiribindi, B. (2016) *Impact of the Major Histocompatibility Complex class I peptide repertoire on Natural Killer cell function*. PhD. University of Southampton.

178. Mbiribindi, B. *et al.* (2019) 'Spatial Clustering of Receptors and Signaling Molecules Regulates NK Cell Response to Peptide Repertoire Changes', *Front Immunol*, 10, p. 605.

179. McKechnie, J.L. *et al.* (2019) 'HLA Upregulation During Dengue Virus Infection Suppresses the Natural Killer Cell Response', *Front Cell Infect Microbiol*, 9, p. 268.

180. McNerney, M.E., Guzior, D. and Kumar, V. (2005) '2B4 (CD244)-CD48 interactions provide a novel MHC class I-independent system for NK-cell self-tolerance in mice', *Blood*, 106(4), pp. 1337-40.

181. Michel, T. *et al.* (2016) 'Human CD56bright NK Cells: An Update', *J Immunol*, 196(7), pp. 2923-31.

182. Middleton, D. and Gonzelez, F. (2010) 'The extensive polymorphism of KIR genes', *Immunology*, 129(1), pp. 8-19.

183. Miletić, A., Krmpotić, A. and Jonjić, S. (2013) 'The evolutionary arms race between NK cells and viruses: who gets the short end of the stick?', *Eur J Immunol*, 43(4), pp. 867-77.

184. Mirandola, P. *et al.* (2004) 'Activated human NK and CD8+ T cells express both TNF-related apoptosis-inducing ligand (TRAIL) and TRAIL receptors but are resistant to TRAIL-mediated cytotoxicity', *Blood*, 104(8), pp. 2418-24.

185. Miyagi, T. *et al.* (2010) 'Altered interferon-alpha-signaling in natural killer cells from patients with chronic hepatitis C virus infection', *J Hepatol*, 53(3), pp. 424-30.

186. Moesta, A.K. and Parham, P. (2012) 'Diverse functionality among human NK cell receptors for the C1 epitope of HLA-C: KIR2DS2, KIR2DL2, and KIR2DL3', *Front Immunol*, 3, p. 336.

187. Momburg, F., Mullbacher, A. and Lobigs, M. (2001) 'Modulation of transporter associated with antigen processing (TAP)-mediated peptide import into the endoplasmic reticulum by flavivirus infection', *J Virol*, 75(12), pp. 5663-71.

188. Moore, P.R. *et al.* (2017) 'Dengue viruses in Papua New Guinea: evidence of endemicity and phylogenetic variation, including the evolution of new genetic lineages', *Emerg Microbes Infect*, 6(12), p. e114.

189. Moradi, S. *et al.* (2015) 'The structure of the atypical killer cell immunoglobulin-like receptor, KIR2DL4', *J Biol Chem*, 290(16), pp. 10460-71.

190. Moretta, L. (2010) 'Dissecting CD56dim human NK cells', *Blood*, 116(19), pp. 3689-91.

191. Mrozek, E., Anderson, P. and Caligiuri, M.A. (1996) 'Role of interleukin-15 in the development of human CD56+ natural killer cells from CD34+ hematopoietic progenitor cells', *Blood*, 87(7), pp. 2632-40.

192. Mullbacher, A. and Lobigs, M. (1995) 'Up-regulation of MHC class I by flavivirus-induced peptide translocation into the endoplasmic reticulum', *Immunity*, 3(2), pp. 207-14.

193. Mungall, A.J. *et al.* (2003) 'The DNA sequence and analysis of human chromosome 6', *Nature*, 425(6960), pp. 805-11.

194. Naiyer, M.M. *et al.* (2017) 'KIR2DS2 recognizes conserved peptides derived from viral helicases in the context of HLA-C', *Sci Immunol*, 2(15).

195. Nattermann, J. *et al.* (2005) 'The HLA-A2 restricted T cell epitope HCV core 35-44 stabilizes HLA-E expression and inhibits cytolysis mediated by natural killer cells', *Am J Pathol*, 166(2), pp. 443-53.

196. Neisig, A., Melief, C.J. and Neefjes, J. (1998) 'Reduced cell surface expression of HLA-C molecules correlates with restricted peptide binding and stable TAP interaction', *J Immunol*, 160(1), pp. 171-9.

197. Neumann, L. *et al.* (1997) 'The active domain of the herpes simplex virus protein ICP47: a potent inhibitor of the transporter associated with antigen processing', *J Mol Biol*, 272(4), pp. 484-92.

198. Newhook, N., Fudge, N. and Grant, M. (2017) 'NK cells generate memory-type responses to human cytomegalovirus-infected fibroblasts', *Eur J Immunol*, 47(6), pp. 1032-1039.

199. Norman, P.J. *et al.* (2013) 'Co-evolution of human leukocyte antigen (HLA) class I ligands with killer-cell immunoglobulin-like receptors (KIR) in a genetically diverse population of sub-Saharan Africans', *PLoS Genet*, 9(10), p. e1003938.

200. Norman, P.J. *et al.* (2016) 'Defining KIR and HLA Class I Genotypes at Highest Resolution via High-Throughput Sequencing', *Am J Hum Genet*, 99(2), pp. 375-91.

201. O'Connor, G.M. *et al.* (2006) 'Functional Polymorphism of the KIR3DL1/S1 Receptor on Human NK Cells', *The Journal of Immunology*, 178(1), pp. 235-241.

202. O'Connor, G.M. *et al.* (2015) 'Peptide-Dependent Recognition of HLA-B*57:01 by KIR3DS1', *J Virol*, 89(10), pp. 5213-21.

203. O'Connor, G.M. *et al.* (2014) 'Mutational and structural analysis of KIR3DL1 reveals a lineage-defining allotypic dimorphism that impacts both HLA and peptide sensitivity', *J Immunol*, 192(6), pp. 2875-84.

204. O'Sullivan, T.E., Sun, J.C. and Lanier, L.L. (2015) 'Natural Killer Cell Memory', *Immunity*, 43(4), pp. 634-45.

205. Ochoa, M.C. *et al.* (2017) 'Antibody-dependent cell cytotoxicity: immunotherapy strategies enhancing effector NK cells', *Immunol Cell Biol*, 95(4), pp. 347-355.

206. Older Aguilar, A.M. *et al.* (2010) 'Coevolution of killer cell Ig-like receptors with HLA-C to become the major variable regulators of human NK cells', *J Immunol*, 185(7), pp. 4238-51.

207. Orr, M.T. and Lanier, L.L. (2010) 'Natural killer cell education and tolerance', *Cell*, 142(6), pp. 847-56.

208. Ortaldo, J.R. *et al.* (1981) 'Determination of surface antigens on highly purified human NK cells by flow cytometry with monoclonal antibodies', *J Immunol*, 127(6), pp. 2401-9.

209. Oszmiana, A. *et al.* (2016) 'The Size of Activating and Inhibitory Killer Ig-like Receptor Nanoclusters Is Controlled by the Transmembrane Sequence and Affects Signaling', *Cell Rep*, 15(9), pp. 1957-72.

210. Papageorgiou, L. *et al.* (2016) 'An updated evolutionary study of Flaviviridae NS3 helicase and NS5 RNA-dependent RNA polymerase reveals novel invariable motifs as potential pharmacological targets', *Mol Biosyst*, 12(7), pp. 2080-93.

211. Parham, P. (2005) 'Influence of KIR diversity on human immunity', *Adv Exp Med Biol*, 560, pp. 47-50.

212. Parham, P. and Moffett, A. (2013) 'Variable NK cell receptors and their MHC class I ligands in immunity, reproduction and human evolution', *Nat Rev Immunol*, 13(2), pp. 133-44.

213. Pegram, H.J. *et al.* (2011) 'Activating and inhibitory receptors of natural killer cells', *Immunol Cell Biol*, 89(2), pp. 216-24.

214. Pelak, K. *et al.* (2011) 'Copy number variation of KIR genes influences HIV-1 control', *PLoS Biol*, 9(11), p. e1001208.

215. Penman, B.S. *et al.* (2016) 'Reproduction, infection and killer-cell immunoglobulin-like receptor haplotype evolution', *Immunogenetics*, 68(10), pp. 755-764.

216. Petitdemange, C. *et al.* (2016) 'Longitudinal Analysis of Natural Killer Cells in Dengue Virus-Infected Patients in Comparison to Chikungunya and Chikungunya/Dengue Virus-Infected Patients', *PLoS Negl Trop Dis*, 10(3), p. e0004499.

217. Petitdemange, C. *et al.* (2014) 'Association of HLA class-I and inhibitory KIR genotypes in Gabonese patients infected by Chikungunya or Dengue type-2 viruses', *PLoS One*, 9(9), p. e108798.

218. Petruzziello, A. *et al.* (2016) 'Global epidemiology of hepatitis C virus infection: An up-date of the distribution and circulation of hepatitis C virus genotypes', *World J Gastroenterol*, 22(34), pp. 7824-40.

219. Phillips, W.H., Ortaldo, J.R. and Herberman, R.B. (1980) 'Selective depletion of human natural killer cells on monolayers of target cells', *J Immunol*, 125(5), pp. 2322-7.

220. Pohla, H. *et al.* (1989) 'Allelic variation in HLA-B and HLA-C sequences and the evolution of the HLA-B alleles', *Immunogenetics*, 29(5), pp. 297-307.

221. Poli, A. *et al.* (2009) 'CD56bright natural killer (NK) cells: an important NK cell subset', *Immunology*, 126(4), pp. 458-65.

222. Praveen, P.V. *et al.* (2010) 'Tapasin edits peptides on MHC class I molecules by accelerating peptide exchange', *Eur J Immunol*, 40(1), pp. 214-24.

223. Presloid, J.B. and Novella, I.S. (2015) 'RNA Viruses and RNAi: Quasispecies Implications for Viral Escape', *Viruses*, 7(6), pp. 3226-40.

224. Prugnolle, F. *et al.* (2005) 'Pathogen-driven selection and worldwide HLA class I diversity', *Curr Biol*, 15(11), pp. 1022-7.

225. Pymm, P. *et al.* (2017) 'MHC-I peptides get out of the groove and enable a novel mechanism of HIV-1 escape', *Nat Struct Mol Biol*, 24(4), pp. 387-394.

226. Qiang, Q. *et al.* (2012) 'Killer cell immunoglobulin-like receptor gene polymorphisms predispose susceptibility to Epstein-Barr virus associated hemophagocytic lymphohistiocytosis in Chinese children', *Microbiol Immunol*, 56(6), pp. 378-84.

227. Rajagopalan, S. and Long, E.O. (2005) 'Understanding how combinations of HLA and KIR genes influence disease', *J Exp Med*, 201(7), pp. 1025-9.

228. Rajagopalan, S. and Long, E.O. (2012) 'KIR2DL4 (CD158d): An activation receptor for HLA-G', *Front Immunol*, 3, p. 258.

229. Rajalingam, R. (2011) 'Human diversity of killer cell immunoglobulin-like receptors and disease', *Korean J Hematol*, 46(4), pp. 216-28.

230. Ramirez, K. *et al.* (2012) 'Gene deregulation and chronic activation in natural killer cells deficient in the transcription factor ETS1', *Immunity*, 36(6), pp. 921-32.

231. Rasmussen, M. *et al.* (2014) 'Uncovering the peptide-binding specificities of HLA-C: a general strategy to determine the specificity of any MHC class I molecule', *J Immunol*, 193(10), pp. 4790-802.

232. Raulet, D.H. (2006) 'Missing self recognition and self tolerance of natural killer (NK) cells', *Semin Immunol*, 18(3), pp. 145-50.

233. Riteau, B., Barber, D.F. and Long, E.O. (2003) 'Vav1 phosphorylation is induced by beta2 integrin engagement on natural killer cells upstream of actin cytoskeleton and lipid raft reorganization', *J Exp Med*, 198(3), pp. 469-74.

234. Rizzo, R. *et al.* (2014) 'Implication of HLA-C and KIR alleles in human papillomavirus infection and associated cervical lesions', *Viral Immunol*, 27(9), pp. 468-70.

235. Robertson, M.J. (2002) 'Role of chemokines in the biology of natural killer cells', *J Leukoc Biol*, 71(2), pp. 173-83.

236. Robertson, M.J. *et al.* (1996) 'Characterization of a cell line, NKL, derived from an aggressive human natural killer cell leukemia', *Exp Hematol*, 24(3), pp. 406-15.

237. Robinson, J. *et al.* (2015) 'The IPD and IMGT/HLA database: allele variant databases', *Nucleic Acids Res*, 43(Database issue), pp. D423-31.

238. Rogalska-Taranta, M. *et al.* (2015) 'Altered effector functions of NK cells in chronic hepatitis C are associated with IFNL3 polymorphism', *J Leukoc Biol*, 98(2), pp. 283-94.

239. Romagnani, C. *et al.* (2007) 'CD56brightCD16- killer Ig-like receptor- NK cells display longer telomeres and acquire features of CD56dim NK cells upon activation', *J Immunol*, 178(8), pp. 4947-55.

240. Santourlidis, S. *et al.* (2002) 'Crucial Role of DNA Methylation in Determination of Clonally Distributed Killer Cell Ig-like Receptor Expression Patterns in NK Cells', *The Journal of Immunology*, 169(8), pp. 4253-4261.

241. Saulquin, X., Gastinel, L.N. and Vivier, E. (2003) 'Crystal structure of the human natural killer cell activating receptor KIR2DS2 (CD158j)', *J Exp Med*, 197(7), pp. 933-8.

242. Saunders, P.M. *et al.* (2015) 'A bird's eye view of NK cell receptor interactions with their MHC class I ligands', *Immunol Rev*, 267(1), pp. 148-66.

243. Schafer, J.L. *et al.* (2015) 'Suppression of a Natural Killer Cell Response by Simian Immunodeficiency Virus Peptides', *PLoS Pathog*, 11(9), p. e1005145.

244. Schellens, I.M. *et al.* (2015) 'Measles Virus Epitope Presentation by HLA: Novel Insights into Epitope Selection, Dominance, and Microvariation', *Front Immunol*, 6, p. 546.

245. Schroder, K. *et al.* (2004) 'Interferon-gamma: an overview of signals, mechanisms and functions', *J Leukoc Biol*, 75(2), pp. 163-89.

246. Serti, E. *et al.* (2014) 'Monocytes activate natural killer cells via inflammasome-induced interleukin 18 in response to hepatitis C virus replication', *Gastroenterology*, 147(1), pp. 209-220 e3.

247. Sharma, D. *et al.* (2009) 'Dimorphic motifs in D0 and D1+D2 domains of killer cell Ig-like receptor 3DL1 combine to form receptors with high, moderate, and no avidity for the complex of a peptide derived from HIV and HLA-A*2402', *J Immunol*, 183(7), pp. 4569-82.

248. Shresta, S. *et al.* (2004) 'Early activation of natural killer and B cells in response to primary dengue virus infection in A/J mice', *Virology*, 319(2), pp. 262-73.

249. Sim, M.J. *et al.* (2017) 'Canonical and Cross-reactive Binding of NK Cell Inhibitory Receptors to HLA-C Allotypes Is Dictated by Peptides Bound to HLA-C', *Front Immunol*, 8, p. 193.

250. Sim, M.J.W. *et al.* (2019) 'Human NK cell receptor KIR2DS4 detects a conserved bacterial epitope presented by HLA-C', *Proc Natl Acad Sci U S A*, 116(26), pp. 12964-12973.

251. Simmonds, P. *et al.* (2017) 'ICTV Virus Taxonomy Profile: Flaviviridae', *J Gen Virol*, 98(1), pp. 2-3.

252. Single, R.M. *et al.* (2007) 'Global diversity and evidence for coevolution of KIR and HLA', *Nat Genet*, 39(9), pp. 1114-9.

253. Smyth, M.J. *et al.* (2005) 'Activation of NK cell cytotoxicity', *Mol Immunol*, 42(4), pp. 501-10.

254. Spencer, C.T. *et al.* (2015) 'Viral infection causes a shift in the self peptide repertoire presented by human MHC class I molecules', *Proteomics Clin Appl*, 9(11-12), pp. 1035-52.

255. Spiroski, M. *et al.* (2013) 'Killer cell immunoglobulin-like receptor genes in four human West Nile virus infections reported 2011 in the Republic of Macedonia', *Hum Immunol*, 74(3), pp. 389-94.

256. Stelma, F. *et al.* (2016) 'HLA-C and KIR combined genotype as new response marker for HBeAg-positive chronic hepatitis B patients treated with interferon-based combination therapy', *J Viral Hepat*, 23(8), pp. 652-9.

257. Stewart-Jones, G.B. *et al.* (2005) 'Crystal structures and KIR3DL1 recognition of three immunodominant viral peptides complexed to HLA-B*2705', *Eur J Immunol*, 35(2), pp. 341-51.

258. Stewart, C.A. *et al.* (2005a) 'Recognition of peptide-MHC class I complexes by activating killer immunoglobulin-like receptors', *Proc Natl Acad Sci U S A*, 102(37), pp. 13224-9.

259. Stewart, C.A. *et al.* (2005b) 'Recognition of peptide-MHC class I complexes by activating killer immunoglobulin-like receptors', *Proc Natl Acad Sci U S A*, 102(37), pp. 13224-9.

260. Strauss-Albee, D.M. *et al.* (2015) 'Human NK cell repertoire diversity reflects immune experience and correlates with viral susceptibility', *Sci Transl Med*, 7(297), p. 297ra115.

261. Stroobant, V. *et al.* (2012) 'Inefficient exogenous loading of a tapasin-dependent peptide onto HLA-B*44:02 can be improved by acid treatment or fixation of target cells', *Eur J Immunol*, 42(6), pp. 1417-28.

262. Strunz, B. *et al.* (2018) 'Chronic hepatitis C virus infection irreversibly impacts human natural killer cell repertoire diversity', *Nat Commun*, 9(1), p. 2275.

263. Sun, J.C., Beilke, J.N. and Lanier, L.L. (2009) 'Adaptive immune features of natural killer cells', *Nature*, 457(7229), pp. 557-61.

264. Sun, J.C. *et al.* (2011) 'NK cells and immune "memory"', *J Immunol*, 186(4), pp. 1891-7.

265. Tardif, K.D., Mori, K. and Siddiqui, A. (2002) 'Hepatitis C virus subgenomic replicons induce endoplasmic reticulum stress activating an intracellular signaling pathway', *J Virol*, 76(15), pp. 7453-9.

266. Tardif, K.D. and Siddiqui, A. (2003) 'Cell surface expression of major histocompatibility complex class I molecules is reduced in hepatitis C virus subgenomic replicon-expressing cells', *J Virol*, 77(21), pp. 11644-50.

267. Targett-Adams, P. and McLauchlan, J. (2005) 'Development and characterization of a transient-replication assay for the genotype 2a hepatitis C virus subgenomic replicon', *J Gen Virol*, 86(Pt 11), pp. 3075-80.

268. Ternette, N. *et al.* (2016) 'Defining the HLA class I-associated viral antigen repertoire from HIV-1-infected human cells', *Eur J Immunol*, 46(1), pp. 60-9.

269. Thananchai, H. *et al.* (2007) 'Cutting Edge: Allele-specific and peptide-dependent interactions between KIR3DL1 and HLA-A and HLA-B', *J Immunol*, 178(1), pp. 33-7.

270. Topham, N.J. and Hewitt, E.W. (2009) 'Natural killer cell cytotoxicity: how do they pull the trigger?', *Immunology*, 128(1), pp. 7-15.

271. Townsend, M.J. *et al.* (2004) 'T-bet regulates the terminal maturation and homeostasis of NK and Valpha14i NKT cells', *Immunity*, 20(4), pp. 477-94.

272. Townsley, E. *et al.* (2016) 'Interaction of a dengue virus NS1-derived peptide with the inhibitory receptor KIR3DL1 on natural killer cells', *Clin Exp Immunol*, 183(3), pp. 419-30.

273. Uhrberg, M., Parham, P. and Wernet, P. (2002) 'Definition of gene content for nine common group B haplotypes of the Caucasoid population: KIR haplotypes contain between seven and eleven KIR genes', *Immunogenetics*, 54(4), pp. 221-9.

274. van den Hurk, A.F. *et al.* (2019) 'Japanese Encephalitis Virus in Australia: From Known Known to Known Unknown', *Trop Med Infect Dis*, 4(1).

275. van der Ploeg, K. *et al.* (2017) 'Modulation of Human Leukocyte Antigen-C by Human Cytomegalovirus Stimulates KIR2DS1 Recognition by Natural Killer Cells', *Front Immunol*, 8, p. 298.

276. van Teijlingen, N.H. *et al.* (2014) 'Sequence variations in HIV-1 p24 Gag-derived epitopes can alter binding of KIR2DL2 to HLA-C*03:04 and modulate primary natural killer cell function', *AIDS*, 28(10), pp. 1399-408.

277. Vidal-Castineira, J.R. *et al.* (2010) 'Effect of killer immunoglobulin-like receptors in the response to combined treatment in patients with chronic hepatitis C virus infection', *J Virol*, 84(1), pp. 475-81.

278. Vivian, J.P. *et al.* (2011) 'Killer cell immunoglobulin-like receptor 3DL1-mediated recognition of human leukocyte antigen B', *Nature*, 479(7373), pp. 401-5.

279. Vivier, E. *et al.* (2018) 'Innate Lymphoid Cells: 10 Years On', *Cell*, 174(5), pp. 1054-1066.

280. Vivier, E. *et al.* (2011) 'Innate or adaptive immunity? The example of natural killer cells', *Science*, 331(6013), pp. 44-9.

281. Vong, Q.P. *et al.* (2014) 'TOX2 regulates human natural killer cell development by controlling T-BET expression', *Blood*, 124(26), pp. 3905-13.

282. Voskoboinik, I., Whisstock, J.C. and Trapani, J.A. (2015) 'Perforin and granzymes: function, dysfunction and human pathology', *Nat Rev Immunol*, 15(6), pp. 388-400.

283. Vossen, M.T. *et al.* (2002) 'Viral immune evasion: a masterpiece of evolution', *Immunogenetics*, 54(8), pp. 527-42.

284. Vukmanović, S. *et al.* (2001) 'Peptide loading of nascent MHC class I molecules', *Arch Immunol Ther Exp (Warsz)*, 49(3), pp. 195-201.

285. Wahl, A. *et al.* (2009) 'T-cell tolerance for variability in an HLA class I-presented influenza A virus epitope', *J Virol*, 83(18), pp. 9206-14.

286. Wahl, A. *et al.* (2010) 'HLA class I molecules reflect an altered host proteome after influenza virus infection', *Hum Immunol*, 71(1), pp. 14-22.

287. Waldmann, T.A. (2015) 'The shared and contrasting roles of IL2 and IL15 in the life and death of normal and neoplastic lymphocytes: implications for cancer therapy', *Cancer Immunol Res*, 3(3), pp. 219-27.

288. Wang, L. *et al.* (2018) 'Killer-cell immunoglobulin-like receptors associate with HIV-1 infection in a narrow-source Han Chinese cohort', *PLoS One*, 13(4), p. e0195452.

289. Wauquier, N. *et al.* (2010) 'Association of KIR2DS1 and KIR2DS3 with fatal outcome in Ebola virus infection', *Immunogenetics*, 62(11-12), pp. 767-71.

290. Wendt, K. *et al.* (2006) 'Gene and protein characteristics reflect functional diversity of CD56dim and CD56bright NK cells', *J Leukoc Biol*, 80(6), pp. 1529-41.

291. WHO (2009) 'Dengue: Guidelines for Diagnosis, Treatment, Prevention and Control: New Edition', in *Dengue: Guidelines for Diagnosis, Treatment, Prevention and Control: New Edition*. Geneva.

292. WHO (2016) 'Guidelines for the Screening Care and Treatment of Persons with Chronic Hepatitis C Infection: Updated Version', in *Guidelines for the Screening Care and Treatment of Persons with Chronic Hepatitis C Infection: Updated Version*. Geneva.

293. WHO (2017) *Global hepatitis report, 2017*.

294. WHO (2018a) *Dengue and severe dengue*. Available at: https://www.who.int/en/news-room/fact-sheets/detail/dengue-and-severe-dengue (Accessed: 16/03/2019).

295. WHO (2018b) *Updates on yellow fever vaccination recommendations for international travelers related to the current situation in Brazil*. Available at: https://www.who.int/ith/updates/20180116/en/ (Accessed: 16/03/2019).

296. WHO (2019a) *Countries and territories with current or previous zika virus transmission*. Available at: https://www.who.int/emergencies/diseases/zika/countries-with-zika-and-vectors-table.pdf?ua=1 (Accessed: September).

297. WHO (2019b) *Dengue and severe dengue*. Available at: https://www.who.int/news-room/fact-sheets/detail/dengue-and-severe-dengue (Accessed: September).

298. WHO (2019c) *West Nile virus*. Available at: https://www.who.int/news-room/fact-sheets/detail/west-nile-virus (Accessed: September).

299. Wiertz, E.J. *et al.* (1996) 'The human cytomegalovirus US11 gene product dislocates MHC class I heavy chains from the endoplasmic reticulum to the cytosol', *Cell*, 84(5), pp. 769-79.

300. Winter, C.C. and Long, E.O. (1997) 'A single amino acid in the p58 killer cell inhibitory receptor controls the ability of natural killer cells to discriminate between the two groups of HLA-C allotypes', *J Immunol*, 158(9), pp. 4026-8.

301. Wu, Y., Tian, Z. and Wei, H. (2017) 'Developmental and Functional Control of Natural Killer Cells by Cytokines', *Front Immunol*, 8, p. 930.

302. Yang, C.M. *et al.* (2017) 'Hepatitis C virus impairs natural killer cell activity via viral serine protease NS3', *PLoS One*, 12(4), p. e0175793.

303. Yawata, M. *et al.* (2008) 'MHC class I-specific inhibitory receptors and their ligands structure diverse human NK-cell repertoires toward a balance of missing self-response', *Blood*, 112(6), pp. 2369-80.

304. Ye, J. *et al.* (2013) 'Immune evasion strategies of flaviviruses', *Vaccine*, 31(3), pp. 461-71.

305. Yokoyama, W.M. *et al.* (2013) 'Tissue-resident natural killer cells', *Cold Spring Harb Symp Quant Biol*, 78, pp. 149-56.

306. Yoon, J.C. *et al.* (2011) 'Cell-to-cell contact with hepatitis C virus-infected cells reduces functional capacity of natural killer cells', *J Virol*, 85(23), pp. 12557-69.

307. Yossef, R. *et al.* (2012) 'Upregulation of MHC class I expression following dengue virus infection: the mechanism at the promoter level', *Expert Rev Anti Infect Ther*, 10(3), pp. 285-7.

308. Young, N.T. *et al.* (1998) 'Expression of HLA class I antigens in transporter associated with antigen processing (TAP)-deficient mutant cell lines', *Tissue Antigens*, 52(4), pp. 368-73.

309. Yousaf M *et al.* (2018) 'Scenario of dengue infection & its control in Pakistan: An up—date and way forward', *Asian Pacific Journal of Tropical Medicine*, 11(1), pp. 15-23.

310. Yu, H. *et al.* (1998) 'Flt3 ligand promotes the generation of a distinct CD34(+) human natural killer cell progenitor that responds to interleukin-15', *Blood*, 92(10), pp. 3647-57.

311. Zahavi, D. *et al.* (2018) 'Enhancing antibody-dependent cell-mediated cytotoxicity: a strategy for improving antibody-based immunotherapy', *Antibody Therapeutics*, 1(1), pp. 7-12.